

Regional Assessment of Fish Health: A Prototype Methodology and Case Study for the Albemarle - Pamlico River Basin, North Carolina

by

M. Craig Barber
Robert M. Baca¹
Sandra L. Bird
John Doherty²
Linda R. Exum
John M. Johnston
Ray R. Lassiter³
Brenda Rashleigh
Michael J. Cyterski
Susan Colarullo⁴
Nicholas T. Loux
Lourdes M. Prieto
Christina J. Wright⁵

published by

Ecosystems Research Division
U.S. Environmental Protection Agency
Athens, GA 30605-2700

¹ Animal and Plant Health Inspection Service
U.S. Department of Agriculture
4700 River Road, Unit 150
Riverdale, MD 20737-1236

² Department of Civil Engineering
University of Queensland
Brisbane, Australia

³ Department of Marine Sciences
University of Georgia
Athens, GA 30602

⁴ U.S. Geological Survey
U.S. Department of the Interior
Trenton, NJ

⁵ National Park Service
U.S. Department of the Interior
4598 Mac Arthur Blvd, NW
Washington, DC 20007

National Exposure Research Laboratory
Office of Research and Development
U.S. Environmental Protection Agency
Research Triangle Park, NC 27711

Notice

The research described in this document was funded by the U.S. Environmental Protection Agency through the Office of Research and Development. The research described herein was conducted at the Ecosystems Research Division of the U.S. Environmental Protection Agency National Exposure Research Laboratory in Athens, Georgia. Mention of trade names or commercial products does not constitute endorsement or recommendation for use.

Acknowledgments

Many persons outside of the immediate BASE (Basin-scale Assessment of Sustainable Ecosystems) research team contributed to this report. Shelly Miller of the Virginia Game and Inland Fisheries provided assistance in compiling data on fish from Virginia, and Tom Jobes of Aquaterra provided assistance in the application of HSPF described in Chapter 6.2. John Doherty, who wrote much of the time series analysis software that underpins the work described in Chapter Sections 6.1 and 6.2, was supported as a Visiting Research Scientist at the University of Idaho, Idaho Falls. We also thank Gary Shenk (USEPA, Chesapeake Bay Program) and Stephen Kraemer (USEPA) for their contributions regarding Chapter sections 6.2 and 6.3.

Foreword

Environmental concerns are primarily ecological concerns. In the past, most regulations that have been implemented to protect ecological resources have done so with only implicit connections to organisms and the habitats and communities in which they live. Research that make such connections explicit is needed to improve current and future ecological risk assessments. Although sustainability of ecological resources is ultimately the goal of all environmental management, identification of what is meant by ecological sustainability is often not well defined. Nevertheless, it is clear that one area of needed research pertaining to this topic is the development of comparative risk approaches that can identify, generate, and evaluate alternative future scenarios. Such research also needs to be focused on regional environmental issues and concerns rather than simply local or site-specific issues. In this regard, river basins, sub-basins, and watersheds, defined by their network of water and material movement, are perhaps the most useful and well defined landscape units for which regional scale environment concerns must be routinely addressed.

To address these issues and needs, the Ecosystems Research Division of the National Exposure Research Laboratory developed a research program in 1999 entitled Basin-scale Assessment of Sustainable Ecosystems (BASE). BASE's goal was to investigate and develop methods and approaches that integrate ecological, hydrological, and landscape processes with projections of socioeconomic demands on regional watersheds and river basins.

Rosemarie C. Russo, Ph.D.
Director
Ecosystems Research Division
Athens, Georgia

Abstract

BASE (Basin-Scale Assessments for Sustainable Ecosystems) is a research program developed by the Ecosystems Research Division of the National Exposure Research Laboratory to explore and formulate approaches for assessing the sustainability of ecological resources within watersheds and larger river basins. To give the program focus, BASE has focused on developing a conceptual framework to assess the sustainability of ecological resources in the Albemarle-Pamlico Basin, NC under the influence of the multiple stressors that might be imposed by human activities across the region. To make this project doable, BASE's focus was narrowed further to deal only with the assessment of projected changes in various dimensions of fish health within the Albemarle-Pamlico Basin. A more complete assessment, however, would consider a wide variety of ecological resources, selected to represent many kinds of potential vulnerability. These could include dwindling habitats, altered climate that places many species of both animals and plants out of their physiological tolerance limits, and the continuing threat to biota across the region from a changing suite of environmental contaminants.

The major components of BASE are: 1) identification and generation of stressor scenarios that directly or indirectly produce ecological effects; 2) hydrologic, hydrodynamic, and water quality simulations; and 3) fish endpoint simulations. Conceptually, analyses of projected socioeconomic and demographic changes within the basin are used to generate input scenarios for regionally distributed hydrological and water quality models. The resulting water quality scenarios are, in turn, used as inputs to various fish endpoint models whose outputs are used to assess the regional sustainability of fish health.

According to the BASE conceptual framework, projected socioeconomic and demographic trends can be translated directly into future land use practices that directly alter 1) regional hydrologic patterns, 2) sediment, nutrient, and contaminant loadings to surface waters, 3) in-stream sediment transport and deposition, and 4) general water quality dynamics. Methods for translating projected urban development into impervious land use cover are described and discussed in detail. Methods for estimating the runoff of water, nutrients, pesticides, and sediments from the landscapes based on current or projected land use are also considered. To complete the framework, models for simulating regional hydrology, water quality, and fish community processes are described and reviewed.

To illustrate how these components can be sequentially linked to assess fish health, a demonstration project aimed at assessing the ecological responses of fish communities within the Contentnea Creek watershed of the Albemarle-Pamlico basin is presented.

Table of Contents

Abstract	iv
1. Introduction	1
1.1. BASE Program Approach and Design	3
1.2. Concepts and Definitions Related to Ecological Sustainability	8
2. Fish Health	10
2.1. Ecological Dimensions	11
2.2. Human Use and Health Perspectives	12
2.3. Stressors	18
2.3.1. Disruption of Nominal Biological Processes	18
2.3.2. Alteration of Physical Habitats	19
2.3.3. Chemical Contaminants	19
2.3.3.1. Water Quality Issues	19
2.3.3.2. Sediment Quality Issues	20
2.3.4. Landscape and Non-point Source Issues	20
3. Description of the Albemarle-Pamlico Basin	22
3.1. Site Description	22
3.2. Socio-economic Development	24
3.2.1. Urban Development	24
3.2.2. Agricultural Patterns and Issues	25
3.3. Regional Climate	25
3.4. Regional Hydrology	26
3.4.1. Surface Water Hydrology	26
3.4.2. Ground Water and Regional Geomorphology	26
3.4.2.1. Effects of Geologic Heterogeneities on Solute Transport	26
3.4.2.2. Coastal Plain Geology	28
3.4.3. Riparian and Wetland Issues	31
3.5. Water Quality Issues	32
3.6. Biological Resources	34
3.6.1. Fish Biogeography and Biodiversity	34
3.6.2. Sport and Commercial Fisheries	35
3.6.3. Endangered and Threatened Fishes	36
4. Identifying Nominal Conditions for Fish Health	37
4.1. Fish Community Associations	37
4.2. Nominal Fish Growth and Related Processes	52
5. Models and Analysis Tools for Regional Assessment	65
5.1. Projecting Land Cover Trends	65
5.2. Hydrology	77
5.2.1. Methods for Projecting Baseflow	77
5.2.2. Predicting Regional Hydrology - HSPF	79
5.2.3. Predicting Regional Hydrodynamics & Sedimentation - EFDC	80
5.2.4. Predicting Riparian Dynamics - REMM	82
5.3. Biological Endpoint Models	83
5.3.1. AQUATOX	84
5.3.2. BASS	84
5.3.3. Habitat Suitability Models	86
5.4. Modeling Issues	89
5.4.1. Models as Ecological Indicators	89
5.4.2. What is a Good Model?	89
5.4.3. Uncertainty	90
5.4.3.1. Mathematical Sensitivity	91
5.4.3.2. Statistical Variability of Parameters, Forcing Functions, & Initial Conditions	93
5.4.3.3. Scientific Uncertainty	95

6. Prototype Assessment - Contentnea Creek Watershed	97
6.1. Hydrological Patterns	97
6.2. Total Suspended Sediment Loadings	119
6.3. Expected Fish Health Trends Using AQUATOX	137
7. Prospectus for Future Regional Assessments	144
References	146

List of Figures

Figure 1. Schematic relationships between models used in the BASE sustainability framework.	4
Figure 2. Schematic ecological sustainability as persistence of ecological resources into a future scenario.	5
Figure 3. Major river basins and 8-digit HUC watersheds of the Albemarle-Pamlico basin.	24
Figure 4. Advective movement of dissolved nutrients and other chemicals through subsurface heterogeneities.	27
Figure 5. Architectural elements in a braided-stream depositional environment (modified from Miall 1985)	29
Figure 6. Atlantic Coastal Plain and Continental Shelf.	30
Figure 7. Regional geologic section (from http://sgl.dnrcr.usgs.gov/albe-html/Maps)	31
Figure 8. Ecoregions of the Albemarle-Pamlico basin.	34
Figure 9. Distribution of fish sample sites with respect to 8-digit HUC watersheds.	38
Figure 10. Fish community clusters based on combinations of 8-digit HUC watersheds. River basin boundaries are outlined in orange, and 8-digit HUC watershed boundaries are outlined in black	40
Figure 11. Fish community clusters based on combinations of 8-digit HUC watersheds and ecoregions. River basin boundaries are outlined in orange; 8-digit HUC watershed boundaries are outlined in black; and ecoregions are outlined in green.	40
Figure 12. Ordination diagram of PCA results. Component loadings are linear combinations of fish species. Labels are the clusters in Figure	41
Figure 13. Ordination diagrams of canonical correlation results. Cluster C fish associations are shown in panel A and cluster E fish associations are shown in panel B. Labels are the species-habitat groups from Table for cluster C and from Table for cluster E.	43
Figure 14. Calculated BAF/BCF for largemouth bass assuming nominal growth and uncontaminated prey.	60
Figure 15. Calculated BAF for largemouth bass assuming nominal growth and contaminated prey.	61
Figure 16. Impervious Cover Results from the DOQQ Interpretation for Frederick County, MD.	69
Figure 17. The three relationships between population density and %TIA presented in Table are shown in Part a (top figure above) along with data collected for this study in watersheds in Frederick County, MD and by Graham (1974) for census tracts in Washington, DC. Part b (bottom figure above) shows the response of the Hicks and Woods (2000) relationship for population densities less than 2000 persons/sq mi compared to data presented on a linear scale.	72
Figure 18. The percentage of impervious cover points sampled from aerial photographs in Frederick County, MD located in land-cover cells summarized by Anderson Level 1 categories.	74
Figure 19. Acreage categorized as residential (combined high and low density) in the NLCD 92 data (NLDC residential) and by residential lot size category from property tax records for Frederick County, MD. The labels for data from the property tax records indicate all the residential lots that are less than the indicated number of acres per unit of housing – e.g., < 5 ac is the sum of all properties in the tax records that are on lots of less than 5 acres per housing unit.	74
Figure 20. Impervious cover for Frederick County, MD watersheds measured from aerial photographs versus that estimated from categorized satellite imagery and category coefficients developed from county wide data.	76
Figure 21. Impervious cover for Frederick County, MD watersheds measured from aerial photographs versus that estimated from property data and impervious coefficients based on lot sizes and land use types.	76
Figure 22. Impervious cover for Frederick County, MD watersheds measured from aerial photographs versus that estimated from a combination of data, including U.S. Census population density, manufacturing and industrial areas from categorized satellite imagery, and major highway networks from U.S. Department of Transportation.	77
Figure 23. Contentnea Creek watershed study area and surroundings. The Contentnea subwatershed is located within the Neuse River basin of North Carolina.	99
Figure 24 a. Measured (bold line) and modeled (light line) flows (in ft ³ /sec) over part of the calibration period.	104
Figure 24 b. Measured (bold line) and modeled (light line) monthly volumes (in ft ³) over calibration period.	104
Figure 24 c. Measured (bold line) and modeled (light line) flow exceedence fractions over the calibration period.	104
Figure 25. Measured (bold line) and modeled (light lines) flows (in ft ³ /sec) over part of the calibration period.	105
Figure 26 a. Measured (bold line) and modeled (light line) flows (in ft ³ /sec) over part of the validation period at Hookerton. Parameters were estimated through simultaneous calibration of all four watershed models.	107
Figure 26 b. Measured (bold line) and modeled (light lines) monthly volumes (in ft ³) over the validation period.	107
Figure 26 c. Measured (bold line) and modeled (light lines) flow exceedence fractions over the validation period.	107
Figure 27. Measured (bold line) and modeled (light line) flows (in ft ³ /sec) over part of the calibration period. Parameters were estimated through simultaneous calibration of all four watershed models.	109
Figure 28. Measured (bold line) and modeled (light line) flows (in ft ³ /sec) over part of the calibration period. Model parameters were estimated through simultaneous calibration of all watersheds using regularization.	111
Figure 29 a. Model-generated (light lines) and measured (bold line) flows in ft ³ /sec over 1993. Model parameters were estimated using PEST's predictive analysis functionality.	115

Figure 29 b. Model-generated (light lines) and measured (bold line) flows in ft ³ /sec over part of the calibration period. Model parameters were estimated using PEST's predictive analysis functionality.	115
Figure 30 a. Model-generated (light lines) and measured (bold line) flows in ft ³ /sec over 1993. Model parameters were estimated using PEST's predictive analysis functionality with DEEPFR adjustable.	116
Figure 30 b. Model-generated (light lines) and measured (bold line) flows in ft ³ /sec over part of the calibration period. Model parameters were estimated using PEST's predictive analysis functionality with DEEPFR adjustable.	116
Figure 31. TSS data gathered over the period 1975 to 1995 at Hookerton Gauging Station.	125
Figure 32. The top part of this figure shows TSS measurements superimposed on stream flow measurements. TSS is plotted against flow in the lower part of the figure.	126
Figure 33. The top graph allows a comparison between TSS measurements and model output to be made on a point-by-point basis. In the bottom graph TSS measurements are superimposed on the model-generated TSS time series. In both of these graphs the model output is depicted in grey.	133
Figure 34. Observed and model-generated TSS values over the calibration period. The total exported suspended mass over the calibration period is minimized in the top graph and maximized in the bottom graph.	135
Figure 35. Diagram of feeding relationships. Solid arrows represent strong feeding preferences and dotted lines represent weak preferences.	138
Figure 36. Response of biomass of the four fish groups to a 10% increase in (a) temperature, (b) nutrients, and (c) sediment.	141
Figure 37. Response of biomass of the four fish groups to a 10% decrease in (a) oxygen, (b) detrital loading, and (c) pH.	142

List of Tables

Table 1. Summary of reported North Carolina fish kills for 1996-2001 (NCDENR 2001).	13
Table 2. Suspected causes of North Carolina fish kills for 1996-2002 expressed as a percent of total.	13
Table 3. Fish species or groups recognized as North Carolina inland game fish (NCWRC 2002).	14
Table 4. Fish species and body sizes recognized by the North Carolina Angler Recognition Program (NCARP), effective July 1, 1997, as a “trophy” fish (NCARP 2002).	15
Table 5. North Carolina fish consumption advisories published by the North Carolina Wildlife Resources Commission (NCWRC 2002).	16
Table 6. Fish consumption advisories published in North Carolina 305B Report, February 2000 (http://h2o.enr.state.nc.us/bepu/files/305b/2000AppendixB.pdf)	17
Table 7. Summary Statistics for the Albemarle-Pamlico major basins (NCDENR 2002e)	23
Table 8. Species-habitat groups within Cluster A.	44
Table 9. Species-habitat groups within Cluster B.	46
Table 10. Species-habitat groups within Cluster C.	48
Table 11. Species-habitat groups within Cluster D.	50
Table 12. Species-habitat groups within Cluster E.	51
Table 13. Summary of daily growth rates (g/g/d) for Albemarle-Pamlico basin fish species.	56
Table 14. Empirical relationships between population density and impervious area.	67
Table 15. Impervious Cover Interpretation of Frederick County, MD by HUC	70
Table 16. Impervious Cover for NLCD 92 Land Cover Categories	73
Table 17. Summary of available Habitat Suitability Models.	87
Table 18. HSPF parameters, their functions, initial values and constraints imposed during the calibration process.	101
Table 19. Estimated parameter values. Parameters sets 2 to 5 were computed using PEST’s regularization functionality.	103
Table 20. Parameters estimated by PEST through simultaneous watershed calibration using its regularization functionality. Parameters estimated through independent model calibration are shown italicized in brackets.	112
Table 21. Estimated parameter values. All parameter sets were estimated using PEST’s predictive analysis functionality.	113
Table 22. HSPF PWATER parameters estimated during the calibration process. Other parameters were assigned values independently of the calibration process. See Doherty and Johnston (2002) for details.	127
Table 23. PERLND SEDMNT parameters estimated during the calibration process.	128
Table 24. RCHRES SEDTRN parameters estimated during the calibration process.	128
Table 25. Sets of estimated parameter values. Units for many of these parameters are complex due to the exponential term in the equations that contain them.	131
Table 26. Selected input parameters of fish groups used for AQUATOX simulations.	139

1. Introduction

An analysis of the ecological sustainability of a large watershed (river basin or multiple basins) obviously could provide essential information for the optimal environmental management of that area. The goal of such an ecological sustainability analysis should be the evaluation of the expected, long-term response of a suite of representative ecological resources to the major stressors that may occur within the basin, with greater emphasis on the more hazardous and more widespread stressors. A basin-scale analysis will generally include a heterogeneous mix of physiographic, hydrographic, ecological, socio-economic, and political characteristics. Many of these complexities are encountered by environmental managers who must decide how to allocate limited resources to a large set of environmental problems. Choices of which of many ecological problems to attempt to solve and which to postpone are limited by human and other resources, so an indication is needed of the relative severity of problems affecting ecosystems within a basin and what resources are sustainable under which practices. Although choices may be made, in part, on political grounds, the better the knowledge of the relative ecological vulnerabilities and environmental management practices that will sustain ecological resources, the more cost effective will be choices for environmental management.

Many ecological problems are inherently non-local. Actions at one geographic location often have large ecological effects at far distant points, so that for some problems, large regions must be considered for an adequate evaluation of consequences. For aquatic resources, a river basin is an appropriate unit in which to consider these interconnected ecological problems. An ecological sustainability analysis, as proposed herein, should use characterization of the geographic distribution and magnitudes of ecological changes that are projected to result from a suite of potential human actions, and identify from this suite those that provide the greatest degree of sustainability. There is, however, no necessity that only basin-wide problems be considered or that an estimate be made of the severity of a problem on a whole-basin basis because both types of analyses are within the scope of our definition of basin-scale sustainability analysis. It would be valuable for a manager to know how to deal with a particularly severe problem confined to a small area within a region, and in general, to know the subregional scope of practices that are damaging and those that are beneficial. When considering which of competing problems to try to solve, a manager could benefit by knowledge of which are more likely to become even more severe under continuation of current uses and what alterations are necessary for sustainability. The ability of the ecological resource to recover when a stressor is removed or a needed support service provided (other species, accessibility of stream reach, etc.) would be valuable knowledge. Estimates of this resiliency must come from knowledge of the resource, and if this knowledge is codified in a working model, it is more widely usable and, therefore, more valuable. Finally, a manager could benefit by knowledge of the specific causes of ecological damage, i.e., what are the human actions to which the resource is vulnerable and what are the specific remedies. It would be valuable to go beyond vulnerability, however. Knowledge of practices that sustain ecological resources encompass, and therefore are more valuable than the more limited knowledge of vulnerabilities. With such information, a manager would be well positioned to allocate resources optimally to environmental protection.

Analyses of the sustainability of ecosystems, as envisioned herein, will consider responses of present-day biota to *potential future stressors and management practices* - the latter represented by scenarios selected for their

plausibility as insights into possible future environmental choices. Scenarios represent not just uncertainty of knowledge of what *will* happen, but also what *might* happen. There are a few factors, such as climate, whose future trajectories are believed to be essentially set - that is we have little power to change this trajectory over the next several decades. In contrast, the magnitudes of many environmental stressors that will occur over the same time period will be determined by choices made over that same period. Future scenarios will consist both of representations of those factors whose trajectories over decades are already set and of other factors whose trajectories will be set by future choices. Comparisons of these response measures of sustainability among scenarios will be directly interpretable. Each scenario will be chosen to reflect real, long-term possibilities for land use, chemical use, forestry and agricultural practices, and other factors that humans control, in addition to those that are essentially outside our control. These analyses will present us with a projection of the consequences of choices that affect the environment long before they occur - in most cases, long enough ahead of time to make optimal choices. The analyses will identify responses with characteristic times that are very long, such as climatic change; of intermediate length, such as alteration in forest composition and soils; and that are short, such as alterations in surface-water hydrology and transport of materials. The longer the characteristic time, the earlier must decisions be made for any intended changes before significant results can be realized.

To assess how resources of today will respond to future stressors, we must assess the current ecological resource base, identify and predict the behavior of future stressors, and predict the response of ecological resources to those anticipated stressors. Clearly the prediction of required stressor and resource dynamics must be performed using mathematical simulation models of some form. Because the predictions of such models will be inherently uncertain, we must develop the ability to characterize results, including the associated uncertainty, in ways that are useful to those with responsibility to steer away from behaviors and choices that carry greater ecological risk. Currently, we have no documented, procedural means with a sound theoretical basis by which questions of the ecological effects of today's socio-economic choices can be evaluated. Ecological sustainability analysis can be the tool by which we preview results of chains of choices on future environments and ecosystems. Change is certain, and choices that are made will establish the nature, rate, and magnitude of that change. A more concrete awareness of the likely results of our actions would give us a better chance to choose environmental policies that support sustainable ecosystems.

The simulation approach can become overburdened with detail. The key to a successful project of this type lies in the abilities of the investigators to define the problem that will both answer the environmental question at hand, and for which the essential abstraction can be made that makes the problem tractable and computationally feasible. Using models to solve problems, even problems of the scope of a large basin, must be a restricted activity by necessity since one can easily define a problem that is too big to be feasible. Therefore, as a demonstration project for the development of a basin-scale ecological sustainability analysis scientists at the Ecosystems Research Division of the National Exposure Research Laboratory have chosen to focus on one particular ecological resource of widespread concern within the Albemarle-Pamlico river basin of North Carolina. In particular, we have focused our efforts on developing a sustainability analysis framework for the *health* of the basin's fish communities and associated fisheries.

For this study of ecological sustainability, we have defined the problem more narrowly to be the effect of water quality changes on fish populations, both resident and migrant. Ideally, a set of feasible management practices

will be identified that will stabilize water quality sufficiently to support sustained resident and anadromous fish communities in these waters indefinitely. Water quality changes are taken to mean the projected changes that will occur in response to human activities that introduce a variety of biological stressors over a selected future time, say 50 years. Questions can be expected to be posed about these effects, including questions of where within the region are the effects most severe, and what management alternative improves water quality the most, or the most economically. The full problem definition should be rich enough to include a wide suite of such questions. The choice of resolution (spatial, temporal, and component-wise) is determined, in part, by the nature of the questions to be answered. The essential components (without getting into detail at this point) include: landscape state in terms of its physiography, land cover, and land use (to determine runoff quantity and quality in terms of suspended and dissolved constituents) for both present and a suite of future scenarios; the quantity and quality of runoff for all of the watersheds at the smallest scale that we will consider; movement of water through the watercourses; flow fields during weather events (long-term drought, high-rainfall event, etc.); water quality as a resultant of both water flowing from upstream and from in-stream processes; and finally, the states of fish populations. These are stated in terms of our perception of essential components of the natural system. In the problem-solution phase, the modeler must apply models that compute the quantities of each of the processes carried out by the essential components, compute differences between current state and a projected future state, and identify scenarios representing management practices that provide sustainability of the fish communities.

1.1. BASE Program Approach and Design

The goals of this research, which will be subsequently referred to as BASE (**B**asin-scale **A**ssessment of **S**ustainable **E**cosystems), are to design and implement a framework for assessing the sustainability of fish communities in the Albemarle-Pamlico basin associated with a suite of alternative management practices over a future time interval, and to contribute knowledge of the conduct of this project to assist with design requirements for a software assessment tool to support such analyses organized on the basis of a discrete hydrologic unit.

Computations in the BASE framework will be carried out by a series of models that are linked according to the topographically driven flows of water and transported material of the natural system. These linkages are portrayed schematically in Figure 1, including the model acronyms.

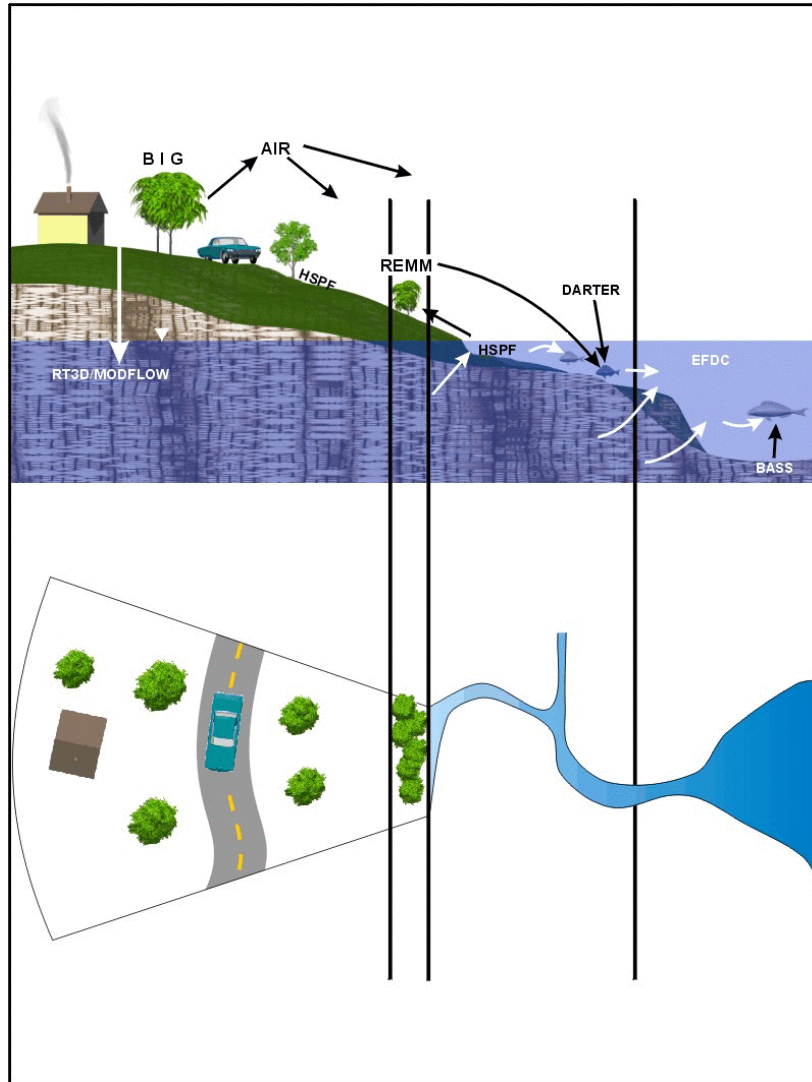


Figure 1. Schematic relationships between models used in the BASE sustainability framework.

The computation of sustainability as a persistence of fish populations or communities between the present environmental state and that presented by scenarios of the future is indicated schematically in Figure 2.

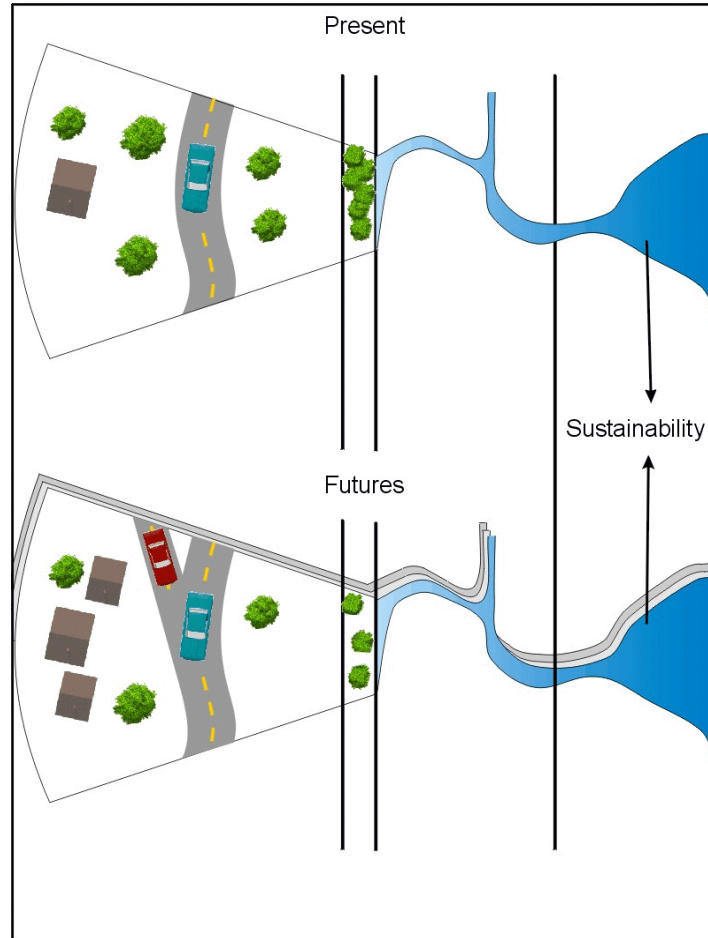


Figure 2. Schematic ecological sustainability as persistence of ecological resources into a future scenario.

Note that multiple scenarios for future environments are indicated in Figure 2, and that both uncertainty and a range of sustainabilities, each associated with a given future scenario, are the outcomes of the use of multiple future scenarios.

Watersheds - The causal chain of influence of environmental factors on fish health within a basin is assumed to be the following. The state of the watershed (forest, field, pavement, etc.), weather, ecological processes and human activities on the watershed control the character of runoff (water production, sediment delivery, allochthonous organic material delivery, concentration of nutrients and toxicants). Both the character of runoff and in-stream processes control water quality. Allochthonous organic material (leaves and woody detritus) is the primary carbon source for small streams, driving the production of benthic insects, which are the primary food source for many stream fishes. In water bodies of larger size and longer water residence times, the allochthonous organic material contributes less per unit of volume or bottom area, and autochthonous organic carbon from primary productivity by phytoplankton dominates.

In streams where allochthonous organic material is the dominant carbon source, the activities of

microorganisms and bottom-dwelling invertebrates decompose and resynthesize the organic detritus, and are the source of food for most fish populations. The presence and composition of riparian vegetation, as well as the distribution of forest cover of the upland portions of the watershed are determinants of the quantity and quality of allochthonous organic material that enters the streams, thereby influencing the density of bottom-dwelling invertebrates that can be supported. Sedimentation destroys habitat for the invertebrate populations, high levels of pesticides lead to higher mortality and lower reproductive rates, and high concentrations of inorganic nutrients can lead to periphyton overgrowth that is detrimental to some and favorable to other invertebrate species. Fish communities are comprised of species whose physiology, behaviors, and ecological interactions favor their presence in streams of given water quality, flow regime, temperature pattern, bottom characteristics, and food source. These quantities, altered by activities that change the character of runoff, in turn, alter fish physiology, behavior, and ecological interactions and consequently, the composition and density of fish communities.

In larger water bodies with residence times long enough that phytoplankton can develop, water clarity, temperature, and the source strengths of the major nutrients (particularly nitrogen species and phosphate) strongly determine the densities of phytoplankton populations that develop. Under favorable conditions, phytoplankton populations tend to develop to densities that reduce the limiting nutrients to background concentrations, which support further growth only at levels that equate to population mortality. Conditions are generally not favorable for long periods, however, so phytoplankton populations tend to increase to high levels and remain there for some time until conditions begin to cause severe mortality. Inorganic nutrients are returned to the water by microbial decomposition of the dead phytoplankton. Where source strengths of nutrients are high and variable, this boom and bust cycle continues, and where nutrient supply is low and more stable, a lower density and more stable phytoplankton population tends to develop. The food web in planktonic systems can be complex, with several planktonic invertebrate populations feeding on the phytoplankton, with several fish species feeding on both the phytoplankton and on the planktonic invertebrates, and with the food habits of many fish species changing from plankton-feeding of the fry, to piscivory later in the fishes' life. Lower reaches of the rivers and the estuaries and sounds support large, transient, anadromous populations that immigrate upriver to spawn and return downriver to the estuaries and ocean, leaving behind large populations of young to feed and grow to sizes where they too leave the sounds and overwinter in the ocean. The characteristics of watersheds and upstream reaches, and processes that occur within the lower reaches control the water quality of the lower reaches, with phytoplankton growth being one of the controlling processes. In addition to the requirement of the continuous existence of a support level of plankton, the flow regime, water temperature, dissolved oxygen, pH, turbidity from suspended sediment and plankton, toxicant concentrations, and other quantities influence the health of resident and anadromous populations of fish.

Activities needed to assess *fish health* can be categorized into discrete phases that follow the above description. These phases are: 1) generation of regional land-use scenarios, 2) runoff modeling (hydrology and source water quality), 3) in-stream hydrodynamics and water quality modeling (including microbial and algal activity), and 4) fish community modeling. These modeling activities will connect the state of the watershed to expectations of the states of fish communities in the watercourses of the region. Given a scenario that projects future states of the regional watersheds, the same modeling activity can be used to connect the projected future states of the watershed to expected future states of fish communities. If a current ecological resource would be detrimentally affected by human activities that could occur in the future, we would naturally say that the ecological resource is

vulnerable to that type of activity, and that for the resource to be sustainable, that activity would necessarily have to be curtailed or altered such that the impact is avoided. If sustainability is the objective, knowledge is required of what practices to substitute for those that create vulnerabilities in ecological resources. Modeling scenarios will include a range of posited human activity patterns, so that those tending to promote sustainable ecosystems can be identified. An additional approach will be evaluated in which the best features of the original set of future scenarios will be compiled to construct the most favorable overall scenario.

Focusing on relationships and causal chains within a watershed underscores a working assumption that fish populations and their health can be evaluated independently across watersheds, but that population interactions must be taken into account within watersheds. From the point-of-view of modeling fish health, this defines a watershed as being hydrologically and ecologically distinct. The eight-digit hydrologic unit code (HUC) defines watersheds that reasonably well meet this criterion. Modeling fish health in small streams, however, requires sub-watershed resolution. This implies that runoff, water flow, water quality, etc. must be computed for each of the small stream, sub-watershed units within the eight-digit HUC. The 11-digit HUC defines smaller watersheds that are of a size that might reasonably well meet the size criteria of associated small stream networks with interacting fish populations. The area of the Albemarle-Pamlico region is about 31,400 square miles and there are 22 eight-digit HUC's within the region. There are 197 11-digit HUC's reported for the region (a few records are duplicated so that there are actually fewer than 197). To model this region's fish health within small streams as well as within large streams, rivers, and estuaries assuming that there will be two or three small streams per 11-digit HUC, the total number of small watershed analyses required would be on the order of 400 – 600. It does not appear feasible to do computations of runoff and streamflow for each of these streams individually without some type of automation, or possibly some type of sampling scheme. One approach that we are pursuing in an attempt to reduce the requirement for local calibration of each watershed is the application of the runoff and streamflow model, HSPF, in small subwatersheds where the physical-chemical properties are more uniform. These HSPF outputs would then be composited to estimate the runoff and streamflow for the whole watershed. If this approach gives usable predictions, it or some modification could be used for computation of runoff and streamflow on the many un-gaged watersheds of the basin.

Analysis of individual watersheds, although assuming that there is little mixing of fish populations among large watersheds, must not assume that the watershed is isolated in other ways. Most watersheds are not headwaters and are part of a much larger airshed. Activity far upstream and far away can have significant effects. Although we are forced to draw artificial boundaries with respect to the airshed and to attempt to obtain fluxes of airborne materials across those boundaries, we are not forced to do so for river basin hydrology and associated transport. Thus, any watershed can be properly placed within the water routing scheme and the analysis done for the watershed in the context of upstream conditions and any cross-watershed transport that is known to occur.

Basins - At the data level, a basin analysis is a collection of watershed analyses, but from a simulation point-of-view, there is the additional requirement that the watershed analyses be conducted in the full context of their watershed and stream-flow connectivity and other factors of basin morphology. At the most downstream points, even the watershed analyses are basin-scale in scope, especially in systems like the Albemarle-Pamlico where the rivers flow into common estuaries and sounds. Analyses of the water quality, fish health, etc., in these downstream systems are inherently basin-scale, because influences on all watersheds contribute to conditions within the sounds.

Anadromous fishes, i.e., those that use the creeks, rivers, and sounds for spawning and nursery areas, require analyses that are supra-watershed. These fishes traverse large distances, passing from sounds into lower rivers and estuaries and then upriver into creeks where they spawn, and then depart from the system. The fry and young then traverse the same systems, albeit much more slowly as they pass through their early life stages in preparation for return to the ocean. Therefore, both the adults and young of these fishes are exposed to conditions in several waterbodies and watersheds annually. Conditions in the river during the time of passage of fry and young can strongly influence the size of the year class and, therefore, the size of the migration supporting the fishery during subsequent years.

Computer simulations will generate a mass of geographic and temporal detail about water quality, fish habitat, and the state of fish health across the region, but comprehension of these data depends on interpretation at a higher and more comprehensive level. Measures of fish health (species composition of communities, population densities, age structure, body burdens of toxic chemicals, etc.) will be generated for mapping, including annual cycles that could show the time of year or life stage that is most vulnerable and the geographic pattern of occurrence of that vulnerability. Other measures of quantities that support or impinge upon fish health will also be available, such as sediment, nutrient, and pesticide loading by stream reach, or larger water body.

1.2. Concepts and Definitions Related to Ecological Sustainability

During the mid 1970's and early 1980's, a great deal of attention was focused on two important concepts related to the sustainability of ecological resources. The first of these was the notion of ecological resistance that was defined to be the ability of an ecological component or process to maintain constant or nearly constant levels of activity when exposed to external stressors. The second concept was that of ecological resilience, which was defined as the ability of an ecological component or process to return to nominal levels of activity after external stressors that depressed the component's or process's activity were relaxed. Having defined these very different types of system response to external perturbation, whether natural or anthropogenic in origin, many researchers attempted to categorize ecosystems, communities, and populations as to whether they are resistant or resilient relative to ecological stressors.

At the same time, systems ecologists began an active dialog focusing on the concept of ecological stability. Although "stability" may be semantically related to "sustainability", early ideas regarding ecological stability were only indirectly related to what today's environmental managers and regulators may have in mind regarding ecological sustainability. Early concepts of ecological stability were largely founded in general systems theory and, in fact, were focused more on the models of ecological components and processes rather than the components or processes themselves. See, for example May(1973). Ecological stability from this perspective largely concerned itself with two different, but related, aspects of "ecosystem" behavior. The first of these behaviors is the ability of an ecosystem to return to its "nominal" trajectory or equilibrium state after being perturbed (Waide and Webster 1976). For linear ecological models or the linearized versions of non-linear ecological models, this type of stability has become synonymous with the Lyapunov stability from applied mathematics (Astor et al. 1976). The second behavior of interest was the ability of an ecosystem to maintain nearly constant population sizes in the face of parameter variations (Waide and Webster 1976). The former ability was generally referred to as "neighbor stability" whereas the latter was referred to as "structural stability".

An important dimension of structural stability as defined above is the property that all system components exhibit bounded growth without catastrophic population crashes. For example, a predator-prey system would be considered stable if both the predator and the prey coexisted in balance with one another. Similarly, a system of two or more competitors would be considered stable if all coexisted with non-zero populations.

Any concept of ecological sustainability, including that of fish health, must include all the concepts mentioned above. Resources that are explicitly exploited for harvest or consumption must be both resistant and resilient to actual or potential over harvest. Many freshwater fisheries are managed and maintained by fish stocking programs that can cause widespread disagreement as to what ecological sustainability really should be. This is particularly true when such programs involve the stocking of non-indigenous species. In such situations, the recreational angler may view resource sustainability simply as the sustainability of the game species of interest. However, from the perspective of ecologists, naturalists, or other outdoors enthusiasts, ecological sustainability must encompass the maintenance of the natural biodiversity of waters being managed by such programs. These two expectations for ecological or resource sustainability are often in conflict with one another since the biodiversity of any native fauna or flora is typically at risk with the introduction of any exotic or non-indigenous species. Consequently, in these situations our ideas of ecological sustainability must include not only the persistence of the game species but also the structural stability of the affected aquatic communities.

2. Fish Health

Fish health can be defined from both an ecological and a human health/value perspective in a wide variety of ways. Questions related to ecological perspectives include:

- 1) Is individual fish growth and condition (e.g., fat reserves) sufficient to enable them to survive periods of natural (e.g., overwintering) and man induced stress?
- 2) Are individual fish species maintaining sustainable populations? In particular, is individual growth adequate for the fish to attain the minimum body size required for reproduction? Is there adequate physical environment for successful spawning? Is there adequate physical habitat for the survival of the young-of-year?
- 3) Do regional fish assemblages exhibit their expected biodiversity or community structure based on biogeographical and physical chemical considerations?
- 4) Are appropriately size fish abundant enough to maintain piscivorous wildlife (e.g., birds, mammals, and reptiles) during breeding and non-breeding conditions?
- 5) Are potential fish prey sufficiently free of contaminants (endocrine disruptors, heavy metals, etc.) so as not to interfere with the growth and reproduction of piscivorous wildlife?

Questions related to human perspectives include:

- 6) Is the fish community/assemblage of concern fishable? That is, are target fish species sufficiently abundant and of the desired quality? Although the two principal dimensions of quality are body size and contaminant burden, another dimension is the outward appearance of the fish. In particular, are the fish free of parasites or signs of disease?

Although such assessment questions clearly identify many of the major issues with which regional environmental managers might be concerned, such questions generally must be further refined in order to be truly useful and relevant for regional assessments of *fish health*. For example, the format of the following assessment questions would seem to be much more useful to regional environmental managers.

- In what percent of lakes in region A are largemouth bass (or other game species) achieving their expected growth rate?
- In what percent of lakes in region A is the mean size of largemouth bass (or other game species) expected to decrease, increase, or remain unchanged over the next 10 years?
- In what percent of lakes in region A are largemouth bass (or other game species) of legal size exceeding fisheries advisories for mercury, PCB, etc?
- In what percent of lakes in region A is the productivity of largemouth bass (or other game species) expected to decrease, increase, or remain unchanged over the next 10 years?
- In what percent of lakes in region A is the recruitment of largemouth bass (or other game species) not sufficient to maintain the fishery for the next 20 years?

- □ In what percent of wetlands in region A are forage fish (e.g., sunfish, killifish, top minnows, etc) expected to attain body concentrations of mercury, PCB, etc that are known to pose an exposure risk to piscivorous wildlife?
- □ In what percent of wetlands in region A are forage fish (e.g., sunfish, killifish, top minnows, etc.) standing stocks sufficient to maintain expected populations of breeding and non-breeding wading birds?
- □ In what percent of streams in region A are native fish species able to successfully compete (i.e., maintain viable population) with projected program stockings of recreational game fish?
- □ In what percent of streams in region A is the productivity of native fish species expected to be inadequate to support anticipated demand of recreational fisheries?

Given appropriate stressor scenarios, each of these example questions concerns either the expected body sizes of a species, the expected body burdens of a species, the productivity of a given species or community at large, or the expected functional/species diversity of community. Consequently, it is not surprising that important metrics or indicators that have been traditionally used to assess *fish health* include 1) the community's species diversity, 2) the community's total biomass (kg/ha or kg/km), 3) the population density (fish/ha or fish/km) or biomass (kg/ha or kg/km) of the community's dominant species, 4) the age or size class structure of the community's dominant species, 5) levels of chemical contaminants in muscle or whole fish for human or ecological exposure assessments, respectively, and 6) the occurrence of disease or other pathologies.

Many natural and anthropogenic stressors effect these characteristics that, in turn, can effect the growth, reproduction, and survival of the piscivorous wildlife that depend on these resources. Water quality parameters such as temperature, dissolved oxygen, and chemical contaminants directly impact the growth and survival of fish species. Excessive nutrient loads often foster algal blooms that can exhaust the water's dissolved oxygen or produce natural toxins. Excessive sediment loads can cause increased siltation that can diminish the abundance of benthic food resources or benthic habitat required for successful spawning and recruitment. Such sediment loadings can also be the source of particle-bound pesticides and toxics. Dredging and benthic scouring due to increased water flow can increase exposures to toxic chemicals as suspended contaminated sediments re-equilibrate with the water. The destruction of riparian vegetation can increase water temperature and sediment loads and reduce allochthonous resources.

2.1. Ecological Dimensions

Ecological dimensions of fish health can be focused at either the single species, the aquatic community, or the larger, coupled, aquatic-terrestrial ecosystem. At the level of single species, management and public concerns may be focused either on rare, threatened, or endangered species or on indicator species that serve as measurement endpoints for the larger communities or ecosystems in which they live. At the community level, there are several aspects of fish health that may be of concern to decision-makers and conservationists. These include: 1) community species diversity; 2) community functional diversity; 3) the presence or absence of exotic or invasive species; 4) community biomass; 5) community productivity; or 6) multivariate indices of biological integrity. At the level of the coupled, aquatic-terrestrial ecosystem, one may be concerned with the ability of fish communities to provide piscivorous, terrestrial wildlife with adequate food resources.

2.2. Human Use and Health Perspectives

Although public perceptions regarding fish health may have many dimensions, four indicators of good regional fish health would undoubtedly be 1) the absence of fish kills, 2) abundant catches of desirable game fish, 3) frequent catches of trophy size fish, and 4) fish that are sufficiently free of contaminant to be safely eaten.

The North Carolina Division of Water Quality (NCDWQ) has maintained statewide records of fish kills since 1996 (NCDENR 1997b, 1998, 1999b, 2000, 2001). Table 1 summarizes the number and locations of fish kills that the NCDWQ has recorded to date. From 1996 to 1998 fish kills within the Albemarle-Pamlico basin accounted for 29 to 35 percent of the state's total recorded fish kills. However, this percentage has steadily increased such that in 1999, 2000, and 2001 fish kills within the Albemarle-Pamlico basin accounted for 52, 65, and 79 percent, respectively, of the state's recorded kill events. Fish kills are attributed to one of six causes: 1) bycatch related mortality; 2) dissolved oxygen depletion; 3) temperature events; 4) toxic algal blooms; 5) waste spills and pesticide; and 6) unknown. Table 2 summarizes the probable causes of all fish kills as identified by the NCDWQ.

Bycatch is the discarded, non-target fish associated with commercial fishing operations. Decomposition of this high protein organic source can result in not only toxic ammonia concentrations but also low dissolved oxygen concentrations. Dissolved oxygen depletions, in the larger context, can be caused by a wide variety of natural or anthropogenic events. Natural causes include heavy rains during drought or low flow conditions. Such rains can flush excessive organic matter into surface waters that, in turn, triggers increased microbial decomposition. Heavy summer rains, which are often significantly cooler than receiving surface waters, not only can cause the turnover of highly reduced anoxic sediments but also can create inversion layers in ponds and other small impoundments. The cooler surface water in such layers can retard reaeration of the underlying water. Excessive nutrient or organic loadings from urban or agricultural sources can cause dissolved oxygen depletions by increasing algal and bacteria metabolism. In addition to their potential to deplete dissolved oxygen concentrations, certain types of algal blooms can also produce extremely hazardous biotoxins. In the Albemarle-Pamlico basin *Pfiesteria* and *Pfiesteria*-like organisms have been the most notorious algal group in this regard. Temperature-related fish kills may be caused by either exceeding the fish's thermal tolerance limits or as a contributing factor to low dissolved oxygen concentrations.

Table 3 summarizes the fish species that are classified as game species in North Carolina. These species may be the most important indicators of acceptable fish health for many regional anglers and outdoorsmen. Whether such persons practice catch-and-release or fish for harvest, their perception of fish health is undoubtedly based not only on their ability to catch an abundance of reasonably sized fish but also on their ability to frequently catch trophy sized fish. Although the notion of what constitutes a trophy fish certainly varies among anglers, the North Carolina Angler Recognition Program provides statewide guidelines for what is considered a trophy fish by average anglers. See Table 4. It is important to note that simple comparison of Tables 3 and 4 reveals that in North Carolina, trophy fish are not necessarily synonymous with game fish. For example, while not recognized as game species, regionally and locally important food species such as catfish and bowfin are recognized as potential trophy fish. Similarly, rough fish such as carp and gar are also recognized for their trophy potential.

Although catch-and-release angling has become a very large percentage of the total fishing effort for many

large game fish such as largemouth bass and trout, fishing for consumption still dominates the sport. Consequently, if anglers cannot eat their catches due to the presence of excessive toxic chemical concentrations, their perception of the resource's health is greatly diminished even without the occurrence of fish kills or other overt ecological effects. Tables 5 and 6 report the most current statewide fish consumption advisories for North Carolina. As can be clearly seen from these tables, dioxin and mercury are issues for some of the sport fisheries in the Albemarle-Pamlico basin.

Table 1. Summary of reported North Carolina fish kills for 1996-2001 (NCDENR 2001).

Basin	1996	1997	1998	1999	2000	2001
Broad	none	none	none	1	none	none
Cape Fear	21	16	23	14	12	5
Catawba	none	3	1	3	2	4
Chowan	2	2	1	1	none	1
French Broad	none	2	3	1	none	none
Lumber	4	3	5	none	2	none
Neuse	14	12	8	16	23	37
Pasquotank	10	2	8	2	none	1
Roanoke	2	none	1	none	none	none
Tar/Pamlico	3	6	5	11	14	23
Watauga	none	none	none	1	none	none
White Oak	3	3	1	3	3	3
Yadkin/Pee Dee	1	10	2	1	2	3
total kills	60	57	58	54	58	77
total fish killed	NR	91,998	593,545	1,298,472	716,141	1,369,140

Table 2. Suspected causes of North Carolina fish kills for 1996-2002 expressed as a percent of total.

Probable Cause	1996	1997*	1998	1999	2000	2001
Bycatch	?	-	?	4	5	1
Dissolved Oxygen Depletion	?	37	49	30	21	34
Toxic Algal Blooms	?	19	2	11	12	4
Temperature / Other	?	-	2	4	5	9
Waste Spills / Pesticides	?	30	7	15	7	8
Unknown	?	28	40	36	50	46

* Kill events were attributed to 1 or more cause and, therefore, annual column sum is greater than 100%.

Table 3. Fish species or groups recognized as North Carolina inland game fish (NCWRC 2002).

Family	Species
Centrarchidae	Black bass (largemouth, smallmouth and spotted)
	Bluegill
	Crappie (white and black)
	Flier
	Green sunfish
	Pumpkinseed
	Redbreast sunfish (robin)
	Redear sunfish (shellcracker)
	Roanoke bass
	Rock bass
	Warmouth
	All other species of the family
	Clupeidae
Hickory shad, in inland waters	
Esocidae	Chain pickerel (jack)
	Muskellunge
	Tiger musky
	All other species of pickerel
Percichthyidae	Bodie bass (striped bass x white bass)
	Striped bass, in inland waters
	White bass
	White perch, in inland waters
Percidae	Sauger
	Walleye
	Yellow perch
	All other species of perch
	Salmonidae
Mountain trout (including but not limited to brook, brown and rainbow)	
Other marine species in inland waters	Flounder
	Red drum (channel bass, red fish and puppy drum)
	Spotted sea trout

Table 4. Fish species and body sizes recognized by the North Carolina Angler Recognition Program (NCARP), effective July 1, 1997, as a “trophy” fish (NCARP 2002).

Family	Species	Weight	Length	
Amiidae	Bowfin	10 lbs	22”	
Centrarchidae	Bluegill	1 lb	11”	
	Crappie (Black or White)	2 lbs	16”	
	Flier	0.4 lb	8”	
	Green Sunfish	1 lb	9”	
	Largemouth Bass	8 lbs	24”	
	Redbreast Sunfish	1 lb	11”	
	Redear Sunfish	1 lb	11”	
	Roanoke Bass	1 lb	11”	
	Rock Bass	1 lb	11”	
	Smallmouth Bass	3 lbs	19”	
	Spotted Bass	2 lbs	15”	
	Warmouth	1 lb	11”	
	Clupeidae	American Shad	3 lbs	16”
		Hickory Shad	2 lbs	13”
Cyprinidae	Carp	20 lbs	34”	
Esocidae	Chain Pickerel	4 lbs	26”	
	Muskellunge	20 lbs	41”	
Ictaluridae	Blue Catfish	30 lbs	41”	
	Channel Catfish	10 lbs	30”	
	Flathead Catfish	30 lbs	41”	
	White Catfish	4 lbs	21”	
Lepisosteidae	Longnose Gar	10 lbs	48”	
Percichthyidae	Bodie Bass	8 lbs	24”	
	Striped Bass	10 lbs	30”	
	White Perch	1 lb	12”	
	White Bass	2 lbs	17”	
Percidae	Walleye	6 lbs	23”	
	Yellow Perch	1 lb	14”	
Salmonidae	Brook Trout (hatchery)	2 lbs	16”	
	Brook Trout (wild)	0.5 lb	10”	
	Brown Trout (wild)	2 lbs	15”	
	Brown Trout (hatchery)	2.5 lbs	18”	
	Rainbow Trout (wild)	0.75 lb	12”	
	Rainbow Trout (hatchery)	2.5 lbs	18”	

Table 5. North Carolina fish consumption advisories published by the North Carolina Wildlife Resources Commission (NCWRC 2002).

Waterbody	Species	Pollutant	Advisory Description
Albemarle Sound (from Bull Bay to Harvey Point west to mouth of Roanoke and Chowan Rivers)	Carp and Catfish	Dioxins	No consumption by women of childbearing age and children. No more than one meal per month for the general population.
Roanoke River (Hwy 17 in Williamston to the mouth of Albemarle Sound)	Carp and Catfish	Dioxins	No consumption by women of childbearing age and children. No more than one meal per month for the general population.
Welch Creek (Martin, Beaufort, and Washington Counties)	Carp and Catfish	Dioxins	No consumption by women of childbearing age and children. No more than one meal per month for the general population.
Walters Lake (Haywood County)	Carp	Dioxins	No consumption by women of childbearing age and children. No more than one meal per month for the general public.
Pages Lake, Pit Links and Watson Lake (Moore County)	Largemouth Bass.	Mercury	No consumption by women of childbearing age and children. No more than two meals per month for the general population.
Big Creek (Columbus County)	Largemouth Bass and Bowfin (blackfish)	Mercury	No consumption by women of childbearing age and children. No more than two meals per month for the general population.
Waccamaw River (Columbus and Brunswick Counties)	Largemouth Bass and Bowfin (blackfish)	Mercury	No consumption by women of childbearing age and children. No more than two meals per month for the general population.
Ledbetter Lake (Richmond County)	Largemouth Bass	Mercury	No consumption by women of childbearing age and children. No more than two meals per month for the general population.
Lumber River basin (Moore, Hoke, Scotland, Richmond, Robeson, Bladen, Columbus and Brunswick Counties)	Largemouth Bass and Bowfin (blackfish)	Mercury	No consumption by women of childbearing age and children. No more than two meals per month for the general population.
Black Lake (Bay Tree Lake) (Bladen Co)	Largemouth Bass and Bowfin (blackfish)	Mercury	No consumption.
Phelps Lake (Washington and Tyrrell Counties)	Largemouth Bass and Bowfin (blackfish)	Mercury	No consumption by women of child bearing age and children. No more than two meals per month for the general population.
South River (Harnett, Sampson, Cumberland and Bladen Counties) and downstream of South River at the lower part of Black River (Sampson, Bladen and Pender Counties)	Largemouth Bass, Bowfin (blackfish) and chain pickerel	Mercury	No consumption by women of childbearing age and children. No more than two meals per month for the general population.
STATEWIDE	Bowfin (blackfish)	Mercury	No consumption by women of childbearing age, pregnant women and children. No more than two meals per month for the general population.

Table 6. Fish consumption advisories published in North Carolina 305B Report, February 2000 (<http://h2o.enr.state.nc.us/bepu/files/305b/2000AppendixB.pdf>)

Waterbody	Species	Pollutant	Advisory Description
Pigeon River (includes Waterville Lake)	Carp, Catfish	Dioxin	All groups should not consume fish
Belews Lake	Carp, Redear Sunfish, Crappie	Selenium	General Population – 1 meal per week. Children and childbearing women – No consumption
Hyc0 Lake	Carp, White Catfish, Green Sunfish	Selenium	General Population – 1 meal per week. Children and childbearing women – No consumption
Baytree Lake	Largemouth Bass	Mercury	All groups should not consume fish
Ledbetter Lake	Largemouth Bass	Mercury	General Population – 2 meals per month. Children and childbearing women – No consumption
Phelps Lake	Largemouth Bass	Mercury	General Population – 2 meals per month. Children and childbearing women - No consumption
Roanoke River (Williamston to Albemarle Sound)	All fish except herring, shad and shellfish	Dioxins	General Population – 2 meals per month. Children and childbearing women – No consumption
Pages Lake, Pit Links and Watson Lake	Largemouth Bass	Mercury	General Population – 2 meals per month. Children and childbearing women – No consumption
Big Creek (Columbus County)	Largemouth Bass	Mercury	General Population – 2 meals per month. Children and childbearing women – No consumption
Waccamaw River	Largemouth Bass	Mercury	General Population – 2 meals per month. Children and childbearing women – No consumption
Welch Creek	All fish except shellfish	Dioxins	All groups should not consume fish
South River and Black River below South River	Largemouth Bass, Chain Pickerel	Mercury	General Population – 2 meals per month. Children and childbearing women – No consumption
Albemarle Sound (Bull Bay to Harvey Point west to mouth of Roanoke and Chowan Rivers	All fish except herring, shad and shellfish	Dioxins	General Population – 2 meals per month. Children and childbearing women – No consumption
All waters in the Lumber River basin including Pages Lake, Lake Tabor, Lake Waccamaw, Maxton Pond and Johns Pond	Largemouth Bass	Mercury	General Population – 2 meals per month. Children and childbearing women – No consumption
All water of North Carolina	Bowfin	Mercury	General Population – 2 meals per month. Children and childbearing women – No consumption

2.3. Stressors

Fish assemblages are influenced by biological processes, environmental factors, and anthropogenic stressors. Biological processes influencing fish assemblages include autoecology, density-dependent interactions of individuals, and competitive interactions among species. Environmental factors affecting fish assemblages include hydrology and physico-chemical habitat. Biological processes and environmental factors determine the structure of fish assemblages in the absence of anthropogenic stressors. Anthropogenic stressors, such as sediment and hydrologic and habitat alteration, can have profound effects at the level of the assemblage. Because of the complexity of influences structuring fish assemblages, mathematical models have been used to gain better understanding. The influence of biological processes, environmental factors, and anthropogenic stressors on fish assemblages, and the uses of mathematical models to integrate these influences are discussed below.

In the absence of anthropogenic stressors, biological processes and environmental factors structure assemblages. Patterns of diversity and the relative abundances of populations in assemblages are thought to be determined by temporal and spatial heterogeneity in environmental factors (Townsend 1989, Reice 1994). Although this hypothesis is generally supported by field studies (Grossman et al. 1982, Rahel et al. 1984, Yant et al. 1984, Jackson et al. 1992, Grossman et al. 1998), other studies have demonstrated that biological processes, in particular species interactions, may at least in part determine the structure fish assemblages (Tonn et al. 1986, Taylor 1996). The relative importance of the influence of biological processes and environmental factors in structuring assemblages remains an open question. Because community structure appears to differ between regions (Hawkes et al. 1986, Whittier et al. 1988, Angermeier and Winston 1999), the answer may vary with region (Matthews 1998).

2.3.1. Disruption of Nominal Biological Processes

The abundance of a fish species is determined in part by autoecological processes including feeding, reproduction, movement, and survival. Fish species display a wide range of feeding and reproductive behaviors (Allan 1995) that are alternatively favored in different environments, leading to difference species abundances among these environments (Karr 1981). Movement, as determined by species-specific stream fish dispersal abilities (Hill and Grossman 1987, Gatz and Adams 1994) in relation to the number, type, and proximity of suitable habitats (Schlosser 1995), controls the number of individuals immigrating to these habitats. Survival of specific age classes, which may be controlled by tolerances to environmental factors such as temperature, oxygen, and acidity, will also affect fish abundances (Matthews 1998).

The abundances of stream fish populations are also influenced by density-dependent interactions among individuals. Density-dependence is the dependence of per capita growth rate on present and/or past population densities, where growth rate typically declines with increasing density as a result of resource limitation. Although it is unlikely in most stream fish populations that juveniles interact strongly with adults due to differences in resource use between these life stages (Lobb and Orth 1991), three types of density-dependent limitation are possible in fish populations: juvenile survival rate may exhibit a density-dependent response to juvenile density (Shuter 1990), and

adult density may have a negative effect on either adult fecundity (Shuter 1990) or adult survival rate (Grossman and Ratajczak In review). It is likely that most populations are regulated biologically by some form of density-dependence (Cappuccino 1995).

The nature and strength of species interactions may also affect species abundance and diversity. Competition may occur among stream fishes for habitat or food (Matthews 1982), and can limit summer growth, pre-winter size, and potentially winter survival in juvenile fishes (Schlosser 1987), which in turn determine abundance. Competition can also prevent the coexistence of species that experience strong interactions, such that similar species will exhibit negative covariation in abundance or presence over time (e.g., Winston et al. 1991). Competition may limit the set of species that can coexist in an assemblage to those that use different sets of resources. Fish species that do coexist typically exhibit resource partitioning (Lobb and Orth 1991, Johnson et al. 1992). Predation of larger fishes on smaller fishes has the direct effect of reducing prey population, and can also produce indirect effects through food web interactions (Allan 1995).

2.3.2. Alteration of Physical Habitats

Fish assemblages are also affected by physical and chemical factors that determine habitat quality and availability. Stream size, as determined by drainage area and channel width, controls characteristics such as canopy cover and organic input (e.g., Vannote et al. 1980). The stability and complexity of the substrate influences all aquatic biota, in particular the invertebrates that serve as food for most stream fishes (Allan 1995). In-stream temperature affects winter survival and fecundity of fishes, particularly in north-temperate areas (Lyons 1996, Donald 1997, Hurst and Conover 1998). Physical characteristics, such as suspended sediment, have also been related to fish assemblage composition (Goldstein et al. 1996, Bilger and Brightbill 1998). In-stream chemical factors, such as oxygen and acidity, can also influence assemblages (Allan 1995).

Stream fish assemblages are influenced by hydrology. Current velocity may determine energetic costs of maintaining position, thereby affecting energy stores and survival (Facey and Grossman 1992). Flow and the flooding regime may determine habitat availability (Grossman and Ratajczak In review), spawning success, and larval abundance (Pearsons et al. 1992, Johnston et al. 1995) for fishes. Flow variability has also been related to fish assemblage structure. For example, Chipps et al. (1994) and Poff and Allan (1995) demonstrated differences in trophic compositions of fish assemblages between more and less variable streams. Yearly variability in flow has also been related to compositional differences through time for a single site (Strange et al. 1992).

2.3.3. Chemical Contaminants

2.3.3.1. Water Quality Issues

During 1992-1995 the USGS analyzed for 47 different pesticides in surface-water samples across the Albemarle-Pamlico basin. Of these, 45 pesticides were detected. Twenty-one streams had detectable concentrations of 1 to 5 pesticides, 30 streams had detectable concentrations of 6 to 20 compounds, and 4 streams, all in the Tar River basin, had detected concentrations of 20 or more pesticides. Metolachlor, atrazine, prometon, and alachlor

were detected in 80, 69, 60, and 63 percent, respectively, of 233 stream samples from 65 sites in the Albemarle-Pamlico basin. Sixteen pesticides, including four insecticides (carbaryl, carbofuran, ethoprop, and diazinon) were measured at concentrations greater than 0.1 µg/L. (USGS 1998).

Herbicides were generally detected during the spring and summer months. Concentrations of several pesticides, including atrazine and metolachlor, were elevated immediately after application in March and April. These concentrations peaked in June and July and then dissipated to low values or the detection limit for most of the year. These data suggested that drinking-water standards for pesticides are most likely to be violated during May through July. An additional concern in this regard, however, was the fact that drinking water or aquatic life standards only existed for only about 50 percent of the compounds detected (USGS 1998).

2.3.3.2. Sediment Quality Issues

As part of the USGS pesticide study discussed above in Section 2.3.3.1, the USGS also analyzed sediments for a wide variety of organochlorines, semivolatile organic compounds (SVOCs), and trace elements. In 1992, streambed sediments were collected at 22 stations and analyzed for 35 organochlorine pesticides, 63 semivolatile compounds, and 44 major, minor, and trace elements (Woodside and Simerl, 1996). DDT, DDD, and DDE were detected in 27, 40, and 63 percent, respectively, of the samples analyzed. Additionally, dieldrin and chlordane were detected in 18 and 9 percent, respectively, of the samples tested.

2.3.4. Landscape and Non-point Source Issues

Land development in a watershed is reflected in the diversity and composition of fish assemblages (e.g., Karr 1981, Paller et al. 1996, Scott and Hall 1997). Species diversity typically decreases with an increase in land development (Karr 1981). A commonly-observed trend in trophic structure is a decrease in insectivores and an increase in omnivores, which are better adapted to feeding in disturbed conditions (Karr et al. 1986). The assemblage may also show shifts in taxonomic composition in response to land development, such as a decrease in minnows, darters, sunfish, or suckers (Karr et al. 1986). Although certain regularities regarding how fish metrics change with land-use have been demonstrated for many geographic regions (e.g., Karr 1981, Angermeier and Schlosser 1987, Leonard and Orth 1988, Miller et al. 1988, Hughes et al. 1998), the nature of the change varies with region (Smoger and Angermeier 1998).

Scientists recognize that fish assemblages in developed watersheds are affected primarily by nonpoint source anthropogenic stressors that result from land use development, in particular altered hydrologic regimes, sedimentation, and habitat degradation (Williams et al. 1989, Richter et al. 1997, Wilcove et al. 1998). Alteration of hydrologic regimes, in terms of the amount and variability of flow affect all aspects of fish life history (e.g., Allan 1995). Sedimentation can increase fish movement, interfere with fish feeding by reducing reactive distance for sight-feeders and lowering the abundance of insects available as food, and impair reproduction of fishes with specific spawning habitat requirements (Newcombe and MacDonald 1991, Bergstedt and Bergersen 1997). Habitat destruction can isolate patches of suitable habitat within a stream, which reduces species' survival. Habitat destruction also changes the natural mosaic of habitat conditions, thereby altering natural fish movement and migration patterns (Reeves et al. 1995).

The response of fish assemblages to anthropogenic stressors in a given region is determined by the interaction of the stressors with the biological processes and environmental factors at these sites, although the mechanism by which this occurs is not well understood. The assemblage response may simply be the net effect of individual autoecological responses to stressors (e.g., Karr 1981). However, the effects of stressors on individuals may be altered by biological processes. For example, Shuter (1990) showed that the effect of stressors in a fish population dynamics model depends on where in the life cycle a population is regulated in density-dependent fashion, and Jaworska et al. (1997) showed that incorporating species interactions in a fish population model distorted the stressor response patterns predicted at the population level. The response may also be due to the shifting in importance of environmental factors compared to biological processes, for example, an increase in density-independent environmental factors could outweigh the counteracting biological process of density-dependence (Turchin 1995, Hayes et al. 1996). A better understanding of how biological processes, environmental factors, and anthropogenic stressors interact to determine fish assemblage structure in specific regions would be of importance to management.

3. Description of the Albemarle-Pamlico Basin

3.1. Site Description

The Albemarle-Pamlico drainage basin is located in southern Virginia, continuing south into north-central and eastern North Carolina. The entire basin encompasses approximately 28,000 square miles and includes the Chowan, Roanoke, Tar-Pamlico, and Neuse River basins (McMahon and Lloyd 1995). See Figure 3. Four physiographic provinces are present within the basin: Ridge and Valley, Blue Ridge, Piedmont, and Coastal Plain (Fenneman 1938). Topography ranges from mountains in the west to very flat areas in the east. Along with topography, a temperature gradient runs west to east with increasing average annual temperatures occurring over the lower eastern elevations (McMahon and Lloyd 1995). Table 7 summarizes basic statistics for each of the four Albemarle-Pamlico river basins.

Land use across the basin is divided into the following categories: 50% forested, 30+% agricultural, 15% wetlands, and <5% urban/developed (McMahon and Lloyd 1995). Land use may be described as a mosaic of these categories across the basin. Agriculture and wetlands, however, are more prevalent in the east and forested lands are typically dominant in the west. Agriculture within the basin introduces high concentrations of fertilizers, pesticides, sediments, and animal wastes into the environment. Portions of the Tar-Pamlico and Chowan River basins have been designated as ‘nutrient sensitive waters’; the Chowan and Neuse River basins are the most heavily impacted by pesticides (McMahon and Lloyd 1995). Sediment loading is typically higher in areas of high relief. The level of non-point source pollutants entering the surface and ground water systems is dependent upon the crops grown, animals raised, tillage practices, waste storage facilities and the climate, slope, soils, and drainage conditions of the watershed. For a detailed description of land use, population demography and non-point source pollution in the basin, please read McMahon and Lloyd (1995) and Harned et al. (1995).

The Chowan River basin is located in the coastal plain of northeastern North Carolina and southeastern Virginia. In North Carolina the basin encompasses all or parts of Bertie (30%), Chowan (67%), Gates (80%), Hertford (100%), Northampton (65%), Perquimans (0.03%), and Washington (0.01%) Counties. The Chowan River is formed by the confluence of the Nottoway and Blackwater Rivers at the Virginia and North Carolina state line. Whereas in North Carolina the drainage of the basin is 1,315 square miles, in Virginia the drainage area of the basin is 3,575 square miles. The two major tributaries of the Chowan River are the Meherrin River and its largest tributary, Potecasi Creek, and the Wiccacon River and its largest tributary, Ahoskie Creek (NCDENR 2002a, e).

The Neuse River basin originates in the northern Piedmont region of North Carolina and terminates into the Pamlico Sound. The drainage area of the basin is 6,192 square miles, making it the third largest river basin in North Carolina. The basin itself is one of only three major North Carolina river basins whose boundaries are located entirely within the state. Within the basin, there are 3,293 miles of freshwater streams and thousands of acres of freshwater impoundments. The basin encompasses all or part of the following counties: Beaufort (2.1%), Carteret (50%), Craven (95%), Duplin (0.16%), Durham (73%), Edgecombe (0.36%), Franklin (10%), Granville (25%), Greene (100%), Harnett (0.02%), Hyde (0.02%), Johnston (98%), Jones (81%), Lenior (99%), Nash (20%), Onslow (1.2%), Orange (49%), Pamlico (83%), Person (32%), Pitt (42%), Sampson (0.79%), Wake (85%), Wayne (91%),

and Wilson (81%). Major tributaries of the Neuse River include: Crabtree Creek, Swift Creek, Little River, Contentnea Creek, and the Trent River (NCDENR 2002b, e).

The Roanoke River basin originates in north central North Carolina and south central Virginia and terminates into the Pamlico portion of the Tar-Pamlico river basin. The drainage area of the basin in North Carolina is 3,493 square miles. Major tributaries of the Roanoke River in North Carolina include the Mayo, Dan and Cashie rivers and the Smith, Country Line, Sweetwater and Conoho creeks. The total stream miles of the basin in North Carolina is 2,414. In Virginia the drainage area of the basin is 6,382 square miles. Whereas major tributaries in the northern section of the basin are the Little Otter, Big Otter, Blackwater and Pigg Rivers, major tributaries in the southern portion of the basin include the Dan River, Smith River, and Banister River. Whereas in North Carolina the basin encompasses all or parts of the following counties: Alamance (0.13%), Beauford (0.91%), Bertie (70%), Caswell (90%), Edgecombe (0.07%), Forsyth (21%), Granville (33%), Guilford (1.7%), Halifax (40%), Martin (75%), Northampton (35%), Orange (2.4%), Person (60%), Rockingham (81%), Stokes (85%), Surry (2.7%), Vance (52%), Warren (38%), and Washington (13%), in Virginia the basin includes all or parts of the following 16 counties: Appomattox, Bedford, Botetourt, Brunswick, Campbell, Carroll, Charlotte, Floyd, Franklin, Halifax, Henry, Mecklenburg, Montgomery, Patrick, Pittsylvania, and Roanoke (NCDENR 2002c, e).

The Tar-Pamlico River basin, which like the Neuse River basin is entirely contained within North Carolina, encompasses all or part of the following counties: Beauford (97%), Carteret (1.5%), Cavern (0.63%), Dare (11%), Edgecombe (99%), Franklin (90%), Granville (43%), Halifax (60%), Hyde (91%), Martin (25%), Nash (80%), Pamlico (17%), Person (7.8%), Pitt (58%), Tyrrell (0.28%), Vance (48%), Warren (62%), Washington (19%), and Wilson (19%) (NCDENR 2002e).

Table 7. Summary Statistics for the Albemarle-Pamlico major basins (NCDENR 2002e)

Basin	Population	Density inds/mi ²	Area (mi ²)	Stream Miles	% of State Stream Miles	Stream Mile to Area Ratio	Impaired Stream Miles	% Stream Miles Impaired
Chowan	62,474	48	1,378	788	2.1	0.57	132	75
Neuse	1,015,511	181	6,235	3,440	9.1	0.55	454	33
Roanoke	263,691	107	3,503	2,389	6.3	0.68	168	23
Tar-Pamlico	364,862	80	5,571	2,335	6.2	0.42	53	9

Population estimates based on 1990 census.

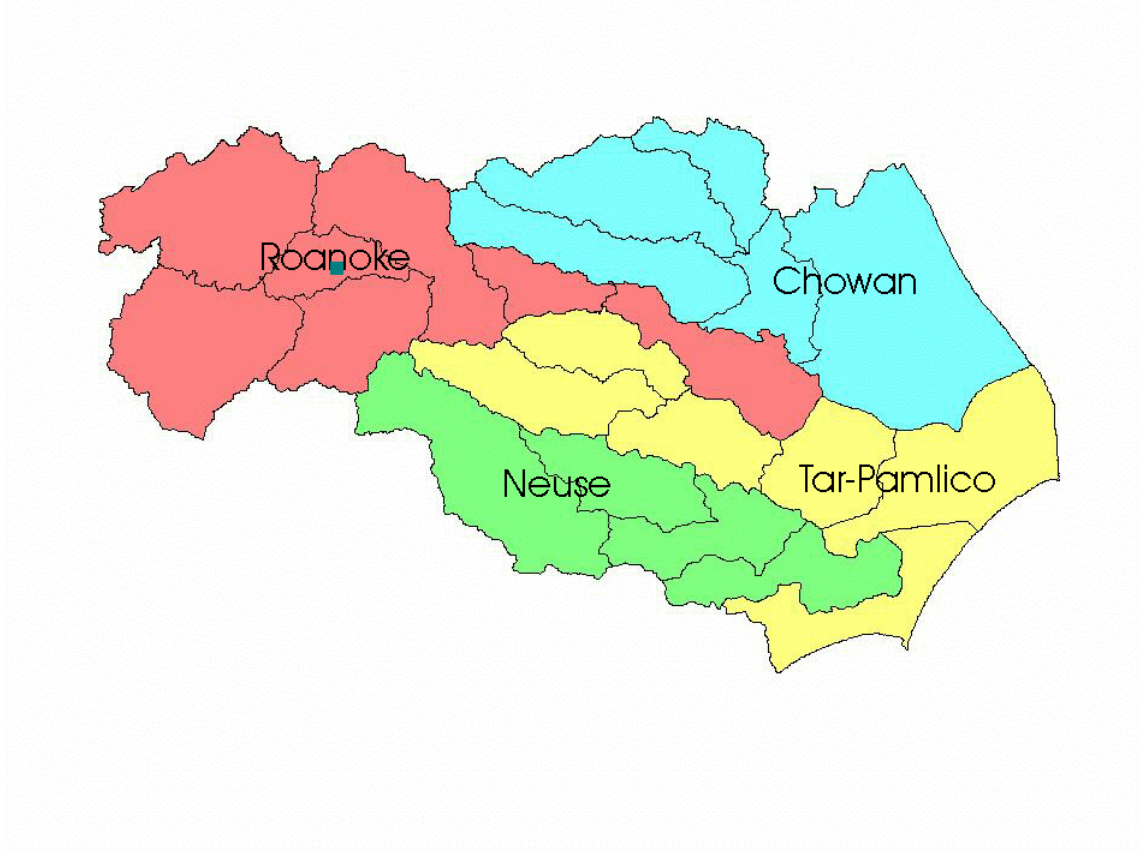


Figure 3. Major river basins and 8-digit HUC watersheds of the Albemarle-Pamlico basin.

3.2. Socio-economic Development

3.2.1. Urban Development

The Chowan River basin approximately 0.9% of North Carolina's total population. The basin's population growth is low to moderate, with most growth occurring around the larger municipalities and in the vicinity of the lower Chowan River. Murfreesboro, Ahsoskie, and Edenton are the largest urban areas in the basin. Rural areas within the basin, however, are declining in population. Based on projections from 1990 to 2020, Chowan and Gates Counties are expected to increase by 17% and 19%, respectively. Populations in Bertie, Hertford, and Northampton Counties, however, are expected to decrease by 1 to 10% (NCDENR 2002a, e).

The Neuse River basin contains approximately 15.3% of North Carolina's total population. Not only is the Neuse River basin the most populated of the four Albemarle-Pamlico basins, but it also the most densely populated. Based on 1987 estimates, approximately 5.1% of the Neuse River basin is urban development with most of this development being concentrated in the upper basin around Raleigh, Durham, Cary and Garner (NCDENR 2002b).

Projected population growths from 1990 to 2020 for counties completely or partially contained within the basin are as follows: Beaufort (8.1%), Carteret (43%), Craven(25%), Durham (35%), Edgecombe (-0.8%), Franklin (63%), Granville (32%), Greene (21%), Johnston (72%), Jones (-0.6%), Lenior (2.8%), Nash (40%), Onslow (33%), Orange (50%), Pamlico (15%), Person (21%), Pitt (46%), Sampson (17%), Wake (101%), Wayne (19%), and Wilson (9.3%)(NCDENR 2002e).

The Roanoke River basin contains approximately 4.0% of North Carolina's total population. Projected population growths from 1990 to 2020 for the North Carolina counties completely or partially contained within the basin are as follows: Beaufort (8.1%), Bertie (-1.0%), Caswell (3.3%), Forsyth (23%), Granville (32%), Guilford (27%), Halifax (8.3%), Martin (2.0%), Northampton (-9.6%), Orange (50%), Person (21%), Rockingham (7.5%), Stokes (41.7%), Surry (18%), Vance (13%), Warren (14%), and Washington (-15%) (NCDENR 2002e).

The Tar-Pamlico River basin contains approximately 5.5% of North Carolina's total population. Although the basin is the second most populated basin within the Albemarle-Pamlico region, its population density is moderate compared to the other basins. Fishing, farming, forestry, and phosphate mining are the most important economic activities in the basin, with agriculture and forest cover each accounting for slightly over 40% of the total land area. Projected population growths from 1990 to 2020 for counties completely or partially contained within the basin are as follows: Beaufort (8.1%), Dare (78%), Edgecombe (-0.8%), Franklin (63%), Granville (32%), Halifax (8.3%), Hyde (-18%), Martin (2.0%), Nash (40%), Pamlico (15%), Person (21%), Pitt (46%), Vance (13%), Warren (14%), Washington (-15%), and Wilson (9.3%) (NCDENR 2002e).

3.2.2. Agricultural Patterns and Issues

Approximately 87% of the land cover in the Chowan River basin is either forest or agriculture. However, from 1982 to 1992, the most significant changes in land cover was the urban/built-up category that increased by 59%. This increase was matched by reductions in forested land (-1%), cultivated cropland (-2%), and pastureland (-23%) and by a slight increase in uncultivated cropland. Swine production has increased significantly from 1990 to 1994 in the upper portion of the Chowan River in North Carolina (327% increase) and the Meherrin River and tributaries (446% increase) (NCDENR 2002a). While the largest cash crop in the basin is peanuts, sorghum, corn, tobacco and potatoes are also important agricultural interests (NCDENR 1997a)

Based on 1987 satellite imagery provided by the North Carolina Center for Geographic Information and Analysis (CGIA), agriculture and forestry accounts for 34.7% and 33.9%, respectively, of the land area in the Neuse River basin. Wetlands and open water (including the Neuse estuary and large impoundments) account for another 20% of the basin's surface area (NCDENR 2002b).

In North Carolina, forested and agricultural land covers account for 61% and 25%, respectively, of the Roanoke River basin. The most dramatic recent changes within the basin occurred from 1982 to 1992 when uncultivated cropland and urban covers increased approximately 60% and 54%, respectively (NCDENR 1996).

3.3. Regional Climate

The mean annual temperature for the Albemarle-Pamlico basin is approximately 52 degrees Fahrenheit. There is a reasonably constant east-west gradient across the coastal plain and piedmont portions of the basin with the southeastern coastal plain area having a mean annual temperature of slightly more than 62 degrees Fahrenheit. This temperature gradient increases by a factor of about four in the Blue Ridge Mountains. The basin's mean annual rainfall also varies on an east-west gradient with the southeastern coastal plain and middle piedmont receiving mean annual rainfall of 52 inches and 44 inches, respectively. The rainfall pattern in the upper piedmont and mountains, however, is much more complex with annual rainfalls varying from 36 to 52 inches. Patterns in temperature and plant growth are such that approximately $\frac{2}{3}$'s of the basin's annual rainfall is evaporated or transpired annually (McMahon and Lloyd 1995).

3.4. Regional Hydrology

3.4.1. Surface Water Hydrology

Only 12 to 18 inches of the basin's annual rainfall enters the Albemarle-Pamlico Sound as streamflow. Of this amount, only about a $\frac{1}{3}$ (approximately 5 inches) represents overland runoff. The remaining $\frac{2}{3}$'s (approximately 11 inches) is ground water baseflow. This fact is reinforced by the observation that long term average monthly streamflows are relatively independent of long term monthly rainfalls (McMahon and Lloyd 1995). Average contributions of ground water to subbasin streamflow are estimated to be 45-53%, 48-58%, 49-57%, and 61-64% for the Neuse River, Chowan River, Tar-Pamlico River, and Roanoke River basins, respectively (McMahon and Lloyd 1995).

3.4.2. Ground Water and Regional Geomorphology

The movement of water carrying dissolved nutrients and chemicals from the land surface, through the subsurface, and into stream channels is an important influence on most measures of fish health. The influence of subsurface baseflow contributions on fish health is especially pronounced within Atlantic coastal plain watersheds, where highly permeable, unconsolidated and poorly-consolidated sedimentary deposits transmit significant quantities of precipitation recharge through the subsurface. In the Albemarle-Pamlico basin, it's estimated that more than 70% of the streamflow in surface water drainages originates from groundwater (McMahon and Lloyd 1995).

Considering the large proportion of streamflow in the Albemarle-Pamlico basin that derives from subsurface baseflow, it's evident that the accuracy of fish health assessments partly hinges on how well we can predict baseflows and their associated nutrient and chemical loadings. Unlike baseflow predictions, however, subsurface nutrient and chemical load predictions strongly depend on the local arrangement of geologic heterogeneities in space. Accurate load predictions thus require that small-scale geologic variability be characterized. As an alternative to high-cost, disruptive, and incomplete sampling of small-scale heterogeneities, it is proposed that subsurface geologic structure beneath the Atlantic coastal plain be inferred using standard gaussian geostatistical techniques and fairly well understood principles of geology.

3.4.2.1. Effects of Geologic Heterogeneities on Solute Transport

While the rate at which water moves through the subsurface is strongly influenced by the spatial arrangement of geologic heterogeneities, the influence of geologic structure is even greater for the case of transport of dissolved chemical species. This extreme sensitivity of solute transport to the distribution of heterogeneities can be traced to the hyperbolic structure of the advection-dispersion equation, which governs the movement of dissolved solutes through porous media. For a conservative solute not subject to sorption or chemical transformation, subsurface movement of solute dissolved in groundwater is governed by the following partial differential equation:

$$\frac{\partial c}{\partial t} = D \nabla^2 c - \mathbf{v} \frac{\partial c}{\partial l} \quad (1)$$

where c is solute concentration, t is time, D is a diffusion coefficient tensor, and \mathbf{v} is average groundwater velocity along direction l .

The first term on the right side of the equation relates to molecular diffusion and small-scale hydrodynamic mixing effects, and is typically negligible compared to the second, advective term. Sensitivity of solute transport to the local distribution of heterogeneities arises from this second term, which describes transport occurring at the same rate and direction as groundwater moves. Figure 4 illustrates how field-scale variations in hydrogeologic properties like hydraulic conductivity (K), caused by the presence of subsurface geologic heterogeneities, can control patterns of both ground water flow and advective movement of dissolved nutrient and chemicals.

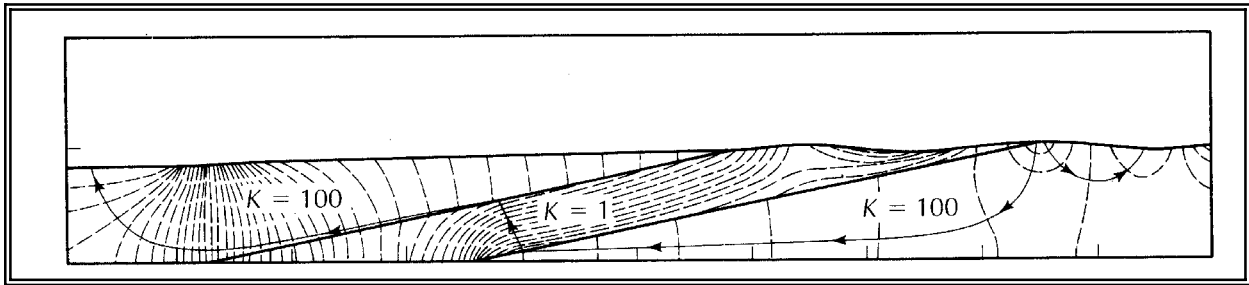


Figure 4. Advective movement of dissolved nutrients and other chemicals through subsurface heterogeneities.

As water flows through the subsurface, it tends to take shorter flowpaths through low-permeability geologic facies and longer flowpaths through highly permeable geologic units. The dominance of advective mechanisms of transport, coupled with the fact that the geometry of advective movement is strongly influenced by the spatial distribution of high- and low-permeability materials, suggests that the single most dominant factor influencing subsurface transport at field and regional scales is the manner in which geologic heterogeneities are arranged in space.

Given this strong dependence of subsurface flow and transport patterns on the spatial arrangement of geologic heterogeneities, accurate prediction of solute transport requires that we characterize all subsurface heterogeneities that may influence advective transport. However, due to the high costs and extreme invasiveness associated with measurement of geologic properties, characterization of all heterogeneities that may influence subsurface transport of nutrients and chemicals is not a realistic option. Instead, we can utilize geologic principles to infer deterministic subsurface geologic statistics, using concepts borrowed from architectural element analysis.

Architectural element analysis relies on descriptions of lithofacies composition, external shape, and internal geometry to identify suites or assemblages of lithofacies unique to a particular depositional setting. In the architectural element classification scheme, depositional units within a package of genetically-related deposits represent primary building blocks that can be physically separated from one another according to a hierarchy of bounding surfaces. Moreover, there is a distinct signature associated with small-scale geologic variability occurring within each unit.

Figure 5 presents a number of genetically-related depositional units commonly encountered in braided-stream environments, based on the classification of Miall (1985). Miall's suite of eight architectural elements for braided-stream environments may provide a sound basis for identifying and classifying subsurface geologic architectures in a wide variety of other depositional environments, including glacial, eolian, lacustrine, deltaic, marine, estuarine, and tidal-flat depositional settings. Of particular interest are sedimentary architectures associated with inner continental shelf and marginal marine deposits, such as those observed within the North Atlantic coastal plain.

3.4.2.2. Coastal Plain Geology

The coastal plain represents the emergent part of a 150-300 m wide belt of Mesozoic and Cenozoic highly-permeable, poorly-indurated sedimentary rock lying between the Piedmont Physiographic Province of the Appalachian Mountains and the north Atlantic coastline, and extending 2400 miles from Florida to the Grand Banks of Newfoundland. Figure 6 illustrates how the coastal plain and the continental shelf represent a single physiographic feature along the margins of the North American continent, separated from the ocean floor by a sharp break known as the continental slope.

Sediments underlying the Atlantic coastal plain were eroded from the Appalachian Highlands to the west, and transported to the continental margins primarily by streamflow. These sediments were subsequently reworked by widespread cyclic transgression and regression of the ocean to produce marginal marine and inner continental shelf deposits. Transgression and regression of the shoreline throughout geologic time has resulted in both vertical aggradation and seaward lateral progradation of sediments, producing a regional coastward-dipping and -thickening homoclinal wedge of unconsolidated and consolidated rocks. A typical regional cross-section of rocks underlying the Coastal Plain is shown in Figure 7. To the east of the Fall Line, the Albemarle-Pamlico basin is underlain by shallow unconsolidated sands and gravels and deeper semiconsolidated sands. Total thickness of these deposits increases from zero near the Fall Line to 10,000 ft along southern NJ and eastern NC. Superimposed on the regional marine sequences are shallow deltaic and fluvial deposits produced by continued transport and reworking of sediment from the continental interior by water. To the west of the Fall Line, the basin is underlain by NE-SW trending belts of metamorphic rock associated with the Appalachian orogeny.

As a consequence of the downdip thickening associated with the coastal plain sediments, many subsurface units beneath the coastal plain have no surface equivalents that can easily be studied. Instead, subsurface geologic structure must be inferred based on our understanding of the depositional setting that likely prevailed over the coastal plain throughout geologic time.

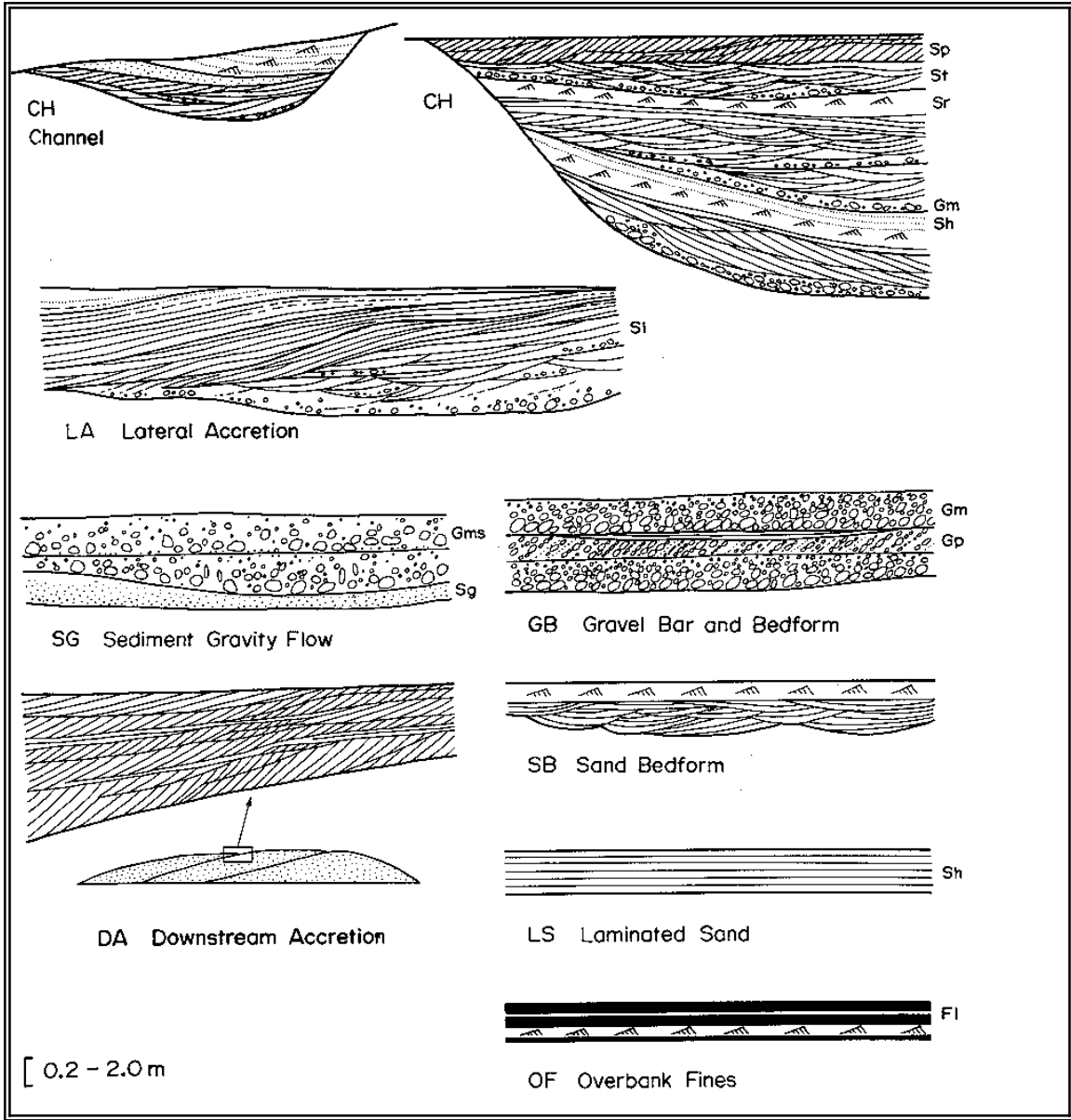


Figure 5. Architectural elements in a braided-stream depositional environment (modified from Miall 1985)

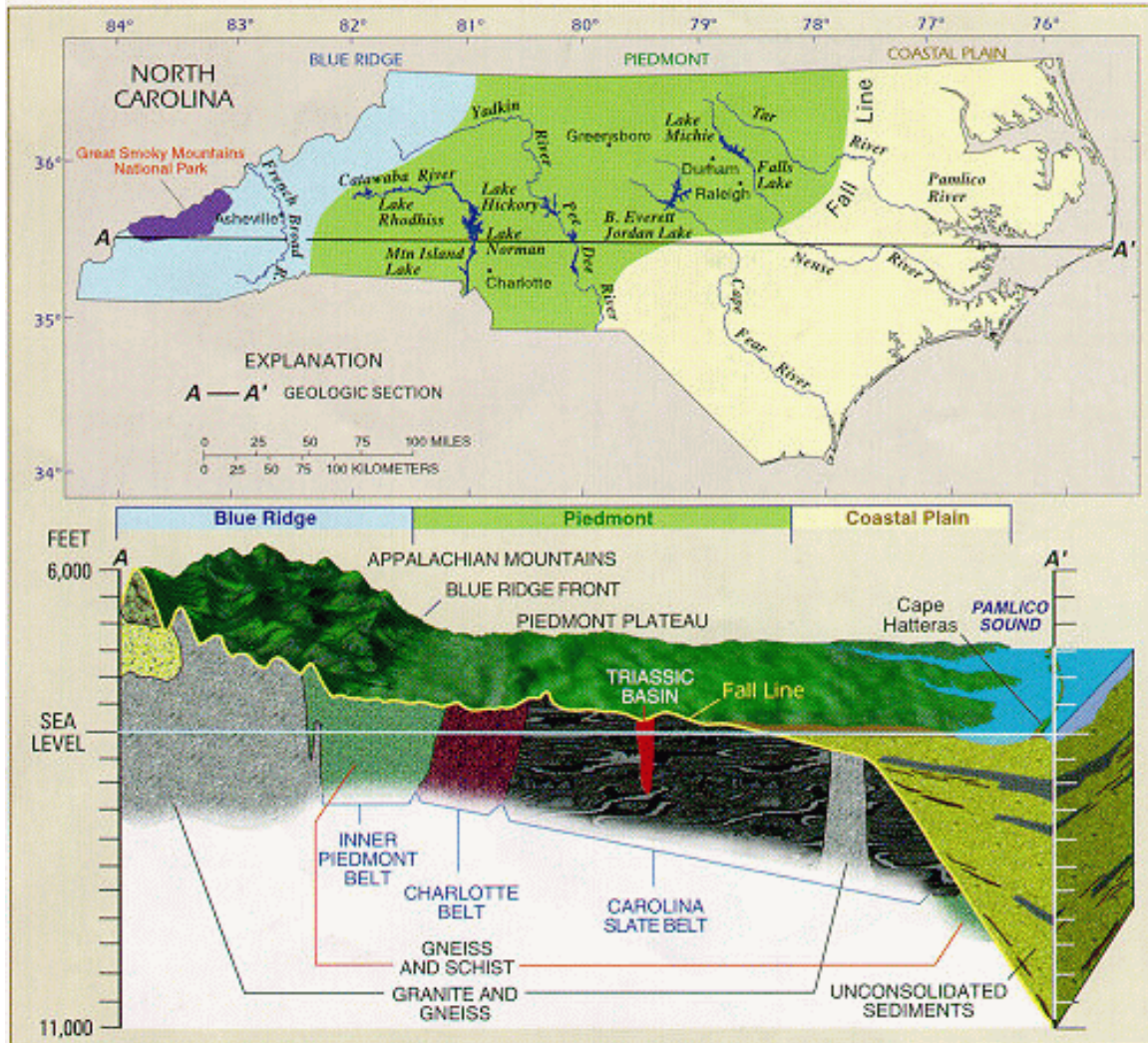


Figure 7. Regional geologic section (from <http://sgil.dnrcrlg.er.usgs.gov/albe-html/Maps>)

3.4.3. Riparian and Wetland Issues

Riparian areas are ecotones that occur at the interface between terrestrial and aquatic environments. Gregory et al. (1991) further defines riparian areas as three-dimensional zones of interaction between terrestrial and aquatic environments that extend horizontally to the limits of the flood plain and vertically into the canopy of near stream vegetation. Riparian areas exist across the United States and encompass a wide variety of vegetation types including grassland, shrubs and forests. Because of their widespread occurrence along small, first order streams to large lowland rivers, riparian ecosystems exhibit a high degree of variability across the landscape. Within riparian areas, topography, hydrology, soils, and plant communities may change rapidly across short distances thus making riparian habitats one of the most diverse and challenging systems to study. However, within this context of diversity, there are certain environmental conditions that are fairly common to riparian ecosystems.

Due to their proximity to the stream or river channel, riparian ecosystems experience repeated disturbances from mild to extreme flooding events. Several studies have linked high plant species-richness in riparian areas to the frequent occurrence of flooding within these ecosystems (Gregory et al. 1991, Planty Tabacchi et al. 1996). However, other studies have found a reduction in plant species-richness following repeated flooding events that skew the plant community towards species that are tolerant of frequent disturbances by floods (Denslow 1985, Wardle et al. 1997). Thus, increased plant species-richness is likely to occur in areas of only low to moderate disturbance and within riparian areas possessing a mosaic of soil types and topographical conditions (Nilsson et al. 1994, Planty Tabacchi et al. 1996, Everson and Boucher 1998). Diversity in land form, soil type, and community composition are defining characteristics of riparian habitats, making them valuable to both terrestrial and aquatic environments.

For example, riparian forests are particularly important for maintaining stream water quality and habitat generation for aquatic and terrestrial organisms. Riparian areas modify hydrology by absorbing and storing rainfall and runoff and filtering surface and subsurface water destined for the stream/river channel or ground water aquifer (Brinson et al. 1981, Gregory et al. 1991, Sharitz et al. 1992). Riparian areas also generate complex aquatic and terrestrial habitats. Collares-Pereira et al. (1995) found that riparian vegetation cover was one of the most important variables affecting fish distributions within Portuguese lowland streams. Riparian areas also alter light regimes and contribute particulate organic matter to the aquatic system that may serve as food or habitat for aquatic flora and fauna (Brinson et al. 1981, Gregory et al. 1991, Sharitz et al. 1992). Finally, riparian areas protect the stream bank from erosion by slowing water flow rates and securing stream bank soils. Thus, riparian areas typically improve water quality and maintain stream habitats over the short and long term.

Riparian areas also affect biogeochemistry within the watershed. Early studies of the importance of riparian areas focused upon the role of riparian buffer zones in intercepting runoff, dissolved nutrients and sediment (Karr and Schlosser 1978, Verry and Timmons 1982, Lowrance et al. 1984). Several studies have found that highly effective riparian areas were comprised of a combination of grass or herbaceous vegetation along the outer limits of the flood plain and immature forests immediately adjacent to the stream channel (Lowrance et al. 1984, Bosch et al. 1994). For example, Peterjohn and Correll (1984) found that riparian buffer zones intercepted 4.1 mg sediment and 11 kg organic N, 0.83 kg ammonium-N, 2.7 kg nitrate-N and 3 kg phosphate bound to sediment per ha of riparian forest, annually. Unfortunately, across the United States, only approximately 40% of the watersheds have forested riparian areas whereas an equal number of watersheds have little or no forest cover, and nearly 10% are completely urban (Jones et al. 1997). Therefore, under typical conditions, it is unlikely that the majority of riparian areas will be able to function in an ideal manner. The use of the REMM model to analyze the function of riparian areas within the Albemarle-Pamlico drainage basin will illustrate the importance of forested riparian buffer systems to water quality and fish health as well as stressing the importance of riparian habitat characterization for future modeling efforts.

3.5. Water Quality Issues

Nutrient enrichment is a primary water quality concern in the Chowan River basin. With the implementation of the Nutrient Sensitive Waters (NSW) management strategy, however, nutrient loads have been reduced, and algal blooms have been less frequent and shorter in duration. Implementation of agricultural nonpoint

source control measures through the Agricultural Cost Share Program had reduced North Carolina's total phosphorus input by 6% (DEM, 1990). Many point source discharges in the basin have also altered their operations to reduce their nutrient loads to the surface waters. Consequently, since 1990, the nitrogen reduction goal of 20% had been accomplished and total phosphorus had been reduced by 29% (goal of 35%) (NCDENR 2002a).

Fish consumption advisories for dioxin remain in effect for the Chowan River from the Virginia border to Albemarle Sound. The primary source of dioxins in the Chowan River is believed to be the Union Camp Fine Paper mill in Franklin, VA. This advisory currently recommends that the general population consume no more than two meals of any fish except herring, shad (including roe), or shellfish in one month and that children and child-bearing women consume no fish until further notice. See Tables 5 and 6. Annual monitoring by Union Camp, however, does indicate that dioxin levels are decreasing in fish from the Chowan and Meherrin Rivers since the advent of new bleaching technologies (NCDENR 2002a). Elevated mercury concentrations in fish have also been reported sporadically within the basin (NCDENR 1997a)

Although the total area of impaired water in the Neuse River basin is less than other basins, it is affected by more severe localized problems. Water use impairment affects 30% of the freshwater stream miles and 9% of the estuarine area. High sediment loads and low dissolved oxygen are the major problems in the basin's freshwaters while nutrient runoff and algal blooms are the major problem in the basin's estuarine areas. Significant concentrations of toxic substances, particularly mercury and dioxin, have been detected at several local sites, and water, sediment, and fish tissue concentrations have indicated areas of concern for both aquatic life and human health. Compared to the other major river basins, the Neuse has the highest water column concentrations of toxic metals. (NCDENR 2002b). The major sources of impaired water quality in the Neuse River basin has been identified as agricultural runoff, defective septic tanks, marinas, and waste water treatment plants. Nonpoint sources are responsible for approximately 80% of the area's impaired water quality. A great portion of this nonpoint source runoff comes from urban development that enables stormwater to move rapidly into estuaries and sounds without adequate in-stream processing. (NCDENR 2002b)

Over half of the waters in the Roanoke River basin are impaired. Suspended sediments (27%), toxics contaminations (11%), excessive nutrient loadings (21.5%), and fecal contamination are the primary causes of impairment. Nonpoint sources account for approximately 85% of pollutant inputs (NCDENR 2002c). North Carolina ambient water quality standards and metal concentration limits have been exceeded at many sites along the Roanoke River and may be due to the relatively high level of industry in the basin (NCDENR 2002c). However, other potential nonpoint sources of metals and toxics in the Roanoke basin include 10 Superfund sites and 4 solid waste sites (NCDENR 2002c). Up until October 2001, all fish species from the lower Roanoke River, Welch Creek, and Albemarle Sound were subject to a fish consumption advisory for dioxin (NCDHHS 2001). See Tables 5 and 6. This advisory, however, has been lifted for all North Carolina game species (see Table 3).

As of April 16, 2002 North Carolina issued a fish consumption advisory for mercury in largemouth bass, chain pickerel, bowfin (blackfish), king mackerel, shark, swordfish, and tilefish taken from North Carolina waters south and east of Interstate 85 (NCDHHS 2002).

3.6. Biological Resources

3.6.1. Fish Biogeography and Biodiversity

The Albemarle-Pamlico basin contains a diverse range of habitats from small mountain streams to large estuaries to the sounds between the coast and Outer Banks (Lloyd et al. 1991). These habitats can be aggregated into five major ecoregions, i.e., the Middle Atlantic Coastal Plain, the Southeastern Plains, the Piedmont, the Blue Ridge Mountains, and the Central Appalachian Ridge and Valley (Figure 8). This rich habitat diversity results in an equally rich diversity of fish communities within the basin. The Neuse drainage has 93 total fish species, with 10 being introduced. The Tar drainage has 82 species, 5 being introduced. The Roanoke drainage has 124 species, with 25 being introduced. Among the native fish species, the Neuse and Tar are about 94% similar, but share only 67% and 68%, respectively, of the native fish with the Roanoke (Hocutt et al. 1986).

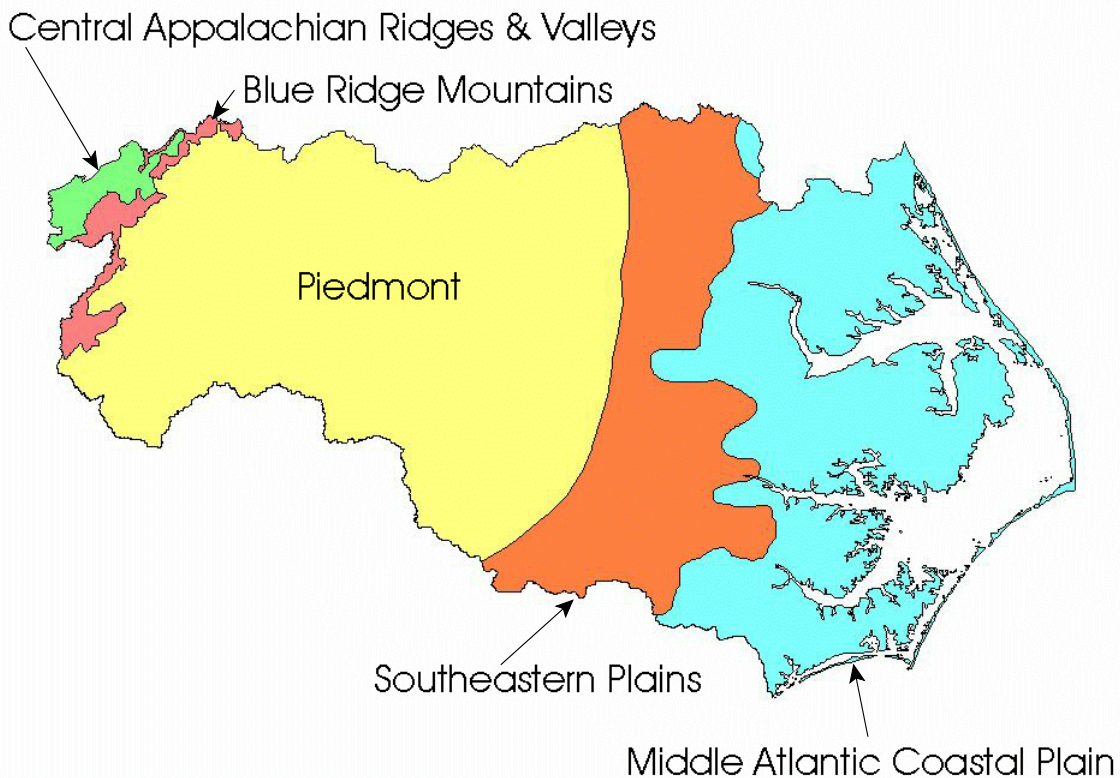


Figure 8. Ecoregions of the Albemarle-Pamlico basin.

3.6.2. Sport and Commercial Fisheries

The Chowan River and its tributaries provides some of North Carolina's finest freshwater fishing. From 1977 to 1980 the total fishing effort within the basin was estimated to be 201,600 angling hours per year (NCDENR 1997a). Additionally, cypress - tupelo swamps that flank virtually the entire Chowan River provides habitat for many coastal plain species. The river and its tributaries provide spawning habitats for anadromous river herring (alewife and blueback herring) and shad (hickory shad and American shad). Although the basin provides over 230 miles of rivers and streams as spawning habitat for these anadromous species, access to additional potential spawning areas is blocked by six dams and culverts throughout the basin (NCDENR 2002a). Not only are these anadromous species important recreational resources in their own right, particularly the American and hickory shad, but these species also provide excellent forage for largemouth bass, the most sought after sport fish in the river. During the summer and fall months, bass concentrate at the mouths of tributary creeks to feed on young-of-year herring. As a result of this abundant food supply, bass frequently attain sizes in excess of five pounds. The river and its tributaries (e.g., Sarem Creek, Bennett's Creek and Wiccacon River) also provide good fishing for sunfish and bream during the spring spawning period (April–May). These waters also produce good catches of black crappie during spring months and white perch during the summer (Ashley 2002).

The Neuse River basin supports both abundant and varied fresh and brackish water sport fisheries. Commercial and sport marine fisheries exist below New Bern for striped bass, southern flounder, Atlantic croaker, spot, bluefish, gray trout and channel bass. Above this point, freshwater sport fisheries exist for largemouth bass, sunfish, catfish, yellow and white perch and chain pickerel. Largemouth bass and sunfish are abundant in the river and its tributaries. Black crappie are among the most sought after fish in late fall and early spring. Important commercial and recreational sport fisheries for American and hickory shad exist in the Neuse during these species' spring spawning run. Prime areas for shad fishing include Pitch Kettle and Contentnea Creeks (see Chapter 6). Striped bass fishing which is popular in both the Neuse and the Trent Rivers, is best in the early spring and fall (Ashley 2002).

The Roanoke River basin provides excellent fishing for striped bass, largemouth bass, sunfish and catfish. The Roanoke River is the principal spawning stream for the Albemarle Sound population of striped bass. Stripers enter the mouth of the river in late March or early April on their annual spawning run to their principal spawning grounds near Weldon. The Roanoke River also offers very good fishing for white perch that spawns in the river from late March to late May. As the weather warms, both striped bass and white perch migrate back downstream to Albemarle Sound. During this same time, however, fishing for largemouth bass, sunfish and catfish begins to peak. Fishing for largemouth bass peaks in May but may remain good until cool weather slows the action in November. Although bluegill is the most abundant sunfish species, fliers, redear (shellcrackers), redbreast and warmouth are also caught frequently. Channel catfish and bullheads are caught along the entire length of the river and provide excellent table fare. Although these catfish generally weigh less than four pounds, channel catfish in excess of 20 pounds are frequently caught (Ashley 2002).

The Tar-Pamlico River basin, like the Neuse River basin, supports both fresh and brackish water sport fisheries. Although often obstructed by dams and culverts, the stream and rivers of the Tar-Pamlico River basin provide almost 400 miles of spawning areas for several anadromous fish species (NCDENR 2002d). The section of

river between Rocky Mount and Old Sparta provides important spawning areas for anadromous American shad, hickory shad, river herring and striped bass. Between Grimesland and Washington, the river supports heavy fishing pressure for striped bass, largemouth bass, various sunfish, white perch, and yellow perch. Largemouth bass are abundant throughout the Tar River watershed and receive heavy fishing pressure during May and early June. Sunfish (bluegill, redbreast, warmouth, flier and pumpkinseed) are also abundant in the river and its larger tributaries (e.g., Tranters Creek, Swift Creek and Fishing Creek) (Ashley 2002).

3.6.3. Endangered and Threatened Fishes

Although no fish species are federally or state listed as threatened or endangered in the Chowan River basin, at least 5 freshwater mussels and 1 crustacean are. These include: the alewife floater (*Anodonta implicata*), the eastern lampmussel (*Lampsilis radiata*), the tidewater mucket (*Leptodea ochracea*), the eastern pond mussel (*Ligumia nasuta*), the triangle floater (*Alasmidonta undulata*), and the Chowanoke crayfish (*Orconectes virginensis*) (NCDENR 1997a).

Threatened and endangered mussel species native to the Neuse River basin include: the Tar spiny mussel (*Elliptio steinstansana*), the dwarf wedgemussel (*Alasmidonta heterodon*), the Atlantic pigtoe (*Fusconaia masoni*), brook floater (*Alasmidonta varicosa*), the green floater (*Lasmigona subviridis*), the yellow lampmussel (*Lampsilis cariosa*), the yellow lance (*Elliptio lanceolata*), the Carolina fatmucket (*Lampsilis radiata conspicua*), the creeper (*Strophitus undulatus*), the Roanoke slabshell (*Elliptio roanokensis*), the triangle floater (*Alasmidonta undulata*), the Cape Fear spike (*Elliptio marsupiobesa*), and the notched rainbow (*Villosa constricta*) (NCNEWP 202).

Eight species of threatened or endangered mussels and fish are indigenous to the Roanoke River basin. The threatened or endangered mussel species include: the eastern pond mussel (*Ligumia nasuta*), the green floater (*Lasmigona subviridis*), the Roanoke slabshell (*Elliptio roanokensis*), the tidewater mucket (*Leptodea ochracea*), and the triangle floater (*Alasmidonta undulata*). The fish species of concern are the cutlips minnow (*Exoglossum maxillingua*), the rustyside sucker (*Thoburnia hamiltoni*), and the shortnose sturgeon (*Acipenser brevirostum*). However, at least four other fish species have also been identified as species of special concern. These are the spotted marginate madtom (*Noturus insignis*), the bigeye jumprock (*Moxostoma ariommun*), the Roanoke hogsucker (*Hypentelium roanokense*) and the riverweed darter (*Etheostoma podostemone*) (NCDENR 1996).

The Tar-Pamlico River basin provides habitats for ten mussel species and three fish species that are state or federally listed as rare, threatened, or endangered. The mussel species of concern include: the Tar spiny mussel (*Elliptio steinstansana*), the dwarf wedgemussel (*Alasmidonta heterodon*), the triangle floater (*Alasmidonta undulata*), the yellow lance (*Elliptio lanceolata*), the Roanoke slabshell (*Elliptio roanokensis*), the Atlantic pigtoe (*Fusconaia masoni*), the yellow lampmussel (*Lampsilis cariosa*), the squawfoot (*Strophitus undulatus*), the eastern lampmussel (*Lampsilis radiata*), and the notched rainbow (*Villosa constricta*). The fish species of concern are the least brook lamprey (*Lampetra aepyptera*), the Roanoke bass (*Ambloplites cavifrons*), and Carolina madtom (*Noturus furiosus*) (NCDENR 1999a, Prince 2002).

4. Identifying Nominal Conditions for Fish Health

4.1. Fish Community Associations

As discussed in Section 3.6.1, the Albemarle-Pamlico basin contains a diverse range of habitats from small mountain streams to large estuaries to the sounds between the coast and Outer Banks (Lloyd et al. 1991). This rich habitat diversity results in an equally rich diversity of fish communities within the basin. Although detailed texts on the biogeography of fish in the basin exist (Menhinick 1991, Jenkins and Burkhead 1993), there has been little effort to describe the distribution and composition of fish communities quantitatively in the basin as a whole. The few studies that have undertaken such analyses have only treated portions of the Albemarle-Pamlico basin. In particular, the Virginia portion of the basin has been analyzed by Angermeier and Winston (1998, 1999) and the basin's coastal plain communities within North Carolina have been studied by Spruill et al. (1998).

Methods for Characterizing Basin Fish Assemblages

The structure of fish communities within the Albemarle-Pamlico basin can be readily characterized using publicly available data. For this study, four data sets were used for this purpose. These included: 1) one USGS National Water-Quality Assessment (NAWQA) program data set, 2) one USEPA Environmental Monitoring and Assessment Program (EMAP) data set, 3) one North Carolina Department of Environment and Natural Resources data set, and 4) one Virginia Game and Inland Fisheries data set. These data sets report fish abundances for wadeable streams not larger than 5th order that were sampled between 1990-1999 using electrofishing. Figure 9 displays the distribution of sample sites represented in these combined data sets with respect to the basin's 8-digit Hydrologic Unit Code (HUC) watersheds. Using these data, a series of site \times species and site \times site matrices were constructed to analyze the biogeography and community structure of fish assemblages in the Albemarle-Pamlico basin.

To perform these analyses, a site \times species matrix was constructed disregarding all species found at only a single site. The abundances in the resulting 302 \times 100 site-species array were then reduced to a binary absence / presence format. Sample sites were then aggregated to produce a 21 \times 100 array based on 8-digit HUC (Hydrologic Unit Code) (see Figure 3) and a 34 \times 100 array based on 8-digit HUC/ecoregion combinations. Finally, similarity matrices were constructed from each site \times species matrix by calculating the mean Jaccard's similarity for all stream pairs within the basin at large, each 8-digit HUC, and each 8-digit HUC/ecoregion combination. These similarity matrices were investigated using the complete linkage clustering technique, which separates the summarized sites into similar groups.

A principal components analysis (PCA) was performed on the 34 \times 100, 8-digit HUC/ecoregion \times species array. Component loadings of the PCA axes were species, and PCA scores were obtained for each site. Ordination diagrams of component loadings for the summarized sites were plotted for comparison with the results of the cluster analysis.

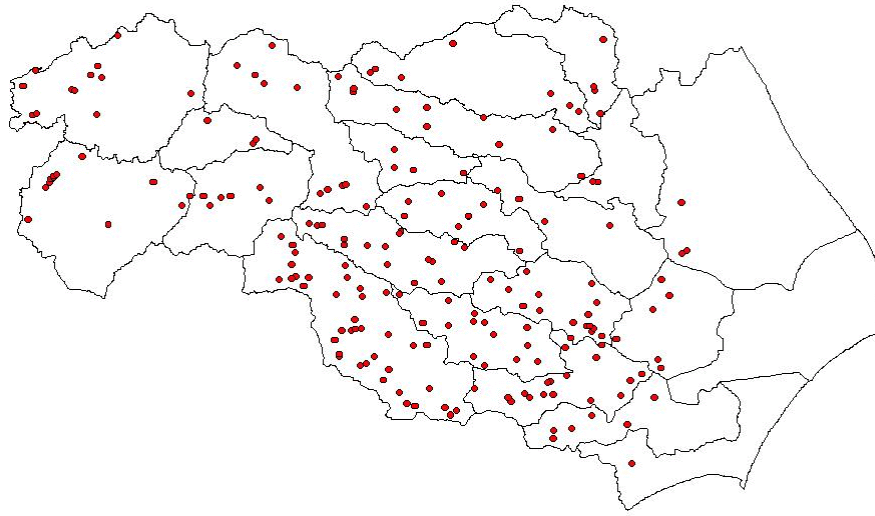


Figure 9. Distribution of fish sample sites with respect to 8-digit HUC watersheds.

Each cluster of streams identified above was analyzed separately for species associations. Two clusters did not have enough sample sites for meaningful analyses. The remaining five were arrayed in site \times species matrices using all of the sample sites within the cluster. Simple matching coefficients were calculated for each species pair in each array and reduced to similarity matrices corresponding to the five original clusters. A cluster analysis using the complete linkage method was conducted on each similarity matrix to define distinct fish associations in each cluster. The species associations within stream clusters were investigated for similarities in habitats used by the fish. Habitat properties shared by the fish in each association were investigated, including substrate preference, stream flow, and stream depth as described in Page and Burr (1991).

Canonical correlations between fish associations in the 8-digit HUC/ecoregion clusters and types of land use in the cluster were run to investigate how fish associations varied with type of human impact within a cluster. Measures of land use included the amount of residential, industrial, agricultural, and forested land within the cluster. Ordination diagrams of the correlations between fish associations and land use canonical variables were plotted.

Results and Discussion

Cluster analysis at the 8-digit HUC level

Cluster analysis of the fish communities at the level of the 8-digit HUC resulted in clusters that formed across the four major river basins, as well as within a single river basin (Figure 10). Fish communities within the

Roanoke River basin fell into three different clusters, while those of the Chowan River basin grouped into four clusters. These clusters formed along an upstream-downstream gradient, consistent with the changes that might be associated with the different ecoregions. Clusters also formed across the major river basins along a north-south gradient, as might be associated within one or a few ecoregions. For example, one cluster included sites in the lower Chowan, Roanoke, and Neuse River basins in the area of the Middle Atlantic Coastal Plain ecoregion. These findings indicate that fish communities are organized at some level other than that of only the river basin.

Cluster analysis at the 8-digit HUC + ecoregion level

The cluster analysis of the fish communities at the level of the 8-digit HUCs and ecoregions produced seven clusters (Figure 11). Five of the clusters (A-E) contained enough samples for interpretation, while clusters F and G contained too few samples for analysis of the fish associations. Cluster F was from two very small areas on the border between ecoregions and may be a transition area between clusters E, C, and D. Cluster G contained only one sample, one of the closest to the ocean and the only one from its 8-digit HUC. The lack of species found there (n=8) resulted in a sample clustering separate from the other sites, and is likely not representative of the 8-digit HUC/ecoregion combination.

The other five clusters were more distinct. Cluster A formed in the upper Roanoke River basin across the Piedmont, Blue Ridge Mountains, and Central Appalachian Ridges and Valleys ecoregions. All of the sample sites in the mountains were grouped in this cluster. Cluster B formed across the Roanoke and upper Chowan River basins but was limited to the Piedmont ecoregion. Cluster C formed in the Tar-Pamlico, Roanoke, and entire Neuse River basins across the Piedmont, Southeastern Plains, and Middle Atlantic Coastal Plain ecoregions. Cluster D was in the Chowan River basin limited to only the Southeastern Plains ecoregion. Cluster E formed across the Chowan, Roanoke, and Tar-Pamlico River basins, but only within the Middle Atlantic Coastal Plain ecoregion. In the formation of a cluster, the influence of the river basins as opposed to the ecoregions became more important with increasing distance from the coast.

The principal components analysis (PCA) revealed the distinctions between clusters A-G in ordination space (Figure 12). PC1 and PC2 accounted for 21% and 13% of the variation in the fish species data, respectively. Fish with high positive loadings on PC1 included the central stoneroller (*Campostoma anomalum*), the fantail darter (*Etheostoma flabelare*), and the finescale dace (*Phoxinus oreas*) all of which are representative of rocky, flowing waters towards the headwaters of the basin. Species with high negative loadings on PC1 included the creek chubsucker (*Erimyzon oblongus*), the American eel (*Anguilla rostrata*) and the pirate perch (*Aphredoderus sayanus*), which were more common down-basin and often associated with vegetation or debris. PC2 was more difficult to interpret based on the habitat of the fish. Species loading high positively on PC2 included the satinfin shiner (*Cyprinella analostana*) and the V-lip redhorse (*Moxostoma pappilosum*), perhaps indicative of deeper flowing waters. Fish with high negative loadings on PC2 included the tessellated darter (*Etheostoma olmstedi*) and the banded sculpin (*Cottus carolinae*), which may be indicative of shallow riffle habitats. However, the habitat differences of the fish on PC2 were not as distinct as on PC1, indicating that some factor other than habitat may better explain the separation of the clusters along the PC2 axis.



Figure 10. Fish community clusters based on combinations of 8-digit HUC watersheds. River basin boundaries are outlined in orange, and 8-digit HUC watershed boundaries are outlined in black

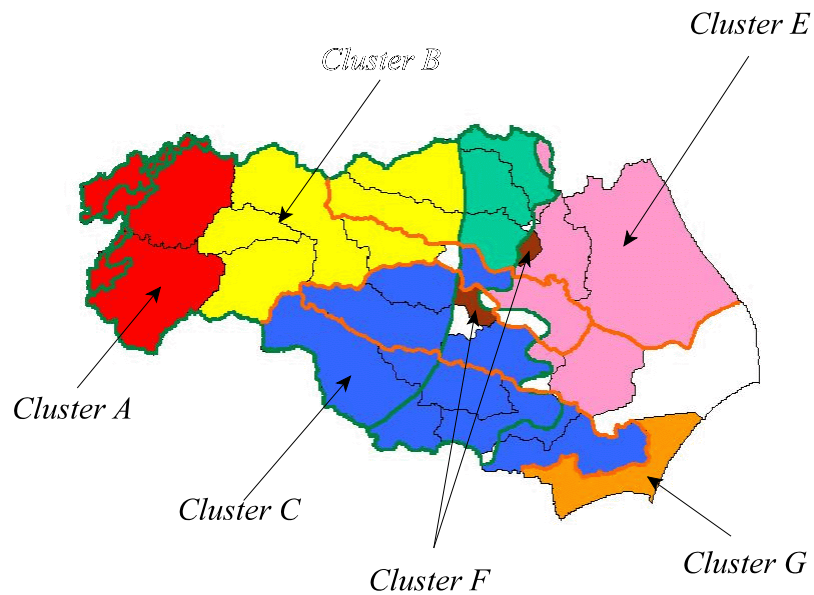


Figure 11. Fish community clusters based on combinations of 8-digit HUC watersheds and ecoregions. River basin boundaries are outlined in orange; 8-digit HUC watershed boundaries are outlined in black; and ecoregions are outlined in green.

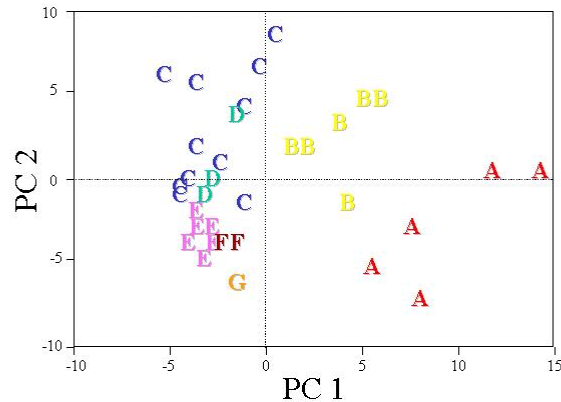


Figure 12. Ordination diagram of PCA results. Component loadings are linear combinations of fish species. Labels are the clusters in Figure 11 .

Fish associations within clusters

The analysis of the fish associations within clusters A-E showed associations that were generally interpretable by the habitat preferences of the fish species, with the habitat preferences being more important upstream than downstream (Tables 8 - 12). Clusters A and B showed clear separation of fish associations grouped by flow, water depth, presence of vegetation, and substrate. The fish associations in clusters C and D also showed separation by habitat, but some of the clusters were more similar than distinct (such as the vegetated pool vs. vegetated swamp associations in cluster C). The cluster furthest downstream, cluster E, showed the least separation based on habitat preferences, with all fish found in some form of vegetated, low-flow water. Rose and Echelle (1981) showed that similar species will associate with each other, even in streams that are separated over a wide area. This similarity appears to be habitat-based upstream. The downstream habitats are either not distinct enough units as described and/or another variable is adding a substantial influence on the fish associations. This other variable may be the presence of humans in the river basins.

Canonical Correlations and the Influence of Humans

Canonical correlations between measures of human use of the land in clusters C (Figure 13 A) and E (Figure 13 B) separated the fish associations in those clusters primarily along a gradient of high to low human impact on the land. Correlations between human impact on the land and fish communities throughout the rest of the basin were not conducted since the data sets used to compile information about the fish did not have similar

variables describing the presence of humans. The first canonical variable of land use for both clusters was a gradient from evergreen forest/wetlands to industrial/mining/transportation, indicating a measure of low to high impact on the land by humans. This variable separated the similar fish associations in cluster E (i.e., ‘uncommon species, vegetated pools’ and ‘vegetated pools/backwater’) as well as in cluster C (i.e., ‘rocky/sandy pools/runs, 1-50 m wide’ and ‘rocky/sandy pools, 1->50 m wide’). The first canonical variable explained 30% of the variation in the fish associations in cluster C, and 39% in cluster E.

The second variable in cluster E was along a gradient from cropland to residential areas, perhaps a measure of the type of impact by humans. Cropland areas might add excess nutrients and pesticides to streams via runoff, while residential areas might introduce other pollutants and cause dramatic habitat alteration. The second variable in cluster C was along a gradient of wetland/evergreen forests to residential areas, again suggestive of another type of low to high human impact gradient. The form of these human impact gradients is speculative without corresponding nutrient, pollutant, and toxicant data from within the streams, but this seems a likely explanation and will be investigated with continued sampling this summer that will collect the associated data necessary to investigate this hypothesis.

Conclusions

- □ Fish communities in streams of the Albemarle-Pamlico basin form distinct groups based on combinations of major river basin and ecoregion characteristics.
- □ Within these groupings of streams, the fish species separated into distinct fish associations. These associations were based on habitat preference by the fish, especially in the upstream groups.

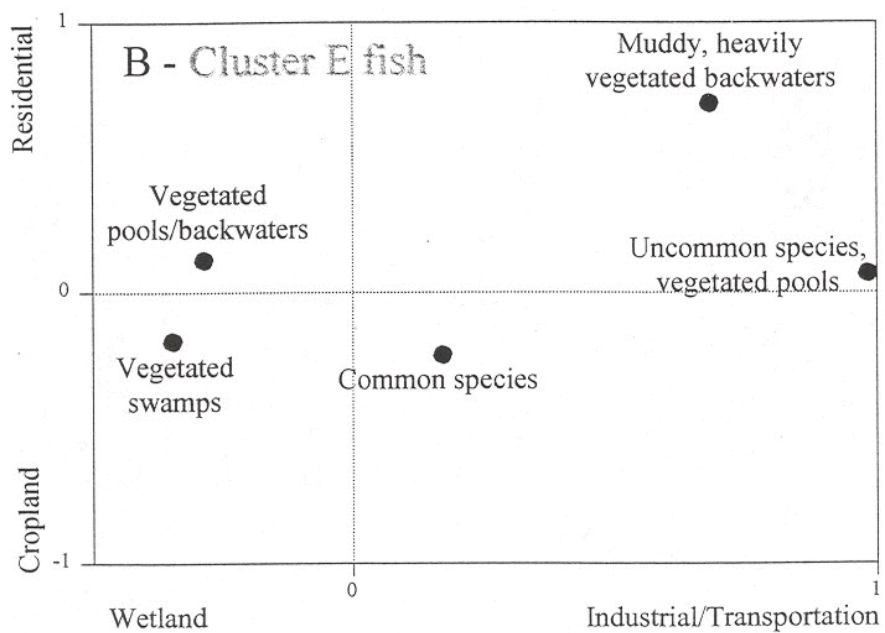
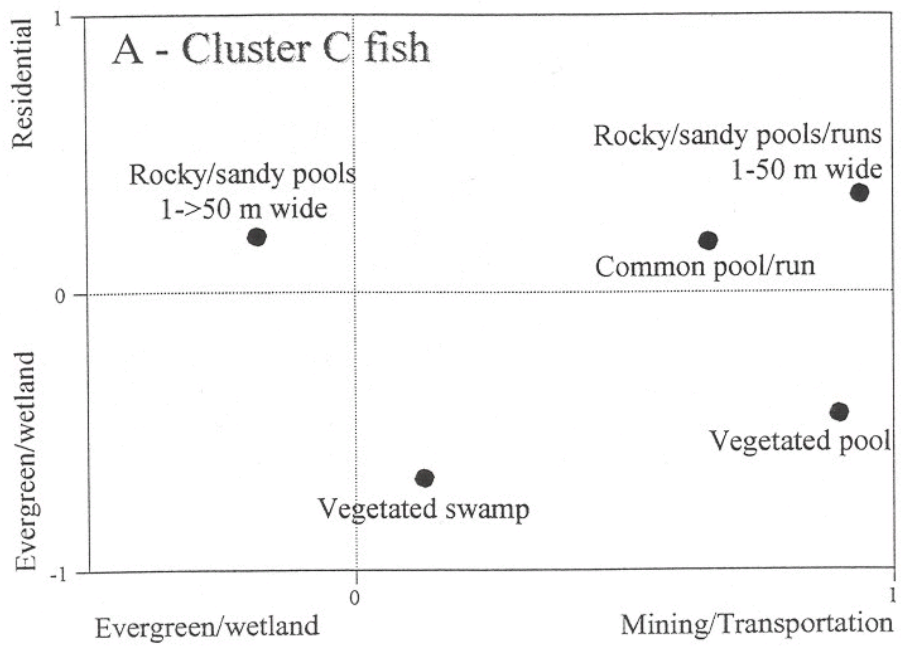


Figure 13. Ordination diagrams of canonical correlation results. Cluster C fish associations are shown in panel A and cluster E fish associations are shown in panel B. Labels are the species-habitat groups from Table 10 for cluster C and from Table 12 for cluster E.

Table 8. Species-habitat groups within Cluster A.

<i>Catostomus commersoni</i>	white sucker	Common species in the cluster
<i>Lepomis auritus</i>	redbreast sunfish	
<i>Etheostoma nigrum</i>	johnny darter	Rocky pool
<i>Etheostoma podostemone</i>	riverweed darter	
<i>Rhinichthys atratulus</i>	blacknose dace	
<i>Semotilus atromaculatus</i>	creek chub	
<i>Campostoma anomalum</i>	central stoneroller	Rocky riffle/pool
<i>Clinostomus funduloides</i>	rosyside dace	
<i>Etheostoma flabellare</i>	fantail darter	
<i>Hypentelium roanokense</i>	Roanoke hog sucker	
<i>Luxilus cerasinus</i>	crescent shiner	
<i>Moxostoma cervinum</i>	black jumprock	
<i>Nocomis leptcephalus</i>	bluehead chub	
<i>Noturus insignis</i>	margined madtom	
<i>Phoxinus oreas</i>	finescale dace	
<i>Etheostoma vitreum</i>	glassy darter	Clear, rocky runs
<i>Hypentelium nigricans</i>	northern hog sucker	
<i>Luxilus albeolus</i>	white shiner	
<i>Lythrurus ardens</i>	rosefin shiner	
<i>Notropis chiliticus</i>	redlip shiner	
<i>Percina roanoka</i>	Roanoke darter	

Continued on next page

Table 8. (continued) Species-habitat groups within Cluster A.

<i>Cottus bairdi</i>	mottled sculpin	Gravel/boulder runs
<i>Exoglossum maxillingua</i>	cutlips minnow	
<i>Moxostoma ariommum</i>	bigeye jumprock	
<i>Percina peltata</i>	shield darter	
<i>Percina rex</i>	Roanoke logperch	
<i>Cyprinella analostana</i>	satinfin shiner	Vegetated pools, 1-25 m wide
<i>Dorosoma cepedianum</i>	gizzard shad	
<i>Lepomis macrochirus</i>	bluegill	
<i>Micropterus salmoides</i>	largemouth bass	
<i>Ambloplites rupestris</i>	rock bass	Vegetated pools, 5-50 m wide
<i>Cyprinus carpio</i>	common carp	
<i>Micropterus dolomieu</i>	smallmouth bass	
<i>Moxostoma anisurum</i>	silver redhorse	
<i>Moxostoma erythrurum</i>	golden redhorse	
<i>Ameiurus natalis</i>	yellow bullhead	Uncommon pool/run species
<i>Ictalurus punctatus</i>	channel catfish	
<i>Lepomis cyanellus</i>	green sunfish	
<i>Lepomis gibbosus</i>	pumpkinseed	
<i>Moxostoma pappillosum</i>	V-lip redhorse	
<i>Moxostoma rhothoecum</i>	torrent sucker	
<i>Notropis hudsonius</i>	spottail shiner	
<i>Oncorhynchus mykiss</i>	rainbow trout	
<i>Pomoxis nigromaculatus</i>	black crappie	

Table 9. Species-habitat groups within Cluster B.

<i>Etheostoma flabellare</i>	fantail darter	Common pool/run species
<i>Etheostoma nigrum</i>	johnny darter	
<i>Lepomis auritus</i>	redbreast sunfish	
<i>Lepomis cyanellus</i>	green sunfish	
<i>Lepomis gibbosus</i>	pumpkinseed	
<i>Lepomis macrochirus</i>	bluegill	
<i>Luxilus cerasinus</i>	crescent shiner	
<i>Lythrurus ardens</i>	rosefin shiner	
<i>Nocomis leptocephalus</i>	bluehead chub	
<i>Noturus insignis</i>	marginated madtom	
<i>Ameiurus platycephalus</i>	flat bullhead	Mixed substrate pool/run
<i>Cyprinella analostana</i>	satinfin shiner	
<i>Micropterus salmoides</i>	largemouth bass	
<i>Notropis procne</i>	swallowtail shiner	
<i>Catostomus commersoni</i>	white sucker	Clear, rocky pool/riffle
<i>Clinostomus funduloides</i>	rosyside dace	
<i>Luxilus albeolus</i>	white shiner	
<i>Percina roanoka</i>	Roanoke darter	
<i>Semotilus atromaculatus</i>	creek chub	
<i>Anguilla rostrata</i>	American eel	Clear, rocky riffle/run
<i>Campostoma anomalum</i>	central stoneroller	
<i>Etheostoma vitreum</i>	glassy darter	
<i>Hypentelium nigricans</i>	northern hog sucker	
<i>Hypentelium roanokense</i>	Roanoke hog sucker	
<i>Lampetra appendix</i>	Amer. brook lamprey	
<i>Moxostoma cervinum</i>	black jumprock	
<i>Phoxinus oreas</i>	finescale dace	
<i>Rhinichthys atratulus</i>	blacknose dace	

Continued on next page

Table 9. (continued) Species-habitat groups within Cluster B.

<i>Ameiurus brunneus</i>	snail bullhead	Sandy pools/backwaters
<i>Ameiurus catus</i>	white catfish	
<i>Ameiurus nebulosus</i>	brown bullhead	
<i>Dorosoma cepedianum</i>	gizzard shad	
<i>Enneacanthus gloriosus</i>	bluespotted sunfish	
<i>Esox americanus</i>	redfin pickerel	
<i>Fundulus rathbuni</i>	speckled killifish	
<i>Gambusia holbrooki</i>	eastern mosquitofish	
<i>Hybognathus regius</i>	eastern silvery minnow	
<i>Lepomis microlophus</i>	redeer sunfish	
<i>Moxostoma anisurum</i>	silver redhorse	
<i>Moxostoma erythrurum</i>	golden redhorse	
<i>Notemigonus crysoleucas</i>	golden shiner	
<i>Notropis alborus</i>	whitemouth shiner	
<i>Notropis altipinnis</i>	highfin shiner	
<i>Notropis amoenus</i>	comely shiner	
<i>Notropis hudsonius</i>	spottail shiner	
<i>Perca flavescens</i>	yellow perch	
<i>Percina peltata</i>	shield darter	
<i>Pomoxis annularis</i>	white crappie	
<i>Pomoxis nigromaculatus</i>	black crappie	
<i>Ameiurus natalis</i>	yellow bullhead	Muddy, vegetated swamp/low flow
<i>Aphredoderus sayanus</i>	pirate perch	
<i>Erimyzon oblongus</i>	creek chubsucker	
<i>Esox niger</i>	chain pickerel	
<i>Lepomis gulosus</i>	warmouth	
<i>Moxostoma pappillosum</i>	V-lip redhorse	

Table 10. Species-habitat groups within Cluster C.

<i>Aphredoderus sayanus</i>	pirate perch	Common pool/run throughout cluster
<i>Erimyzon oblongus</i>	creek chubsucker	
<i>Etheostoma olmstedii</i>	tessellated darter	
<i>Gambusia holbrooki</i>	eastern mosquitofish	
<i>Lepomis auritus</i>	redbreast sunfish	
<i>Lepomis macrochirus</i>	bluegill	
<i>Micropterus salmoides</i>	largemouth bass	
<i>Noturus insignis</i>	marginated madtom	
<i>Cyprinella analostana</i>	satinfin shiner	Rocky/sandy pools/runs, 1-50 m wide
<i>Etheostoma nigrum</i>	johnny darter	
<i>Lepomis cyanellus</i>	green sunfish	
<i>Luxilus albeolus</i>	white shiner	
<i>Lythrurus ardens</i>	rosefin shiner	
<i>Nocomis leptocephalus</i>	bluehead chub	
<i>Notropis procne</i>	swallowtail shiner	
<i>Percina peltata</i>	shield darter	
<i>Percina roanoka</i>	Roanoke darter	
<i>Ambloplites cavifrons</i>	Roanoke bass	Rocky/sandy pools, 1->50 m wide
<i>Ameiurus nebulosus</i>	brown bullhead	
<i>Catostomus commersoni</i>	white sucker	
<i>Clinostomus funduloides</i>	rosyside dace	
<i>Etheostoma vitreum</i>	glassy darter	
<i>Hybognathus regius</i>	eastern silvery minnow	
<i>Hypentelium nigricans</i>	northern hog sucker	
<i>Ictalurus punctatus</i>	channel catfish	
<i>Lepomis microlophus</i>	redeer sunfish	
<i>Lepomis sp. - hybrid</i>	hybrid sunfish	
<i>Moxostoma anisurum</i>	silver redhorse	
<i>Moxostoma cervinum</i>	black jumprock	
<i>Moxostoma pappillosum</i>	V-lip redhorse	
<i>Nocomis raneyi</i>	bull chub	
<i>Notropis altipinnis</i>	highfin shiner	
<i>Notropis hudsonius</i>	spottail shiner	
<i>Notropis volucellus</i>	mimic shiner	
<i>Pomoxis nigromaculatus</i>	black crappie	
<i>Semotilus atromaculatus</i>	creek chub	

Continued on next page

Table 10. (continued) Species-habitat groups within Cluster C.

<i>Ameiurus natalis</i>	yellow bullhead	Vegetated pools, sluggish current
<i>Anguilla rostrata</i>	American eel	
<i>Enneacanthus gloriosus</i>	bluespotted sunfish	
<i>Esox americanus americanus</i>	redfin pickerel	
<i>Lepomis gibbosus</i>	pumpkinseed	
<i>Lepomis gulosus</i>	warmouth	
<i>Acantharchus pomotis</i>	mud sunfish	Vegetated swamps
<i>Amia calva</i>	bowfin	
<i>Centrarchus macropterus</i>	flier	
<i>Esox niger</i>	chain pickerel	
<i>Etheostoma serrafer</i>	sawcheek darter	
<i>Notemigonus crysoleucas</i>	golden shiner	
<i>Notropis amoenus</i>	comely shiner	
<i>Notropis cummingsae</i>	dusky shiner	
<i>Noturus gyrinus</i>	tadpole madtom	
<i>Umbra pygmaea</i>	eastern mudminnow	

Table 11. Species-habitat groups within Cluster D.

<i>Ictalurus punctatus</i>	channel catfish	Deep pools of larger streams
<i>Lepisosteus osseus</i>	longnose gar	
<i>Cyprinella analostana</i>	satinfish shiner	Rocky/sandy runs
<i>Etheostoma vitreum</i>	glassy darter	
<i>Gambusia holbrooki</i>	eastern mosquitofish	
<i>Lampetra appendix</i>	Amer. brook lamprey	
<i>Moxostoma anisurum</i>	silver redhorse	
<i>Moxostoma pappillosum</i>	V-lip redhorse	
<i>Notropis procne</i>	swallowtail shiner	
<i>Pomoxis nigromaculatus</i>	black crappie	
<i>Amia calva</i>	bowfin	Sandy pools
<i>Etheostoma olmstedii</i>	tessellated darter	
<i>Hybognathus regius</i>	eastern silvery minnow	
<i>Notropis amoenus</i>	comely shiner	
<i>Ameiurus natalis</i>	yellow bullhead	Sluggish pools with vegetation
<i>Erimyzon oblongus</i>	creek chubsucker	
<i>Esox americanus</i>	redfin pickerel	
<i>Noturus gyrinus</i>	tadpole madtom	
<i>Anguilla rostrata</i>	American eel	Vegetated muddy/sandy swamps/pools
<i>Aphredoderus sayanus</i>	pirate perch	
<i>Enneacanthus gloriosus</i>	bluespotted sunfish	
<i>Esox niger</i>	chain pickerel	
<i>Lepomis auritus</i>	redbreast sunfish	
<i>Lepomis gibbosus</i>	pumpkinseed	
<i>Lepomis gulosus</i>	warmouth	
<i>Lepomis macrochirus</i>	bluegill	
<i>Micropterus salmoides</i>	largemouth bass	
<i>Percina peltata</i>	shield darter	

Table 12. Species-habitat groups within Cluster E.

<i>Anguilla rostrata</i>	American eel	Common species, found in pools
<i>Aphredoderus sayanus</i>	pirate perch	
<i>Enneacanthus gloriosus</i>	bluespotted sunfish	
<i>Erimyzon oblongus</i>	creek chubsucker	
<i>Esox americanus</i>	redfin pickerel	
<i>Lepomis macrochirus</i>	bluegill	
<i>Acantharchus pomotis</i>	mud sunfish	Vegetated pools/backwater
<i>Centrarchus macropterus</i>	flier	
<i>Lepomis gibbosus</i>	pumpkinseed	
<i>Amia calva</i>	bowfin	Uncommon species, vegetated pools
<i>Dorosoma cepedianum</i>	gizzard shad	
<i>Esox niger</i>	chain pickerel	
<i>Etheostoma fusiforme</i>	swamp darter	
<i>Etheostoma olmstedii</i>	tessellated darter	
<i>Etheostoma serrifer</i>	sawcheek darter	
<i>Gambusia holbrooki</i>	eastern mosquitofish	
<i>Lepomis auritus</i>	redbreast sunfish	
<i>Lepomis marginatus</i>	dollar sunfish	
<i>Micropterus salmoides</i>	largemouth bass	
<i>Noturus gyrinus</i>	tadpole madtom	
<i>Chologaster cornuta</i>	swampfish	Muddy, heavily vegetated backwaters
<i>Enneacanthus obesus</i>	banded sunfish	
<i>Ameiurus natalis</i>	yellow bullhead	Vegetated swamps
<i>Lepomis gulosus</i>	warmouth	
<i>Notemigonus crysoleucas</i>	golden shiner	
<i>Umbra pygmaea</i>	eastern mudminnow	

4.2. Nominal Fish Growth and Related Processes

Because many of the assessment questions related to *fish health* concern, either explicitly or implicitly, the individual growth rates of fish, estimation of expected or nominal growth rates for ecologically dominant, recreational, and commercial fish species is an important issue for both fisheries ecologists and environmental decision-makers. Examples of important assessment questions that directly pertain to individual growth rates of fish species of concern include:

- 1) Is individual fish growth and condition sufficient to enable them to survive periods of natural (e.g., overwintering) and man induced stress?
- 2) Is individual growth rate adequate for juvenile fish to attain the minimum body size required for reproduction?
- 3) Is the growth rate of piscivorous species adequate to allow them accessible to appropriately sized prey? Conversely, are the growth rates of potential prey species within the range that makes them available to piscivorous species of concern?
- 4) Are appropriately sized fish abundant enough to maintain piscivorous wildlife (e.g., birds, mammals, and reptiles) during breeding and non-breeding conditions?
- 5) Is the growth of game species sufficient to meet public expectations of the fishery?
- 6) Is the growth rate of fish high enough to biodilute residues of persistent bioaccumulative chemicals to levels that are safe for the fish themselves, piscivorous wildlife, and humans?

Having recognized the need to assess individual growth rates of fish, the question that immediately follows is what model should be used to for this purpose? This model selection, like most model selections, is not a trivial concern since over the past 60 years at least four different models have become standards for characterizing the growth of fishes; these are the von Bertalanffy, Richards, Gompertz, and Parker-Larkin models. See Ricker (1979) for a detailed discussion of these models and other less commonly used models.

According to the von Bertalanffy model, the body weight growth of fish can be formulated as a simple mass balance of anabolic processes that are directly proportional to the fish's surface area and catabolic processes that are directly proportional to the fish's body weight. Assuming isometric growth (i.e., $W = \lambda L^3$), the fish's body weight is therefore governed by the following differential equation

$$\frac{dW}{dt} = \phi W^{2/3} - \rho W \quad (2)$$

where W is the fish's body weight; ϕ is the fish's rate of feeding and assimilation; and ρ is the fish's total

metabolic rate. In terms of body length, this model is also equivalent to

$$\frac{dL}{dt} = \frac{\rho}{3} (L_{\max} - L) \quad (3)$$

where L is the fish's body length and $L_{\max} = \phi \rho^{-1} \lambda^{-1/3}$ is the fish's "maximum" body length which results from setting Eq.(2) to zero. For further discussion, see Parker and Larkin (1959) and Paloheimo and Dickie (1965).

The Richard's model (Richards 1959) is a generalization of the von Bertalanffy model that relaxes the assumption of isometric growth and strict proportionality between a fish's feeding/assimilatory processes and its absorptive surface areas. In the Richards model, all these processes are simply assumed to be an allometric power function of the fish's body weight. The fish's growth is then described by the differential equation

$$\frac{dW}{dt} = \phi_1 W^{\phi_2} - \rho W \quad (4)$$

Although both the von Bertalanffy and Richards models appear to be based on a strong physiological foundation, a more critical look at these models cast doubts on the generality of such conclusions or assertions. One particular point of contention in this regard is the assumption that fish metabolism (i.e., respiration and excretion) is directly proportional to the fish's body weight. Although this assumption is certainly satisfied or closely approximated for some fish species, most fish species have metabolic demands that are best described as power functions of their body weights. Consequently, from a purely physiologically-based perspective a much better anabolic-catabolic process model for fish growth could be argued to be

$$\frac{dW}{dt} = \phi_1 W^{\phi_2} - \rho_1 W^{\rho_2} \quad (5)$$

See Paloheimo and Dickie (1965). Unlike the von Bertalanffy and Richards models, however, this model generally does not have a closed analytical solution. Furthermore, when this model is fit to observed data, there is no guarantee that the fitted exponents will match expected physiological exponents unless the analysis is suitably constrained.

In light of such interpretative problems, simpler empirical growth models may be more than adequate for many applications. Two such models that have proved useful in this regard are the Gompertz and Parker-Larkin models. Both of these models are intended to describe specific growth rates (i.e., $W^{-1} dW/dt$) that decrease with the age or size of the individual. According to the Gompertz model, fish growth is described by

$$\frac{dW}{dt} = \epsilon_1 \exp(-\epsilon_2 t) W \quad (6)$$

On the other hand, the Parker-Larkin model (Parker and Larkin 1959) describes fish growth using the simple allometric power function formulation

$$\frac{dW}{dt} = \alpha W^\beta \quad (7)$$

Although each of these growth models can potentially describe very different growth trajectories, much of the discussion surrounding their use has focused on whether the models predict asymptotically zero or indeterminate growth (Parker and Larkin 1959, Paloheimo and Dickie 1965, Knight 1968, Schnute 1981). Although the growth rates of individual fish almost always decrease with increasing age or body size, Knight (1968) argued that the traditional notion of asymptotically zero growth is seldom, if ever, supported by studies that have focused on actual growth increments rather than on size at age. Because the Parker-Larkin model is the only model outlined above that assumes that the growth of fish is fundamentally indeterminate, this model might have an important conceptual advantage over the von Bertalanffy, Richards, and Gompertz, models. The Parker-Larkin model also may have an additional advantage over both the von Bertalanffy and Richards models in that the Parker-Larkin model does not rely on an apparently unrealistic assumption that the respiration of fishes can be generally described by a linear function of the fish's body weight.

In the following sections, a procedure for estimating nominal growth rates for fish species in the Albemarle-Pamlico basin using the Parker-Larkin growth model is outlined. Following this discussion, methods for comparing observed and expected growth rates will be considered. Finally, the importance of accurately estimated growth rates for assessing regional patterns of chemical bioaccumulation and population dynamics is discussed.

Methods

There are three basic types of data that have been traditionally used to calculate fish growth rates; these are: 1) length at age data, 2) back-calculated length at age for specific age classes sampled over multiple years, and 3) back-calculated length at age for specific year classes or cohorts. Back-calculated body lengths for the later two data types are generally calculated by regression using growth increments indicated by annular features of body scales, otoliths, pectoral spines, or other "hard" structures. Whereas for a length at age dataset each individual fish contributes only one observation (i.e., its current length), each individual fish contributes a time series of body lengths for both of the remaining types of growth data.

Nominal growth rates for fish species occurring in the Albemarle-Pamlico basin were estimated from data summarized by Carlander (1969, 1977b, 1997). For each species, reported body lengths at age, whether back-calculated or not, were converted to live body weights using the geometric mean of the weight-length regressions summarized by Carlander (1969, 1977b, 1997) for that species. Estimated live body weights were then fit to the analytical solution Parker-Larkin growth model using the NL2SOLV non-linear regression and optimization software. The standard form of the solution of the Parker-Larkin growth model for any time interval $[t_0, t]$ is

$$W(t) = \left(W(t_0)^{1-\beta} + \alpha (1-\beta) (t - t_0) \right)^{1/(1-\beta)} \quad (8)$$

However, because this expression is discontinuous at $\beta = 1$, Eq.(8) was not used directly for estimating the growth

parameters α and β . Instead, the equivalent expression

$$W(t) = \left(W(t_0) \exp(-b) + \alpha \exp(-b) (t - t_0) \right) \exp(b) \quad (9)$$

where $\exp(-b) = (1 - \beta)$ was used for this purpose. After obtaining estimates for the parameters α and b ,

specific growth rates $\gamma = W^{-1} dW/dt$ were calculated using the identity

$$\gamma = \gamma_1 W^{\gamma_2} = \alpha W^{\beta-1} = \alpha W^{-\exp(-b)} \quad (10)$$

Results

Table 13 summarizes the calculated daily growth rates (g/g/d) for ecologically and recreationally important fish species found in the Albemarle-Pamlico basin. The growth coefficients and exponents that were estimated for these species display a wide range of values, i.e., $0.0017 < \gamma_1 < 4.0321$ and $-1.361 < \gamma_2 < -0.044$. It is interesting to note that the redbfin pickerel (*Esox americanus*) had both the smallest growth coefficient and the largest growth exponent. This situation, however, is not too surprising since when power functions are fit to most data, the resulting coefficients and exponents are generally negatively correlated. See Section 5.4.4.2.

What is more interesting are the trends in the growth coefficients and exponents displayed by closely related fish species. For example, whereas growth coefficients and exponents within each of the centrarchid genera *Lepomis*, *Micropterus*, and *Pomoxis* are generally very similar to one another, these same parameters for the closely related catfish genera *Ameiurus* and *Ictalurus* demonstrate a relatively wide range of values, i.e., $0.0053 < \gamma_1 < 0.0456$ and $-0.595 < \gamma_2 < -0.294$. This divergent pattern of growth parameters for congeneric species was also displayed by the two species of *Alosa* (shad), *Esox* (pickerel), and *Moxostoma* (redhorses) that were analyzed. An intermediate pattern of growth parameters was displayed by the two *Morone* species analyzed. In particular, striped bass (*M. saxatilis*) and white perch (*M. americana*) displayed very similar growth exponents but vastly different growth coefficients that undoubtedly reflect their relative adult sizes.

Discussion

Comparing Observed and Expected Growth Rates

For any species of concern, let $\bar{\gamma} = \bar{\gamma}_1 W^{\bar{\gamma}_2}$ denote the species' nominal or expected specific growth rate within a watershed or basin of concern. Also let $\gamma_i = \gamma_{1,i} W^{\gamma_{2,i}}$ denote that species' observed specific growth rate at the i -th sample station within that watershed or basin. In order to evaluate how the species' actual growth rates

Table 13. Summary of daily growth rates (g/g/d) for Albemarle-Pamlico basin fish species.

Species	daily growth rate (g/g/d)
<i>Alosa pseudoharengus</i>	0.0165 W[g] ^{-0.619} (n= 18; r ² =0.92)
<i>Alosa sapidissima</i>	0.3516 W[g] ^{-0.907} (n= 47; r ² =0.98)
<i>Ambloplites cavifons</i>	0.0933 W[g] ^{-0.703} (n= 328; r ² =0.96)
<i>Ameiurus catus</i>	0.0053 W[g] ^{-0.294} (n= 42; r ² =0.95)
<i>Ameiurus natalis</i>	0.0456 W[g] ^{-0.595} (n= 23; r ² =0.86)
<i>Ameiurus nebulosus</i>	0.0123 W[g] ^{-0.378} (n= 13; r ² =0.97)
<i>Catostomus commersoni</i>	0.0909 W[g] ^{-0.731} (n= 105; r ² =0.95)
<i>Centrarchus macropterus</i>	0.0214 W[g] ^{-0.803} (n= 34; r ² =0.95)
<i>Cyprinus carpio</i>	0.0153 W[g] ^{-0.389} (n= 350; r ² =0.96)
<i>Dorosoma cepedianum</i>	0.3682 W[g] ^{-1.307} (n= 26; r ² =0.89)
<i>Erimyzon oblongus</i>	0.2569 W[g] ^{-0.878} (n= 10; r ² =0.95)
<i>Erimyzon sucetta</i>	0.1070 W[g] ^{-0.863} (n= 19; r ² =0.92)
<i>Esox americanus vermiculatus</i>	0.0017 W[g] ^{-0.044} (n= 18; r ² =0.87)
<i>Esox niger</i>	0.0567 W[g] ^{-0.630} (n= 83; r ² =0.96)
<i>Hypentilium nigricans</i>	0.3906 W[g] ^{-1.021} (n= 22; r ² =0.87)
<i>Ictalurus punctatus</i>	0.0146 W[g] ^{-0.346} (n= 256; r ² =0.99)
<i>Lepisosteus osseus</i>	0.3508 W[g] ^{-0.928} (n= 36; r ² =0.99)
<i>Lepomis auritus</i>	0.0154 W[g] ^{-0.577} (n= 33; r ² =0.90)
<i>Lepomis cyanellus</i>	0.0172 W[g] ^{-0.562} (n= 251; r ² =0.91)
<i>Lepomis gibbosus</i>	0.0341 W[g] ^{-0.512} (n= 126; r ² =0.90)
<i>Lepomis gulosus</i>	0.0283 W[g] ^{-0.524} (n= 211; r ² =0.88)
<i>Lepomis macrochirus</i>	0.0144 W[g] ^{-0.612} (n= 879; r ² =0.90)
<i>Lepomis microlophus</i>	0.0498 W[g] ^{-0.761} (n= 102; r ² =0.94)
<i>Micropterus dolomieu</i>	0.1114 W[g] ^{-0.723} (n= 621; r ² =0.92)
<i>Micropterus salmoides</i>	0.0701 W[g] ^{-0.705} (n=1241; r ² =0.96)
<i>Morone americana</i>	0.0212 W[g] ^{-0.613} (n= 149; r ² =0.92)
<i>Morone saxatilis</i>	1.5661 W[g] ^{-0.687} (n= 170; r ² =0.97)
<i>Moxostoma anisurum</i>	1.0441 W[g] ^{-0.819} (n= 29; r ² =0.96)
<i>Moxostoma macrolepidotum</i>	0.0323 W[g] ^{-0.401} (n= 89; r ² =0.96)
<i>Notemigonus crysoleucas</i>	0.1788 W[g] ^{-1.361} (n= 21; r ² =0.81)
<i>Notropis hudsonius</i>	4.0321 W[g] ^{-0.920} (n= 14; r ² =0.89)
<i>Oncorhynchus mykiss</i>	0.0034 W[g] ^{-0.342} (n= 222; r ² =0.93)
<i>Perca flavescens</i>	0.0387 W[g] ^{-0.730} (n= 597; r ² =0.92)
<i>Polyodon spathula</i>	0.0561 W[g] ^{-0.487} (n= 13; r ² =0.96)
<i>Pomoxis annularis</i>	0.0717 W[g] ^{-0.602} (n= 745; r ² =0.91)
<i>Pomoxis nigromaculatus</i>	0.0307 W[g] ^{-0.584} (n= 598; r ² =0.92)
<i>Semotilus atromaculatus</i>	0.1094 W[g] ^{-0.763} (n= 24; r ² =0.92)

compare to its expected growth rate, a well defined metric describing the difference between γ_i and $\bar{\gamma}$ is needed. Perhaps the most straightforward measure of this difference would be the average ratio $\gamma_i/\bar{\gamma}$ over the species' expected size range. In particular,

$$A_i = \frac{\int_{W_l}^{W_u} \gamma_i/\bar{\gamma} dW}{W_u - W_l} = \frac{\int_{W_l}^{W_u} (\gamma_{1,i}/\bar{\gamma}_1) W^{\gamma_{2,i} - \bar{\gamma}_2} dW}{W_u - W_l} \quad (11)$$

where W_l and W_u denote the species lower and upper body weights, respectively. If the species realized growth rate γ_i is on average less than its expected growth rate $\bar{\gamma}$, then $A_i < 1$. Conversely, if the species realized growth rate γ_i is on average greater than its expected growth rate $\bar{\gamma}$, then $A_i > 1$. These calculated ratios could then be used to construct a cumulative distribution function (CDF) to evaluate the overall condition of the species' realized growth within the basin. Using such a CDF, watershed and basin managers and decision-makers could easily determine whether the majority of their surveyed populations are actually maintaining their expected growth rates. These ratio's could also be used to generate maps displaying the actual distribution of species growth rates.

Bioaccumulation of Persistent Organic Pollutants (POPs)

Growth rates of fish affect their rates and levels of chemical bioaccumulation in two different but interrelated ways. Firstly, growth rates determine to what extent fish can biodilute existing chemical body burdens to physiologically safe concentrations or chemical activities. Secondly, because growth is simply the mass balance between feeding/assimilation and total metabolic demands (i.e., total respiration and excretion), growth rates of fish are positively correlated with their realized feeding rates. Thus, although high growth rates would generally indicate that fish can potentially biodilute existing chemical burdens, such rates would also indicate a more rapid uptake of additional chemical burdens in the face of continuing dietary exposures. Although these growth effects are generally unimportant for low to moderate bioaccumulative chemicals (e.g., organic chemicals with octanol/water partition coefficients less than 10^4 or 10^5), such effects can be extremely important for highly bioaccumulative chemicals such as PCBs, dioxins, and mercury.

To illustrate the effects of growth rates on chemical bioaccumulation in fish, consider the following simple bioaccumulation model presented by Barber et (1991 Eq.(31))

$$\frac{dC_f}{dt} = k_1 C_w + \phi C_p - \left(\frac{k_1 + K_e \epsilon}{K_f} + \gamma \right) C_f \quad (12)$$

In this equation,

C_f denotes the fish's whole body concentration ($\mu\text{g/g}$) of the chemical;

k_1 is the chemical's uptake rate (day^{-1}) across the fish's gills;

C_w is the chemical's environmental water concentration ($\mu\text{g/ml}$);

ϕ is the fish's specific feeding rate (g/g/day);
 C_p is the concentration ($\mu\text{g/g}$) of the chemical in the fish's "average" prey;
 ϵ is the fish's specific egestion rate (g/g/day);
 K_e is a thermodynamically based partition coefficient for the chemical in egested feces;
 K_f is a thermodynamically based partition coefficient for the chemical in the fish's whole body;
 γ is the fish's specific growth rate (day^{-1}).

This model assumes that chemical exchange across the gill is by simple diffusion and that the chemical uptake from food and excretion to feces occur by simple thermodynamic chemical partitioning. Although the former assumption is well accepted (Yalkowsky et al. 1973, Thomann and Connolly 1984, Gobas et al. 1986, Gobas and Mackay 1987, Barber et al. 1988, Erickson and McKim 1990, Barber et al. 1991), many of the available fish bioaccumulation models use non-thermodynamically based approaches to describe chemical uptake from food. In particular, these models (Norstrom et al. 1976, Jensen et al. 1982, Thomann and Connolly 1984, Thomann 1989, Madenjian et al. 1993) assume that fish are able to assimilate a constant fraction of the chemical they ingest. In terms of mass fluxes, these models assume that

$$M_d = \alpha_c C_p F \quad (13)$$

where M_d is the fish's chemical uptake from food (g/day); α_c is the chemical's assimilation efficiency; and $F = \phi W$ is the fish's daily feeding rate (g/day). The formulation presented in Eq.(12), however, is equivalent to assuming that the chemical assimilation efficiency α_c , rather than being a physiological constant, is a thermodynamic variable. In particular,

$$\alpha_c = 1 - (1 - \alpha_f) \frac{C_f K_e}{C_p K_f} \quad (14)$$

where α_f is the fish's food assimilation efficiency (Barber et al. 1991 Eq.(30)). In other words, the fish's chemical assimilation efficiency is a decreasing function of its whole body concentration. At equilibrium the fish's chemical assimilation efficiency would therefore be

$$\alpha_c = 1 - (1 - \alpha_f) \frac{BAF_f K_e}{BAF_p K_f} \quad (15)$$

where BAF_f and BAF_p are the steady state bioaccumulation factors for the fish and its prey, respectively. Assuming 1) a nominal food assimilation efficiency of $\alpha_f = 0.825$, 2) a nominal fish lipid content of 5%, and 3) the formulations for K_e and K_f outlined by Barber et al. (1991) and Barber (2002), a fish's chemical assimilation efficiency would therefore be expected to range from near $\alpha_c = 1$ at the beginning of an exposure to

$$\alpha_c = 1 - 0.58 \frac{BAF_f}{BAF_p} \quad (16)$$

at equilibrium. If the fish's and its prey's bioaccumulation factors are approximately equal, then $\alpha_e \approx 0.4$, which agrees with recent findings reported by Moser and McLachlan (2001a, 2001b) for dietary uptake for humans. If the prey's BAF becomes larger than that of the fish, then the fish's chemical assimilation efficiency will increase above $\alpha_e \approx 0.4$. It is more likely, however, that the fish's BAF will exceed that of its prey, in which case the fish's chemical assimilation efficiency will continue to decrease. If the fish's BAF becomes significantly larger than that of its prey, the above expression can even become negative, which implies that food rather than being a net source of chemical becomes a net route of excretion. Refer back to Eq.(13).

To illustrate how growth rates affect the bioaccumulation of organic pollutants in fish, we will now focus our discussion on largemouth bass (*Micropterus salmoides*) that are exposed to constant aqueous exposure concentrations at 15 Celsius. In this case, Eq.(12) is equivalent to

$$\frac{dBAF_f}{dt} = k_1 + \phi BAF_p - \left(\frac{k_1 + K_e \epsilon}{K_f} + \gamma \right) BAF_f \quad (17)$$

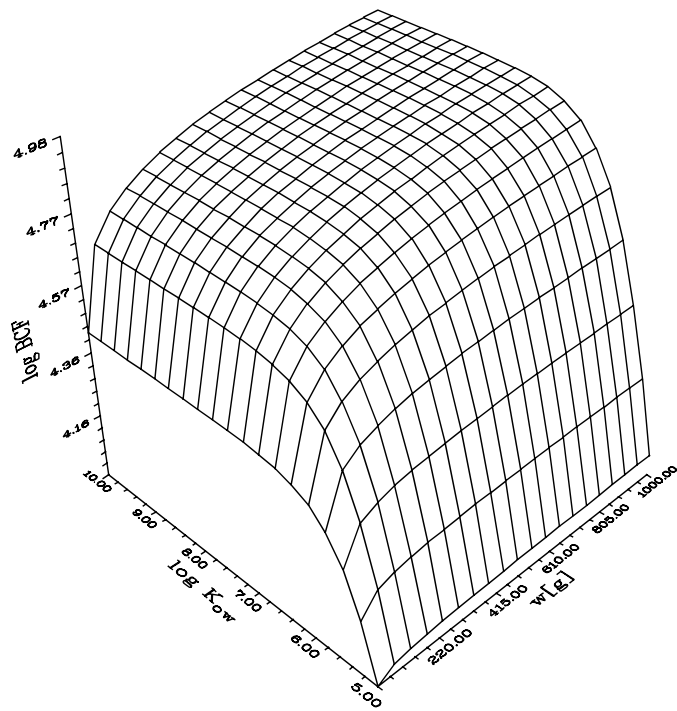
where $BAF_f = C_f / C_w$ and $BAF_p = C_p / C_w$ now denote the realized bioaccumulation factors for the fish and its prey. Using this equation with the Parker-Larkin growth model (i.e., Eq.(7)), the realized BAF for any size of largemouth bass and any persistent organic pollutant (POP) characterized by its octanol-water partition coefficient K_{ow} can be easily generated. For these simulations, daily specific feeding rates ϕ for bass were back-calculated from their estimated daily specific growth rate function $\gamma = 9.06E-02 W^{-0.682}$ using routine respiratory demand estimated from the OXYREF fish oxygen consumption database (CEAM 2002) as outlined in Barber (2002).

Figures 14 and 15 display the realized BAFs for largemouth bass for two different scenarios. In Figure 14, largemouth bass are assumed to be exposed only to polluted surface waters. In this case, the bass's BAFs actually correspond to bioconcentration factors (BCF). Although this exposure scenario is not realistic of actual field exposures, it is presented here to illustrate the effect of growth dilution. In particular, if the bass's growth was zero, their realized BAF/BCF would be expected to be directly proportional to K_{ow} for all chemicals, rather than plateauing for chemical's with K_{ow} greater than 10^7 . In Figure 15, on the other hand, bass are assumed to be feeding on contaminated prey that come to equilibrium with the surrounding water. For this figure the bass's prey BAFs are assumed to be given by the Quantitative Structure Activity Relationship (QSAR) proposed by Mackay(1982), i.e.,

$$BAF_p = 0.0479 K_{ow} \quad (18)$$

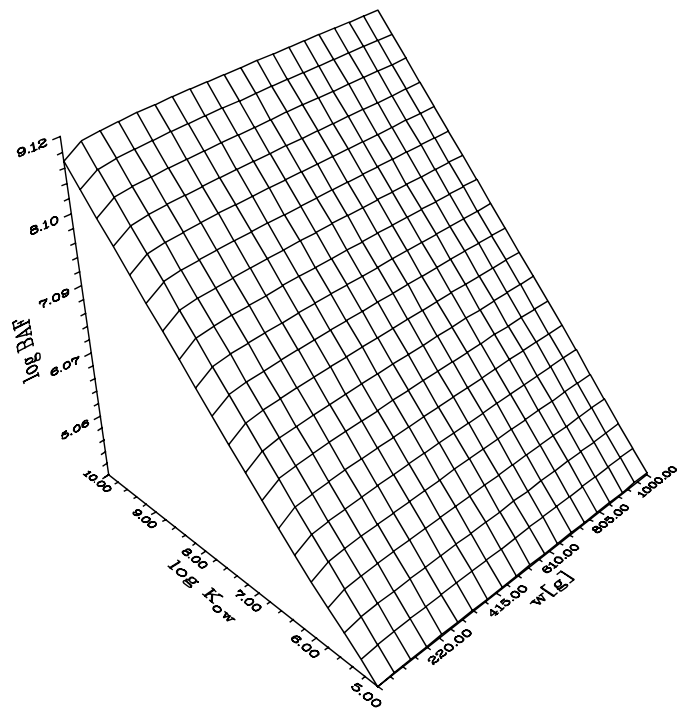
Although growth dilution is still theoretically occurring in these simulations, the effect of growth dilution is completely masked by the bass's dietary uptake.

Both of these results are important since QSAR-based models (e.g., Eq.(18)) are perhaps the most widely used tools currently employed to predict chemical bioaccumulation in fish. Although Figures 14 and 15 clearly demonstrate that biological factors such as size and growth rates have profound effects on the ultimate levels of



Micropterus salmoides

Figure 14. Calculated BAF/BCF for largemouth bass assuming nominal growth and uncontaminated prey.



Micropterus salmoides

Figure 15. Calculated BAF for largemouth bass assuming nominal growth and contaminated prey.

chemical bioaccumulation in fish, QSAR models by their very construction assume that only physico-chemical properties of the pollutants of concern greatly influence these levels. Because other growth rate and size-dependent processes such as dietary compositions and “reproductive excretion” via toxicant transfer to eggs and sperm were ignored even in Eqs.(12) and (17) for simplicity of discussion, it is important to realize that fish size and growth rates would be expected to influence the bioaccumulation patterns of fish in additional ways to those discussed above.

Interrelationship Between Growth Rates and Mortality Rates

Numerous studies (Damuth 1981, Peters and Raelson 1984, Juanes 1986, Robinson and Redford 1986, Boudreau and Dickie 1989, Gordo and Duarte 1992, Randall et al. 1995, Dunham and Vinyard 1997, Steingrímsson and Grant 1999) have shown that the population densities of vertebrates are generally correlated with their mean body size. In particular,

$$N = a W^{-b} \quad (19)$$

where N is the population density (inds/area) of the species or cohort and W is the mean body weight of that species or cohort. Although an interspecific analysis of data for a variety of fish by Randall et al. (1995) suggested a mean exponent close to unity, data reported by Boudreau and Dickie (1989) and Gordo and Duarte (1992) for individual fish species suggest an average exponent closer to 0.75. In either case, an expression for a species' total mortality rate can be obtained by differentiating Eq. (19) as follows

$$\frac{dN}{dt} = -b a W^{-b} \left(W^{-1} \frac{dW}{dt} \right) = -b N \hat{\gamma} \quad (20)$$

where $\hat{\gamma}$ is the species “specific growth” rate. From this equation, it immediately follows that the species' total mortality rate is simply $\mu = b \hat{\gamma}$. Readers interested in detailed discussions concerning the underlying process-based interpretation and general applicability of this result should consult Peterson and Wroblewski (1984), McGurk (1993, 1999) and Lorenzen (1996).

The “specific growth” rate $\hat{\gamma}$ in Eq.(20) is not automatically synonymous with the somatic or physiological specific growth rate γ in Eqs. (7) - (10). In particular, because $\hat{\gamma}$ simply quantifies how the mean body weight of the species or cohort changes in time, there are at least three different possibilities for what this parameter actually models or represents. If the physiological growth of individuals actually determines most of the species' or cohort's mean body size dynamics, then $\hat{\gamma}$ should obviously be identical to γ . However, it is also possible that the species' or cohort's body size dynamics is primarily determined by predatory or environmentally induced mortality that is specific to certain size ranges within that species or cohort. In this case, $\hat{\gamma}$ would be expected to be largely independent of γ . Lastly, the species' or cohort's mean body size dynamics could be determined by a mixture of these physiological and ecological processes. Of these alternatives, however, there are at least four lines of reasoning that would suggest that the most likely situation is in fact that $\hat{\gamma} = \gamma$. In this case, the species' or cohort's mortality rate is given by

$$\mu = b \gamma_1 W^{\gamma_2} \quad (21)$$

The first observation that strongly suggests that $\hat{\gamma} = \gamma$ is the simple fact that Eq.(21) describes the allometric dependence of estimated mortality on body weight equally well for both forage and predatory fish species (see Lorenzen 1996). Because physiological growth is obviously the one process that these fish have in common for generating mean body weight dynamics, it seems only logical to conclude $\hat{\gamma} = \gamma$. Additionally, because mortality rate exponents for fish in pond/cage aquaculture, where predatory and environmentally imposed mortality are presumably minimized, are typically not significantly different from those estimated for fish in natural ecosystems (see Lorenzen 1996), it again seems logical to conclude that $\hat{\gamma} = \gamma$. The remaining arguments suggesting that $\hat{\gamma} = \gamma$, however, relies heavily on the fact that the exponent γ_2 of a species-specific growth function is generally negative, which then implies that the species' or cohort's mortality rate is a decreasing function of increasing body size.

Mortality rates as decreasing functions of increasing body size are certainly consistent with intuitive notions concerning the survivorship and mortality for most fish species that are either benthivores, insectivores, or piscivores. For such species, large individuals generally have a significant competitive advantage over smaller individuals for both prey and spatial resources (Garman and Nielsen 1982, East and Magnan 1991). This large size competitive advantage, in turn, would be expected to translate into lower mortality rates for large individuals as compared to smaller individuals. In terms of predator-prey dynamics, size-dependent competitive abilities would be expected for two reasons. The first of these is based on the observation that reactive distances, swimming speeds, and territory sizes of fish tend to be positively correlated with their body size (Minor and Crossman 1978, Breck and Gitter 1983, Wanzenböck and Schiemer 1989, Grant and Kramer 1990, Miller et al. 1992, Keeley and Grant 1995, Minns 1995). Thus, given two differently sized predators competing for the same potential prey, one would expect that the larger predator is more likely to encounter that prey than is the smaller. Because prey handling times are generally inversely correlated with body size (Werner 1974, Miller et al. 1992), one would also expect that having encountered the prey, the larger predator would dispatch the prey and resume its foraging more quickly than the smaller predator.

Another argument or justification for $\hat{\gamma} = \gamma$ is based on intuitive notions concerning the predation of forage fish by piscivores. Numerous food web studies have shown that there is generally a strong positive correlation between the body sizes of piscivorous fish and the forage fish that they consume (Parsons 1971, Lewis et al. 1974, Timmons et al. 1980, Gillen et al. 1981, Knight et al. 1984, Moore et al. 1985, Stiefvater and Malvestuto 1985, Storck 1986, Jude et al. 1987, Johnson et al. 1988, Yang and Livingston 1988, Brodeur 1991, Elrod and O'Gorman 1991, Hambright 1991, Juanes et al. 1993, Mattingly and Butler 1994, Hale 1996, Madenjjan et al. 1998, Margenau et al. 1998, Mittelbach and Persson 1998, Bozek et al. 1999). If W_l and W_u denote the lower and upper body weights, respectively, of forage fish generally consumed by a population of piscivores, one would expect the mortality rate of fish just entering the predator's prey window to be greater than the mortality rate of the larger fish leaving the predator's prey window. Clearly, this expectation is satisfied if $\hat{\gamma} = \gamma$ with $\gamma_2 < 0$.

Forage fish that have attained sufficient body size to escape predation and piscivores are faced with the common dilemma of having only finite prey resources within any given geographical area that they inhabit. When such resources become limiting and dispersal is possible, many of the effected individuals will emigrate from that specific geographical area. Such migrations, however, from the perspective of sampling community populations or

biomasses are indistinguishable from mortality. Consequently, one would expect that the effective “mortality” rates of large forage fish and piscivores to be directly related to their growth rates. Moreover, one might also expect that larger individuals are less likely to migrate than are smaller individuals not only because larger individuals can better protect established foraging territories but also because of the relative metabolic demands of dispersal. In this case, the “mortality” rates of larger fish would again be expected to be less than the “mortality” rates of smaller fish.

Having justified the assertion that a species growth rate function directly determines its population mortality rate, we can now utilize that relationship to project short and intermediate term future population densities. Assume, for example, that given a cohort’s current population size and growth function at time t_0 , one wants to project the cohort’s population density at some future time t . From Eq.(20) it immediately follows that

$$\begin{aligned}\frac{dN}{dt} &= -b N \left(W^{-1} \frac{dW}{dt} \right) \\ \frac{dN}{N} &= -b \frac{dW}{W} \\ \ln \frac{N}{N(t_0)} &= \ln \left(\frac{W}{W(t_0)} \right)^{-b}\end{aligned}\tag{22}$$

When Eq.(8) is now substituted into this expression, the resulting equation can be manipulated to yield

$$N(t) = N(t_0) \exp \left(\ln \frac{W(t_0)^b}{(W(t_0)^{1-\beta} + \alpha (1-\beta) (t-t_0)^{b/(1-\beta)})} \right)\tag{23}$$

5. Models and Analysis Tools for Regional Assessment

This chapter summarizes different modeling approaches and analysis techniques that can be used to construct an integrated, multi step analysis of fish health for a watershed to regional scale assessment. Implicit in this discussion is the understanding that the actual implementation of such spatially explicit assessments can be straightforwardly facilitated with Geographical Information System (GIS) technology that not only can analyze the output from a network of spatially distributed models, but also can be used to formulate and execute that network of models.

5.1. Projecting Land Cover Trends

Projecting Impervious Cover Trends

Nonpoint source pollution (NPS), or pollution from diffuse sources such as urban/suburban areas and farmlands, is now recognized as the primary threat to water quality in the United States (USEPA 1994). NPS pollution threats from urban and suburban development are increasing as the U.S. population rises. Along with this increase in development comes an increase in impervious surfaces, areas where infiltration of water into the underlying soil is prevented. Roadways and rooftops account for the majority of this impervious area.

Research in recent years has consistently shown a strong relationship between the percentage of impervious cover in a drainage basin and the health of the receiving stream. In a review of research on impervious cover, Schueler (1994) concluded that despite a range of different criteria for stream health and the use of widely varying methods and a range of geographic conditions, stream degradation consistently occurred at relatively low levels of imperviousness (10 to 20%). A recent survey of Maryland streams found that brook trout (*Salvelinus fontinalis*), a species very sensitive to water temperature, were not present in any streams where the watershed was greater than 2% impervious cover. The strength of the relationship between stream health and impervious cover is not surprising since impervious cover contributes directly to hydrologic changes that degrade waterways and channels pollutants directly into waterways, thereby preventing the processing of pollutants in soils. In addition impervious cover is significantly warmer in the summer than the vegetated cover that it replaces, resulting in higher stream temperatures during summer months. Arnold and Gibbons (1996) strongly advocate use by planners of impervious surface coverage as an indicator for water resource protection in urbanizing areas.

The goal of the Office of Research and Development (ORD) Regional Vulnerability Assessment (ReVA) Program is to develop and demonstrate an approach to quantify and communicate regional vulnerabilities so that risk management activities (both restoration and risk reduction) can be targeted and prioritized (Smith 2000). The geographic area of interest for this program is EPA's Region III, which includes five states in the mid-Atlantic area of the U.S. Impervious cover is proposed as an indicator of aquatic conditions for subwatersheds throughout this region. Although there is a strong relationship between impervious cover and stream health, the utility of impervious cover as an indicator is a function of the ease and accuracy for estimating it.

A number of approaches have been used for measuring and estimating impervious cover. While ground-

based surveys can be extremely accurate, such surveys are typically prohibitively expensive for anything other than small areas. Readily available and higher resolution satellite imagery is providing rapidly expanding use of remote sensing techniques for impervious cover estimation. The National Land Cover Data 1992, developed for the Multi Resolution Land Characteristics Consortium, identifies urban areas based on impervious cover. A number of relationships between population density and impervious cover have been developed (Stankowski 1972, Graham et al. 1974, Hicks and Woods 2000). City planners often use land-use zoning to do rapid estimates of total impervious area (TIA). Both population density and land-use zoning based estimation methods provide a means for projecting increase in impervious cover in a watershed using either projected population growth or build-out scenarios. Population density data are available from the U.S. Census Bureau, but no comprehensive data base of land use zoning is available for the region.

The objective of this section is to compare and evaluate the utility of different approaches for estimating and projecting impervious cover. The focus is on methods that would be useful in doing region-wide assessments. Methods evaluated include: empirical relationships using population density data; analysis of categorized, land-cover data; use of impervious cover coefficients and parcel level property records; and the use of a combination of data sources (Vogelmann et al. 1998, Vogelmann et al. 2001).

Materials and Method

Test Data Set Development

An impervious cover test data set for 56, 14-digit subwatersheds in Frederick County, MD was developed using DOQQs from the U.S. Geological Survey (USGS) taken in 1989. DOQQs are computer-generated versions of aerial photographs that have been orthorectified so they represent true map distances. They are available for any area of the country from the USGS. The DOQQs have a 1 m² resolution and their analysis provides a high level of accuracy in the determination of impervious cover at a subwatershed scale (Zandbergen et al. 1999). A point sampling method with a 200 m regular grid was used to evaluate the impervious area; a detailed description of the methodology and quality assurance assessment is provided in Bird, et al. (2000). The DOQQ sampling yielded an average of approximately 800 sample points per 14-digit HUC—with a total of 43,816 points in the study area. Quality assurance objectives for these data were to obtain a measure of the %TIA within +/- 1% for watersheds with a TIA of less than 10% of the total watershed area and within 10% of the TIA for watersheds with a TIA greater than 10%.

The greatest potential introduction of error identified in the quality assurance assessment was from an individual analyst's interpretation of the images. In order to control this error, sampling points overlaid on the DOQQs were characterized by two independent analysts as either pervious or impervious. A third individual served as a quality assurance checker. The quality assurance checker imported the results of the first two analysts into a program that compared the two grids on a point-by-point basis. Points with discrepancies in categorization of results by the first two analysts were reviewed by the quality assurance checker, who made the final determination of assignment of categories.

Impervious cover is not a single homogenous quantity. Generally, paved surfaces and buildings fall

unambiguously under the definition of impervious surfaces. Ambiguity can exist, however, even for these categories since there is now a pervious asphalt paving material that allows some infiltration. Other areas, such as dirt and gravel roads and parking lots, railroad yards and quarries that may not be coated with manmade, impervious materials are in many instances so heavily compacted as to be functionally impervious. Actual surface material in these cases is often hard to determine from the aerial photography. These features were categorized as impervious in our interpretation of the photography.

Impervious Cover Estimation

Impervious cover is a result of human settlement, and therefore, population density should be a reasonable predictor of it. Use of population density as a means to estimate impervious cover is attractive since it provides a rapid technique for generating a quantitative estimation of both present and projected land surface cover. Stankowski (1972), Graham, et al. (1974) and Hicks and Woods (2000) developed empirical relationships with different functional forms to relate population density to percent impervious cover. Stankowski (1972) developed his relationship using county scale data from New Jersey with population densities ranging from 120 to 13,800 persons/mi². The impervious cover was estimated from land use data available from the state planning office. Graham, et al. (1974) evaluated selected census tracts for the Washington, DC metropolitan region where population densities ranged from 350 to 53,300 persons/mi² and developed impervious cover estimates ranging from 14% to 98% using 1:50,000 aerial photography. Hicks and Woods (2000) developed their relationship based on data for the greater Vancouver, BC area using impervious cover estimated from land use zoning categories. All three relationships are summarized in Table 14.

Table 14. Empirical relationships between population density and impervious area.

Source	Relationship
Stankowski (1972)	$\%TIA = 0.0218 P^{1.206} - 0.100 \log P$
Graham et al. (1974)	$\%TIA = 91.32 - 69.34 (0.9309^{P/640})$
Hicks and Woods (2000)	$\%TIA = 95 - 94 \exp(-0.0001094 P)$

Land use and land cover data are frequently used as a basis for estimating impervious area. Categorized land use and land cover systems derived from remote sensing data define developed land cover classes based on the fraction of impervious cover in a specified area (Anderson et al. 1976, Vogelmann et al. 1998). Sleavin et al. (2000) generated percent impervious coefficients for generalized land use and land cover classes developed from 30 m Landsat Thematic Mapper imagery, as well as from land use and parcel size class data. The 1992 National Land Cover Data (NLCD 92) is a categorized land cover data set for the continental United States based on 30 m Thematic Mapper data from the early 1990s plus a variety of auxiliary data sources (Loveland and Shaw 1996, Vogelmann et al. 1998). The Frederick County, MD impervious surface data, derived from the DOQQs, were used to develop estimates of the percentage of impervious surface for each NLCD 92 category based on data for the entire county and the estimated contribution of each class to the TIA. These coefficients were then used with the land cover

data to see how well these values were able to estimate impervious surface values for individual watersheds.

Researchers have also developed coefficients of impervious cover based on land use and zoning classes. Arnold and Gibbons (1996) reported coefficients for impervious cover based on residential lot size, industrial uses, general commercial use and shopping centers. Data from property records for Frederick County (Maryland Office of Planning 1999) were used in combination with these coefficients to estimate impervious surface area by watershed. Only properties listing a construction date prior to 1990 were included in this analysis since the aerial photographs were from 1989.

Finally, three different data types were combined to estimate impervious cover. Data types used for this estimation were: 1) population density from block level census data, 2) the commercial-industrial and quarrying-mining land cover category from NLCD 92, and 3) interstates and major US highway coverages. Population density served as an indicator of impervious cover generated by residential development. The residential contribution was estimated from the Hicks and Woods (2000) relationship. The two NLCD 92 categories provided information on the contributions from major manufacturing, commercial, and quarrying areas that can be more reliably detected by satellite imagery. These areas were assumed to be 90% impervious (the definition of the commercial-manufacturing category is defined as 80% or greater for the NLCD 92). The highway coverages provided information on impervious cover contributed by major highways (interstate and other US highways) that aren't necessarily related to local residential development. Highway contribution was calculated based on the number of lanes and a 12 ft lane width.

Results

Impervious cover results from the DOQQ interpretation for Frederick County, MD are illustrated in Figure 16. The highest intensity impervious area centers on the town of Frederick, with the watershed containing most of the town having 23% TIA. Only three of the Frederick County watersheds have impervious cover greater than 10%. The mean value is 5.1% TIA and the median is 4.6 % TIA. Data by 14-digit HUC are presented in Table 15. This table also indicates whether the watershed was totally contained within Frederick County or only partially located within the county. The area of the watershed contained within the county is also presented in the table. An ideal data set for testing impervious cover estimation for use as an environmental indicator would have more representatives in the 10 % to 20% range where stream impairment is initially observed. Accurately identifying watersheds in the 5% to 10% range may be even more critical, however, since these are ones that, while not yet significantly impaired, may benefit from good preventative planning in the near future.

Figure 17a shows the %TIA predicted by the relationships developed by Stankowski (1972), Graham, et al. (1974), and Hicks and Woods (Hicks and Woods 2000). Also shown in this figure are the data for the combined Frederick County watersheds and the Washington, DC census tracts. Whereas the Stankowski (1972) relationship seriously under predicts %TIA at population densities greater than 1000 persons/mi², the Graham et al. (Graham et al. 1974) relationship seriously over predicts %TIA for population densities under 500 persons/mi². Although the Hicks and Woods (2000) relationship appears to provide the best fit overall, closer inspection of the data for population densities under 2000 person/mi² (Figure 17b) indicates that this function

Measured Impervious Cover Frederick County, MD

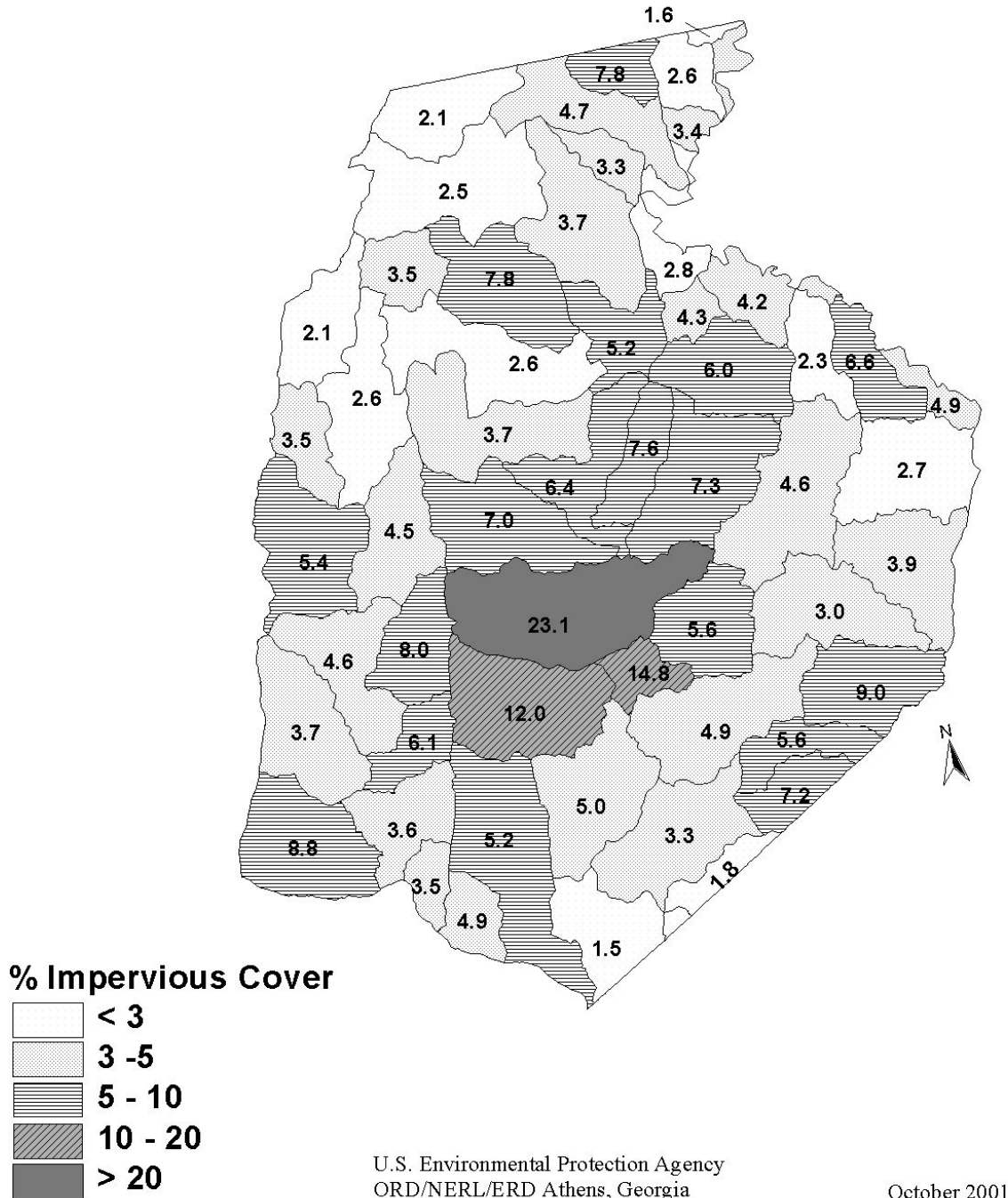


Figure 16. Impervious Cover Results from the DOQQ Interpretation for Frederick County, MD.

Table 15. Impervious Cover Interpretation of Frederick County, MD by HUC.

14-digit HUC	Impervious Cover (% TIA)	Area (Sq Mi)	HUC within County
02070009040124	1.6	0.9	Completely
02070009040128	3.4	4.4	Partially
02070009030101	2.1	11.0	Completely
02070009030104	4.7	13.2	Completely
02070009030102	7.8	5.5	Completely
02070009040127	2.6	5.8	Completely
02070009060176	2.5	21.6	Completely
02070009060177	3.7	18.0	Completely
02070009060201	3.3	4.7	Completely
02070009060202	2.8	6.6	Partially
02070008010026	2.1	10.8	Partially
02070009060227	7.8	16.5	Completely
02070009060226	3.5	6.9	Completely
02070008010028	2.6	15.2	Completely
02070009060228	2.6	18.3	Completely
02070009050171	4.2	8.0	Partially
02070009060204	5.2	9.4	Completely
02070009060203	4.3	3.5	Completely
02070009060205	3.7	18.3	Completely
02070008010027	3.5	7.3	Completely
02070009050170	2.3	7.3	Completely
02070009060251	6.0	14.0	Completely
02070009050169	6.6	8.3	Partially
02070009060206	6.4	12.3	Completely
02070009050168	4.9	3.7	Partially
02070008010029	5.4	17.3	Completely
02070008010030	4.5	12.8	Completely
02070009060208	7.6	8.1	Completely

Continued on next page

Table 15. (continued) Impervious Cover Interpretation of Frederick County, MD by HUC.

14-digit HUC	Impervious Cover (% TIA)	Area (Sq Mi)	HUC within County
02070009060252	7.3	19.1	Completely
02070009060209	7.0	17.8	Completely
02070009070280	4.6	21.1	Completely
02070009070276	2.7	16.3	Partially
02070008010032	8.0	10.2	Completely
02070008010031	4.6	14.1	Completely
02070009060210	23.0	28.3	Completely
02070009070278	3.9	15.1	Partially
02070008010036	3.7	15.9	Partially
02070009070286	5.6	12.3	Completely
02070009070283	3.0	15.8	Completely
02070009080301	12.0	20.0	Completely
02070009080302	14.8	5.1	Completely
02070008010035	6.1	6.5	Completely
02070009080305	4.9	19.4	Completely
02070009080303	9.0	13.6	Completely
02070009080306	5.0	17.1	Completely
02070008010037	8.8	17.4	Partially
02070008010052	5.2	24.0	Completely
02070008010038	3.6	10.6	Completely
02070009080326	5.6	7.1	Partially
02070009080330	3.3	17.3	Completely
02070009080327	7.2	6.6	Partially
02070008010039	3.5	4.0	Completely
02070008010051	4.9	5.7	Completely
02070009080328	1.8	4.2	Partially
02070009080308	1.5	11.5	Partially
02070008020076	0.0	0.7	Partially

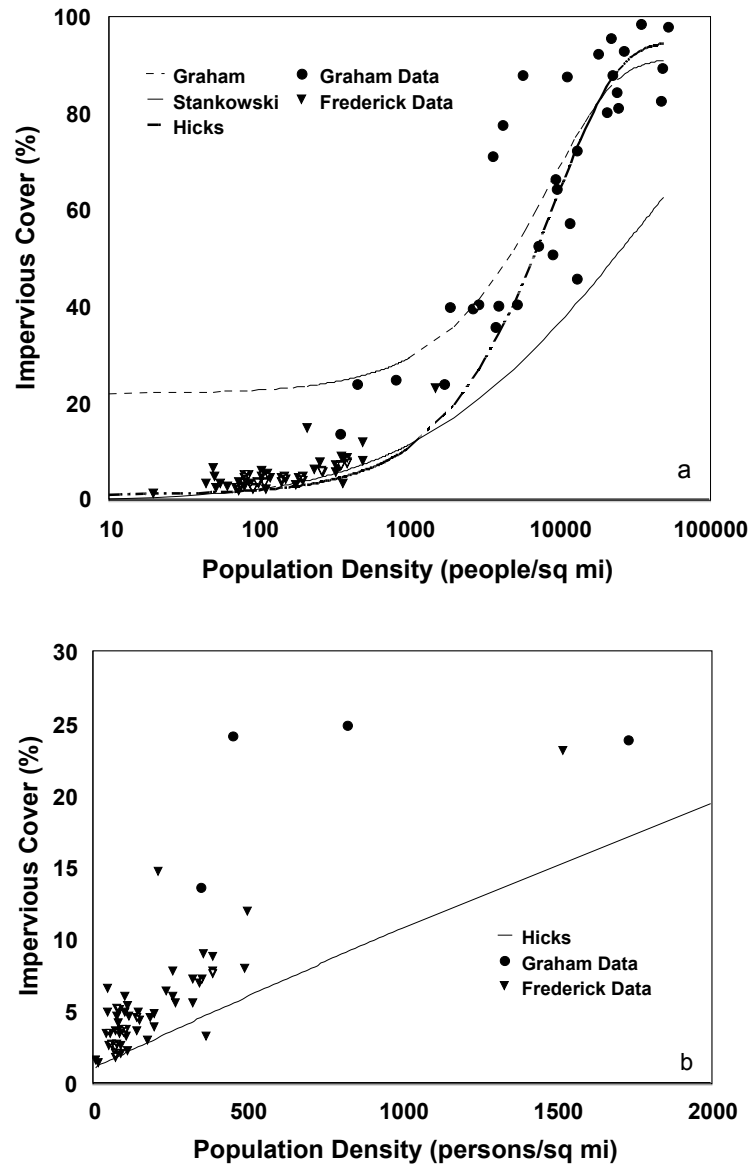


Figure 17. The three relationships between population density and %TIA presented in Table 14 are shown in Part a (top figure above) along with data collected for this study in watersheds in Frederick County, MD and by Graham (1974) for census tracts in Washington, DC. Part b (bottom figure above) shows the response of the Hicks and Woods (2000) relationship for population densities less than 2000 persons/sq mi compared to data presented on a linear scale.

consistently underestimates %TIA within this range. This fact is important since these population densities are of particular interest in development of an environmental indicator. On average, the Hicks and Woods (2000) relationship underestimated the impervious cover for Frederick County by 2.2%

Impervious surface coefficients developed for the NLCD 92 land cover categories for Frederick County as a whole are summarized in Table 16. The percentage of the category estimated as impervious is the percentage of the points sampled from the DOQQs located in a specific land cover class that were categorized by analysts as impervious. The sample size is the number of the DOQQ sampling points that were geographically located within the specific land cover class. The final column of Table 16 is the percentage of the sampling points in Frederick County that were categorized as impervious that were located in the cells of that land cover category. Figure 18 illustrates the percentage of impervious cover points found in the Anderson, et al. (1976) Level 1 land cover categories. Only 23% of the sampling points categorized as impervious in Frederick County are located in cells of the developed land cover categories and over 50% are located in the agricultural categories. Frederick County is a suburban county and the land cover data does not include a category that picks up a substantial fraction of very low density development. To be classified as low density residential, a 30 m cell must include at least 30% impervious cover. Figure 19 shows the amount of developed residential land in different lot size categories (Maryland Office of Planning 1999) and total land in the residential cover classes from the NLCD 92 data. The amount of residential land identified by the NLCD 92 data is consistent with the acreage in residences on lots less than about ½ acre. Larger lot residential properties are not identified as residential areas by the NLCD 92 data set and are frequently classified as agricultural or forested.

Table 16. Impervious Cover for NLCD 92 Land Cover Categories

Land Cover Category	Percentage of the Category Impervious	Sample Size	Percent of Impervious Area in Frederick County Accounted
low density residential	42	990	16.9
high density residential	77	76	2.4
commercial/industrial	57	156	3.6
quarries/mines/gravel pits	62	117	2.9
transitional barren	17	29	0.2
deciduous forest	2	11159	9.1
evergreen forest	4	697	1.1
mixed forest	5	3400	6.9
hay/pasture	5	23497	47.7
row crops	8	2663	8.6
other grasses	9	33	0.1
woody wetland	3	368	0.4
herbaceous wetland	1	138	0.1

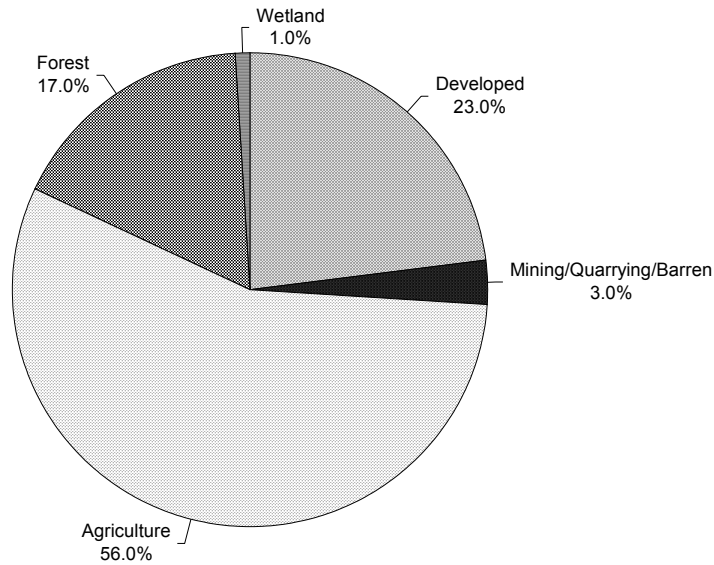


Figure 18. The percentage of impervious cover points sampled from aerial photographs in Frederick County, MD located in land-cover cells summarized by Anderson Level 1 categories.

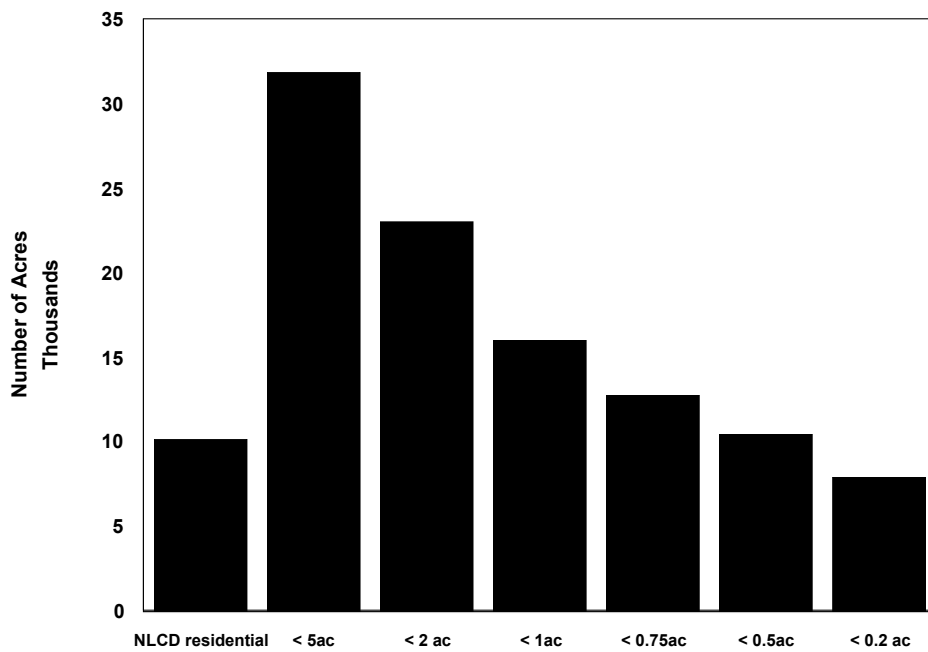


Figure 19. Acreage categorized as residential (combined high and low density) in the NLCD 92 data (NLDC residential) and by residential lot size category from property tax records for Frederick County, MD. The labels for data from the property tax records indicate all the residential lots that are less than the indicated number of acres per unit of housing – e.g., < 5 ac is the sum of all properties in the tax records that are on lots of less than 5 acres per housing unit.

Impervious surfaces were estimated for the 56 individual 14-digit HUCs in Frederick County based on the coefficients in Table 16. Figure 20 shows measured and estimated (from NLCD 92 coverage and these coefficients) %TIA for each watershed in Frederick County. Since the impervious surface coefficients were derived from the data for the whole county, on average the impervious cover estimates are expected to match closely the measured data. The mean error between estimated and measured values is 0.2% TIA. Figure 20 also indicates that using these coefficients, %TIA is overestimated for low impervious cover watersheds and underestimated for the more developed watersheds in the county. The mean absolute error for Figure 20 data is 1.4%.

Results from the use of coefficients of impervious cover by land use class as a method for estimating impervious cover are illustrated in Figure 21. Generally, the estimates for impervious cover are low except in the over 10% impervious cover areas. The over estimates arise from large acreage, commercially zoned properties that have been built on but are not fully developed. The property data base does not include records for publically owned and other tax-exempt properties, nor does this method account for roadway areas.

Accuracy of estimates of impervious cover based on combining the Hicks and Woods (2000) population density, estimates of industrial and commercial contributions from the NLCD 92 and contributions from highways (Interstates and other major U.S. highways) are illustrated in Figure 22. Figure 22 compares the estimated impervious cover using the combined data set to the measured values for Frederick County. The straight line indicates a one to one match between the estimated and measured %TIA values. Overall, this technique underestimated impervious cover by 0.8% TIA with an average, absolute error of 1.4 %TIA. This estimate was obtained without fitting to the test data set. For Frederick County as a whole, the residential area calculated from population density contributed 65% of the imperviousness, commercial/industrial land cover from the NLCD contributed 25%, the major highways contributed 6% and quarrying and mining contributed 4%.

Summary and Conclusions

Population density is a good basis for screening level estimation of impervious cover. The exponential relationship of Hicks and Woods (2000) captures the general shape of the relationship between population density and impervious cover, but somewhat underestimates the impervious cover. The other relationships do not adequately characterize the relationship over the full range of impervious area.

Combining information from multiple data sources provided the best approach to calculate a reasonably accurate impervious cover indicator that can be calculated quickly for large areas. Use of NLCD coverage that identifies commercial, manufacturing, mining and quarrying areas along with road network information effectively augmented the population-based relationship with identification of non-residential sources of impervious cover. The categorized NLCD data, however, does not adequately quantify impervious cover since larger lot, suburbanized areas where initial degradation of water quality may be occurring are not identified as developed classes. Impervious area coefficients for agricultural and forested categories that account for the majority of impervious cover appear to be a function of population density. Use of impervious area coefficients with size of property and type of land use also do not appear to accurately characterize percentage impervious area.

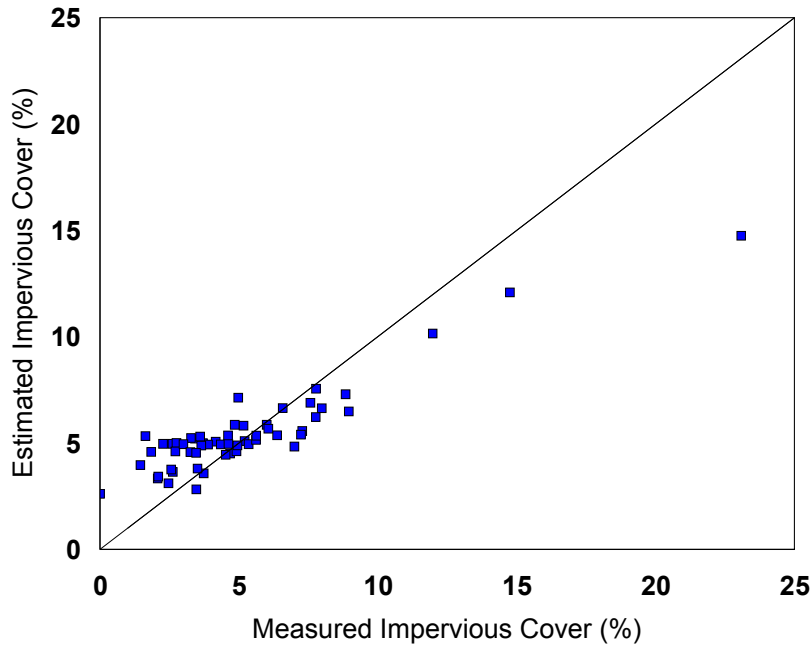


Figure 20. Impervious cover for Frederick County, MD watersheds measured from aerial photographs versus that estimated from categorized satellite imagery and category coefficients developed from county wide data.

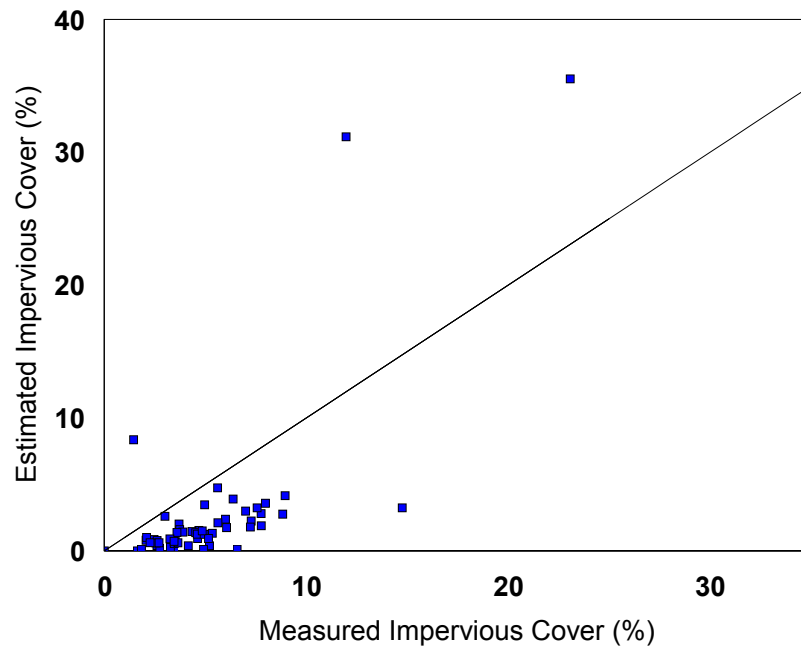


Figure 21. Impervious cover for Frederick County, MD watersheds measured from aerial photographs versus that estimated from property data and impervious coefficients based on lot sizes and land use types.

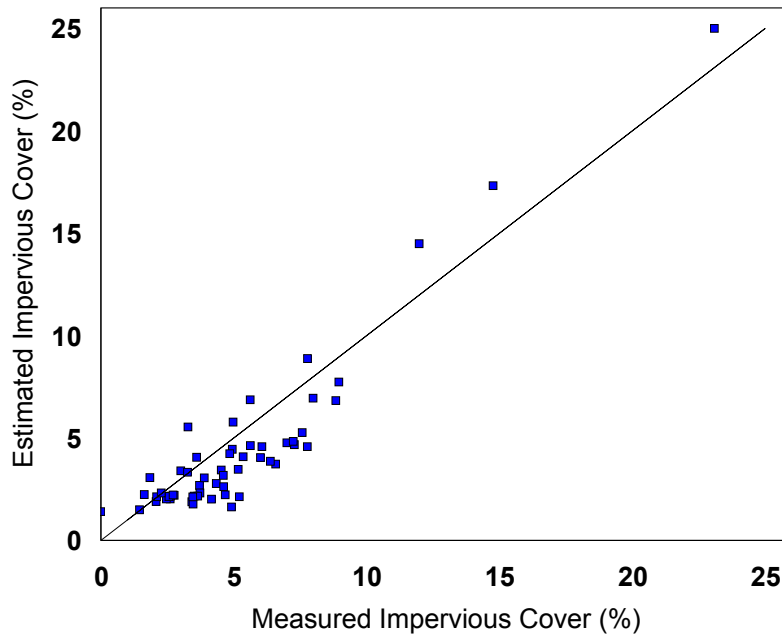


Figure 22. Impervious cover for Frederick County, MD watersheds measured from aerial photographs versus that estimated from a combination of data, including U.S. Census population density, manufacturing and industrial areas from categorized satellite imagery, and major highway networks from U.S. Department of Transportation.

5.2. Hydrology

5.2.1. Methods for Projecting Baseflow

The Groundwater Modeling System (GMS) MODFLOW flow and RT3D transport models can be used to predict future baseflow rates and nitrogen loads into each reach of every drainage system within the Albemarle-Pamlico basin, based on recharge and surficial nitrogen loading estimates provided by the BASINS NPSM (HSPF) model as described below.

The GMS model runs proceed as follows:

- Design a three-dimensional, finite-difference grid, aligned perpendicular and parallel to the Albemarle-Pamlico basin axis, with uniform cell spacing size dictated by limits of available computational resources;
- Assign distributed geologic properties, such as hydraulic conductivity(K), porosity(n), and storativity(S), by importing datasets generated by a Visual Basic geologic characterization application using USGS borehole log data and NCSC bathymetric data to define terrestrial aquifer structure and sub-estuary marine aquifer structure, respectively;

- Assign precipitation recharge (N) and nitrogen concentrations at the water table (c_N), assumed uniform within a given 8- or 11-digit HUC, by importing an ArcView HUC shapefile containing NPSM recharge and water table concentration fields, and mapping the fields to GMS recharge and concentration attributes;
- Assign well discharge rates by importing an ArcView county shapefile containing a discharge field, constructed from the USGS GWSI database and from well records made available by state environmental agencies, and mapping well discharge to GMS attributes;
- Import the BASINS rfl shapefile for the Albemarle-Pamlico basin, modified to include fields for streambed elevation, mean stream stage, and vertical streambed conductance in each reach, and map the fields to GMS model attributes;
- Assign initial and boundary hydraulic heads by importing a grid generated in ArcInfo using USGS GWSI data;
- Assign first-order chemical reaction rate coefficients (λ) for nitrogen transformation.

Prior to execution of the flow and transport models in predictive mode, the models must be calibrated. Recharge and nitrogen water table load estimates from the NPSM simulation can be assumed to be known and invariant during the calibration procedure. Calibration involves variation of certain GMS model parameters until observed baseflows and stream nitrogen concentrations, obtained from the last 5-yr period of record, are matched at selected USGS gaging and sampling stations to within some acceptable error tolerance. Parameters that affect steady-state flow and transport are varied during a steady-state calibration, while those influencing transient flow and transport are adjusted during a subsequent transient calibration. Details of the calibration procedure are as follows:

- Well discharge, streambed elevation, streambed conductance, and boundary heads are assumed to be known and invariant;
- Hydraulic conductivity (K), porosity (n), and storativity (S) are varied in proportion to one another, constrained only by the subsurface geometry imposed by the Visual Basic geologic characterization model;
- For the steady-state phase of calibration, only K and n are varied during execution of MODFLOW and RT3D, respectively; these parameters are varied until observed time-averaged baseflows and nitrogen concentrations at selected gaging stations are matched to within some acceptable tolerance;
- For the transient phase of calibration, only S , λ , and stream stage are varied during execution of MODFLOW and RT3D, respectively; the parameters are changed until errors associated with matching baseflow and nitrogen time series average, over time, to be within some acceptable tolerance;
- Constant stage conditions are maintained in every reach during steady-state flow calibration, but these heads are allowed to vary during the transient flow calibration.

Observed baseflows are obtained from daily streamflow data using the HYSEP baseflow separation code, with observed nitrogen contributions from baseflow estimated according to nitrogen signatures characteristic of surface water and groundwater within the reach drainage. USGS data that will likely prove useful for estimating such signatures include:

- a series of surface-water samples collected at primary and secondary USGS surface-water sites during the rise and recession stages following a precipitation event, and analyzed for CFCs and tritium to determine residence time and surface water source;
- the amount of nitrate in surface water derived from ground-water discharge estimated on the basis of the chemical characteristics of ground water and from recharge rates; and
- relative streamflow contributions from surface runoff and ground-water discharge determined from CFC and tritium measurements according to the chemical signatures associated with ground water and surface recharge.

Following calibration, the models can be run in predictive mode using actual precipitation input and nitrogen recharge values estimated from HSPF using the most likely future land-use scenario. Ideally, Monte Carlo methods can be used to quantify uncertainty in future baseflow and nitrogen load predictions caused by uncertainty in geologic structure at the unresolved catchment scale. However, synthesis of multiple realizations, particularly over the 28,000-mi² Albemarle-Pamlico drainage basin, would quickly overwhelm our current computational resources. Future extensions of the BASE research should include such Monte Carlo simulation to assess the spatial distribution of prediction error, and help to pinpoint locations where measurement of catchment scale geologic structure would most improve the assessment of ecosystem sustainability.

5.2.2. Predicting Regional Hydrology - HSPF

HSPF (**H**ydrocomp **S**imulation **P**rogram-**F**ortran) is a comprehensive watershed simulation model that has its origins in the Stanford Watershed Model developed by Crawford and Linsley (1966). HSPF is frequently cited in the literature as one of the first comprehensive watershed models and is designed to simulate all water quantity and water quality processes that occur in a watershed, including sediment transport and movement of contaminants. HSPF can be applied to most watersheds that possess the requisite meteorologic and hydrologic data. Although usually classified as a lumped parameter model, it can simulate spatial variability by dividing the basin into hydrologically homogeneous segments and using different meteorologic input data and watershed parameters for each segment. HSPF includes both fitted parameters as well as parameters that can be measured in the watershed.

HSPF simulates watershed hydrology as a series of flows and storages. In general, each flow is an outflow from a storage and is described mathematically as a function of the current storage amount and physical characteristics of the watershed system. Although the overall model is physically based, flows and storages are conceptually represented in a simplified manner. As mentioned above, the model also employs the use of calibration parameters for certain conceptually aggregated processes.

HSPF represents a basin of interest as a series of land segments and in-stream reaches/reservoirs. Although the boundaries of these units are established according to the user's needs, they are generally defined by similar hydrologic characteristics. Land segments that allow enough infiltration to influence the water budget are considered pervious; otherwise they are considered impervious. Pervious land segments move water along three paths: overland flow, interflow and groundwater flow. Impervious land segments move water by overland flow and evaporation, and transport various water quality constituents (pollutants) directly to the stream channels.

In-stream hydraulic and water quality processes are simulated by reach. The outflow from a reach or reservoir can be distributed to one or more other reaches or reservoirs to represent realistic flow patterns. Flow routing is accomplished by a modified version of the kinematic wave equation. Evaporation, precipitation and other fluxes that take place at the water's surface are also simulated by the model.

The modeling capabilities of HSPF have recently been integrated with the BASINS GIS (Geographical Information System) modeling system supported by the Office of Water.

5.2.3. Predicting Regional Hydrodynamics & Sedimentation - EFDC

To supply the current velocities, sedimentation rates, and other water quality conditions relevant for assessing the health of stream and river fish populations and communities, a three-dimensional, finite-difference, hydrodynamic, water quality and sediment transport model, EFDC (Environmental Fluid Dynamics Code), can be set up using existing data to model seventh order and higher streams, rivers, and reservoirs in the Albemarle-Pamlico basin.

EFDC can be used to model a wide variety of geometrically and dynamically complex water bodies such as stratified estuaries, rivers, lakes, and coastal regions. It solves the three-dimensional, vertically hydrostatic, free surface, turbulent averaged equations of motion for a variable density fluid (Hamrick 1992, Hamrick 1996, Hamrick and Wu 1997). The physics programmed in EFDC and many aspects of the computational finite difference scheme are equivalent to the widely used Blumberg-Mellor model (Blumberg and Mellor 1987) and the U.S. Army Corps of Engineers' Chesapeake Bay model (Johnson et al. 1993). The model uses a sigma (or stretched) vertical coordinate and Cartesian or curvilinear orthogonal horizontal coordinates. Dynamically coupled equations for the transport of turbulent kinetic energy, turbulence length scale, salinity and temperature are also solved. The two turbulence transport equations implement the Mellor-Yamada level 2.5 turbulence closure scheme (Mellor and Yamada 1982) as modified by Galperin et al. (1988). An optional bottom boundary layer module allows for wave-current boundary layer interaction using an externally specified, wind-generated, surface-gravity wave field. EFDC also simultaneously solves an arbitrary number of Eulerian transport-transformation equations for dissolved and suspended constituents, and simulates drying and wetting in shallow areas using a mass conservative scheme. In addition, it includes: 1) vegetation resistance formulations for flow simulations in vegetated water bodies (Hamrick and Moustafa 1995), 2) a near field mixing zone model that is fully coupled with the far field transport of salinity, temperature, sediment, and contaminant and eutrophication variables, 3) hydraulic structure representation and Lagrangian particle tracking, and 4) accepts radiation stress fields from wave refraction-diffraction models, which allows simulation of longshore currents and sediment transport. The following quotation from the EFDC User Manual (Hamrick 1996) summarizes the computational scheme incorporated in EFDC.

“The numerical scheme employed in EFDC to solve the equations of motion uses second order accurate spatial finite difference on a staggered or C grid. The model's time integration employs a second order accurate three time level, finite difference scheme with an internal-external mode splitting procedure to separate the internal shear or baroclinic mode from the external free surface gravity wave or barotropic mode. The external mode solution is semi-implicit, and simultaneously computes the two-dimensional surface elevation field by a preconditioned conjugate gradient procedure. The external solution is completed by the calculation of the depth averaged barotropic velocities using the new surface elevation field. The model's semi-implicit external solution allows large time steps which are constrained only by the stability criteria of the explicit central difference or upwind advection scheme used for the nonlinear accelerations. Horizontal boundary conditions for the external mode solution include options for simultaneously specifying the surface elevation only, the characteristic of an incoming wave (Bennett and McIntosh 1982), free radiation of an outgoing wave (Bennett 1976, Blumberg and Kantha 1985) or the normal volumetric flux on arbitrary portions of the boundary. The EFDC model's internal momentum equation solution, at the same time step as the external, is implicit with respect to vertical diffusion. The internal solution of the momentum equations is in terms of the vertical profile of shear stress and velocity shear, which results in the simplest and most accurate form of the baroclinic pressure gradients and eliminates the over determined character of alternate internal mode formulations. Time splitting inherent in the three time level scheme is controlled by periodic insertion of a second order accurate two time level trapezoidal step. The EFDC model is also readily configured as a two-dimensional model in either the horizontal or vertical planes.”

“The EFDC model implements a second order accurate in space and time, mass conservation fractional step solution scheme for the Eulerian transport equations at the same time step or twice the time step of the momentum equation solution (Smolarkiewicz and Margolin 1993). The advective step of the transport solution uses either the central difference scheme used in the Blumberg-Mellor model or a hierarchy of positive definite upwind difference schemes. The highest accuracy upwind scheme, second order accurate in space and time, is based on a flux corrected transport version of Smolarkiewicz's multidimensional positive definite advection transport algorithm (Smolarkiewicz 1984, Smolarkiewicz and Clark 1986, Smolarkiewicz and Grabowski 1990) which is monotone and minimizes numerical diffusion. The horizontal diffusion step, if required, is explicit in time, while the vertical diffusion step is implicit. Horizontal boundary conditions include time variable material inflow concentrations, upwinded outflow, and a damping relaxation specification of climatological boundary concentration. For the heat transport equation, the NOAA Geophysical Fluid Dynamics Laboratory's atmospheric heat exchange model (Rosati and Miyakoda 1988) is implemented. The Lagrangian particle transport-transformation scheme implemented in the model utilizes an implicit tri-linear interpolation scheme (Bennett and Clites 1987). To interface the Eulerian and Lagrangian transport-transformation equation solutions with near field plume dilution models, internal time varying volumetric and mass sources may be arbitrarily distributed over the depth in a specified horizontal grid cell. The EFDC model can be used to drive a number of external water quality models using internal linkage processing procedures described in Hamrick (1994).”

The EFDC model has been used for a study of high fresh water inflow events in the northern portion of the Indian River Lagoon, Florida, and a flow through high vegetation density-controlled wetland systems in the Florida Everglades. The model has been used for discharge dilution studies in the Potomac, James and York Rivers. Salinity intrusion studies include the York River, Indian River Lagoon and Lake Worth. Sediment transport studies include the Blackstone River, James River, Lake Okeechobee, Mobile Bay, Morro Bay, San Francisco Bay, Elliott Bay, Duwamish River and Stephens Passage. Power plant cooling studies include Conowingo Reservoir, the James River and Nan Wan Bay. Contaminant transport and fate studies include the Blackstone and Housatonic Rivers, James River, San Francisco Bay, Elliott Bay and the Duwamish River. Water quality eutrophication studies include Norwalk Harbor, Peconic Bay, the Christina River Basin, the Neuse River, Mobile Bay, the Yazoo River Basin, Arroyo Colorado, Armand Bayou, Tenkiller Reservoir, and South Puget Sound. The Peconic Bay water quality application is particularly noteworthy. The model was calibrated using a one year data set and subsequently verified by simulation of an eight year historical period having extensive field data. The model was then executed for alternative 10 year management scenarios to develop a Comprehensive Conservation and Management Plan for the estuary system.

5.2.4. Predicting Riparian Dynamics - REMM

The Riparian Ecosystem Management Model (REMM) was developed by the USDA to simulate ecological processes in riparian zones (Altier et al. In press). Riparian zones in REMM are based on the three zone riparian buffer system described by Welsch, 1991. As a best management practice, the three zone system consists of an outer grass strip (zone 3), a middle conifer forest strip (zone 2), and an inner (adjacent to the stream) hardwood forest strip (zone 1). Within REMM, the riparian zone need not follow the BMP model of three zones and, thus, may be used to describe the riparian buffer system under both natural and managed conditions.

REMM brings together the following four components to simulate ecological processes within the buffer zone: hydrology (surface and subsurface), sediment transport, nutrients (C, N, and P), and vegetation (growth and resource allocation). Together, these components interact to simulate the effects of riparian buffer systems on multiple water quality parameters. For example, REMM may be used to simulate the sequestration of nutrients (both in the riparian vegetation and soil) and sediment from water that flows through the riparian zone. REMM may also be used as a management tool for assessing the effect of riparian buffer systems on water quality, as part of a system of agricultural best management practices (BMP's). This model is particularly suited for coastal plain riparian ecosystems, which comprises a large proportion of the land area in the Albemarle-Pamlico drainage basin. With minimal modification, the model is also usable in the Piedmont, Blue Ridge, and Ridge and Valley ecoregions of the basin, with equal success.

A detailed description of the four main components of REMM is presented in the model documentation (Altier et al. In press). In general, the model uses algorithms to simulate the interactions between hydrology, sediment, nutrients, and vegetation using a combination of mass balance and rate controlled calculations. The hydrology component encompasses surface and subsurface water flow and models surface runoff, vertical and lateral subsurface flow, interception, evapotranspiration, plant water uptake and evaporation directly from the soil/litter surface layers. Erosion calculations utilize the universal soil loss equation (USLE) approach but also take into account routing, transport capacity and deposition. Nutrients are modeled by accounting for interactions between

plant biomass and the soil and through the association between nutrients and sediment. Vegetation types include herbaceous (annuals or perennials) and deciduous or coniferous woody vegetation. Vegetation type thus has a large impact upon the cycling of nutrients through the soil and litter layers.

In order to parameterize REMM, data can be gathered from the following sources: soil (STATSGO); topography (DEM, 30 or 90 m); land use scenarios (other BASE researchers); climate (HSPF in BASINS); surface hydrology (other BASE researchers); sediment and nutrient loading (other BASE researchers); and the condition of the riparian zone (US-EPA EMAP and USGS NAWQA). Simulations by REMM can then predict the ability of the riparian ecosystem to remove nutrients and sediments prior to entering the stream channel. Because sediment and nutrient loadings are primary determinants of the quality and quantity of stream fish habitat and of water quality in down-stream rivers and reservoirs, REMM, or models like it, must be considered an integral component of any framework aimed at assessing fish health.

Parameters for Upland Watershed Description

As soils develop, the primary rock or parent material is broken down into smaller and smaller constituent mineral particles. Near surface mineral soil is made up of varying amounts of sand, silt and clay (terms that describe particle size - clay <0.002 mm, silt 0.002-0.05 mm, and sand 0.05-2 mm). The relative proportions of these particle size classes are described by a factor termed soil texture. Water infiltration, water holding capacity, drainage, hydraulic conductivity and other soil properties are determined primarily by soil texture and are modified by the amount of organic matter present in the soil surface horizons. In general, sandy soils have good drainage and aeration but poor water holding capacity. Clayey soils have high water holding capacities but may be prone to water logging and poor drainage. The texture class of a particular soil is not naturally modified in the short term and may be thought of as a defining characteristic of soils on a spatially explicit basis. Thus, the development of a soil texture data base for the region will be highly important for use with the REMM model due to the direct link between soil texture and factors such as hydrology and erosion. Soil texture data will also be modified by the use of slope data for the watershed. The greater the slope in a region, the more susceptible the area is to erosion and thus sediment in surface runoff.

Another factor that is important to consider when characterizing the condition of the upland areas of a watershed is land use. Areas that are highly impacted by development or agriculture often exhibit changes in soil texture, soil structure, and hydraulic conductivity that are quite different from the original soil conditions. Thus land use also drastically affects the rate of water infiltration and water interception by covering the soil surface with structures or materials that are impervious to water. In addition, land use within the watershed is the primary source of non-point source pollutants (nutrients, sediments, and pesticides). The proximity of different land use types to the riparian zone may greatly modify the potential for these pollutants to move through the riparian area towards the stream. Therefore, land use as well as soil parameters are included in the characterization of the watershed for the parameterization of REMM.

5.3. Biological Endpoint Models

Because of the complexity of influences structuring fish assemblages, mathematical models have been used

to gain a better understanding. Roell and Orth (1998) used a model of species interactions to predict the effect of a pest control chemical on a stream fish assemblage. DeAngelis et al. (1997) developed a model for the effects of alternative hydrologic regimes on Everglades ecosystems. Jager et al. (1997) developed an individual-based, spatially-explicit, stage-structured model to predict in-stream flow effects on chinook salmon in regulated rivers. The process-based approach used in these models allows for the exploration of multiple environmental settings and ecological communities, and provides the predictive capability that is necessary to explore management options and future stressor scenarios.

5.3.1. AQUATOX

AQUATOX is a general ecological risk assessment model that simulates the fate and transport of conventional pollutants, such as nutrients and sediments, in surface waters in association with their effects on aquatic ecosystems. Aquatic ecosystems are considered as a series of trophic levels, e.g., attached and planktonic algae, submerged aquatic vegetation, invertebrates, and forage, bottom-feeding, and game fish. Interactions between these components may be varied from that of a simple food chain to that of a complex food-web. The model can be implemented for a wide variety of surface water environments including: streams, small rivers, ponds, lakes, and reservoirs. The model is designed to evaluate the likelihood of past, present, and future adverse effects from various stressors including: toxic organic chemicals, nutrients, organic wastes, sediments, and temperature. These stressors may be simulated individually or collectively (Park 2000a, b).

The fate portion of AQUATOX is specifically designed to model the chemical and physical behavior of organic toxicants. Processes considered by the model include: 1) partitioning among organisms, suspended and sedimented detritus, suspended and settled inorganic sediments, and water, 2) volatilization, 3) hydrolysis, 4) photolysis, 5) ionization, and 6) microbial degradation. Constant, dynamic, and multiplicative loadings can be specified for atmospheric, point- and nonpoint sources. Loadings of pollutants can be turned off at the click of a button to obtain a **control** simulation for comparison with the **perturbed** simulation.

Any ecosystem model consists of multiple abiotic and biotic state variables or compartments. In AQUATOX the biotic state variables may represent trophic levels, guilds, or species. AQUATOX can simulate either detrital-based or algal-based food chains and foodwebs. Ecosystem forcing functions are assumed to include temperature, light, and nutrients. The effects portion of the model includes: chronic and acute toxicity to the various organisms modeled; and indirect effects such as release of grazing and predation pressure, increase in detritus and recycling of nutrients from killed organisms, dissolved oxygen sag due to increased decomposition, and loss of food base for animals.

5.3.2. BASS

BASS (**B**ioaccumulation and **A**quatic System Simulator) is a Fortran 95 simulation model designed to simulate the population and bioaccumulation dynamics of age-structured fish communities using a temporal and spatial scale of resolution of a day and a hectare, respectively. BASS currently ignores the migration of fish into and out of this simulated hectare. The duration of a species' age class can be specified as either a month or a year. This

flexibility enables users to simulate small, short-lived species such as daces, live bearers, and minnows with larger, long-lived species such as bass, perch, sunfishes, and trout. The community's food web is specified by defining one or more foraging classes for each fish species based on either body weight, body length, or age. The user then specifies the dietary composition of each of these foraging classes as a combination of benthos, incidental terrestrial insects, periphyton, phytoplankton, zooplankton, and/or other fish species including its own. Presently, the standing stocks of all nonfish prey are handled only as external forcing functions rather than as simulated state variables. See Barber (2001)

Although BASS was specifically developed to simulate the bioaccumulation of chemical pollutants within a community or ecosystem context, it can also be used to simulate population and community dynamics of fish assemblages that are not exposed to chemical pollutants. For example, BASS could be used to simulate the population and community dynamics of fish assemblages that are subjected to altered thermal regimes associated with various hydrological alterations or industrial activities. BASS could also be used to simulate the population and community dynamics of fish assemblages that are subjected to introductions of exotic species or stockings of recreational sport fishes.

BASS is an extremely flexible model in that

- □ there are no restrictions to the number of chemicals that can be simulated;
- □ there are no restrictions to the number of fish species that can be simulated;
- □ there are no restrictions to the number of cohorts that fish species may have;
- □ there are no restrictions to the number of feeding classes that fish species may have;
- □ there are no restrictions to the number of foraging classes that fish species may have.

BASS's input data needs are broadly classified into three categories: simulation control parameters, chemical parameters, and fish parameters. Simulation control parameters provide information that is applicable to the simulation as a whole, e.g., length of the simulation, the ambient water temperature, nonfish standing stocks, and output options. Chemical parameters specify not only the chemical's physico-chemical properties (e.g., the chemical's molecular weight, molecular volume, n-octanol/water partition coefficient, etc.) but also exposure concentrations in the environment (i.e., in water, sediment, benthos, insects, etc.). Fish parameters identify the fish's taxonomy (i.e., genus and species), feeding and metabolic demands, dietary composition, predator-prey relationships, gill morphometrics, body composition, initial weight, initial whole body concentrations for each chemical, and initial population sizes.

BASS's output includes:

- □ Summaries of all model input parameters and simulation controls.
- □ Tabulated annual summaries for the bioenergetics of individual fish by species and age class.
- □ Tabulated annual summaries for the chemical bioaccumulation within individual fish by species and age class.
- □ Tabulated annual summaries for the community level consumption, production, and mortality of each fish species by age class.

- Plotted annual dynamics of model variables as requested by the user as a function of age or size classes.

Using the results of Section 4.2, one could straightforwardly identify the dominant species of the major habitat types (e.g., rocky pools, vegetative pools, mixed substrate pools, clear rocky riffles/runs, muddy low flow runs, swamps, etc.) within each fish association cluster of the Albemarle-Pamlico basin. These species lists could then be used to construct either actual or average community representations for each major habitat/association cluster combination. In general, each of these major habitat/associations communities would be represented by 4-8 species that account for at least 80-90% of the habitat's total fish biomass. Having identified the species composition of these major habitat/association cluster combinations, one could then construct a generalized food web for each community based on the published natural histories of its dominant species. Finally, given the necessary data for determining initial conditions for fish species comprising these communities (i.e., initial body sizes and population densities) and for establishing the standing stocks of nonfish food resources (i.e., benthic invertebrates, insect drift, zooplankton, etc.), BASS could be used to simulate several different aspects of fish health for the Albemarle-Pamlico basin. These might include: 1) growth rates and projected population sizes of important recreational and food species such as largemouth bass, crappie, sunfish, and catfish as related to the availability of lower trophic level resources that, in turn, are influenced by water quality and sedimentation, 2) growth rates and projected population sizes of important recreational and food species as related to temperature and hydrology, and 3) bioaccumulation dynamics of dioxin, mercury, and complex pesticide mixtures.

5.3.3. Habitat Suitability Models

Early in the 1980's the U.S. Fish and Wildlife Service began development of a planning and evaluation technique known as the Habitat Suitability Index (HSI). The intent of these HSI models was to provide wildlife managers and decision-makers with a numerical index for evaluating the impacts of water or land use changes on fish and wildlife habitats. These models formulate quantitative relationships between key environmental variables and habitat suitability that integrate life history information of specific species and their habitat requirements for food, cover, reproduction, and survival. Each HSI model provides a numerical index of habitat suitability on a 0 to 1 scale and assumes that there is a positive relationship between the index and carrying capacity of the habitat being evaluated. Although HSI models should be considered as hypotheses of species-habitat relationships rather than proven statements of cause and effect, they provide an objective approach for improved decision-making regarding actual or expected habitat impacts associated with water quality changes and land use practices. Because the goal of HSI models is to assess the impacts of water quality and land use changes on fish and wildlife populations indirectly via habitat considerations, HSI models are, in ecological risk assessment terminology, measurement rather than assessment endpoint models.

Two features of HSI models make them potentially useful tools for regional assessments. The first of these features is the fact that the habitat variables used in HSI calculations can be either measured or model-generated for any particular region of concern. For example, variables for a stream fish HSI typically include:

average, maximum, or minimum current velocity (food, cover, reproduction)
average, maximum, or minimum pH (growth, survival)

average, maximum, or minimum water temperature (growth, survival, reproduction)
 average, maximum, or minimum dissolved oxygen (survival, reproduction)
 turbidity (survival)
 % designated aquatic vegetation (food, cover, reproduction)
 % designated substrate type (food, reproduction)
 % riparian cover (food)
 % shade (cover)
 % pools (food, cover)
 % runs (food, cover)
 Stream gradient
 average stream depth
 average stream width

The second feature of HSI models that make them amenable to regional assessments is their mathematical simplicity. These two features make implementation of HSI models within a GIS framework a very straightforward undertaking.

Table 17 summarizes HSI models that have been developed for various freshwater and marine fish that could be used directly to assess fish habitat relationships in the Albamarle-Pamlico basin or that could be used to pattern the development of new HSI models.

Table 17. Summary of available Habitat Suitability Models.

Species	Common Name	HSI Model
<i>Acipenser brevirostrum</i>	Shortnose sturgeon	Crance (1986)
<i>Alosa aestivalis</i>	Blueback Herring	Pardue (1983)
<i>Alosa pseudoharengus</i>	Alewife	Pardue (1983)
<i>Alosa sapidissima</i>	American Shad	Stier and Crance (1985)
<i>Ameiurus melas</i>	Black Bullhead	Stuber (1982)
<i>Brevoortia tyrannus</i>	Menhaden	Christmas et al. (1982)
<i>Catostomus catostomus</i>	Longnose sucker	Edwards (1983b)
<i>Catostomus commersoni</i>	White Sucker	Twomey et al. (1984a)
<i>Cynoscion nebulosus</i>	Spotted Seatrout	Kostecki (1984)
<i>Cyprinus carpio</i>	Carp	Edwards and Twomey (1982a)
<i>Dorosoma cepedianum</i>	Grizzard Shad	Williamson et Nelson (1985)
<i>Esox lucius</i>	Northern Pike	Inskip (1982)
<i>Esox masquinongy</i>	Muskellunge	Cook and Solmon (1987)
<i>Etheostoma gracile</i>	Slough Darter	Edwards et al. (1982a)
<i>Ictalurus punctatus</i>	Channel Catfish	McMahon and Terrell (1982)
<i>Ictiobus bubalus</i>	Smallmouth Buffalo	Edwards and Twomey (1982b)
<i>Ictiobus cyprinellus</i>	Bigmouth Buffalo	Edwards (1983a)
<i>Leiostomus xanthurus</i>	Spot	Stickney and Cuenco (1982)

<i>Lepomis auritus</i>	Redbreast Sunfish	Aho et al. (1986)
<i>Lepomis cyanellus</i>	Green Sunfish	Stuber et al. (1982b)
<i>Lepomis gulosus</i>	Warmouth	McMahon et al. (1984c)
<i>Lepomis macrochirus</i>	Bluegill	Stuber et al. (1982a)
<i>Lepomis microlophus</i>	Redear Sunfish	Twomey et al. (1984b)
<i>Menidia beryllina</i>	Inland Silverside	Weinstein (1986)
<i>Menticirrhus americanus</i>	Southern Kingfish	Sikora and Sikora (1982)
<i>Micropogonias undulatus</i>	Atlantic Croaker	Diaz and Onuf (1985)
<i>Micropterus dolomieu</i>	Smallmouth Bass	Edwards et al. (1983a)
<i>Micropterus punctulatus</i>	Spotted Bass	McMahon et al. (1984b)
<i>Micropterus salmoides</i>	Largemouth Bass	Stuber et al. (1982c)
<i>Morone chrysops</i>	White Bass	Hamilton and Nelson (1984)
<i>Morone saxatilis</i>	Striped Bass	Bain and Bain (1982), Crance (1984)
<i>Notropis cornutus</i>	Common Shiner	Trial et al. (1983a)
<i>Oncorhynchus clarki</i>	Cutthroat Trout	Hickman and Raleigh (1982)
<i>Oncorhynchus gorbuscha</i>	Pink Salmon	Raleigh and Nelson (1985)
<i>Oncorhynchus keta</i>	Chum Salmon	Hale et al. (1985)
<i>Oncorhynchus kisutch</i>	Coho Salmon	McMahon (1983)
<i>Oncorhynchus mykiss</i>	Rainbow Trout	Raleigh et al. (1984)
<i>Oncorhynchus tshawytscha</i>	Chinook Salmon	Raleigh et al. (1986a)
<i>Paralichthys albigutta</i>	Gulf Flounder	Enge and Mulholland (1985)
<i>Paralichthys lethostigma</i>	Southern Flounder	Enge and Mulholland (1985)
<i>Perca flavescens</i>	Yellow Perch	Krieger et al. (1983)
<i>Pleuronectes vetulus</i>	English Sole	Toole et al. (1987)
<i>Polyodon spathula</i>	Paddlefish	Hubert et al. (1984)
<i>Pomoxis annularis</i>	White Crappie	Edwards et al. (1982c)
<i>Pomoxis nigromaculatus</i>	Black Crappie	Edwards et al. (1982b)
<i>Pylodictis olivaris</i>	Flathead Catfish	Lee and Terrell (1987)
<i>Rhinichthys atratulus</i>	Blacknose Dace	Trial et al. (1983c)
<i>Rhinichthys cataractae</i>	Longnose Dace	Edwards et al. (1983b)
<i>Salmo trutta</i>	Brown Trout	Raleigh et al. (1986b)
<i>Salvelinus fontinalis</i>	Brook Trout	Raleigh (1982)
<i>Salvelinus namaycush</i>	Lake Trout	Marcus et al. (1984)
<i>Sciaenops ocellatus</i>	Red Drum	Buckley (1984)
<i>Semotilus atromaculatus</i>	Creek Chub	McMahon (1982)
<i>Semotilus corporalis</i>	Fallfish	Trial et al. (1983b)
<i>Stizostedion vitreum</i>	Walleye	McMahon et al. (1984a)
<i>Thymallus arcticus</i>	Arctic Grayling	Hubert et al. (1985)

5.4. Modeling Issues

5.4.1. Models as Ecological Indicators

Although EMAP's Indicator Development Strategy (Barber 1994) correctly suggested that the output of dynamic simulation models that are parameterized with monitoring data could be used as ecological indicators, there has been little or no effort to date to explore either the feasibility or the utility of such methods. Because of financial and logistical constraints, most traditional monitoring programs, including EMAP, have focused only on structural measures of system condition, e.g., fish or zooplankton densities, concentration of chlorophyll a, Secchi depth, water concentration of toxics, etc. There are assessment needs, however, for which functional measures of system fluxes or flows might be more useful indicators of the system's overall condition. In such cases, dynamic simulation models could be used to estimate the needed system measures. Dynamic simulation models could also be used to enumerate time series of structural indicators of system condition that cannot be repeatedly monitored for fiscal or logistical reasons.

5.4.2. What is a Good Model?

The question of what constitutes a “good” model is neither a trivial nor straightforward question since there are multiple ways to analyze how a model corresponds to an observational dataset. For example, let x_{data} and x_{model} denote the measured and predicted values of a system output of interest. Perhaps the most obvious measures of goodness of fit might be the norm

$$\left| x(t)_{model} - x(t)_{data} \right| < \epsilon \quad (24)$$

In other words, how close does the model come to matching the observed values pointwise? An alternative norm, however, might measure how well the model predicts changes in the observed data. In this case, the norm

$$\left| \frac{dx_{model}}{dt} - \frac{dx_{data}}{dt} \right| < \delta \quad (25)$$

would be a better measure for evaluating the model's goodness of fit. Although measures like Eq.(24) are used much more frequently than measures like Eq.(25), there is no a priori reason to do so, particularly if $\delta \ll \epsilon$.

Consequently, a “good” model is not necessarily the one that gives the best prediction in terms of closeness to reality, for this might be just an accident. If data are not there to provide good estimates for model parameters and boundary conditions, then the bottom line is simply that the data are not there. A “good” model is really one for which the right answer can be guaranteed to lie within its quantified uncertainty range. It is data, and data alone, that will reduce this uncertainty range through a priori or posteriori reduction of parameter and input uncertainty intervals.

Another complicating factor that is generally ignored when comparing model output to observed data is the fact that the data being used for model evaluation is itself a physical model of the phenomena that the mathematical model is designed to describe. Observational data has its own implicit and explicit assumptions as well as its own limitations. In some cases, predicted model results can be better than measured results (e.g., measured vs. predicted K_{ow} 's for extremely hydrophobic chemicals).

5.4.3. Uncertainty

There are many heuristic ideas concerning model uncertainty. One of the most common, and yet the most difficult to address, is the notion of uncertainty as a probability statement. For example, what is the probability that a prediction of a model will be observed in the field? This is an intriguing question since most models are by assumption, construction, or definition the most probable or expected description of the system of interest. Questions of this type are equivalent to

$$P[X_{model}(t, x, y, z) = X_{data}(t, x, y, z)] \quad (26)$$

where $X_{model}(t, x, y, z)$ and $X_{data}(t, x, y, z)$ denote a particular model prediction and field observation for a particular time and spatial location. Despite the difficulty in aligning the temporal and spatial coordinates of the model and the observed data, such probability statements are meaningless if one assumes that model outputs represent a continuous random variable, or more precisely a function of continuous variables (i.e., parameters, forcing functions, and initial conditions that have associated distributions). In particular, because the probability of any one “value” of a continuous random variable is by definition zero, it follows that Eq.(26) would be zero for any prediction or observation.

On the other hand, probability statements of the form

$$P[|X_{model}(t, x, y, z) - X_{data}(t, x, y, z)| < \delta] \quad (27)$$

over some specified time interval $[t_1 < t < t_2]$ or spatial coordinates are entirely meaningful. Such probabilities could be evaluated empirically if the statistical distributions of all model parameters, forcing functions, and initial conditions were known under the assumption that the model's structure is a “reasonable” representation of the actual processes that it is intended to simulate. By model structure we mean 1) number of state variables, 2) the connectance between those state variables, and 3) the “appropriate” functions describing the interactions between state variables and other state variables, system inputs, and system outputs.

Perhaps a more useful alternative to this probability approach is the construction of confidence limits on selected model outputs. If more than one output is of interest, however, the next question that must be addressed is how to generate simultaneous confidence limits. Generation of such confidence limits are not an easy proposition since one needs to know or assume covariances between the model parameters, forcing functions, and state variables.

Ramifications of Uncertainty

Model uncertainty analysis can be, and has been, used for a number of ends. On the positive side, uncertainty analysis can be used to focus future research and model development. Understanding what processes and parameters generate the greatest range in prediction and which of those processes and parameters are the least well characterized is essential for determining optimal strategies for data acquisition and research direction. For example, the statistical distributions for most parameters of many environmental models are poorly known or characterized. Consequently, with limited resources it is important to determine whether new algorithm development and process research is more important than better characterization of existing model parameters and processes. Ideally, the answer to such questions should be based on knowing what activities have the most effect (per dollar) in lowering the uncertainty of key model predictions.

Understanding the factors that contribute to model uncertainty is also essential for objective verification/validation of models. For example, validation of a model that generates a wide range of prediction for a key process or output of interest may be virtually impossible if one has access to only 1 or 2 validation datasets. In such cases, if additional datasets are either unavailable or unattainable, model verification/validation would have to be undertaken indirectly. Indirect model verification activities could focus on other model outputs for which additional observational data were available or on extensive peer review of the model's theoretical foundations, assumptions, structure, implementation, and application.

On the negative side of things, uncertainty analysis has often been used to discredit models without a full appreciation of what such analyses really are telling us. This is particularly true in the case of environmental regulation when the regulatory and regulated communities are using different models for their respective analyses. In such cases, there has been a strong tendency to argue that the model with the smaller “uncertainty” is by definition the better model. Although such assertions on the surface may seem entirely reasonable, there is no a priori reason to believe that the “better science-based model” in point of fact has the smaller model uncertainty for any specific application. Such paradox arises directly from the fact that model uncertainty is not a one dimensional property of a model. Rather, it is the product of several different properties of the model and its parametric data that collectively determine the model's bounds of prediction. These factors may be broadly grouped under the headings of model sensitivity, statistical variability of parameters, and “true” scientific uncertainty.

5.4.3.1. Mathematical Sensitivity

There are four major classes of mathematical sensitivity regarding a model's behavior. These are the model's sensitivity to parameter changes, forcing functions, initial state variables, and structural configuration. The first three of these classes are generally defined in term the following partial derivatives

$$\frac{\partial Y_i}{\partial p_j} ; \quad \frac{\partial Y_i}{\partial Z_j} ; \quad \frac{\partial Y_i}{\partial X_j(0)} \quad (28)$$

where Y_i is a system output of interest; p_j is some state parameter; Z_j is some external forcing function; and $X_j(0)$

is the initial value of some state variable of interest. In general, the output Y_i may be either a state variable, a flux, or a function of a state variable or flux. Structural sensitivity, however, generally cannot be formulated in this manner since this form of model sensitivity typically concerns the number and connectivity between the system's state variables. Examples of questions regarding a model's structural sensitivity would include:

1. How does model output change using 4 segments vs. 10?
2. How does model output change using 10 compartments vs. 7?
3. How does model output change when the connectivity between components change?
4. How does model output change when a process of interest is formulated using the function $G(x_i, x_j, z_k, t)$ rather than $F(x_i, x_j, z_k, t)$? Although this particular question could be formulated in term of partial derivatives if the functions under consideration were by some definition mathematically convergent, in general no such formalism is possible.

It should be noted that structural sensitivity is related to the issue of model complexity for which there are at least 2 “fundamental” rules. These are:

1. If complexity is added to a model in a way that increases the range of prediction for key model outputs, then the point of diminishing return for model complexity (at least as far as making that prediction goes) is reached when the range of prediction starts to flatten out. It can also be shown that potential bias due to over-simplification has also been reduced to near-zero at this point.
2. Model complexity does not, on its own, guarantee that the model will give the “right answer”. It only helps to guarantee that the “right answer” will lie within the quantified uncertainty margins.

Many environmental models (e.g., watershed models like HSPF) can not be parameterized completely using first principles and application-independent parameteric datasets. Such models must be calibrated to known conditions in order to parameterize certain processes that they simulate. If such models are too complex, they may have too many parameters to be calibrated uniquely. On the other hand, if such models are too simple (yet can be well calibrated), they may not be capable of simulating valuable aspects of system fine detail. This inability, in turn, may introduce serious bias into the model's predictions. Thus, if a calibrated model is required to simulate fine detail (e.g., groundwater/surface water interaction, response to extreme climatic events, etc.), then it will have uncertainty by virtue of parameter nonuniqueness (and all of the other uncertainties mentioned above).

Because model sensitivity as defined above is simply a mathematical characteristic of a model, model sensitivity in and of itself is neither good nor bad. If the system being modeled is insensitive, then model sensitivity is obviously undesirable. On the other hand, sensitivity is desirable if the system being modeled is itself sensitive. Even though increasing model sensitivity may generate very large confidence limits for system outputs of interest, it is important to acknowledge that model sensitivity and uncertainty are not one and the same (Summers et al. 1993, Wallach and Genard 1998). Model uncertainty, or at least one of its most common manifestations, is the product of

both the model's sensitivity to particular components and the statistical variability associated with those components.

There are at least three key points to remember when addressing issues of model sensitivity. These are

1. Sensitivity with respect to parameters, initial conditions, and forcing functions is a fixed property of a model. To change these aspects of uncertainty, the model's structure must be changed.
2. Sensitivity is a major factor for calibrating models, i.e., how can one change parameters or forcing functions to have model output match a set of observations.
3. Unqualified questions regarding the sensitivity of generalized models such as 3MRA, BASS, EXAMS, WASP, etc. are generally meaningless. The only meaningful sensitivity analyses of such models are those performed for specific applications. Any of these models can be sensitive or insensitive depending on the particular application of concern.

Readers interested in issues and techniques related to model sensitivity and uncertainty should consult the following papers: Giersch (1991), Elston (1992), Summers et al. (1993), Håkanson (1995), Norton (1996), Loehle (1997), and Wallach and Genard (1998).

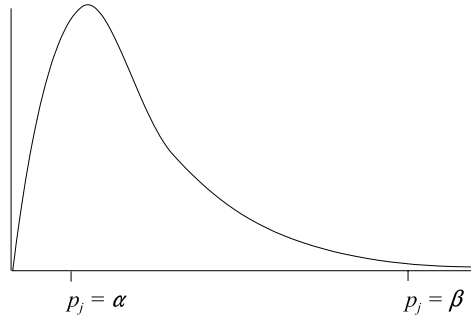
5.4.3.2. Statistical Variability of Parameters, Forcing Functions, & Initial Conditions

The statistical variability of a model's parameters, forcing functions, and initial conditions refines one's perceptions regarding the model's realizable sensitivity. Consider, for example, the following results for a parameter sensitivity analysis.

$$\left. \frac{\partial Y_i}{\partial p_j} \right|_{p_j = \alpha} = s_1$$

$$\left. \frac{\partial Y_i}{\partial p_j} \right|_{p_j = \beta} = s_2$$
(29)

where s_1 and s_2 denote a very small and very large real number, respectively. In terms of model uncertainty, the real question of interest is what is the statistical distribution of p_j ? Therefore, assume for the sake of discussion that the actual distribution of p_j is described by the following graph.



In this case, one would probably conclude that although the model may exhibit some very sensitive behavior in its global parameter space, in its operational or anticipated parameter space the model is, in fact, very insensitive.

Actual distributions of all of a model's parameters, forcing functions, and state variables are seldom, if ever, known. If the distributions of parameters, forcing functions, or state variables are poorly known, more research will obviously provide a better characterization of the needed distributions. However, there will always be a limit of diminishing returns when making such investments.

The covariance structure between parameters, forcing functions, and state variables is another factor that can greatly alter one's perception of a model's realizable sensitivity. For example, many biological and physical processes are represented by power functions, i.e.,

$$P = p_1 X^{p_2} \quad (30)$$

When such relationships are fitted using standard regression techniques after logarithmic transformation of Eq.(30), i.e.,

$$\log P = \log p_1 + p_2 \log X = \hat{p}_1 + p_2 \log X \quad (31)$$

the resulting estimates for \hat{p}_1 and p_2 are always negatively correlated with one another. Consequently, if one were to analyze this model's parameter sensitivity to \hat{p}_1 without covarying the exponent p_2 appropriately, the resulting analysis, at the very least, would be biased and at the worst would actually tell one little, if anything, about the model's realized or expected sensitivity.

Another interesting problem arises for models that must be calibrated to estimate parameters for certain lumped, empirically based processes. Generating the actual, or even the approximate, distribution of such parameters is generally a very complex task since the parameter's distribution for any given set of model calibrations is

obviously conditioned on the particular datasets used to parameterize the rest of the model. The parameter's “true” distribution must, therefore, be constructed using Bayes Theorem and knowledge of the distributional properties of the model's other parameters. This task is much easier if the model is not particularly sensitive to the calibration parameter of interest. If this is not the case, however, predictions may become quite uncertain and very dependent on the a priori parameter distribution rather than on any constraints enforced by the calibration process.

All of the above concepts will greatly influence one's notions concerning the expected behavior of any given model. To illustrate this fact, let the vector \mathbf{p} denote the parameters of a model. If one now conceptually treats any given model output of interest as a vector function $\mathbf{y}(t) = \mathbf{G}(\mathbf{p}, t)$, the model's average prediction for the output of interest would be given by the following definition of mathematical expectation

$$E[\mathbf{y}(t)] = \int \mathbf{G}(\mathbf{p}, t) dP(\mathbf{p}) \neq \frac{\sum_{i=1}^n \mathbf{G}(\mathbf{p}_i, t)}{n} \quad (32)$$

where $P(\mathbf{p})$ is the cumulative joint density function of the model's parameters. Thus, in order to quantify a model's expected behavior, one must quantify the distributions of the model's parameters, forcing functions, and initial conditions which is not equivalent to executing the model “mindlessly” a large number of times and calculating sample means.

5.4.3.3. Scientific Uncertainty - Model Structure, Process Representation, etc.

If we acknowledge that the parameters, forcing functions, and initial conditions of our environmental models have associated statistical distributions, then we are, in fact, acknowledging that the predictions of those models have associated errors or equivalently statistical distributions of prediction. When making any type of prediction that admits to prediction error, it is only natural then to ask how can predictions be made less uncertain? Consequently, when models are used for environmental regulation or decision-making, the question that is often asked is how can one reduce the model's uncertainty? Based on the preceding materials, two fundamental facts should be obvious. First, because the mathematical sensitivity of a model is a fixed property of the model, prediction error related to model sensitivity cannot be reduced except by changing the model structure itself. However, if model processes should be sensitive, then they should be sensitive, end of story. The second fundamental fact is that one can better characterize the distributions of model parameters, forcing functions, and initial conditions just so far. Once the statistical moments of a variable's distribution are “adequately” estimated more sampling will not significantly improve those estimates.

The only dimension of model uncertainty that can be effectively reduced is what can be identified as the model's scientific or conceptual uncertainty. This aspect of model uncertainty is in fact closely related to the notion of structural sensitivity discussed above. There are at least three major dimensions of this source of uncertainty. These are:

- 1) Model Structure - That is, how many components are needed to satisfy implicit or stated model objectives? Furthermore, how should these components be connected?

2) Process Representation - What functions or algorithms should be used to describe model processes and their interactions? The answer to this question will often depend both on the state of the science and overall model objectives.

3) Application Issues - What are the implicit temporal and spatial scales of the model and the object of its application?

Remember, all models are abstractions or simplifications of real world phenomena. Good models may often be more the result of ignoring those things that are not relevant to the model's objectives rather than including as much detail as possible.

6. Prototype Assessment - Contentnea Creek Watershed

To illustrate how water quality and biological endpoint models can be sequentially linked to assess different dimensions of fish health, this chapter presents a demonstration of this process for which the aim is to assess the ecological responses of fish communities in the Contentnea Creek watershed of the Albemarle-Pamlico basin to sediments and nutrients.

In Section 6.1 calibration of the HSPF (Hydrologic Simulation Program Fortran) hydrologic model to the Contentnea Creek watershed is presented. Although HSPF is a lumped parameter model that is only moderately physically-based, it has been widely used for TMDL development. The art of effectively using HSPF, however, requires a great deal of experience in fitting the adjustable parameters in the calibration process. Due to resource and time constraints, a modeler may not have the opportunity to fully explore various parameter suites or place confidence bounds on model predictions, thereby addressing the critical issue of uncertainty that will arise as TMDLs are generated, scrutinized, and challenged. Here we present the automated parameter optimization software PEST (for **P**arameter **E**stimation) in combination with HSPF for the parameterization of four neighboring watersheds in the Contentnea River basin of North Carolina.

In Section 6.2 a procedure for calibrating HSPF to simulate sediment dynamics is presented. The use of nonlinear parameter estimation techniques using the PEST software is demonstrated by incorporating TSS data into the model calibration process. Recognizing that no parameter set estimated through the calibration process is unique, the model's predictive uncertainty arising from parameter uncertainty using the PEST predictive analyzer is then considered.

Finally, in Section 6.3 the aquatic ecosystem simulation model AQUATOX is parameterized and applied to Contentnea Creek using the hydrologic and sediment trends predicted by the above HSPF calibrations.

6.1. Hydrological Patterns

In spite of the fact that calibration of lumped and distributed parameter watershed models is a difficult and time-consuming task, it is general modeling practice for such models to be calibrated manually. While a number of studies have reported on the use of various parameter estimation methodologies in the calibration of watershed models (e.g., Kuczera 1983, Wang 1991, Duan et al. 1992, Sorooshian et al. 1993, Yapo et al. 1998, Thyer et al. 1999), the use of computer-assisted watershed model calibration outside academic circles is not widespread, and is sometimes even discouraged on the basis that the use of such techniques erodes the modeler's ability to bring his/her expertise to the task of model calibration (e.g., Lumb et al. 1994).

There can be little doubt that attempts to calibrate watershed models using nonlinear parameter estimation software meet with difficulties that are not found to the same extent in the calibration of other types of environmental models. Included amongst these difficulties are: 1) the highly nonlinear (with respect to adjustable parameters) nature of such models; 2) the potential for local minima to exist in whatever mathematical formulation is

chosen as a measure of model-to-measurement misfit (normally called the objective function); 3) the number of parameters requiring adjustment in many such models and hence the nonuniqueness with which they can be estimated; 4) the large data sets that must be handled; 5) the large amounts of noise associated particularly with constituent and sediment data; and 6) the lack of expertise in parameter estimation methods that exists in the watershed modeling community.

A related issue to that of model calibration, and one that is rarely addressed in the literature, is that of estimating the uncertainty associated with predictions made by a model once it has been calibrated. The fact that most model parameters are nonunique, even after calibration constraints have been imposed, raises the spectre that predictions made by a calibrated model may also be nonunique; see for example, Beven (2000). Integrity in the deployment of environmental models as a basis for environmental management requires that the extent of such predictive uncertainty be explored (National Research Council 2001).

The present exercise demonstrates the use of nonlinear parameter estimation and predictive uncertainty analysis in the calibration and deployment of a model that simulates streamflow in neighboring watersheds. A number of different applications of these methodologies are discussed in the context of exploring, and partially overcoming, many of the difficulties noted above. It should be noted, however, that it is not the purpose of this paper to compare the merits and weaknesses of different parameter estimation and predictive analysis algorithms. Rather, this study reveals some of the powerful and innovative data-processing achievements that can be made with relatively little trouble in applying readily available software in everyday modeling contexts.

Methods

The Contentnea Creek basin, a coastal plain watershed, is located in the Neuse River basin in North Carolina (Figure 23). Rainfall in the region averages 127 cm per year (Giese et al. 1997). The mean annual minimum and maximum temperatures are approximately 8 Celsius and 22 Celsius, respectively; the mean monthly minimum temperature is 15 Celsius (Wilson, NC). The physiography is relatively uniform throughout the four modeled watersheds, with relatively low relief. The soils are well-drained sands and sandy loams developed on sediments of marine origin.

Models were built for four, non-overlapping watersheds of the Contentnea Creek basin, viz. Contentnea Creek above Hookerton, Moccasin Creek, Nahunta Swamp and Little Contentnea Creek; areas of these watersheds are 311924, 100208, 52815 and 57692 acres, respectively. Each model was calibrated using daily streamflow records from gauging stations situated at their respective outlets (operated and maintained by the U.S. Geological Survey). When a gauging station was not located at a watershed pour point, the watershed boundary was corrected to reflect the appropriate contributing area. The models were built as part of a wider study dedicated to predicting alterations to water quality within the Contentnea Creek basin as a result of increasing urbanization, changing farming practices and climatic change (Johnston 2001).

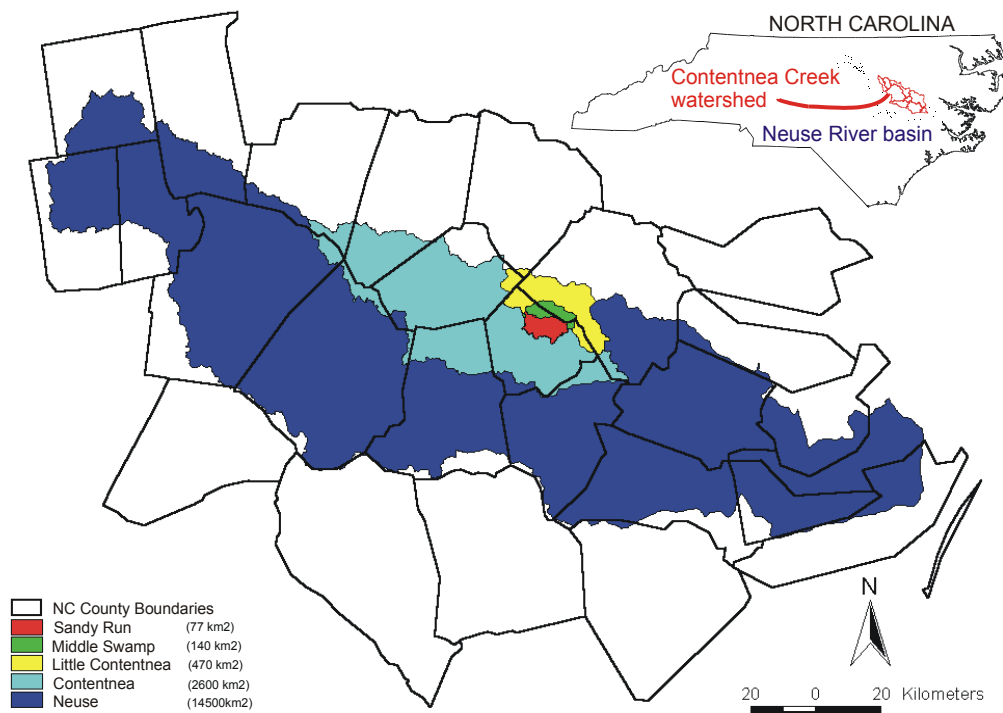


Figure 23. Contentnea Creek watershed study area and surroundings. The Contentnea subwatershed is located within the Neuse River basin of North Carolina.

The primary land covers within all watersheds are forest, agriculture, grassland and urban. Land use classifications were taken from the MRLC national land cover dataset (Vogelmann et al. 2001) with selected thematic map scenes and a composite of data acquired between 1990 and 1994. Of these four land use classes, the land use with the largest difference in hydrological characteristics is the urban land use class. The increased amount of impervious cover comprising this land use type results in increased flashiness of streamflow (i.e., higher flows immediately after rain and possibly lower flows during dry times) in addition to a higher potential for increased chemical constituent and sediment loading into streams that drain the basin.

Software

Simulation of hydrologic processes within the watersheds comprising the Contentnea Creek study area was undertaken using version 12 of HSPF (Bicknell et al. 2001). Each watershed was simulated using four HSPF PERLNDs, one IMPLND and a RCHRES (a PERLND is a pervious land segment, an IMPLND is an impervious land segment and a RCHRES is a free-flowing reach or mixed reservoir). The four PERLNDs were used to represent the four major land use types mentioned above. The IMPLND was used for the simulation of urban impervious areas. The RCHRES was used to simulate flow of water in the stream reach that drains each watershed.

Because the major hydrological difference between land use types is that between pervious and impervious land, initial model deployment was such that all four PERLNDs within each modeled watershed were assigned the same hydrologic parameters, except for the FOREST parameter that governs the amount of evapotranspiration taking place during winter. Parameters related to the dimensions of the system (e.g., land use areas, lengths of overland flow paths, average slopes) were assigned in accordance with known watershed geometry and topography.

Model calibration was undertaken using PEST (Doherty 2001a) in conjunction with a suite of utility software written to support the use of PEST in the surface water modeling context (Doherty 2001b); the principal member of this suite is TSPROC, a time-series processor optimized for use in the calibration context. PEST is a model-independent parameter estimator with advanced predictive analysis and regularization features. Its model-independence rests on the fact that it is able to communicate with a model through the latter's own input and output files, thus allowing easy calibration setup with an arbitrary model. This capability allows the model that is to be calibrated to be encapsulated in a batch or script file if desired. Hence both model pre- and postprocessing software (such as TSPROC) can be used as part of the calibration process.

PEST implements a particularly robust variant of the Gauss-Marquardt-Levenberg method of parameter estimation. While this method requires that a continuous relationship exist between model parameters and model outputs, it can normally find the minimum in the objective function in fewer model runs than any other parameter estimation method. This is important where model run times are lengthy, or even moderate. (In the present case model runs took about 1 minute on a Pentium III 550 MHz machine.) The Gauss-Marquardt-Levenberg method has been accused of being too easily trapped in local objective function minima; see, for example, Abbaspour et al. (2001). In the present instance, this problem was circumvented by formulating a calibration objective function that included not just flows, but processed flow data as well. Also, parameter nonuniqueness was accommodated during model calibration and predictive uncertainty analysis using the methods described below.

TSPROC is able to read time-series data from a variety of sources including ASCII files and USGS Watershed Data Management (i.e., WDM) files. It can: 1) undertake temporal interpolation of one time series to another; 2) carry out mathematical manipulations of arbitrary complexity between one or more time series; 3) calculate various derived quantities from time series including exceedence times and volumetric/mass accumulation between one or many arbitrary dates and times; and 4) compute indices of biotic health based on continuous high or low values beyond a threshold value. Also, it facilitates the use of both raw and processed time series data in the calibration process by automatically generating PEST input files for calibration runs involving some or all of these quantities. Hence, use of TSPROC eliminates many of the problems associated with the handling and processing of large data sets that accompany the use of nonlinear parameter estimation techniques in the surface water-modeling context.

The remainder of this section briefly describes some of the methodologies used to calibrate HSPF and to analyze the uncertainty of predictions made by HSPF, employing PEST in conjunction with TSPROC and using the Contentnea Creek drainage area as an example. The methods described herein can be easily extended to other models and other watersheds.

Calibration of a Single Watershed Model

Calibration of each of the watershed models discussed above was undertaken by adjusting certain model parameters to obtain as good a match as possible between model outputs and gauged flows over the period 1970 to 1985. Adjusted parameters, and their role in HSPF, are listed in Table 18. All of these parameters pertain to the HSPF PERLND module. As was mentioned above, the same values for these parameters were assigned to all four PERLNDs representing the four dominant land use types within each watershed. The third column of Table 18 lists the initial values assigned to the pertinent parameters prior to calibration adjustment, these values being considered reasonable for these watersheds (USEPA 1999, 2000a). The fourth column of Table 18 lists bounds on parameter values imposed through the calibration process. As is documented in Doherty (2001a), PEST is able to impose bounds on adjustable parameter values in a way that enhances numerical stability of the parameter estimation process as these bounds are imposed.

Table 18. HSPF parameters, their functions, initial values and constraints imposed during the calibration process.

Parameter Name	Parameter function	Initial value	Bounds*
LZSN	Lower zone nominal storage	5.0 in	2 - 15 in
UZSN	Upper zone nominal storage	0.5 in	0.01 - 2 in
INFILT	Related to the infiltration capacity of the soil	0.08 in/hour	0.001 - 0.5 in/hr
BASETP	The fraction of potential ET that can be sought from baseflow.	0.1	0.01 - 0.2
AGWETP	Fraction of remaining potential ET that can be satisfied from active groundwater storage	0.05	0.001 - 0.2
LZETP	Lower zone ET parameter - an index to the density of deep-rooted vegetation.	0.5	0.1 - 0.9
INTFW	Interflow inflow parameter	2	1.0 - 10.0
IRC	Interflow recession parameter	0.4 day ⁻¹	0.001 - 0.999 day ⁻¹
AGWRC	Groundwater recession parameter	0.95 day ⁻¹	0.001 - 0.999 day ⁻¹
DEEPFR	Fraction of groundwater inflow that goes to inactive groundwater	0.1	fixed

* taken from (USEPA 2000a)

For most of the model calibration runs documented herein the DEEPFR parameter was fixed at 0.1. This low value was assumed to be reasonable since loss of water to deep aquifers is considered unlikely to occur in any of the watersheds of concern.

In order to reduce the nonlinearity of the parameter estimation problem (and hence render it numerically more stable), PEST was actually used to estimate transformed interflow and groundwater recession parameters that are related to the native HSPF recession parameters depicted in Table 18 by the following relationships:

$$IRCTTRANS = IRC / (1 - IRC) \quad (33)$$

and

$$AGWRCTTRANS = AGWRC / (1 - AGWRC) \quad (34)$$

These transformed parameters approach infinity as the native parameters approach 1. All adjusted parameters were log-transformed during the parameter estimation process undertaken by PEST to further increase the linearity of the problem and thereby reduce the chances of numerical instability.

To estimate parameter values for HSPF, PEST was used to minimize an objective function comprised of three components. These were the weighted differences between: 1) model-generated and observed flows, 2) monthly volumes calculated on the basis of modeled and observed flows, and 3) exceedence times for various flow thresholds calculated on the basis of modeled and observed flows.

The relative weights assigned to each of these three observation groups was such that the contribution made to the total objective function by each of them was about the same. Within the first of the above groups, weights assigned to individual flow observations were calculated using the formula:

$$w = c \times (1/f)^{1.5} \times (1 + \cos(2\pi d/365.25)/4) \quad (35)$$

where w is the weight assigned to a flow observation; f is the flow magnitude; c is a factor used to make the contribution to the objective function from each observation group about the same; and d is the day of the year (counting from 1st January).

If observation weights are calculated as the reciprocals of the observations themselves, it can be shown that this is mathematically equivalent to calibration against the logs of the observations. In calibrating a hydrologic model, such a strategy ensures that high flows do not dominate the parameter estimation process simply because of their large numerical value. In the present instance, the second factor in Eq.(35) is such that low flows are provided with an even greater weight than that provided through inverse magnitude weighting. This was done in order to focus the calibration process on these low flows, thus hopefully enhancing the calibrated models' ability to furnish accurate predictions under low-flow conditions. These conditions are the focus of part of the present investigation since they have the potential to impose risks on the fish population of the creeks.

The third factor in Eq.(35) provides a means of partial discrimination against flows measured during the summer months when rainfall is likely to show a high degree of spatial heterogeneity. This can result in discrepancies between rainfall supplied to a model and rainfall that actually fell in the watershed that the model represents.

For the initial parameter values listed in Table 18, the objective function for each of the watershed models was about 3×10^6 , the contribution from each of the three observation groups (i.e., flows, monthly volumes and exceedence times) being about 1×10^6 each. For the Contentnea Creek model calibrated against flows recorded at Hookerton (henceforth referred to as the Hookerton model), PEST was able to reduce this objective function to 4.6×10^5 in about 100 model runs. Optimized parameter values are shown as "set 1" in Table 19. A graphical comparison between modeled and measured flows through part of the calibration period, between modeled and observed monthly volumes over the entirety of the calibration period, and between modeled and observed

exceedence times pertaining to the whole of the calibration period are shown in Figures 24a–c. Note that the restriction of graphed flows in Figure 24a to only a part of the calibration period was done for the sake of clarity. Graphs over the remainder of the calibration period are similar. Note also that the flow axis is logarithmic in this plot in order to afford a better comparison between flows under both high and low flow conditions. Calibration results for the other watershed models were similar to those documented above for the Hookerton model.

Table 19. Estimated parameter values. Parameters sets 2 to 5 were computed using PEST’s regularization functionality.

Parameter Name	Set 1	Set 2	Set 3	Set 4	Set 5	Set 6
LZSN	2	2	2	2	2	2
UZSN	2	1.79	2	2	1.76	2
INFILT	0.0526	0.0615	0.0783	0.034	0.0678	0.0687
BASETP	0.2	0.182	0.199	0.115	0.179	0.2
AGWETP	0.0011	0.0186	0.00232	0.0124	0.0247	0.0407
LZETP	0.5	0.5	0.2	0.72	0.5	0.5
INTFW	10	3.076	1	4.48	4.78	2.73
IRC	0.677	0.571	0.729	0.738	0.759	0.32
AGWRC	0.983	0.981	0.972	0.986	0.981	0.966
DEEPR	0.1	0.1	0.1	0.1	0.1	0.1

Parameter Nonuniqueness

Is it possible to calibrate a rainfall-runoff model against a flow time series by adjusting only 4 or 5 parameters if the model is designed in such a way as to ensure maximum parameter sensitivity and minimum correlation between parameters; see, for example, Jakeman and Hornberger (1993). Correlation is the term used to describe the phenomenon whereby two or more parameters can be varied in harmony in such a way as to have virtually no effect on the calibration objective function. In the calibration process described in the previous section, nine HSPF parameters were adjusted in order to achieve an acceptable fit between model outcomes and measured flows (though adjustment for some parameters ceased when they hit their bounds). It would thus appear that there is some redundancy in the parameterization of the model, probably resulting in at least some degree of correlation between the various parameters appearing in Table 18.

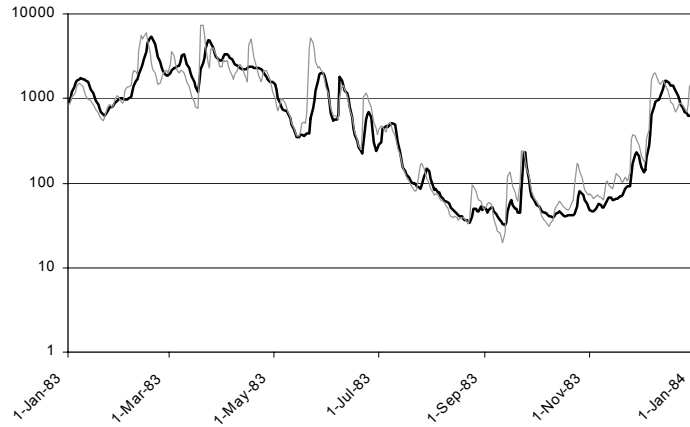


Figure 24a. Measured (bold line) and modeled (light line) flows (in ft³/sec) over part of the calibration period.

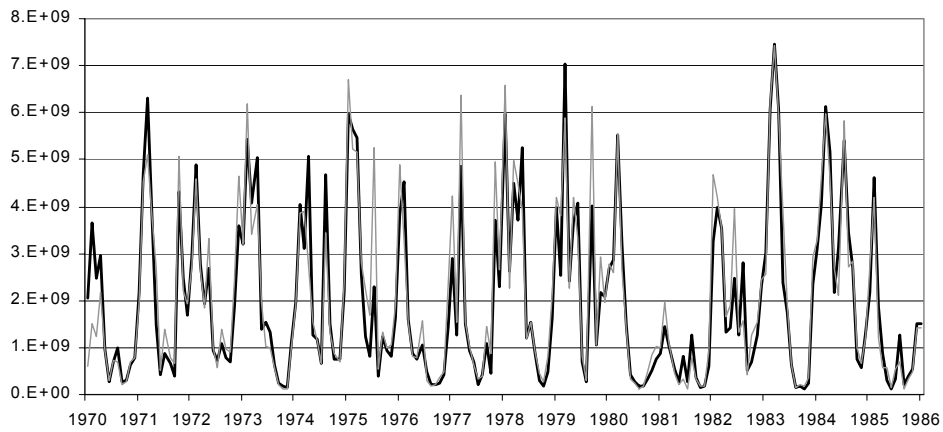


Figure 24b. Measured (bold line) and modeled (light line) monthly volumes (in ft³) over calibration period.

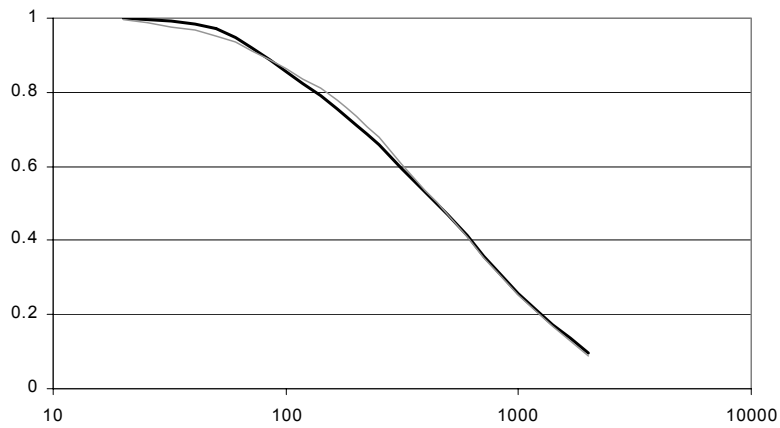


Figure 24c. Measured (bold line) and modeled (light line) flow exceedance fractions over the calibration period.

To determine if there were other sets of parameters that could be considered to adequately calibrate the model, PEST was used in regularization mode. When run in this mode, the user supplies PEST with a default system condition expressed in terms of preferred values for parameters and/or preferred values for mathematical relationships between parameters. PEST is then used to calibrate the model to within a preferred model-to-measurement fit tolerance (defined through a limiting *measurement* objective function below which the model is deemed to be calibrated), while simultaneously minimizing a *regularization* objective function calculated on the basis of the misfit between optimized parameter values and their user-supplied default values or relationship values.

In order to find a number of different parameter sets that calibrate the Hookerton model, a number of different default system conditions were defined in terms of preferred values for the parameters listed in Table 18. In all cases these preferred values lay within the bounds depicted in the fourth column of this table. A limiting measurement objective function of 5×10^5 was supplied for all PEST runs. This is slightly above that which it is possible to achieve without any regularization conditions being imposed, as was established during the previous calibration exercise; it is also such as to allow a visually pleasing fit between measurements and model outcomes. The model was then re-calibrated a number of different times, with PEST's regularization functionality ensuring that each calibrated parameter set departed to the smallest extent possible from the default parameter set supplied for that run. Four of the parameter sets determined in this way are listed as sets 2 to 5 in Table 19. In all cases the fit between model outcomes and raw and processed observation data was commensurate with that depicted in Figures 24a-c. Figure 25 shows the comparison of modeled and measured flows for 1983 using parameter sets 2 to 5 from Table 19.

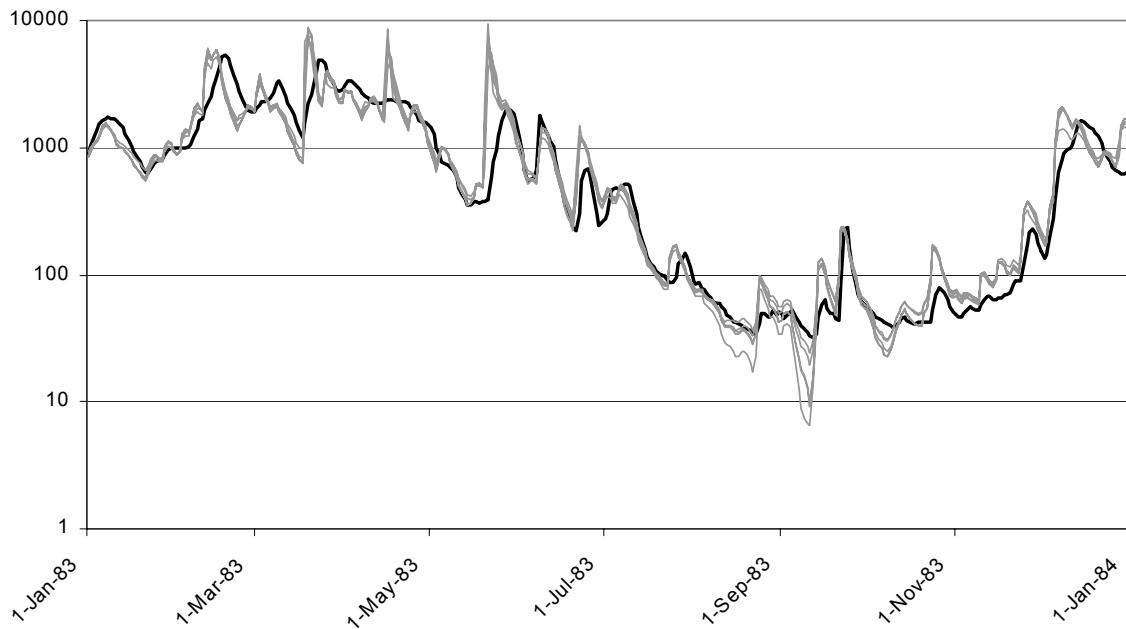


Figure 25. Measured (bold line) and modeled (light lines) flows (in ft³/sec) over part of the calibration period.

The nonuniqueness of parameters estimated through this calibration process is readily apparent from these results. However, the extent of this nonuniqueness is not as bad as it could have been if LZSN had not consistently

hit its lower bound and UZSN had not mostly hit its upper bound. The imposition of these bounds thus left PEST with two less parameters to estimate, thus reducing the amount of parameter redundancy. However, PEST's insistence on lowering LZSN to its 2 inch lower bound and raising UZSN to its 2 inch upper bound is noteworthy; perhaps PEST's tendency to alter these parameters to values outside of their respective ranges indicates that they may play a role that is at least partly different from that which their names suggest. Also note that the extreme sensitivity of parameter AGWRC as its value approaches 1.0 disguises the fact that there is more nonuniqueness associated with its estimation than is indicated by Table 19. Estimates for the value of the transformed parameter AGWRCTRANS defined in Eq.(34) vary between 35.7 and 74.1.

Finally, it is worthy of remark that the methodology demonstrated herein could be used to undertake a kind of calibration-constrained Monte Carlo analysis as a basis for model predictive uncertainty analysis. Parameter sets lying within the allowable ranges shown in Table 19 could be generated at random. Then, for each such generated set, the model could be recalibrated using PEST in regularization mode in order to determine a parameter set that calibrates the model, while departing minimally from the randomly-generated parameter set. Model predictions would then be made using all such calibrated parameter sets.

Model Validation

As discussed above, the Contentnea Creek models were all calibrated using flows recorded over the period 1970 to 1985. Flows recorded over the period 1986 to 1995 were then used for validation of the calibrated models. Figure 26a shows a comparison between observed and model-generated flows for the Hookerton model over part of the validation period. Observed and model-generated monthly volumes and observed and model-generated exceedence fractions pertaining to the whole of the validation period are shown in Figures 26b and 26c. In these figures predictions made on the basis of parameter sets 2 to 5 listed in Table 19 are provided as grey lines. Bold lines represent measured flows, or quantities derived directly from them.

Inspection of Figures 26a and 26b reveals that the fits between prediction and observation are not entirely without merit. Hence, at least for the types of predictions discussed thus far (all based on flow), even though the model calibration process resulted in a nonunique parameter set, predictions made by the calibrated model appear to be sensitive to the same *combinations* of parameters as those that can be estimated through calibration. In general this is more likely to occur when a model is used to make predictions that are of the same type as those against which it was calibrated. Where a model is used to make predictions of different types from those against which it was calibrated, or where model inputs are significantly different under predictive conditions from those that prevailed under calibration conditions, opportunities arise for predictions to be sensitive to parameters, or parameter combinations, that are not well determined through the calibration process. In such circumstances predictive uncertainty may be high. This occurred to some extent in the period around 1st September 1993 when flows were very low. It is during such periods of climatic extremes that conditions are most likely to deviate from those encountered under calibration conditions, and hence when the reliance on individual parameters, or on combinations of parameters, that are different from those for which the information content of the calibration data set was greatest is most likely to occur. This is further discussed below.

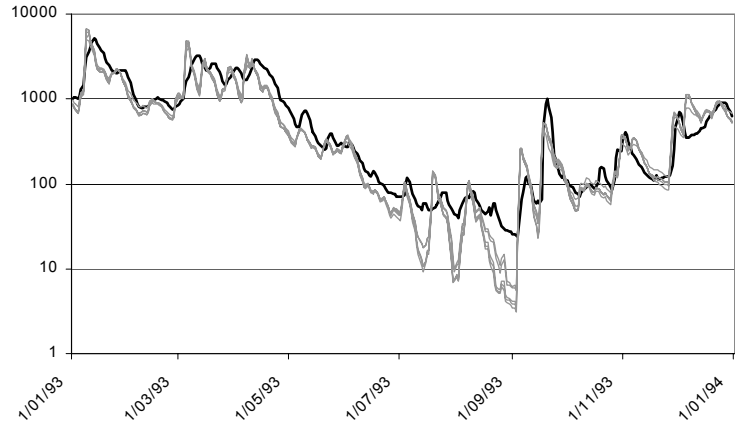


Figure 26a. Measured (bold line) and modeled (light line) flows (in ft³/sec) over part of the validation period at Hookerton. Parameters were estimated through simultaneous calibration of all four watershed models.

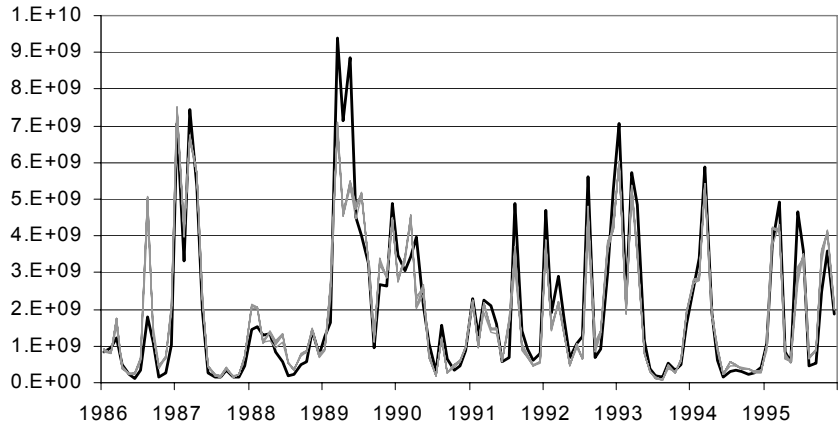


Figure 26b. Measured (bold line) and modeled (light lines) monthly volumes (in ft³) over the validation period.

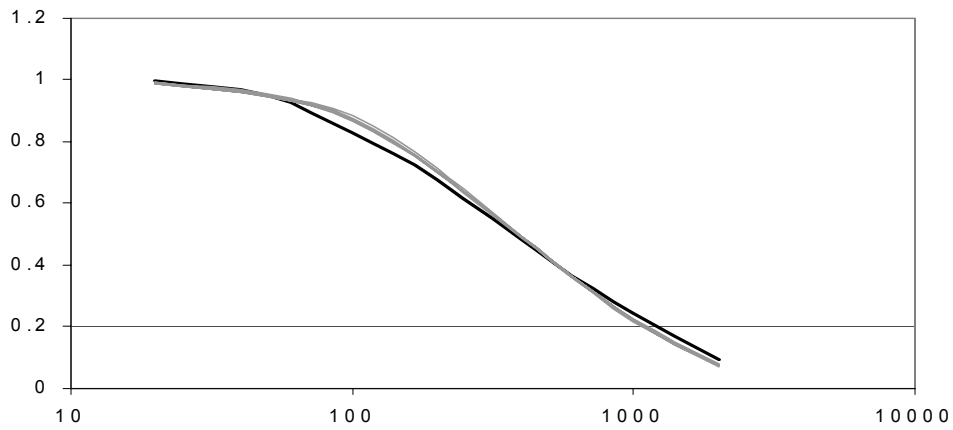


Figure 26c. Measured (bold line) and modeled (light lines) flow exceedence fractions over the validation period.

Simultaneous Calibration of Multiple Watershed Models Using Identical Parameter Values

From the forgoing discussion it is apparent that parameter uniqueness cannot be expected in the calibration of our simple watershed, even though many simplifications were made in order to reduce the number of parameters requiring estimation, including constraints imposed on parameters to ensure that they are assigned reasonable values (possibly at the cost of goodness of fit in the case of LZSN). Calibration of the other three watershed models led to similar conclusions.

In an attempt to reduce the degree of nonuniqueness in parameter estimates extra information was introduced into the calibration process. It was mentioned above that the same land use categories are featured in all of the watershed models that are the focus of the present investigation. It is thus to be hoped that parameters assigned to the PERLNDs representing these land use types are consistent across the different watersheds. If they are not, then this constitutes evidence that there are limitations in the ability of the model to simulate watershed processes either because of poor model construction or because of limitations in the ability of a lumped parameter model such as HSPF to simulate complex natural systems, or both. The issue of whether anything can be done in practice about either of these conditions is a matter for conjecture.

In expanding Popper's (1959) exposition of the scientific method to the application of numerical simulation models in environmental management, Beck (1987) noted that environmental models can only be used to test hypotheses, and that any given hypothesis can only be rejected, not accepted, on the basis of model usage. In following that principle, the hypothesis that all four watershed models can be assigned identical hydrologic parameter values for each land use type was tested. Rejection of this hypotheses can take place if a good fit between model outcomes and corresponding field measurement in all watersheds cannot be achieved using a reasonable set of hydrologic parameter values that are identical for all models.

Note the sharp distinction between this method of comparing parameters used by different models in neighboring watersheds and that employed by Yokoo et al. (2001). The latter authors attempted to establish regression relationships between model parameters on the one hand and observable watershed characteristics on the other. However, these relationships were sought only after calibration of the individual models had taken place in a manner that was quite independent of the regression relationships being sought. Given the nonuniqueness of watershed model parameterization that is illustrated above, such a methodology is flawed, for too much is left to chance in estimating parameters as an outcome of the calibration process. In the present instance, the posited inter-model parameter relationships (i.e., parameter equality in this case) are built into the calibration process. If an acceptable calibration does not occur with these relationships directly incorporated into the calibration process, then the hypothesis of parameter equality must be rejected. In contrast, given the extent of parameter nonuniqueness illustrated above, the failure of a separate and independent calibration of each watershed to yield identical parameter values does not provide sufficient basis for rejection of the hypothesis that parameter values for all watersheds are the same.

A composite model was constructed through inclusion of all watershed models in a single batch file. PEST was used to calibrate this composite model as if it were a single model. TSPROC acted as postprocessor for all four models, enabling daily flow rates, monthly volumes and exceedence times for all four watersheds to be used in the

calibration process. Nine parameters were then estimated, viz. those listed in Table 18 under the constraint that all watershed models employ the same parameter values.

Parameter values estimated as an outcome of this process are those labeled as “set 6” in Table 19. The fit between model outcomes and field measurements was, however, a little disappointing in all four watersheds. Figure 27 shows modeled and observed flows for the Hookerton model over 1983 (this being part of the 1970-1985 calibration period). The fit is not as good as that depicted in Figure 24b, particularly at low flows. The failure at low flows is unfortunate because, as was discussed above, the calibration process was to a degree focussed on low flows.

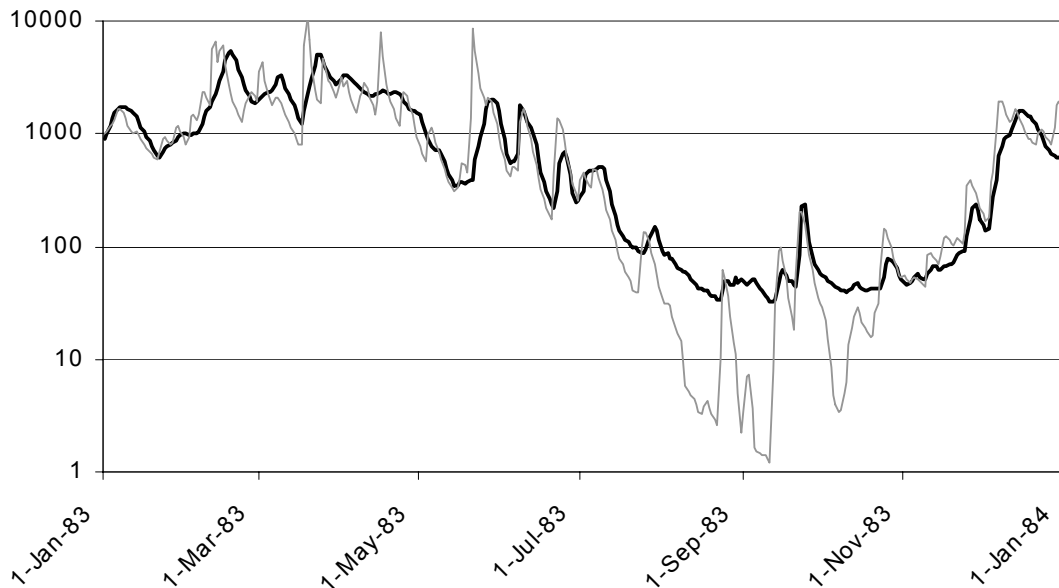


Figure 27. Measured (bold line) and modeled (light line) flows (in ft^3/sec) over part of the calibration period. Parameters were estimated through simultaneous calibration of all four watershed models.

As a result of our attempt to calibrate multiple models simultaneously with identical parameter values, can we reject the hypothesis that all of these parameters are the same? Our attempt to answer this question raises yet another question. The fit between model outcomes and field measurements illustrated in Figure 27 is not entirely inadequate over the complete time series. However, our ability to make accurate predictions at low flows would probably be seriously degraded if we were to insist on using identical parameters for all watershed models. Nevertheless, the extent of misfit illustrated in Figure 27 (and also apparent from an inspection of the outputs of the other watershed models) may not be bad enough to reject the parameter set if used for other purposes, for example to parameterize an ungauged watershed in the same area for a preliminary analysis of its rainfall-runoff characteristics. For this latter application, the more watersheds that are involved in the simultaneous calibration exercise, the more robust the parameter estimates are likely to be. The idea of prediction-specific parameters that follows from this argument, together with the inherent nonuniqueness of parameters estimated through the calibration process, brings

into question the idea that the model construction, calibration and deployment process should ever yield a unique set of parameter values. Rather, model calibration should be viewed as a form of data interpretation. The manner in which data is most appropriately interpreted depends very much on the context in which that interpretation takes place as set by the environmental management issue that the model is being used to address.

Simultaneous Calibration of Multiple Watershed Models Using Regularization

In the previous section it was established that the ability of the Hookerton model to simulate low flows was seriously compromised by insisting that its parameters adopt values that allow the calibration of other watershed models as well. Nevertheless, the hydrologic response of neighboring watersheds should not be ignored, for there is information content in the assertion that variation of parameter values between the watersheds that are the subject of the present investigation should be minimal. As was discussed above, the extent of parameter nonuniqueness (and hence the element of luck associated with parameter estimates) is such that cross-watershed parameter similarity will be an unlikely outcome of the calibration of individual watershed models unless that concept is included directly in the calibration process.

By using PEST in regularization mode in the simultaneous calibration of all four watershed models a parameter similarity condition can, in fact, be introduced to the parameter estimation process without compromising the level of model-to-measurement fit achieved through that process. Recall from the discussion in a previous section that PEST's regularization functionality is such that the user sets the objective function below which the model is deemed to be calibrated. In attempting to attain that objective function, PEST varies parameter values in such a way as to minimize the departure of these values from their preferred condition; however, attainment of the desired level of model-to-measurement fit is still PEST's primary goal.

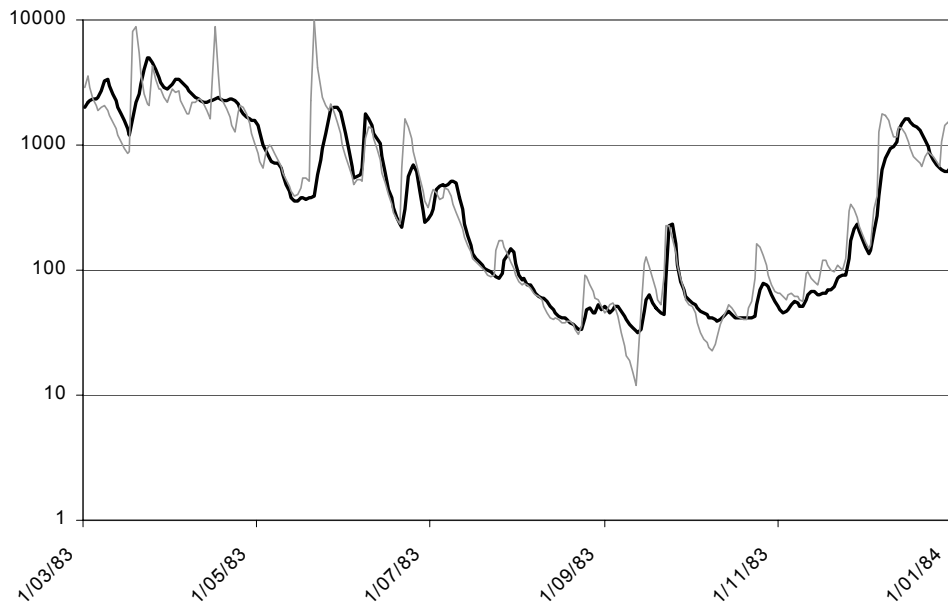


Figure 28. Measured (bold line) and modeled (light line) flows (in ft^3/sec) over part of the calibration period. Model parameters were estimated through simultaneous calibration of all watersheds using regularization.

In applying regularization to the simultaneous calibration of all four watershed models a preferred condition of cross-watershed parameter equality was imposed (in contrast to the previous use of regularization where the preferred condition pertained directly to parameter values themselves). Because the limiting measurement objective function used in the parameter estimation process was set suitably low, a good fit between model outputs and field measurements was obtained for all watersheds. For the Hookerton model, the fits resemble those illustrated in Figures 24a-c; see Figure 28. Estimated parameter values for all watersheds are listed in Table 20. PEST's regularization functionality is such that any parameter differences between watersheds that are apparent in Table 20 are there because they *have to be there* in order to obtain the high level of fit illustrated in Figure 28. (For comparison purposes, parameters estimated through independent watershed calibration are shown italicized in brackets in Table 20. Inter-watershed variation is obviously much greater for these parameters.)

The regularization process, when used in this way, while reducing parameter nonuniqueness considerably, does not necessarily eliminate it. This is because there may be other sets of parameters that result in just as good a fit between model outcomes and field measurements, and which also result in inter-watershed variation that is no greater than that depicted in Table 20. Nevertheless, the regularization process has been used to inject a vital piece of knowledge into the parameter estimation process that would have otherwise been neglected (that is, the notion that inter-watershed parameter variability should be minimal). Furthermore, it allowed the inclusion of this information to take place in a way that did not detract from the primary purpose of the model, viz. to provide as accurate a simulation as possible of flows (particularly low flows), volumes and exceedence times in each watershed.

Table 20. Parameters estimated by PEST through simultaneous watershed calibration using its regularization functionality. Parameters estimated through independent model calibration are shown italicized in brackets.

Parameter Name	Contentnea at Hookerton	Moccasin at Lucama	Nahunta Swamp	Little Contentnea
LZSN	2.29 (2.00)	2.01 (2.00)	2.58 (3.244)	2.00 (2.00)
UZSN	2.00 (2.00)	2.00 (2.00)	2.00 (2.00)	1.55 (1.93)
INFILT	0.0533 (0.0526)	0.0317 (0.0194)	0.0706 (0.117)	0.0276 (0.00518)
BASETP	0.163 (0.20)	0.182 (0.118)	0.157 (0.20)	0.166 (0.114)
AGWETP	0.0201 (0.00108)	0.0269 (0.0493)	0.0222 (0.00358)	0.0268 (0.00814)
LZETP	0.50 (0.50)	0.50 (0.50)	0.50 (0.50)	0.50 (0.50)
INTFW	1.21 (10.0)	1.00 (1.00)	1.17 (1.406)	1.31 (3.253)
IRC	0.533 (0.670)	0.506 (0.794)	0.512 (0.220)	0.499 (0.799)
AGWRC	0.988 (0.984)	0.967 (0.980)	0.976 (0.967)	0.942 (0.956)
DEEPFR	0.1 (fixed)	0.1 (fixed)	0.1 (fixed)	0.1 (fixed)

Predictive Analysis

Attention has been drawn to the fact that where a model attempts to make predictions under conditions that are different from those prevailing under calibration conditions, the margin of uncertainty surrounding such predictions is likely to be larger than that surrounding predictions made under similar conditions to those prevailing at calibration. The same applies to the prediction of system fine detail (e.g., temporal or spatial detail, depending on the type of model). Even under calibration conditions, a model is unlikely to replicate every nuance of an environmental system's response over the whole of the calibration period, for the cost of fitting certain observations at certain times very well is often a loss of ability to fit other observations at other times quite as well.

This phenomenon is exemplified in the Hookerton model's failure to accurately predict the low flows that occurred over the few days centered on 1st September 1993. Figure 26a shows that all of the calibrated models for this watershed underpredict flow over this time, a particularly worrying phenomenon since the calibration process attempted to optimize the model's ability to predict such low flows. Also apparent from Figure 26a is the fact that there is some uncertainty surrounding flow predictions made over this time, this following from the range of predictions displayed in that figure, all of which were made with well calibrated models.

Multiple re-calibration using PEST's regularization functionality in conjunction with different default parameter values is one way of exploring model predictive uncertainty. A model can be calibrated many times, with a different parameter set estimated each time; predictions can then be made using all estimated parameter sets. However, a far more efficient way to explore predictive uncertainty is to first identify a specific prediction whose uncertainty requires exploration, and then to find a parameter set that maximizes/minimizes that prediction while maintaining the model in a calibrated state (as defined by an upper objective function limit below which the model is deemed to be calibrated). This can be accomplished using PEST's predictive analysis functionality. Like nonlinear parameter estimation, predictive analysis, as implemented by PEST, is an iterative procedure involving many model runs; however, notwithstanding the fact that it is a numerically intensive process, it is by far the most efficient means available for exploration of the uncertainty surrounding a specific prediction made by a calibrated model. The

algorithm underpinning PEST’s predictive analysis functionality requires no linearity assumption on the part of the model; it is based on the theory presented by Vecchia and Cooley (1987); see either that reference, or Doherty (2001a), for further details.

Total flow volume over the period 29th August to 3rd September 1993 was identified as the specific model prediction which PEST was used to maximize, and then minimize, while maintaining the model in a calibrated state relative to measured flows, volumes and exceedence times spanning the period 1970 to 1985; the limiting calibration objective function was the same as that used above in exploring the role of regularization in estimating parameter sets that deviate minimally from a set of user-supplied preferred values. Figure 29a shows predictions made by the two calibrated models (i.e., that for which the key prediction is maximized and that for which it is minimized) over 1993, while Figure 29b shows model-to-measurement fits for these two models over part of the calibration period. In each of these figures the dashed light-colored curve represents the output of the minimization model, whereas the full light-colored curve represents the output of the maximization model. Because the predictive period is actually within the validation period, measured flows are also shown in Figure 29a (bold line) for comparison with model predictions.

The range of uncertainty accompanying the prediction of flows on and near 1st September 1993 is apparent from an inspection of Figure 29a. As Figure 29b demonstrates, both the model used for prediction maximization and that used for prediction minimization fit measured flows well under calibration conditions. However, as is expected, the model that was calibrated for prediction minimization tends to produce lower flows through the time window of the calibration period illustrated in Figure 29b than that calibrated for prediction maximization. Calibrated parameters for the minimization and maximization models are sets 7 and 8, respectively, in Table 21.

Table 21. Estimated parameter values. All parameter sets were estimated using PEST’s predictive analysis functionality.

Parameter Name	Set 7	Set 8	Set 9	Set 10
LZSN	2	2	2	2
UZSN	1.9	2	1.58	1.91
INFILT	0.0675	0.03	0.0871	0.029
BASETP	0.2	0.2	0.2	0.2
AGWETP	0.0169	0.001	0.022	0.001
LZETP	0.5	0.5	0.5	0.5
INTFW	4.73	10	5.44	10
IRC	0.587	0.671	0.65	0.833
AGWRC	0.98	0.99	0.979	0.995
DEEPPFR	0.1 (<i>fixed</i>)	0.1 (<i>fixed</i>)	0.166	0.262

Model Complexity

It is unfortunate that even with the predicted flow maximized over the 6 day period of interest, the model-

generated flow is less than the flow that was actually observed over this period. The range of predictive uncertainty would have been wide enough to include measured flows if the limiting objective function (i.e., the objective function below which the model is deemed to be calibrated) was set higher than it actually was during the predictive analysis process described above, thus giving PEST more room to move in seeking parameter values that maximize the predicted flows while still calibrating the model. However, the model's failure to include measured flows in its predictive uncertainty range can also be construed as a lack of ability on the part of the model to replicate all of the temporal fine detail of the system's behavior, a topic that was briefly discussed above. (Whether it is actually necessary for a model to replicate such fine detail depends on the uses to which the model will be put.)

In general, if a model is to simulate system fine detail, it must be endowed with an appropriate level of complexity. The introduction of complexity to a model is generally accompanied by the introduction of extra parameters. It has already been demonstrated that, even though the Hookerton model can be quite adequately calibrated with the number of adjustable parameters already at its disposal, those parameters cannot be uniquely estimated. Hence, even if it increases the model's ability to replicate system fine detail, the introduction of more parameters is likely to increase the extent of parameter nonuniqueness.

In order to introduce more complexity into the model, the DEEPFR parameter, which for all runs documented up until now had been fixed at a low value in accordance with current understanding of the system, was allowed to vary. PEST was then used to adjust this parameter, along with the parameters that it had already been adjusting, in order to minimize and maximize flow at Hookerton over the period 29th August to 3rd September 1993 while, once again, maintaining the model in a calibrated state over the period 1970 to 1985. Figure 30a shows flows over 1993 predicted by the maximization and minimization models, while Figure 30b shows flows during 1983 (part of the calibration period) produced by the two models. Estimated parameters for minimization and maximization of flow are listed as set 9 and set 10, respectively, in Table 21.

As an inspection of Figure 30a reveals, measured flow volume over the 6 day period spanning 29th August to 3rd September 1993 is now just within the margin of predictive uncertainty of the model, the latter now being wider (both upwards and downwards) as a result of the introduction of the extra complexity. This illustrates an extremely important (and seldom recognized) aspect of model usage in environmental simulation. In general, while it is true that system fine detail can often be replicated only if the necessary complexity is introduced into a model, the heightened extent of parameter correlation and insensitivity that results from the addition of that complexity often results in high levels of uncertainty surrounding the predictions of that system fine detail made by the model. Hence, just because a model *can* simulate complex processes, this does not mean that it *will* simulate them with any precision. *If the appropriate level of complexity is included in the model, all that can be guaranteed is that true system behavior will lie somewhere within the uncertainty limits of predictions made by that model.* The introduction of complexity into a model endows the modeler (by using the model in conjunction with a predictive analyser such as PEST) to calculate these uncertainty limits and thereby to know the limits (*and only the limits*) of future real world behavior. The need for predictive uncertainty analysis in conjunction with model deployment (especially if a model is deployed to investigate system fine detail) is thus paramount.



Figure 29a. Model-generated (light lines) and measured (bold line) flows in ft^3/sec over 1993. Model parameters were estimated using PEST's predictive analysis functionality.

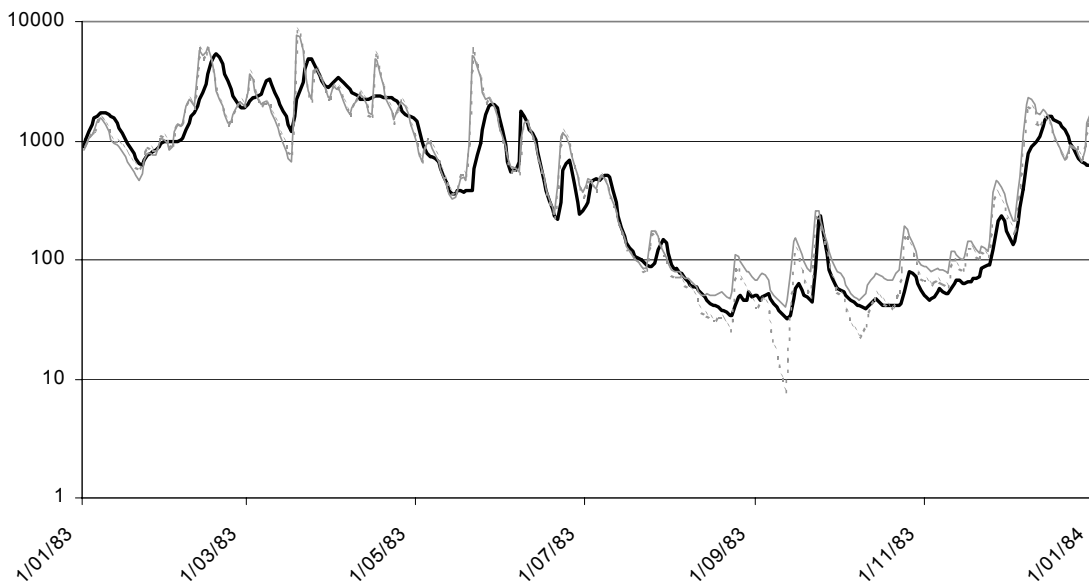


Figure 29b. Model-generated (light lines) and measured (bold line) flows in ft^3/sec over part of the calibration period. Model parameters were estimated using PEST's predictive analysis functionality.

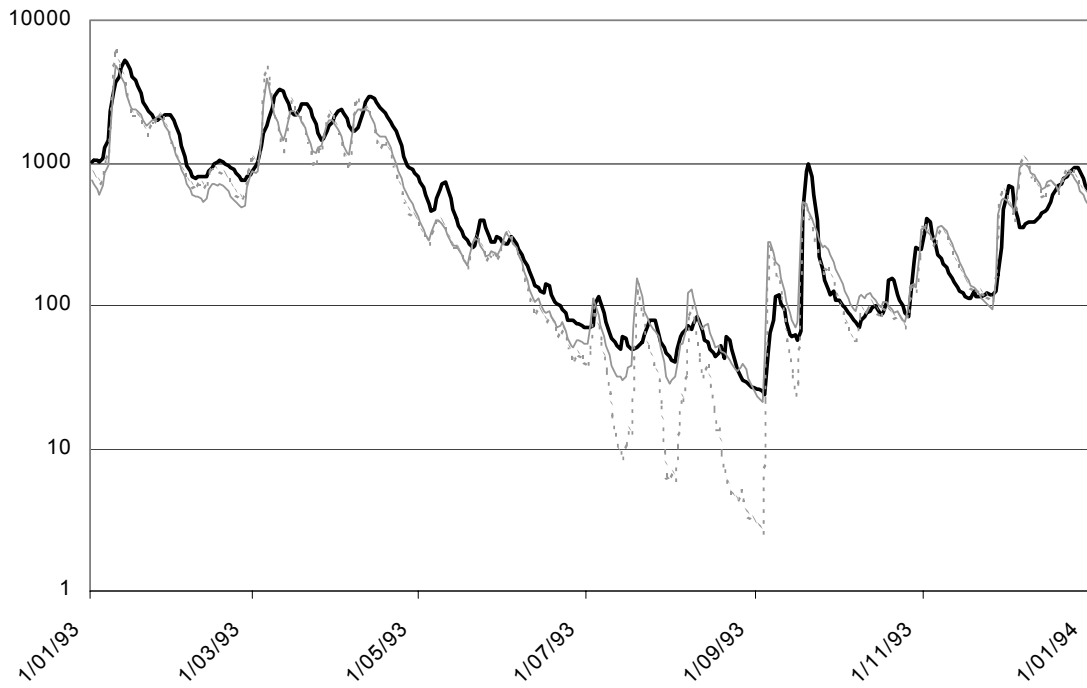


Figure 30a. Model-generated (light lines) and measured (bold line) flows in ft^3/sec over 1993. Model parameters were estimated using PEST's predictive analysis functionality with DEEPFR adjustable.

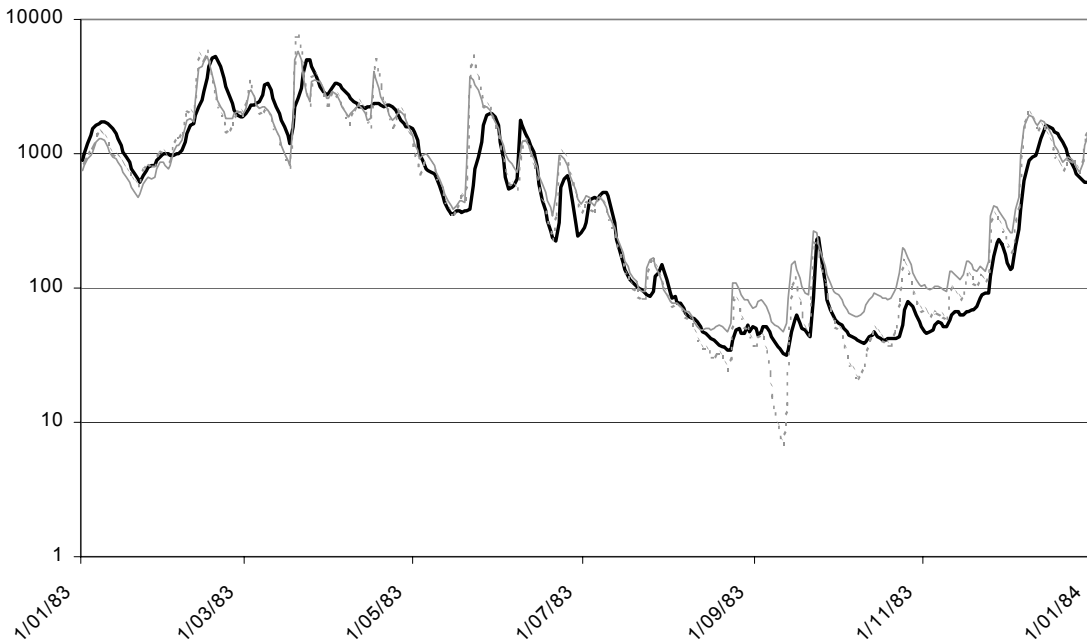


Figure 30b. Model-generated (light lines) and measured (bold line) flows in ft^3/sec over part of the calibration period. Model parameters were estimated using PEST's predictive analysis functionality with DEEPFR adjustable.

It is interesting that PEST actually increased, rather than decreased, DEEPFR in order to raise the low flows within the predictive window. Part of the reason for this is that, under calibration conditions, the model-predicted total flow volume was slightly above the observed total flow volume with DEEPFR fixed at 0.1. Hence, the model needed to lose water. To the extent that the original DEEPFR setting of 0.1 prevented it from easily losing water, other parameters had to be adjusted to compensate for this so that water could be lost in other ways. Obviously they did a good job, because the fit between model outputs and field data under calibration conditions was very good. However, the cost of this load shifting to other parameters may have been the estimation of inappropriate values for these other parameters. Furthermore, while it may have helped in some ways, it cannot be said that the inclusion of DEEPFR as an adjustable parameter is not more of a parameter fiddling device than a reflection of reality. As has been mentioned above, losses to deep groundwater are expected to be minimal in this watershed. Other possible reasons for the volumetric discrepancy between modeled and observed flows may include inaccuracies in spatial rainfall interpolation, inaccurate calculation of potential evaporation, variation of impervious area as development occurred during the calibration period, and other reasons as well. Loss of water to unknown deep aquifers (as represented by DEEPFR) may thus be a surrogate for some or all of these processes.

The Effect of Urbanization

One of the reasons for construction of the Contentnea basin watershed models is to assess the effects of urbanization on the aquatic ecosystem. While there are many changes that occur as a result of urbanization, we focus on just one, viz. the hydrologic effect of urbanization on low flows. With increased impervious land in a watershed, a stream is expected to become more flashy, having higher peak flows during significant rain events and lower fair-weather flows due to the smaller amount of infiltration and reduced subsurface recharge.

If flow becomes low enough the adverse effects on the health of fish can be considerable. When flows become so low that no aeration occurs, dissolved oxygen can drop close to the level at which it is harmful to fish (generally accepted to be 4 to 5 ppm). In summer, in-stream temperatures rise as a result of sun exposure and higher atmospheric temperatures. This can also stress fish and lead to algal growth that, in turn, can further deplete dissolved oxygen. Furthermore, the possibilities offered to fish for refuge from stress are rapidly diminished as flow is lowered.

A flow of 30 ft³/sec was selected as the threshold of concern. The model was then used to explore the effect of urbanization on increasing the number of days for which flow is likely to be below this threshold. Because the model cannot be expected to predict flows exactly (especially low flows, as has been demonstrated above), a direct model prediction of the number of days for which flow is below this threshold under conditions of increased urbanization would be almost meaningless. Hence the following strategy was adopted in order to make low-flow predictions following urbanization with as much accuracy as possible:

- 1) The model was run over the period 1970 to 1995 based on current land use. It was also calibrated over this period. To increase the model's predictive ability at low flows, an extra observation was added to the calibration data set; the model was used to match, as accurately as possible, the observed time for which flows were below 30ft³/sec over the calibration period.

2) The model was then run over the same period using the same historical inputs but with impervious area increased from 1.7% to 5% of the Hookerton model watershed. A time series representing the difference between model-generated non-urbanized and urbanized daily flows was then generated. This difference provides a measure of the effect of urbanization on streamflow.

3) The flow difference time series calculated above was added to the observed flow time series over the calibration period to generate a kind of high fidelity model-predicted streamflow showing the effects of urbanization. The fact that model-generated flow *differences* were used in the predictive process, rather than model-generated flows themselves, does much to mitigate the effects of the model's inability to replicate system response in fine temporal detail.

4) The amount of time for which the high-fidelity streamflow (calculated as above) was below 30ft³/sec was computed. This estimate was then maximized/minimized while maintaining the model in a calibrated state (according to point 1 above) using PEST's predictive analyser.

All of the calculations required to generate the high fidelity streamflow (and to accumulate the time for which this flow was below the critical threshold) were carried out following each model run using the time series processor TSPROC discussed above. Furthermore, each model run as undertaken by PEST in the course of carrying out this complex predictive analysis process required that two HSPF runs, together with TSPROC-based processing, be carried out. The model as run by PEST was thus comprised of a batch file containing the commands to run HSPF twice in succession followed by TSPROC. TSPROC was also used to generate PEST input files for this complex problem.

On the basis of historical flows it is easily calculated that, over the period between 1970 and 1995, a total of 17.3 days was spent with flow below 30ft³/sec. Model-predicted days below this threshold for a more urbanized watershed range from 9 days to 14 days (these being the limits calculated using PEST's predictive analyser). The fact that the number of low-flow days will actually decrease, rather than increase, as a result of urbanization reflects the fact that sporadic rain falling on impervious areas during summer months is able to rapidly top up river flow on most occasions before the latter reaches the 30 ft³/sec threshold. Because the model was used to calculate flow *alterations* rather than flows themselves, and because this result was subject to rigorous uncertainty analysis using PEST's predictive analyser, a high degree of confidence surrounds this prediction. It should be noted, however, that this method of analysis presumes that future climate will not depart from past climate. This will quite possibly not be the case. Unfortunately, however, under an assumption of altered climatic inputs, the analysis of differential flows discussed above that led to the calculation of results of reasonably high integrity is not possible. The development of other methods of differential flow analysis suitable for deployment in a calibration/predictive analysis setting for scenarios that involve climatic change awaits further research.

Conclusions

Though focused on a particular environmental management problem, the purpose of this work has been to demonstrate new methodologies for environmental data processing based on the use of numerical simulation models in conjunction with sophisticated parameter estimation and predictive analysis software.

It has been demonstrated that even after imposition of a set of simplifying assumptions that are necessary for the construction of a numerical simulator of real-world behavior, it may not be possible to estimate model parameters uniquely through the calibration process, even when these parameters are constrained to take on reasonable values. Furthermore, the greater the level of system detail that a model attempts to replicate, the greater will normally be the number of parameters that require estimation, and the less likely it becomes that such parameters can be uniquely estimated.

Parameter nonuniqueness may result in predictive nonuniqueness when a model is deployed to predict the environmental effects of altered land management. The extent of this predictive nonuniqueness may not be so large as to negate the effort required for model development. In general, the more broad-scale the type of prediction made by a model, the more likely is that prediction to be made with a high degree of certainty. However, where a model is required to predict the temporal fine detail of system response, and/or where model inputs are significantly different under predictive conditions from what they were under calibration conditions, the margin of uncertainty surrounding at least some of those predictions may be quite large. If these predictions are important then integrity demands that the magnitude of this uncertainty be analysed using, for example, the type of software discussed herein.

Whenever possible, a modeler's knowledge and intuition should play an important role in the parameter estimation process. In many instances this can be accomplished by supplying a default system state from which model parameters should depart only to the extent necessary to calibrate the model. This can be accomplished by using the regularization techniques discussed herein. Where knowledge of an area is insufficient to define a unique default system state, a number of such states can be generated (e.g., using a random number generator) while adhering to the bounds imposed by reality. Repeated model re-calibration can then be undertaken in such a way as to deviate to the smallest extent possible from each one of them. Predictions should then be made using each such parameter set. In this way a kind of calibration-constrained Monte-Carlo analysis can be undertaken.

Finally, this work demonstrates that an environmental model cannot be used to furnish the elusive "answer at the back of the book" regarding the effects of a particular environmental management scenario on future system behavior. Modeling is simply a form of data processing. When used creatively in a way that is tuned to the environmental issue at hand, in conjunction with sophisticated parameter estimation and predictive analysis software such as that described herein, a model can be used to undertake powerful and comprehensive data interpretation in a way that is most relevant to that issue. Together, the model and the parameter estimator allow the modeler to pose hypotheses, and then to test them. If a model can be parameterized in such a way that it is able to match field measurements acceptably well using parameters that are acceptably realistic, then the hypothesis that is encapsulated in the model structure, inputs and boundary conditions cannot be rejected. This does not mean, however, that other hypotheses can also not be rejected. Thus, when all available data are processed to the maximum possible extent using state-of-the-art simulation and parameter estimation software, a modeler may still be left with a high degree of uncertainty concerning the predicted outcomes of some environmental management scenarios. An integral part of modeling practice must be to quantify this uncertainty.

6.2. Total Suspended Sediment Loadings

The use of advanced nonlinear parameter estimation techniques in the calibration and predictive analysis of

watershed models was documented by Doherty and Johnston (2002). Use of these techniques was restricted solely to the processing of streamflow data and to the estimation of parameters that govern hydrologic output. Here we document the use of nonlinear parameter estimation methods in estimating parameters associated with the erosion and sediment transport components of the watershed model HSPF (Hydrologic Simulation Program Fortran (Bicknell et al. 2001)). The sporadic and noisy nature of sediment data makes the estimation of these parameters a much more difficult procedure than the estimation of hydrologic parameters. This difficulty is exacerbated by the insensitivity of model output to some of these parameters over at least part of their allowable range, as well as the sometimes extremely nonlinear nature of the relationship between these parameters and model output. Parameter correlation is also a problem: it is often possible to vary two or more parameters simultaneously with very little effect on model output. When high correlation and parameter insensitivity combine, estimation of individual parameters is virtually impossible.

The result of low parameter sensitivity and high parameter correlation is parameter non-uniqueness, even after reality checks have been placed on values using expert knowledge of the physical or chemical processes simulated. Uncertainty in the estimated values of model parameters can then lead to uncertainty in the values of predictions made by the model. This, in turn, leads to the necessity to analyze the uncertainty associated with model predictions. We also address the issue of model predictive uncertainty analysis regarding in-stream sediment transport.

The principal member of the PEST suite is TSPROC, a time-series processor optimized for use in the calibration context. PEST is a model-independent parameter estimator with advanced predictive analysis and regularization features. Its model-independence rests on the fact that it is able to communicate with a model through the latter's own input and output files, thus allowing easy calibration setup with an arbitrary model. Such a model can be encapsulated in a batch or script file if desired. Hence model pre-and post-processing software (such as TSPROC) can be used as part of the calibration process.

PEST implements a particularly robust variant of the Gauss-Marquardt-Levenberg method of parameter estimation. While this method requires that a continuous relationship exist between model parameters and model output, it can normally find the minimum of the objective function in fewer model runs than any other parameter estimation method. This is important when model run times are lengthy, or even moderate.

TSPROC is able to read time-series data from a variety of sources including ASCII files and USGS Watershed Data Management (WDM) files. It can undertake temporal interpolation of one time series to another, carry out mathematical manipulations of arbitrary complexity between one or more time series, compute time series statistics, and calculate various quantities derived from time series including exceedence times, and volumetric/mass accumulation between one or many arbitrary dates and times. It also facilitates the use of both raw and processed time series data in the calibration process by automatically generating PEST input files for calibration runs involving some or all of these quantities. Use of PEST and TSPROC in calibrating the hydrologic component of the Hookerton model (and its three neighboring watershed models) is fully documented in Doherty and Johnston (2002).

When there is a strong correlation between stream discharge and sediment load, the sediment-rating curve can be a powerful tool for the analysis of stream sediment transport. Discharge acts as a surrogate for sediment load

over those periods for which TSS measurements are not available, which, in most cases, is the majority of the period of record. If a rating curve can be determined with sufficient accuracy, the total sediment transported from a watershed over a given period of time can be evaluated by first calculating daily sediment concentrations from daily stream discharges using the sediment rating curve and then summing daily sediment concentrations times daily flows over the period of interest. If it is further assumed that the amount of bed sediment is the same at the end as at the beginning, then total transported sediment is the total amount of sediment eroded or washed from the watershed. This quantity is an estimate of long-term erosion and transport. While such a calculation is conceptually possible, there is a considerable associated uncertainty. Uncertainty exists in parameters that describe the sediment-rating curve, and there are issues with the assumption that streambed sediment storage does not change over the analysis period. Although situations of rapid buildup and loss of bed sediment are rare, they do occur and are impossible to verify without ancillary data.

An alternative means of calculating the total amount of sediment exported from a watershed is that afforded by the use of a calibrated model. Use of a model has the advantage that it can be applied to all sediment size classes (including silt and clay). Estimates of sediment export made using a model will also be subject to a large amount of uncertainty. However, it is possible (and also desirable) to quantify this uncertainty in the application of the model. The ability to quantify the degree of predictive uncertainty associated with sediment calculations in a mathematical model, rather than simply an empirical relationship, is preferred to regression methods for many environmental data processing contexts.

HSPF simulation of suspended sand concentration has a number of important repercussions for the calibration of HSPF using TSS data. As long as sand is available in bed storage, no direct relationship can be made between the amount of suspended sand in the stream and the erosional characteristics of any contributing PERLND or IMPLND. The amount of suspended sand is a function solely of the velocity (and hence current discharge rate) of the stream. Any sand that is delivered in excess of stream sand carrying capacity will be deposited to the bed. Similarly, if a shortfall in stream sand transport potential exists, the difference will be filled with any available sand storage. Under these circumstances, measurements of suspended sand only provide information pertaining to the estimation of those parameters that govern the relationship between stream discharge and stream sediment carrying capacity. That is, the calibration process can only be used to infer the sediment rating curve (or rather the sand rating curve) of the stream.

In contrast, if there is no sand in the bed of a stream, any suspended sand carried by the stream will be the direct result of erosion taking place within the PERLNDs and IMPLNDs. In such a case measurements of suspended sand concentration can provide information for estimation of parameters governing watershed erosion. However, this condition is most likely to prevail in upland watersheds drained by young streams than in lowlands drained by more mature streams.

Transport of silt and clay is simulated differently than sand transport. No carrying capacity is defined for these size classes. A threshold approach is adopted whereby silt and clay are scoured from the streambed if the shear stress exceeds the critical shear stress for scouring (HSPF parameter TAUCS). Silt and clay are deposited if the shear stress is less than the critical shear stress for deposition (HSPF parameter TAUCD). Shear stress is calculated from a number of internal quantities that depend on stream discharge, slope and geometry.

Sediment eroded from PERLNDs and IMPLNDs is routed to RCHRES suspended storage. It is then deposited at a rate determined by sediment settling velocity if the shear stress is below TAUCD. During periods of high flow when a RCHRES receives most of its suspended sediment, sediment can be quickly transported from the system. Because of this, and the fact that there is no means available to achieve an equilibrium sediment level at any flow rate (as is assumed when using the sediment rating curve concept), HSPF simulation of suspended silt and clay normally results in large variations of these quantities over short periods of time. Suspended silt and clay concentrations rise quickly with high flow rates, resulting in active scouring and sediment influx, and quickly fall as suspended sediment settles or is transported from the system.

Normally TAUCS is set above TAUCD. In a given parameterization there is a zone where neither deposition nor scouring occur. If it happens that streamflow is within this zone, these parameters become insensitive in the estimation and calibration process. The chance of this situation occurring is increased when the shear stress output time series (RCHRES HYDR TAU) is not evaluated explicitly. A modeler should have knowledge of this important quantity relative to the TAUCS and TAUCD values. Typically, TAUCS is set such that only storm events go over this value, and similarly, TAUCD is set so that most baseflow occurs below this threshold (T. Jobes, Pers. Comm.). The absence of scouring can also be disguised when silt and clay enter the system during periods of high surface runoff and transport of detached sediment storage. Under these circumstances TAUCS and its associated parameter M (erodability coefficient) are very insensitive. The same can occur with TAUCD and W (settling velocity) when transport of suspended sediment out of the system substantially reduces the impact of deposition rate on suspended sediment concentration.

Estimation of RCHRES silt and clay transport parameters is also difficult because of their correlation with PERLND/IMPLND erosion parameters. Suspended sediment concentrations can be increased by incrementing the storage and/or washoff rate of detached sediment on the watershed in addition to in-stream transport parameters that can be altered. In some instances these problems can be overcome by supplying values for these parameters from outside of the calibration process. However, if a value thus supplied results in rapid scouring or deposition of streambed sand/clay (as can easily happen), then there is no alternative but to adjust its value during the calibration process.

Similar considerations apply to the amount of sand and silt stored in bed sediments as those that were discussed above with respect to sand bed storage. There exist parameter sets that scour all silt and clay from the bed in a short time span or add an unrealistic mass of silt/clay in association with large rainfall events. One way to prevent this is to set TAUCD very low and TAUCS very high so that virtually no interaction between the stream and its bed takes place. While this ensures that bed silt/clay storage remains unchanged during calibration, so that observations of stream silt/clay loads can be used to infer PERLND/IMPLND sediment supply parameters, it may not result in a realistic simulation of system behavior.

The algorithms used by HSPF to compute suspended sediment concentration for both the sand and silt/clay fractions rely on the calculation of in-stream variables such as shear stress and stream velocity. Calculation of these quantities depends as well on the cross-sectional geometry of the reach as supplied in the RCHRES FTABLE (which provides the relationship between discharge, surface area, depth and volume). Only one FTABLE is specified for each stream reach, hence quantities derived from this and other parameters that are used in the calculation of

sediment transport are necessarily lumped. Since the representation of a stream or river reach in HSPF is highly simplified, the shear stress calculated within the RCHRES exists no place in particular, even though the geometry is known to be variable. Furthermore, it is possible to construct an FTABLE that appears suitable but results in counter-intuitive quantities for stream depth and shear stress. This problem is exacerbated by the piecewise linear nature of the FTABLE, resulting in artifacts such as the constant velocity calculated for the entire first segment in the FTABLE. This in turn affects the calculation of suspended sediment concentrations for sand and silt/clay. Parameter values supplied from outside the parameter estimation process based on the physics of sediment scour, transport and deposition may not always result in a good fit of observed suspended sediment concentrations to model predictions. Such parameter estimates are also prone to a high degree of nonuniqueness, relating as well to predictive nonuniqueness.

The Study Area

Contentnea Creek basin, a Coastal Plain tributary of the Neuse River, is located in North Carolina (refer back to Figure 23). Rainfall in the area averages 127 cm per year (Giese et al. 1997). The mean annual maximum temperature is approximately 10 Celsius, while the mean monthly minimum temperature is 30 Celsius. The physiography is relatively uniform throughout the basin, with relatively low relief. The soils are well-drained sands and sandy loams developed on sediments of marine origin. The primary land covers within the basin are forest, agriculture, grassland and urban, with the first two land use types accounting for nearly 70% of the area of the basin.

As described by Doherty and Johnston (2002), parameter estimation of four separate model simulations was completed for neighboring watersheds situated within this basin. These models were developed as part of a study dedicated to predicting alterations to water quality within the Contentnea Creek basin as a result of increasing urbanization and climatic change (Johnston 2001). The present investigation focuses on the most downstream watershed model segment with the best available total suspended solids data on record, Contentnea Creek above Hookerton. This basin is labeled Contentnea in Figure 23 but will be referred to as the Hookerton model to be consistent with Doherty and Johnston (2002). This is also consistent with the USGS name for the gauging station at this location. The area of this watershed is about 100,000 acres.

Methods

Simulation of watershed hydrologic and sediment erosion/transport processes was undertaken using HSPF v.12 (Bicknell et al. 2001). The watershed was simulated using four HSPF PERLND units, one IMPLND and a RCHRES (a PERLND is a pervious land segment, an IMPLND is an impervious land segment and a RCHRES is a free-flowing reach or mixed reservoir). The four PERLNDs were used to represent the four major land use types mentioned above. The IMPLND was used for the simulation of urban impervious areas (this comprising less than 2% of the total area of the watershed). The RCHRES simulates flow of water and constituents in the river system draining the watershed, providing dynamics at the pour point of the watershed.

Model calibration was undertaken using PEST (Doherty 2001a) in conjunction with a suite of utility software written to support the use of PEST in the surface water modeling context (Doherty and Johnston 2002). Total suspended sediment (TSS) samples were collected at irregular intervals at the Hookerton Gauging Station

since 1975. In the present study, data gathered after the end of 1995 were ignored so that the time period used for calibration of the sediment component of the model would coincide with that used for calibration of the hydrologic component of the model (Doherty and Johnston 2002). Unfortunately, partitioning of TSS samples into sediment size classes was not feasible; hence only total sediment data were available for use in model calibration.

Figure 31 shows TSS data plotted on both linear and logarithmic scales. In Figure 32 TSS data are compared with flow data. In Figure 32 TSS measurements are superimposed on flow measurements. While there are occasions when TSS readings appear to have been made during periods of high flow, many of the TSS measurements were taken during periods of comparatively low flow. The dataset as a whole does not provide a suitable basis for model hand calibration during those periods when erosion and sediment movement are most active. Such is the case with many suspended sediment datasets.

The lower part of Figure 32 depicts the sediment-rating curve, showing the relationship between TSS and stream discharge. The increase of TSS with flow rate is apparent in this figure. However, a high degree of scatter would exist around any regression line fitted to these data, such as when using ESTIMATOR. See, for example, Cohn et al. (1989) and Cohn and Gilroy (1991). In HSPF sediment eroded from a PERLND is directed to a RCHRES. There, the delivery of sediment downstream (or to storage within the bed of a stream) is simulated using the SEDTRN group of the RCHRES block. No attempt is made herein to evaluate the erosion and sediment transport algorithms employed by this group. Nevertheless, a few comments will be made on those aspects of the algorithms that have a bearing on the present investigation.

The amount of sand in suspension in a flowing stream is calculated by HSPF in a different manner than for silt and clay fractions. Three options are provided by HSPF for suspended sand calculation: the Toffaleti equation, the Colby method, and the power function method. In all cases HSPF first calculates the *potential* suspended sand concentration based on the velocity of the stream. If the existing suspended sand concentration exceeds this potential, sand is deposited; if it is less than this potential, sand is scoured from the bed of the stream to the extent available. In the present study the power function method was employed, though in a slightly modified form.

A small alteration was made to the algorithm that describes sand transport in a HSPF RCHRES. In the power function option, potential sand carrying capacity (PSAND) of the stream is calculated using the equation:

$$PSAND = KSAND * AVVELE ** EXPSND \quad (36)$$

where *AVVELE* is the average streambed velocity over the RCHRES during a particular time step and *KSAND* and *EXPSND* are parameters to be determined during the calibration process. For this study, this equation was replaced by the following equation:

$$PSAND = KSAND * ROM ** EXPSND \quad (37)$$

where *ROM* is the average stream discharge over the time step. Use of Eq.(37) eliminates the constant velocity problem over the first FTABLE segment mentioned previously. It also resembles the sediment-rating curve

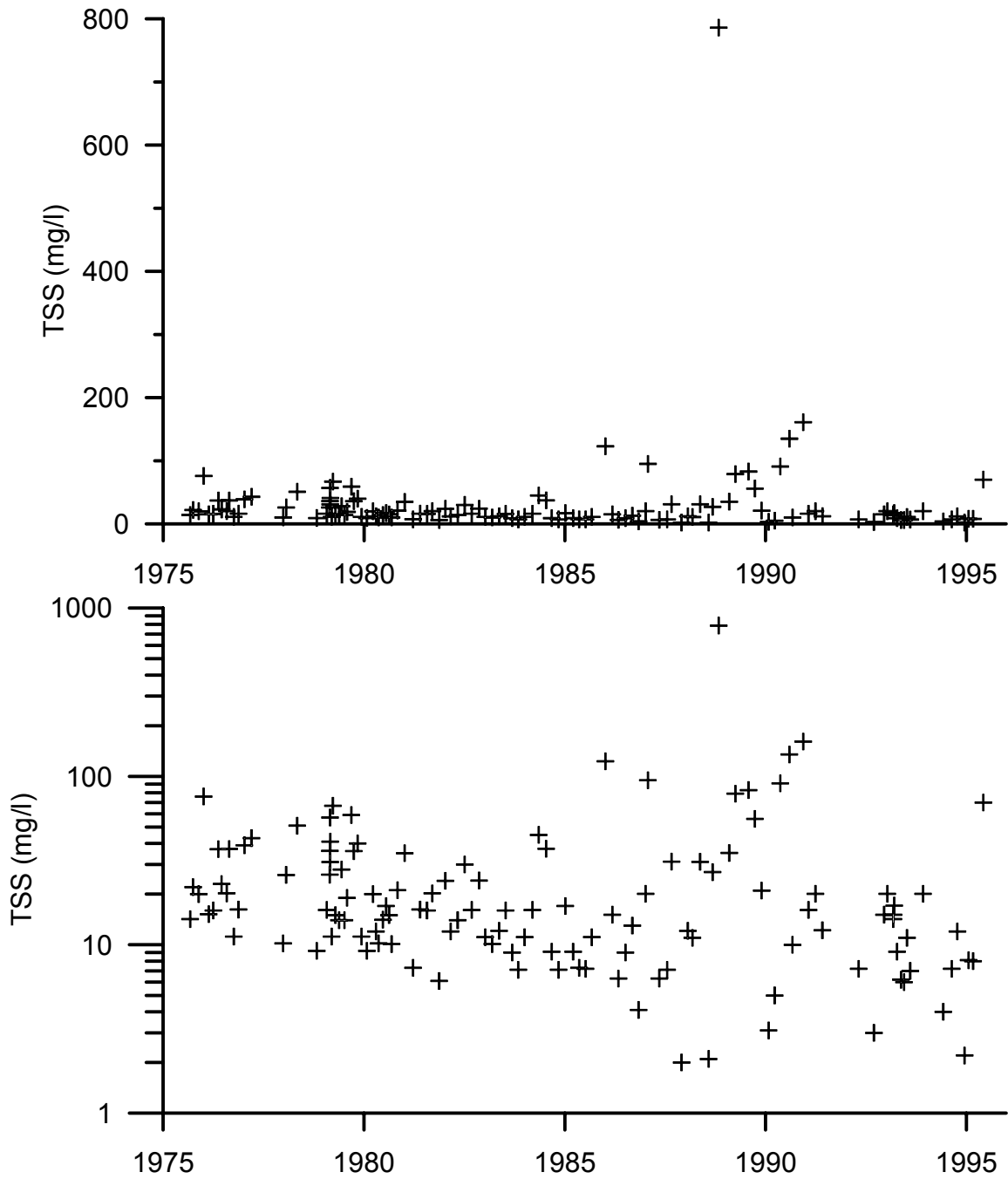


Figure 31. TSS data gathered over the period 1975 to 1995 at Hookerton Gauging Station.

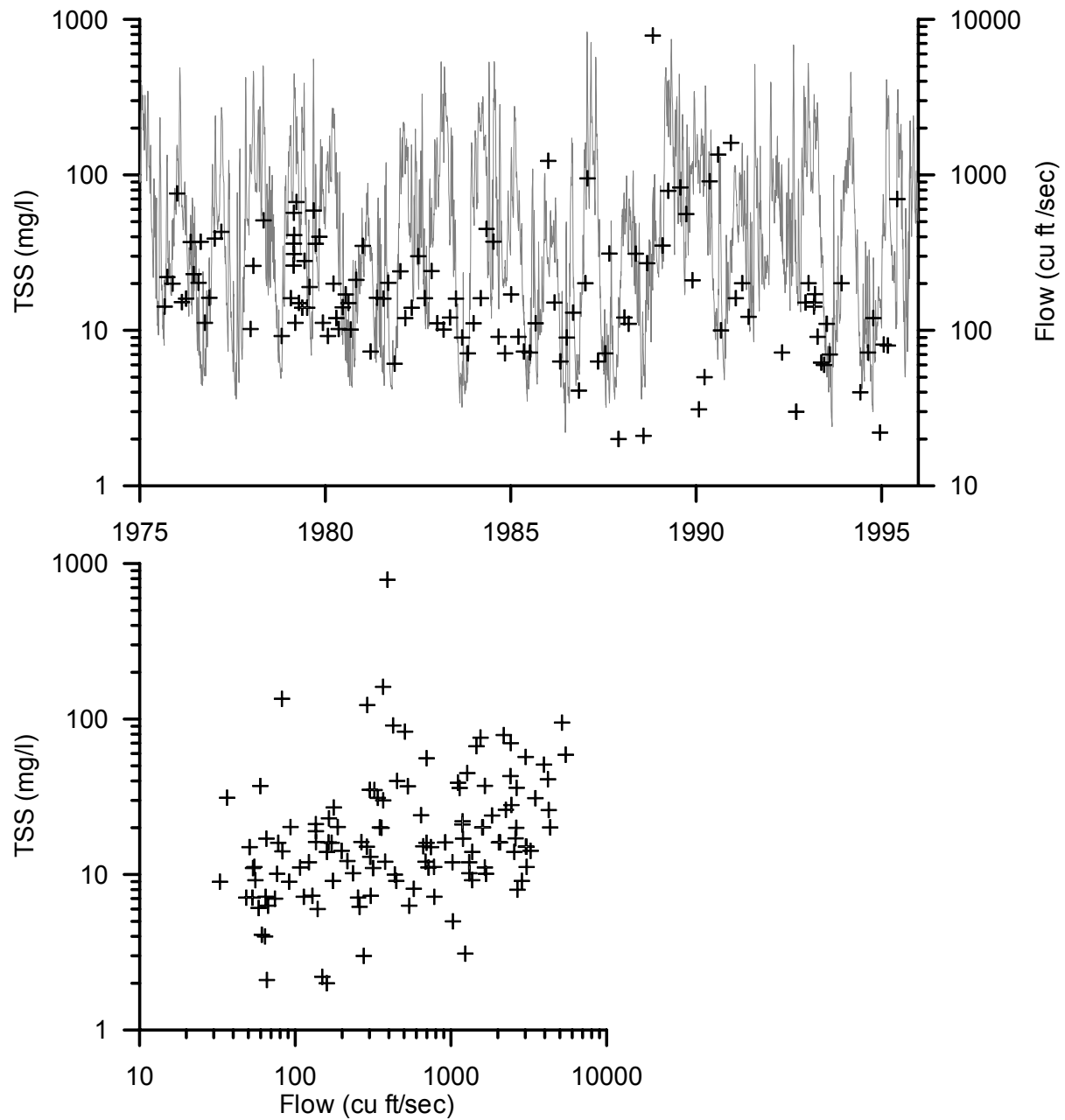


Figure 32. The top part of this figure shows TSS measurements superimposed on stream flow measurements. TSS is plotted against flow in the lower part of the figure.

description of stream sand content. It is possible that higher order terms are preferred in the relationship between PSAND and ROM as employed by Cohn et al. (1989). Use of the above Eq.(37) also required minimal alteration to HSPF, as no new parameters were required. Inspection of Figure 32 suggests that it is unlikely that the scatter around the rating curve of best fit would be substantially reduced by the introduction of higher order terms.

As was discussed above, the Hookerton Model is comprised of four PERLND units and an IMPLND all linked to a single RCHRES. In order to reduce the number of parameters requiring estimation, all four PERLNDs were initially assigned the same hydrologic parameters (the PWATER group of the HSPF PERLND module), except for the FOREST parameter that governs the amount of evapotranspiration taking place during winter. Parameters related to the dimensions of each PERLND (e.g., land use areas, lengths of overland flow paths, average slopes) were assigned in accordance with watershed known geometry and topography. PWATER parameters estimated for the PERLNDs through the calibration process are listed in Table 22. Values for IMPLND parameters were assumed rather than estimated, since this did not affect the calibration process due to the very small size of the IMPLND relative to the PERLNDs. See Doherty and Johnston (2002) and Section 6.1 for full details of the calibration process.

Table 22. HSPF PWATER parameters estimated during the calibration process. Other parameters were assigned values independently of the calibration process. See Doherty and Johnston (2002) for details.

Parameter name	Parameter function	One set of estimated values from Doherty and Johnston (2002)
LZSN	Lower zone nominal storage	2.0 in
UZSN	Upper zone nominal storage	2.0 in
INFILT	Related to the infiltration capacity of the soil	0.0526 in/hr
BASETP	The fraction of potential ET that can be sought from baseflow.	0.20
AGWETP	Fraction of remaining potential ET which can be satisfied from active groundwater storage	0.00108
LZETP	Lower zone ET parameter - an index to the density of deep-rooted vegetation.	0.50
INTFW	Interflow inflow parameter	10.0
IRC	Interflow recession parameter	0.677 day ⁻¹
AGWRC	Groundwater recession parameter	0.983 day ⁻¹

A similar strategy was adopted for the estimation of PERLND sediment parameters (group SEDMNT). The relevant SEDMNT parameters are listed in Table 23 along with a brief description. During the calibration process KRER, JRER, JSER and JGER were assigned identically for all PERLNDs except for the forest PERLND where KRER was assumed zero. KSER and KGER were similar for agricultural and urban PERLNDs, with grasslands a fifth of that value (for KSER) and a fourth of the value in forests (for KGER). Agricultural/urban parameter values are reported with the calibration results in Table 25. Sediment parameters for the IMPLND were not estimated in the calibration process.

Table 23. PERLND SEDMNT parameters estimated during the calibration process.

Parameter name	Parameter function
KRER	Coefficient in the sediment detachment equation
JRER	Exponent in the sediment detachment equation
KSER	Coefficient in the sediment removal equation
JSER	Exponent in the sediment removal equation
KGER	Coefficient in the sediment scour equation
JGER	Exponent in the sediment scour equation

Table 24 lists the RCHRES transport parameters estimated through the calibration process (group SEDTRN). KSAND and EXPSAND pertain to the transport of suspended sand. In order to reduce the number of parameters requiring estimation, M for clay was assumed equal to M for silt while TAUCD for clay was assumed to be 0.8 times that of silt. TAUCS for clay was estimated separately from that of silt. To ensure that TAUCS is always greater than TAUCD, the ratio of these two parameters (named TAUCRAT) was estimated, instead of TAUCS directly. For each sediment type a lower bound of 1 was placed on this ratio.

Table 24. RCHRES SEDTRN parameters estimated during the calibration process.

Parameter Name	Parameter function
KSAND	Coefficient in Eq.(37) for sand carrying capacity
EXPSND	Exponent in Eq.(37) for sand carrying capacity
TAUCD (silt)	Initial shear stress for deposition of silt
TAUCRAT (silt)	Ratio of TAUCS to TAUCD for silt
M (silt)	Erodibility coefficient of silt
TAUCD (clay)	Initial shear stress for deposition of clay
TAUCRAT (clay)	Ratio of TAUCS to TAUCD for clay
M (clay)	Erodibility coefficient of clay

In carrying out the parameter estimation process, PEST minimizes an objective function comprised of the sum of squared weighted deviations (i.e., residuals) between model output and corresponding field measurements; see Doherty (2001a) for more details. When estimating the parameters listed in Tables 23 and 24, the parameter estimation problem was set up in such a way that three types of observations contributed to the objective function. These are now discussed in detail.

TSS Measurements

The 103 TSS measurements illustrated in Figures 31 and 32 comprised one subgroup of the observation dataset used in the parameter estimation process. The weight assigned to each was calculated as the inverse of the measurement itself, thereby preventing the handful of very large TSS measurements from dominating the inversion process. Suspended sediment concentrations calculated by HSPF were time-interpolated to measurement dates and times TSPROC to allow a direct comparison to be made between field TSS measurements and their model-generated counterparts.

TSS Statistics

Whether calibrated by hand or with the help of nonlinear parameter estimation software, it is unrealistic to expect that a set of parameters can be derived that produce a good fit between each individual TSS measurement and its model-generated counterpart. Often the best that can be hoped for is the estimation of a set of parameters that reproduce the statistical properties of the measured dataset. Toward this end, two statistical observations were included in the observation dataset used by the parameter estimation process: the mean and standard deviation of the TSS observations. The model outputs corresponding to these measurement statistics were calculated on the basis of model-generated sediment concentrations time-interpolated to the dates and times of sediment observations. That is, each was calculated on the basis of the 103 model-generated counterparts to field TSS measurements. This allows a direct comparison to be made between two aspects of the character of the respective TSS datasets, with the modeled dataset undergoing a selection process identical to that to which field TSS dataset was subjected.

In formulating the objective function to be minimized, the mean and standard deviation observations were assigned equal weights. These weights were chosen such that, at the beginning of the parameter estimation process (where the model uses initial parameter values selected by the user) the contribution made to the overall objective function by the residuals pertaining to these two observations together was equal to the contribution made to the objective function by all of the TSS residuals. This strategy ensured that neither the statistical observations nor the native TSS observations dominated the parameter estimation process. Thus PEST was able to take both of these observation types into account, reducing the residuals associated with each of them if possible when upgrading parameter values.

RCHRES Bed Composition

Three extra observations were included in the calibration dataset, all of which were provided with a measured value of zero. The first was the difference between the amount of sand in the bed of the RCHRES at the beginning of the calibration period and that at the end of the calibration period. The second and third observations pertained to similar differences taken for silt and clay. Inclusion of these as components of the calibration dataset prevented the occurrence of large amounts of scouring or deposition by the model over the calibration period, this being in accord with direct observations of the condition of the watershed. Each of these observations was provided with the same weight. The weight was such that the contribution made to the overall objective function by the residuals associated with these three bed sediment difference observations was roughly the same as that contributed by native TSS data on the one hand, and the statistics pertaining to TSS data on the other hand, at the

commencement of the parameter estimation process.

Simultaneous Calibration against Head and Flow

An attempt was made to estimate both flow and transport parameters as part of the same calibration process by including discharges (and postprocessed discharges as discussed by Doherty and Johnston), as well as TSS measurements (and postprocessed TSS measurements as discussed above) in the calibration dataset, and estimating all of the parameters listed in Tables 22, 23, and 24 simultaneously. As is documented in Doherty and Johnson and Section 6.1, calibration of the hydrologic parameters listed in Table 22 against a single discharge time series leads to nonunique estimates of these parameters. Joint estimation of flow and sediment parameters on the basis of both flow and discharge data was undertaken to test whether inclusion of sediment data in the calibration process would reduce the range of uncertainty of at least some of the hydrologic parameters.

It was found that PEST's performance was somewhat disappointing during runs of this type due to the deleterious effects of low sensitivity and high correlation of some parameters. The adverse effects of parameter insensitivity and correlation are always worse when there are a large number of parameters to estimate than when there are only a few. In the present case these problems were overcome through judicious use of PEST's user-intervention functionality, by which troublesome parameters were temporarily held at their current values at critical stages of the parameter estimation process, leaving PEST free to adjust the other parameters. However, this can be a labor-intensive process. Hence, it was decided to estimate sediment parameters using a model for which the hydrologic parameters had already been estimated using the methodology discussed in Doherty and Johnston (2002). The hydrologic parameter values used in the present study are listed in the third column of Table 22.

Sediment Parameter Values

Sediment parameters estimated by PEST using the methodology outlined above are listed in the first column of Table 25. Convergence to this set of parameter values took place within 5 optimization iterations; no numerical difficulties were encountered by PEST.

As is discussed in Doherty (2001a) and Section 6.1, as a by-product of the Gauss-Marquardt-Levenberg method of parameter estimation, PEST is able to calculate the uncertainty associated with each estimated parameter. While uncertainty calculation by this means is based on a linearity assumption that is grossly violated in most modeling contexts, the uncertainty values achieved as a result of this process do serve to indicate the confidence levels that can be placed on parameters determined through model calibration. However, in the present instance the uncertainty calculation was impossible due to singularity of the parameter covariance matrix resulting from parameter nonuniqueness. The fact that the parameters listed in Tables 23 and 24 could not be estimated uniquely on the basis of the TSS data depicted in Figures 31 and 32 comes as no surprise. If desired, other sets of calibration-constrained sediment parameters, different from those in the first column of Table 25, but which calibrate the model just as well as these parameters, could have been estimated in the same manner as that in which multiple hydrologic parameter sets were calculated by Doherty and Johnston. This was not done in the present study; nevertheless, as is documented in the next section, the effects of sediment parameter nonuniqueness on model predictive nonuniqueness were explored using PEST.

Table 25. Sets of estimated parameter values. Units for many of these parameters are complex due to the exponential term in the equations that contain them.

Parameter name	Best-fit parameter set	Parameter set for minimized prediction	Parameter set for maximized prediction
KRER	35.0	35.0	35.0
JRER	1.0	1.0	1.0
KSER	1.01	0.5	1.93
JSER	3.005	2.73	3.73
KGER	0.33	0.27	0.40
JGER	4.49	5.00	3.74
KSAND	3.58	3.93	3.32
EXPSND	0.49	0.43	0.55
TAUCD (silt)	0.103 kg/m ²	0.102 lb/ft ²	0.106 lb/ft ²
TAUCRAT (silt)	2.29	2.30	2.27
M (silt)	0.0037 kg/m ² /hr	0.0039 lb/ft ² /day	0.00416 lb/ft ² /day
TAUCD (clay)	0.083 kg/m ²	0.082 lb/ft ²	0.085 lb/ft ²
TAUCRAT (clay)	3.045	3.038	3.02
M (clay)	0.0037 kg/m ² /hr	0.0038 lb/ft ² /day	0.00416 lb/ft ² /day

In the course of undertaking the parameter estimation process, PEST calculates the composite model-output sensitivity to each adjustable parameter, this being the sensitivity of that parameter to the model-generated counterparts to observations taken as a whole. If the composite sensitivity of a parameter is very low or zero, that parameter cannot be estimated through the inversion process. In a highly nonlinear parameter estimation problem such, as that documented herein, some parameters can be locally insensitive; unfortunately, even local insensitivity makes estimation of the pertinent parameters very difficult.

The composite sensitivities calculated by PEST for the parameters KRER and JRER were both zero. These parameters describe the ability of rain to detach sediment from the soil matrix. Detached sediment is then transported to a stream by overland flow if the sediment carrying capacity of overland flow is sufficient. This capacity is determined by parameters KSER and JSER. If these latter parameters are such that all detached soil cannot be transported overland, then the detachment parameters become insensitive since KSER and JSER determine sediment export rather than KRER and JRER. This was the case for the current PEST run. However, if another set of initial parameter values had been chosen to begin the parameter estimation process, the opposite may have been the case as sediment export would then have been limited by the capacity of rainfall to detach sediment, rather than by the capacity of overland flow to transport it. The situation becomes even more complicated when it is considered that, on the basis of in-stream TSS measurements alone, it is impossible to distinguish detachment from scouring as the mechanism for sediment production. Hence, estimation of the scour parameters KGER and JGER at the same time as the other sediment parameters mentioned above is virtually impossible.

It is thus apparent that, even without the problems incurred by the necessity to simultaneously estimate

RCHRES SEDTRN parameters, estimates of PERLND SEDMNT parameters will always be accompanied by a large margin of uncertainty.

Comparison of Model Output with Measurements

In undertaking the parameter estimation process, PEST had little difficulty in reducing the discrepancies between TSS statistics (i.e., mean and standard deviation as discussed above) and their model-calculated counterparts to almost zero. Similarly, PEST was able to ensure that the amounts of sand, silt and clay stored in the stream bed were unchanged over the calibration period. However, not surprisingly, a perfect fit could not be obtained between individual TSS measurements and the corresponding model output.

The top part of Figure 33 shows measured TSS values joined by straight line segments (dark lines). Model-calculated TSS values interpolated to measurement dates and times are joined by grey lines. This connection of measurements using linear segments is not meant to imply linearity of TSS concentrations between measurement times; it is simply a graphical means of conveying the character of the dataset, and of allowing a comparison to be made with the character of corresponding model output. It is apparent from Figure 33 that, as expected, the point-by-point matching of the two datasets is far from excellent. However, as was specifically sought through appropriate formulation of the objective function, the mean and standard deviation of the two datasets are very close, thus ensuring that modeled TSS values, when interpolated to the same dates and times as measured TSS values, have the same look when plotted and inspected.

In the bottom part of Figure 33, measured TSS values are superimposed on the complete model-generated TSS time series. Though far from perfect, the fit is easily as good as that which could have been achieved by manual calibration. Furthermore, the inclusion of bed storage information in the objective function ensured that this fit was not achieved at the cost of unnatural erosion or deposition of the stream bottom.

Predictive Analysis - General Considerations

Given the lumped nature of the parameters employed by a model such as HSPF, and given the fact that these parameters can be estimated with only a high degree of nonuniqueness through the calibration process, determination and documentation of a unique set of parameter values that purport to represent the erosion and transport characteristics of a watershed is a questionable activity. A more fruitful way to use a model such as HSPF in the investigation of sediment erosion and transport processes is to dispense with the idea of parameter uniqueness altogether. Instead, it is better to acknowledge that there is a (possibly large) range of parameter values that can result in acceptable fits between model output and field data (especially when the best fit that can be achieved is not very good), and that are in accord with outside knowledge of these values based on an understanding of the processes that they represent. It follows that there is also a (possibly large) range of parameter values that should be used when the model is deployed to make a prediction, and that there is thus a high potential for predictive nonuniqueness. Hence, no prediction should be made by a model without some attempt being made to quantify the magnitude of uncertainty associated with that prediction. Such predictive uncertainty analysis can be undertaken with the help of PEST's predictive analyzer.

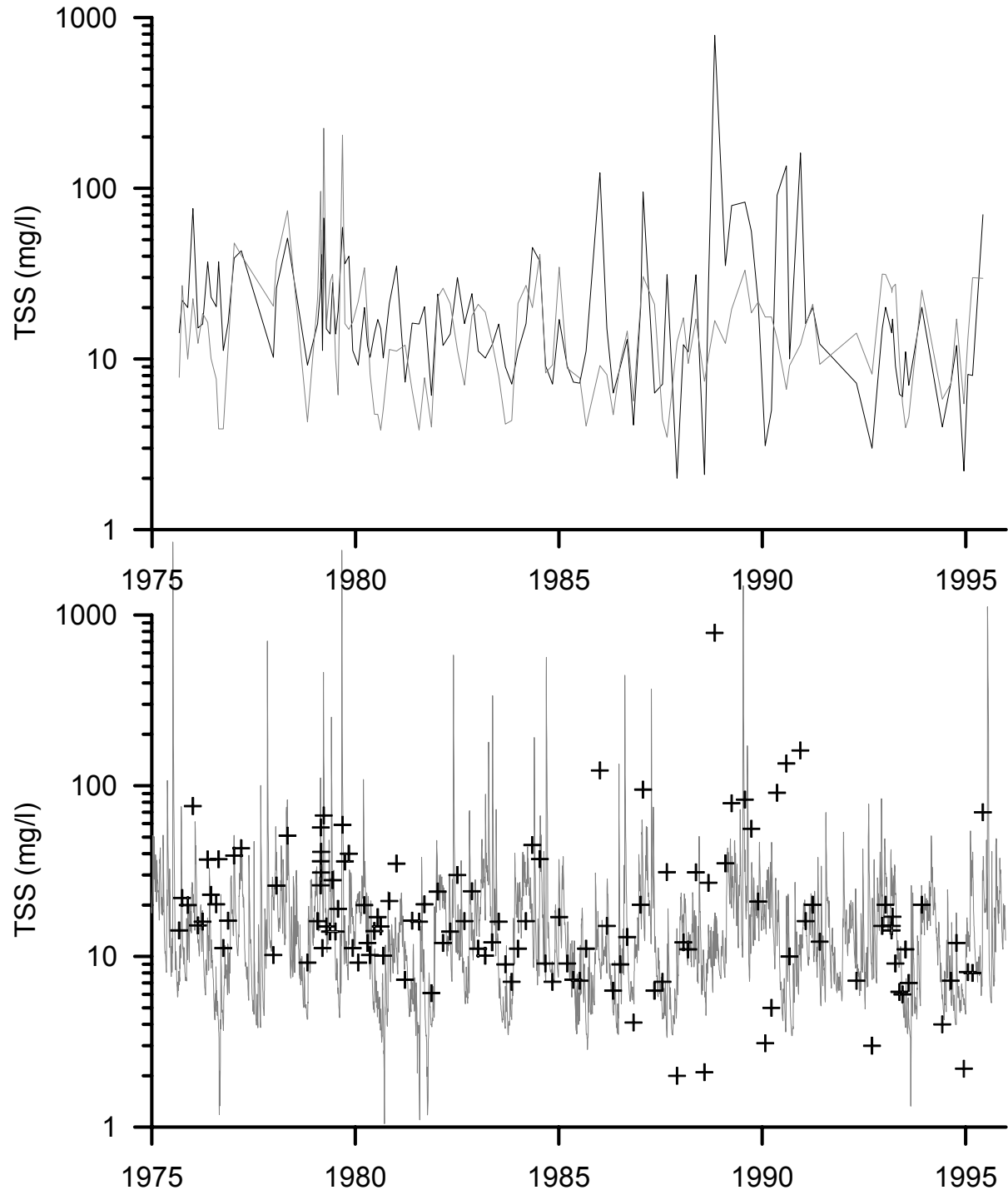


Figure 33. The top graph allows a comparison between TSS measurements and model output to be made on a point-by-point basis. In the bottom graph TSS measurements are superimposed on the model-generated TSS time series. In both of these graphs the model output is depicted in grey.

As is documented in Doherty (2001a) and Section 6.1, PEST's predictive analyzer can calculate the maximum and minimum value that a model prediction can take, while ensuring that parameters used by the model are such as to maintain that model in a calibrated state. Thus, in calculating the range of model predictive uncertainty, the calibration and prediction processes are combined. The user supplies a limiting objective function above which the model is deemed to be uncalibrated. PEST then adjusts parameter values in order to maximize or minimize the user-specified model prediction, while ensuring that estimated parameter values are such that the calibration criterion is not violated; the use of PEST's parameter bounds functionality ensures that parameters remain within acceptable ranges during this process.

The value selected for the limiting objective function depends on the types of observations used in the calibration process and the weights assigned to them. On the basis of the calibration strategy discussed in the previous section, PEST was able to lower the objective function to a value of 4.2×10^4 . For the purpose of analyzing model predictive uncertainty, the limiting objective function threshold was set at 4.8×10^4 ; this resulted in a model-to-measurement fit that is only slightly different from that achieved at the objective function minimum. Given the tightness of this limit, the extent of predictive uncertainty may have been underestimated in the process described below.

The prediction

The prediction in the present example is the total amount of sediment exported from the system over the period spanning 1975 to 1995, i.e., over the total calibration period. Used in this way, HSPF acts as a temporal interpolator of the sporadic TSS measurements taken over the study period, thus assuming a role not too different from that of a sediment rating curve in performing calculations of this type. However, as has already been discussed, the advantage of using a model rather than a regression line to undertake such interpolation is that the model incorporates, at least to some extent, the mechanics of the operative processes. This, in turn, should enhance a modeler's ability to undertake predictive uncertainty analysis through using a tool such as PEST's predictive analyzer in conjunction with the model, for a model has the capacity to perform calculations for conditions that are different from those occurring during the calibration period using equations based on physical principles to perform extrapolation to the new conditions. Nevertheless, the model also relies on curve fitting for the assignment of parameters through the calibration process; furthermore, some of these parameters occur in equations that employ power functions of discharge (or quantities related to discharge). This could result in the calculation of inappropriately high uncertainty ranges when the model is used to predict sediment concentrations at flows that are much higher than those at which TSS measurements were made.

The total mass of sediment exported from the watershed over the model calibration period calculated using the best-fit parameters listed in the first column of Table 25 was 1.13×10^6 tonnes. Maximized and minimized sediment masses calculated using PEST's predictive analysis functionality in the manner discussed above, were 1.5×10^6 tonnes and 7.9×10^5 tonnes, respectively. Parameters giving rise to these predictions are listed in columns 2 and 3 of Table 25. Visually, the fit between model output and field measurements over the calibration period for the maximization and minimization parameters is not too different from that depicted in the top part of Figure 33 for the best-fit parameters. The major differences between the respective model-calculated TSS time series, however, occurred at extreme flow events where no TSS measurements were made. Figure 34 compares TSS measurements

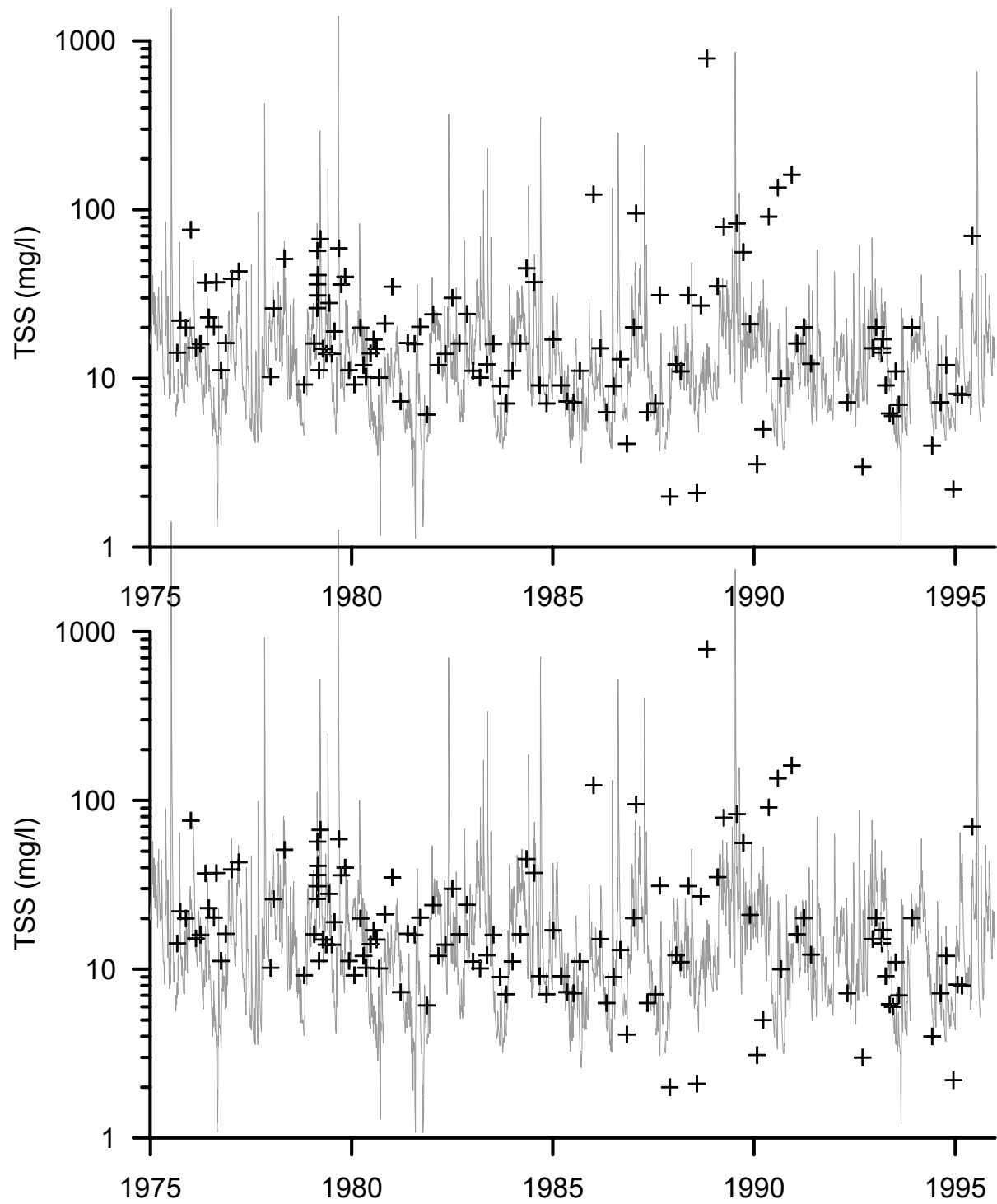


Figure 34. Observed and model-generated TSS values over the calibration period. The total exported suspended mass over the calibration period is minimized in the top graph and maximized in the bottom graph.

with the model-generated TSS time series for minimized (top picture) and maximized (bottom picture) total sediment export.

Conclusions

The use of nonlinear parameter estimation and predictive analysis methods in conjunction with a watershed simulation model to process suspended sediment data has been demonstrated. In common with most studies of this type, the data available for processing was sparse and unrepresentative of extreme system conditions. It was also noisy in the sense that it spanned a large range of measurement magnitudes, and was not directly amenable to fitting with the output of a process-based model. On the other hand, the data was not of such poor quality that its information content was zero. Thus, environmental management of the watershed in which the data was gathered demands that it be processed, and that the results of this processing be incorporated into any predictions made of future watershed behavior under the same or altered land use practices.

Unlike many investigations based on computer simulation of environmental processes, use of a model in the present study was not based on the premise that a unique parameter set could be established that could then be used by the model to make all future predictions. Rather, it was freely acknowledged that for a variety of reasons, including improper knowledge of watershed sediment processes and the availability of only a noisy and inadequate dataset, it would not be possible to ascribe to the model a set of parameters that would allow it to make precise predictions of sediment-related quantities. Hence, the calibration process was seen as a means of imposing a complex set of constraints on parameter values used by the model; that is, no parameter set could be used by the model to make a prediction unless the parameters comprising that set were reasonable (while accepting the fact that the lumped nature of these parameters may broaden the bounds of what is considered reasonable), and unless that parameter set results in a satisfactory fit between model output and field measurements under historical conditions. A total of 13 adjustable parameters pertaining to watershed sediment erosion and transport were estimated. Unique estimation of all parameters on the basis of the limited dataset displayed in Figures 31 and 32 is impossible, even with the application of expert knowledge. As discussed by Doherty and Johnston (2002), if environmental models are to be used correctly, the idea that a single unique parameter set exists and can be estimated should be abandoned. The calibration process can do no more than impose a set of complex constraints on parameter values to ensure that the parameters derived enable the model to replicate observed system behavior as well as possible.

Once parameter nonuniqueness is accepted as a fact of life, use of a model to make predictions of system behavior, or to process data in order to derive secondary quantities of interest to watershed managers (as was done in the present investigation) must include an analysis of the uncertainty associated with model output. A further, perhaps more subtle, outcome of the acceptance of parameter nonuniqueness, is recognition of the fact that the model prediction process cannot be entirely separated from the model calibration process. This is because, in attempting to ascertain the uncertainty associated with key model predictions, the modeler must, with the help of tools such as PEST's predictive analyzer, vary parameters in such a way as to establish the range of uncertainty of those predictions while simultaneously ensuring that constraints imposed by the calibration process are respected.

We conclude by reminding the reader that it was not our purpose to present the results of a detailed study of sediment erosion and transport processes operating in the Contentnea Creek system, for it is readily accepted that

parameters presented herein are in need of further refinement. Rather, the purpose of this study was to explore, and then document, the use of nonlinear and predictive analysis methods in processing TSS data of the type depicted in Figures 31 and 32 to exemplify the type of processing methodology that is now readily available to all modelers. It is hoped that use of the techniques described herein will free the modeler from the heavy burden (often thrust upon him/her by those with a poor understanding of environmental modeling) of having to make a definitive prediction of some aspect of watershed behavior. Rather, the use of software such as PEST, in combination with complex, process-based models such as HSPF, allows the modeler to process all available data to the maximum possible extent and, in the course of doing this, quantify the limits with which it is possible to predict system behavior. This represents a new, and much needed, addition to contemporary modeling practice.

6.3. Expected Fish Health Trends Using AQUATOX

Physical and chemical nonpoint source stressors and the resulting habitat degradation are the primary stressors to the eastern stream fishes (e.g., Richter et al. 1997). The impact of these anthropogenic stressors on stream ecosystems is generally reflected in the diversity and composition of fish assemblages (e.g., Karr 1981). The complexity of the response of ecological populations and communities to anthropogenic stressors makes prediction of this response difficult. Process-based models can be useful for ecological assessment of such complex systems.

This analysis uses a process-based model, AQUATOX (ver. 1.69), to assess the effect of nonpoint source pollutants on aquatic biota. AQUATOX is a model for ecological risk assessment that can represent the effects of both toxic chemicals and conventional pollutants on the aquatic ecosystem (Park 2000a). The model uses a daily timestep to simulate the physical environment (e.g., flow, light, and sediment) and the chemical environment (e.g., nutrients, oxygen, carbon, and pH). The dynamics of biotic components such as detritus, algae, benthic invertebrates and fish can be simulated. Although the model has been applied to lake settings (Park 2000b), no examples of stream applications have been published.

Here, the model is applied to a southeastern coastal plain stream site, the Contentnea Creek in North Carolina. The model is used to assess sensitivity of four fish groups to six habitat factors -temperature, nutrients, sediment, oxygen, pH, and detrital loading. This analysis allows us to evaluate the utility of the AQUATOX model for assessment of stream ecosystems.

Methods and Materials

The model was applied to Contentnea Creek at the site of the U.S. Geological Survey (USGS) gage at Hookerton in the coastal plain ecoregion of east-central North Carolina. The length of the site is 200 m, which is the standard sampling site length used by the state of North Carolina. Values for latitude (35.4423), channel slope (0.00012), mean stream width (31.4 m), inflow pH (6.5), and oxygen concentration (6.8 mg/L) were taken from the USEPA reach file 1 database (USEPA 1998). Values of light intensity (i.e., mean 378 Ly/d and range 447 Ly/d) were taken from the U.S. Department of Energy National Renewable Energy Laboratory solar radiation database for Raleigh, NC. Mean evaporation was set to zero, which is appropriate for stream applications (Park, pers. comm.). Carbon dioxide was set at a constant default loading of 0.7 mg/L. Detrital input was specified at a constant loading of 28 mg/L organic matter, of which 5% was assumed to be particulate and 75% was estimated to be refractory

(Cuffney 1988). The default remineralization parameters are considered widely applicable (Park 2000a), so they were not changed for this site.

Daily values of flow (m³/d), temperature (C), nutrients (mg/L), and sediment (mg/L) were read in directly from output of the HSPF watershed model (USEPA 2000b). The application and calibration of the HSPF model to this watershed has been described above in Section 6.1. In AQUATOX, Manning’s equation for natural streams was selected as the method to calculate dynamic mean depth (m) from the input flow data.

Two groups of algae and three groups of benthic invertebrates were included in the model (Figure 35). Default parameter sets in AQUATOX were used to model algal dynamics, and a constant input of 0.005 g/m² of each algae type was assumed (all biomass units are wet weight). Default parameter sets for representative benthic invertebrates were used to characterize invertebrate groups: chironomid for gatherers, mayfly for filterers, and stonefly for predators. The benthic invertebrate groups correspond to invertebrate communities reported for the coastal plain (Smock and E. Gilinsky 1992).

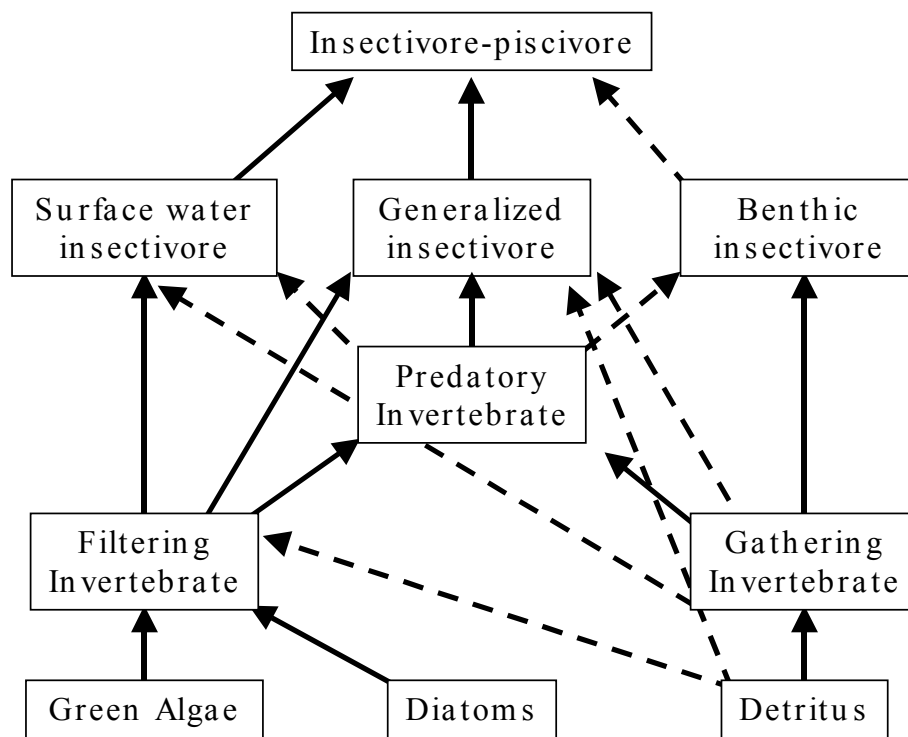


Figure 35. Diagram of feeding relationships. Solid arrows represent strong feeding preferences and dotted lines represent weak preferences.

Four fish groups identified by Paller (1994) for the coastal plain ecoregion were included in the model (Figure 35). Default values were used for the excretion:respiration ratio (0.05), the gametes:biomass ratio (0.09), and

the minimum prey for feeding (0.2); all of these parameters were the same for all fish species. Biomass of the fish groups showed less than a 1% change in response to an order of magnitude increase in carrying capacity parameters, which are used only during spawning, so AQUATOX default values were used.

Parameters for temperature response slope, optimum temperature, maximum temperature, and specific dynamic action were taken from the Wisconsin Bioenergetics model (Hanson et al. 1997 Appendix A). Dace values were used for both surface-water and benthic insectivores; bluegill adult values were used for generalized insectivores; and largemouth bass values were used for insectivore-piscivores (Table 26). The minimum adaptation temperature was taken as the lower lethal temperature from Leidy and Jenkins (1977 Table 13) using sunfish values for the generalized insectivores fish group, black bass values for insectivore-piscivores, and minnow values for surface-water and benthic insectivore groups (Table 26).

Bluegill and largemouth bass mortality rates from Leidy and Jenkins (1977) were used to parameterize the generalized insectivore and insectivore-piscivore groups, respectively (Table 26). Mortality for surface-water and benthic insectivores was assumed to be an order of magnitude greater. Respiration parameters were taken from the OXYREF database (CEAM 2002) for representative species. Maximum consumption parameters for the generalized insectivores and insectivore-piscivores were calculated from Hanson et al. (1997), using an average fish weight taken from sampling data available from the USGS National Water Quality Assessment Program. Half-saturation and maximum consumption parameters for surface-water and benthic insectivores were adjusted in calibration (Table 26).

Table 26. Selected input parameters of fish groups used for AQUATOX simulations.

Parameter (units)	Surface-water insectivores	Benthic insectivores	Generalized insectivores	Insectivore-piscivores
Maximum consumption (g/g/d)	0.36	0.25	0.073	0.056
Respiration rate (1/d)	0.015	0.009	0.006	0.006
Half-saturation (g/m ²)	0.05	0.05	0.75	5
Temperature Response Slope	2.4	2.4	2.3	2.65
Optimum temperature (C)	29	29	22	27.5
Maximum temperature (C)	32	32	33.8	37
Minimum adaptation temperature (C)	10	10	2.5	10
Mortality rate (1/d)	0.01	0.01	0.002	0.001
Gamete mortality (1/d)	0.01	0.01	0.8	0.1

Feeding interactions among biota are represented in the AQUATOX model by preference values (Figure 35). These relationships were specified based on information from Smock and Gilinsky (1992), Carlander (1977a), and Benke et al. (2001). Constant values were used for the egestion fraction of algae and detritus by invertebrates (0.5), invertebrates by invertebrates (0.15), detritus by fish (0.2), invertebrates by fish (0.16), and fish by fish (0.05).

The model was run with time series data for a six-year period 1989-1995. Algae and benthic invertebrates

were initialized at their carrying capacities, benthic invertebrate groups were initialized at 10 mg/L, and fish groups were initialized at 5 mg/L. A sensitivity analysis to temperature, nutrients, sediment, oxygen, pH, and detrital loading was conducted by sequentially increasing or decreasing each of these driving variables by 10% and then assessing the change in biomass for each fish group.

Results and Discussion

The total fish biomass from the calibrated simulation was within the range reported for coastal plain streams, 5-37 g/m² (Sheldon and Meffe 1995). Percentage occurrences of the different fish groups were consistent with those reported by Paller (1994). Total biomass of invertebrates was similar to that reported by Smock et al. (1989) for a coastal plain stream in Virginia; they noted that their results were applicable to other streams in the ecoregion. It was not possible to verify the seasonal patterns produced by the model because fish sampling data were not available at such a frequency.

Fish groups in AQUATOX appeared most sensitive to temperature (Figure 36a). Sensitivity to temperature is a result of the response of fishes to optimum temperature parameters. Generalized insectivores, the fish group with the lowest optimum temperature, showed a decrease in response to increased water temperature. It appears that the insectivore-piscivore group decreased in biomass as a result of the decrease in generalized insectivores, which are its most-preferred food source. The responses of surface-water and benthic insectivores were very similar to each other because they had been parameterized with the same optimum temperature.

Biomass of all fish groups showed very low sensitivity to nutrients; 10% increases in nutrients resulted in less than 2% changes in the biomass of the fish groups (Figure 36b). The role of nutrients in the model is to support photosynthesis. The model uses a multiple-limitation concept, so this result indicates that nutrients are not limiting for this study site. Algae may be more limited by light and stable substrate than by nutrients in the coastal plain (Smock and E. Gilinsky 1992).

Biomass of all fish groups also showed very low sensitivity to sediment (Figure 36c). Low sensitivity of fish groups to sediment is most likely due to the lack of direct effects of sediment on higher taxa in the AQUATOX model. The model includes two effects of sediment on the aquatic ecosystem: increased shading that can reduce light input and affect algal production and increased sedimentation that can increase the burial benthic detritus. The model results indicates that fishes are not sensitive to these two effects. However, certain known direct effects of sediment on fishes and invertebrates, such as interference with feeding or spawning (Newcombe and MacDonald 1991), are not represented in the model.

Biomass of the four fish groups also showed a low sensitivity to a 10% decrease in oxygen (Figure 37a). In the model, oxygen does not affect biota directly until the oxygen concentration is less than 1.0 mg/L, at which time total mortality occurs. Indirect effect of oxygen on detrital decomposition occurs at levels less than 4 mg/L, but these levels did not occur in this analysis.

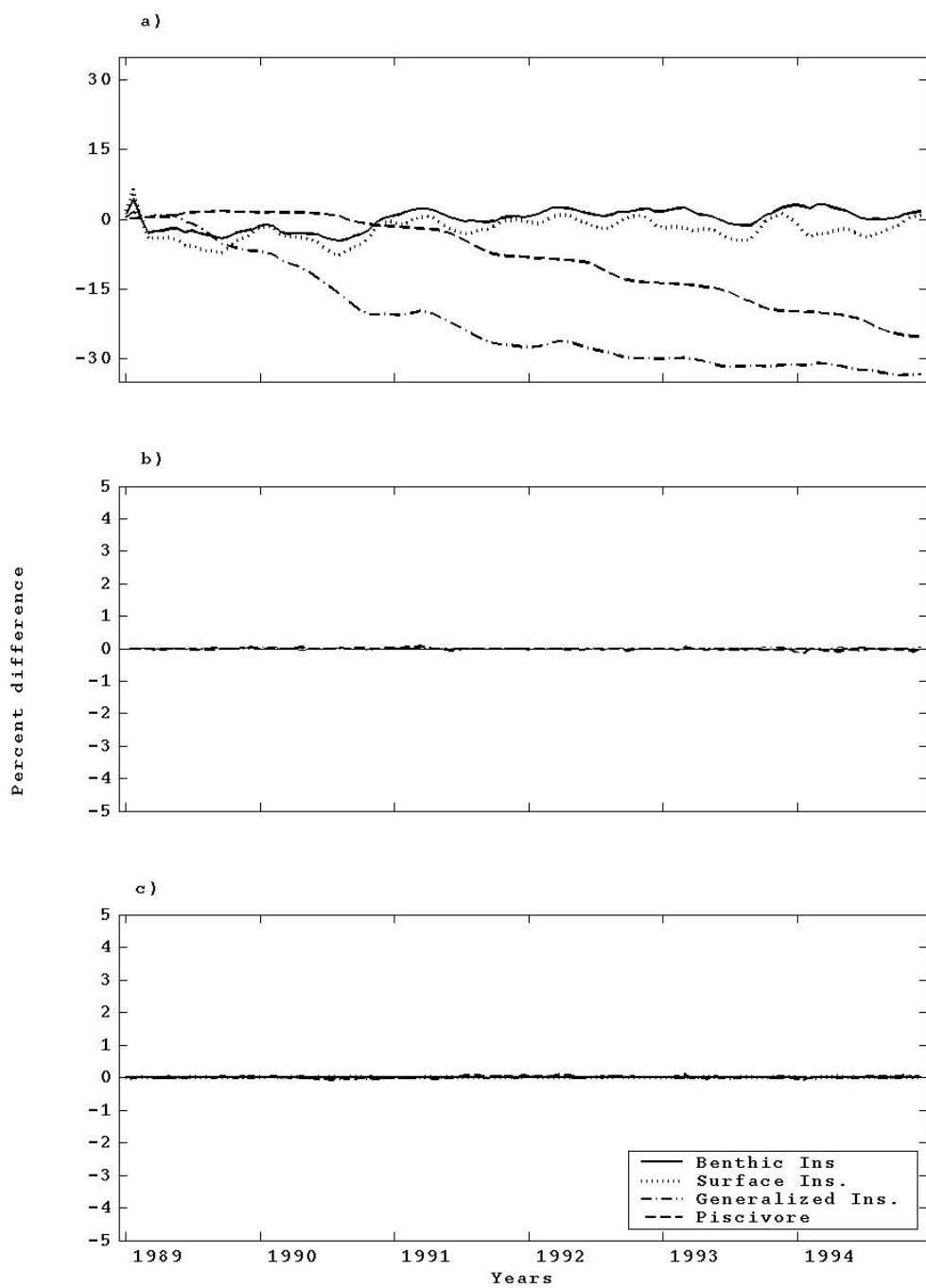


Figure 36. Response of biomass of the four fish groups to a 10% increase in (a) temperature, (b) nutrients, and (c) sediment.

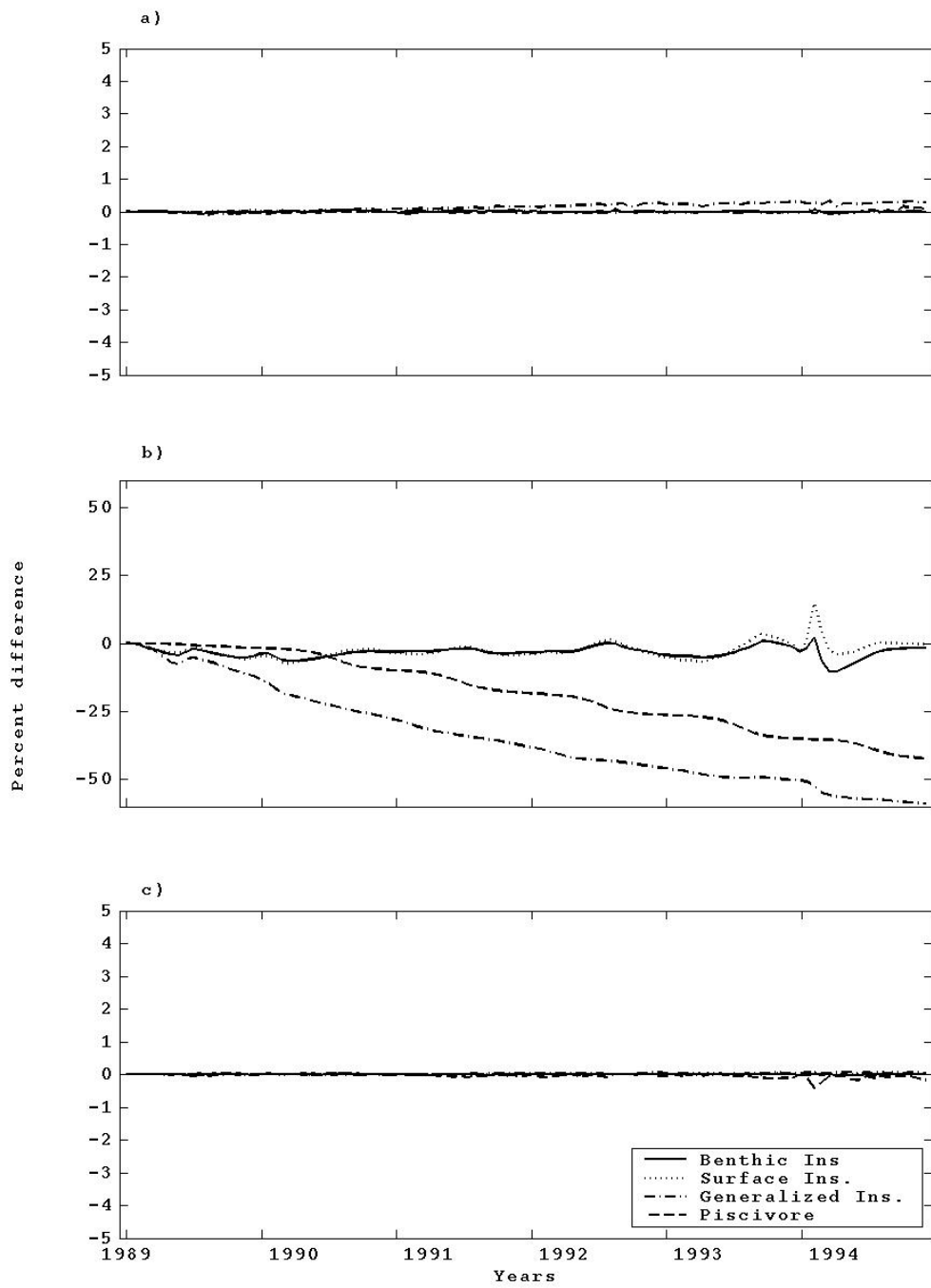


Figure 37. Response of biomass of the four fish groups to a 10% decrease in (a) oxygen, (b) detrital loading, and (c) pH.

The fish groups showed moderate sensitivity to a 10% decrease in detritus loading (Figure 37b). The generalized insectivores, that consume detritus, were most affected. The insectivore-piscivore group was also affected since it feeds on the generalized insectivore group. Benthic insectivores were affected very little because they have access to the sedimented detritus.

Biomass of the four fish groups showed a very low sensitivity (<1%) to a 10% decrease in pH (Figure 37c). In this analysis, the pH stayed within the range 5-8.5; in the model pH does not affect decomposition within this range. The pH can affect nitrification in the model, but levels of ammonia in this simulation were relatively low so this effect did not occur.

The AQUATOX model provides a good representation of the aquatic ecosystem. Detrital and nutrient processes appear to be well-represented, and unlike some other aquatic ecological models, there are feedbacks to algae from both chemicals and fish. It is easy to use the AQUATOX model, and also to use time series outputs from a watershed model as driving variables. AQUATOX, however, does not represent interactions between the stream ecosystem and the flood plain, which are particularly important in the coastal plain ecosystem (Cuffney 1988). Also, it was difficult to verify seasonal patterns in the model results, since data were not collected in a temporal fashion at the study site. Certain limitations, such as lack of multiple age classes and spatial dimension, will be addressed in future versions of AQUATOX (Park, pers. comm.). Currently, the model is useful for assessing the response of the fish groups to only certain types of stressors. Its utility should be determined further by model applications in other study areas and ecoregions.

7. Prospectus for Future Regional Assessments

When the BASE research program was originally conceived and initiated in 1999, the research product presented herein was planned as a prototype computer software modeling tool and case study of fish health across the entire Albemarle-Pamlico basin rather than simply a conceptual framework and general discussion of fish health issues within the Albemarle-Pamlico basin. BASE's failure to realize its original programmatic goal is can be attributed to both logistical and technological factors.

With regard to logistical considerations, the most important factor that hampered the program's overall research efforts was the lost of key federal staff. In particular, approximately 9 FTE were assigned to the BASE research program in FY99. However, during FY00 and FY01 BASE lost 4.5 of its 9 FTEs to retirement and staff accepting federal positions outside of ERD/NERL. With regard to technical considerations, three factors that should be mentioned are: 1) the availability of appropriate models that satisfy assessment and modeling objectives; 2) availability of complete input datasets for models that were judged appropriate for assessment and modeling objectives; and 3) the availability of GIS and other software frameworks that could implement regional parameterization, execution, and output analysis of multiple interacting models.

Although the REMM and HSPF models were initially assumed to be adequate models for describing the interaction of riparian and hydrologic processes for the Albemarle-Pamlico basin, the contrary was discovered to be true due to the inherently different and non-scalable, spatial scales of these models. In particular the field scale focus of the REMM riparian model simply could not be scaled or made to interact with the integrated/lumped watershed processes represented in HSPF. Similarly, the geologically based Groundwater Modeling System (GMS) MODFLOW, described in Section 5.2.1, could not be interfaced with HSPF despite the overwhelming importance of groundwater discharges to surface flow across the Albemarle-Pamlico basin. It would appear that the only way to resolve such modeling issues would be to develop new model codes, either de novo or from state-of-the-art revisions of existing codes, with the explicit objective of dynamic integration of conceptually related, process-based models.

Other models that were considered to be appropriate for regional fish health assessments could not be completely parameterized for the Albemarle-Pamlico basin. Notable in this regard was the BASS bioaccumulation and community model. Although BASS could have been parameterized for most of the fish species that are the ecological dominants in the habitat groups/communities identified in Section 4.1, BASS could not be objectively parameterized for the food webs within these communities since monitoring data detailing these communities' invertebrate stocking stocks, that are the foundations of these food webs, were either fragmentary or wholly lacking. Similarly, the lack of comprehensive, regional contaminant datasets precluded water quality/fate and transport modeling that might have been focused on mercury, dioxins, pesticides, or other persistent organic pollutants (POPs) that are known to be of concern in the Albemarle-Pamlico basin. To overcome such problems, dynamic simulation models must be considered was environmental indicators in the same light as are individual field measurements or composite multivariate indices. Model developers and users must interact and have input into major biological and physical monitoring programs to insure that such data collections can be used not only to assess the current condition of resources of concern but also to evaluate the vulnerability and sustainability of those resources to different future environmental use scenarios.

Even if BASE had access all of the appropriate modeling components and their requisite datasets, the availability of GIS and other software frameworks that could have implemented the regional parameterization, execution, and output analysis of these models would have been a significant impediment toward achieving a transparent assessment technology. As asserted by one peer reviewer “...*formal adoption of a modeling system framework is absolutely necessary if this work is to continue. The framework will serve two critical purposes; first, it will provide a computer-based blueprint for moving the work forward (this includes providing a clear picture of status and basis for making research project decisions in a consistent and prioritized manner); and second, it will provide the means by which the technology configured for the case study can be smoothly evolved to serve both future research and assessments in different river basins.*” Importantly, the selection of such a framework is not a trivial issue since several efforts are already under way inside and outside of the USEPA.

References

- Abbaspour, K.C., R. R. Schulin, and M.T. van Genuchten. 2001. Estimating unsaturated soil hydraulic properties using ant colony optimization. *Advances in Water Resources* 24: 827-841.
- Aho, J.M., C.S. Anderson, and J.W. Terrell. 1986. Habitat suitability index models and instream flow suitability curves: Redbreast sunfish. U.S. Department of the Interior, Fish and Wildlife Service, Washington, DC. Biological Report 82(10.119).
- Allan, J.D. 1995. *Stream ecology*. Chapman & Hall, London, England.
- Altier, L.S., R.R. Lowrance, R.G. Williams, S.P. Inamdar, D.D. Bosch, J.M. Sheridan, R.K. Hubbard, and D.L. Thomas. In press. The riparian ecosystem management model: Simulator for ecological processes in riparian zones. U.S. Department of Agriculture, Washington, DC. Conservation Research Report.
- Anderson, J.F., E.E. Hardy, J.T. Roach, and R.E. Witmer. 1976. A Land Use and Land Cover Classification System for Use with Remote Sensor Data. U.S. Department of the Interior, Geological Survey. Professional Paper 28.
- Angermeier, P.L. and I.J. Schlosser. 1987. Assessing biotic integrity of the fish community in a small Illinois stream. *North American Journal of Fisheries Management* 7: 331-338.
- Angermeier, P.L. and M.R. Winston. 1998. Local vs. regional influences on local diversity in stream fish communities of Virginia. *Ecology* 79: 911-927.
- Angermeier, P.L. and M.R. Winston. 1999. Characterizing fish community diversity across Virginia landscapes: prerequisite for conservation. *Ecological Applications* 9: 335-349.
- Arnold, C.L., Jr. and C.J. Gibbons. 1996. Impervious surface coverage: the emergence of a key environmental indicator. *Journal of the American Planning Association* 62: 243-258.
- Ashley, K.W. 2002. Freshwater Fishing Opportunities in Eastern North Carolina. North Carolina Wildlife Resources Commission, Division of Inland Fisheries. http://www.ncwildlife.org/pg03_Fishing/pg3d6.htm
- Astor, P.H., B.C. Patten, and G.N. Estberg. 1976. The sensitivity substructure of ecosystems. *In Systems Analysis and Simulation in Ecology: Volume IV. Edited by B.C. Patten*. Academic Press, New York, NY. pp. 330-371
- Bain, K.B. and J.L. Bain. 1982. Habitat suitability index models: Coastal stocks of striped bass. U.S. Department of the Interior, Fish and Wildlife Service, Washington, DC. FWS/OBS-82/10.1.
- Barber, M.C. 1994. Environmental Monitoring and Assessment Program: Indicator Development Strategy. U.S. Environmental Protection Agency, Office of Research and Development, Environmental Research Laboratory,

Athens, GA. EPA/620/R-94/022.

Barber, M.C. 2001. Bioaccumulation and Aquatic System Simulator (BASS) User's Manual Beta Test Version 2.1. U.S. Environmental Protection Agency, Office of Research and Development, Athens, GA. EPA 600/R-01/035.

Barber, M.C. 2002. A review and comparison of models for predicting dynamic chemical bioconcentration in fish. *Environmental Toxicology and Chemistry* (in review).

Barber, M.C., L.A. Suárez, and R.R. Lassiter. 1988. Modeling bioconcentration of nonpolar organic pollutants by fish. *Environmental Toxicology and Chemistry* 7: 545-558.

Barber, M.C., L.A. Suárez, and R.R. Lassiter. 1991. Modelling bioaccumulation of organic pollutants in fish with an application to PCBs in Lake Ontario salmonids. *Canadian Journal of Fisheries and Aquatic Sciences* 48: 318-337.

Beck, B. 1987. Water quality modeling: a review of the analysis of uncertainty. *Water Resources Research* 23: 1393-1442.

Benke, A.C., J.B. Wallace, J.W. Harrison, and J.W. Koebel. 2001. Food web quantification using secondary production analysis: predaceous invertebrates of the snag habitat in a subtropical river. *Freshwater Biology* 46: 329-346.

Bennett, A.F. 1976. Open boundary conditions for dispersive waves. *Journal of the Atmospheric Sciences* 32: 176-182.

Bennett, A.F. and P.C. McIntosh. 1982. Open ocean modeling as an inverse problem: tidal theory. *Journal of Physical Oceanography* 12: 1004-1018.

Bennett, J.R. and A.H. Clites. 1987. Accuracy of trajectory calculation in a finite-difference circulation model. *Journal of Computational Physics* 68: 272-282.

Bergstedt, L.C. and E.P. Bergersen. 1997. Health and movements of fish in response to sediment sluicing in the Wind River, Wyoming. *Canadian Journal of Fisheries and Aquatic Sciences* 54: 312-319.

Beven, K.J. 2000. Uniqueness of place and process representations in hydrological modelling. *Hydrology and Earth Systems Sciences* 4: 203-213.

Bicknell, B.R., J.C. Imhoff, J.L. Kittle, T.H. Jobs, and A.S. Donigan. 2001. HSPF User's Manual. Aqua Terra Consultants, Mountain View, CA.

Bilger, M.D. and R.A. Brightbill. 1998. Fish communities and their relation to physical and chemical characteristics of streams from selected environmental settings in the lower Susquehanna River basin, 1993-95. U.S. Geological Survey, Lemoyne, PA. Water Resources Investigations Report 98-4004.

- Bird, S.L., S.W. Albery, and L.R. Exum. 2000. Generating high quality impervious cover data. *Journal of Quality Assurance* 8: 91-103.
- Blumberg, A.F. and L.H. Kantha. 1985. Open boundary condition for circulation models. *Journal of Hydrologic Engineering* 111: 237-255.
- Blumberg, A.F. and G.L. Mellor. 1987. A description of a three-dimensional coastal ocean circulation model. *In* Three-Dimensional Coastal Ocean Models, Coastal and Estuarine Science, Vol. 4. *Edited by* N.S. Heaps. American Geophysical Union, pp. 1-19
- Bosch, D.D., R.K. Hubbard, L.T. West, and R.R. Lowrance. 1994. Subsurface flow patterns in a riparian buffer system. *Transactions of the ASAE* 37: 1783 – 1790.
- Boudreau, P.R. and L.M. Dickie. 1989. Biological model of fisheries production based on physiological and ecological scalings of body size. *Canadian Journal of Fisheries and Aquatic Sciences* 46: 614-623.
- Bozek, M.A., T.M. Burri, and R.V. Frie. 1999. Diets of muskellunge in northern Wisconsin lakes. *North American Journal of Fisheries Management* 19: 258-270.
- Breck, J.E. and M.J. Gitter. 1983. Effect of fish size on the reactive distance of bluegill (*Lepomis macrochirus*) sunfish. *Canadian Journal of Fisheries and Aquatic Sciences* 40: 162-167.
- Brinson, M.M., B.L. Swift, R.C. Plantico, and J.S. Barclay. 1981. Riparian ecosystems: their ecology and status. U.S. Fish and Wildlife Service, Biological Services Program, Washington, DC. FWS/OBS-81/17.
- Brodeur, R.D. 1991. Ontogenetic variations in the type and size of prey consumed by juvenile coho, *Oncorhynchus kisutch*, and chinook, *O. tshawytscha*, salmon. *Environmental Biology of Fishes* 30: 303-315.
- Buckley, J. 1984. Habitat suitability index models: Larval and juvenile red drum. U.S. Department of the Interior, Fish and Wildlife Service, Washington, DC. FWS/OBS-82/10.74.
- Cappuccino, N. 1995. Novel approaches to the study of population dynamics. *In* Population dynamics: new approaches and synthesis. *Edited by* N. Cappuccino and P.W. Price. Academic Press, San Diego, CA. pp. 3-16
- Carlander, K.D. 1969. Handbook of Freshwater Fishery Biology. Volume One: Life History Data on Freshwater Fishes of the United States and Canada, Exclusive of the Perciformes. Iowa State University Press, Ames, IA.
- Carlander, K.D. 1977a. Handbook of freshwater fishery biology Volume 2: Life history data on centrarchid fishes of the United States and Canada. The Iowa State University Press, Ames, IA.
- Carlander, K.D. 1977b. Handbook of Freshwater Fishery Biology. Volume Two: Life History Data on Centrarchid Fishes of the United States and Canada. Iowa State University Press, Ames, IA.

- Carlander, K.D. 1997. Handbook of Freshwater Fishery Biology. Volume Three: Life History Data on Ichthyopercid and Percid Fishes of the United States and Canada. Iowa State University Press, Ames, IA.
- CEAM. 2002. OXYREF: Oxygen Requirements of Fishes Database. U.S. Environmental Protection Agency, Center for Exposure Assessment Modeling. Athens, GA. <http://www.epa.gov/ceampubl/swater/oxyref/>
- Chipps, S.R., W.B. Perry, and S.A. Perry. 1994. Fish assemblages of the central Appalachian mountains: an examination of trophic group abundance in nine West Virginia streams. *Environmental Biology of Fishes* 40: 91-98.
- Christmas, J.Y., J.T. McBee, R.S. Waller, and F.C. Sutter, III. 1982. Habitat suitability index models: Gulf menhaden. U.S. Department of the Interior, Fish and Wildlife Service, Washington, DC. FWS/OBS-82/10.23.
- Cohn, T.A. and E.J. Gilroy. 1991. Estimating loads from periodic records. U.S. Geological Survey, Branch of Systems Analysis. Technical Memo 91.01.
- Cohn, T.A., L.L. DeLong, E.J. Gilroy, R.M. Hirsch, and D.K. Wells. 1989. Estimating constituent loads. *Water Resources Research* 25: 937-942.
- Collares-Pereira, M.J., M.F. Magalhaes, A.M. Geraldes, and M.M. Coelho. 1995. Riparian ecotones and spatial variation of fish assemblages in Portuguese lowland streams. *Hydrobiologia* 303: 93-101.
- Cook, M.F. and R.C. Solomon. 1987. Habitat suitability index models: Muskellunge. U.S. Department of the Interior, Fish and Wildlife Service, Washington, DC. Biological Report 82(10.148).
- Crance, J.H. 1984. Habitat suitability index models and instream flow suitability curves: Inland stocks of striped bass. U.S. Department of the Interior, Fish and Wildlife Service, Washington, DC. FWS/OBS-82/10.85.
- Crance, J.H. 1986. Habitat suitability index models and instream flow suitability curves: Shortnose sturgeon. U.S. Department of the Interior, Fish and Wildlife Service, Washington, DC. Biological Report 82(10.129).
- Cuffney, T.F. 1988. Input, movement, and exchange of organic matter within a subtropical coastal blackwater river-floodplain system. *Freshwater Biology* 19: 305-320.
- Damuth, J. 1981. Population density and body size in mammals. *Nature (London)* 290: 699-700.
- DeAngelis, D.L., W.F. Loftus, J.C. Trexler, and R.E. Ulanowicz. 1997. Modeling fish dynamics and effect of stress in a hydrologically pulsed system. *Journal of Aquatic Ecosystem Stress and Recovery* 6: 1-13.
- Denslow, J.S. 1985. Disturbance-mediated coexistence of species. *In The Ecology of Natural Disturbance and Patch Dynamics. Edited by S.T.A. Pickett and P.S. White. Academic Press, New York. pp. 307-321*
- Diaz, R.J. and C.P. Onuf. 1985. Habitat suitability index models: Juvenile Atlantic croaker (revised). U.S.

Department of the Interior, Fish and Wildlife Service, Washington, DC. Biological Report 82(10.98) [First printed as: FWS/OBS-82/10.21, July 1982].

Doherty, J. 2001a. PEST-ASP User's Manual. Watermark Numerical Computing, Brisbane, Australia.

Doherty, J. 2001b. PEST Surface Water Utilities User's Manual. . Watermark Numerical Computing, Brisbane, Australia.

Doherty, J. and J. Johnston. 2002. Methodologies for Calibration and Predictive Analysis of a Watershed Model. Journal of the American Water Resources Association (accepted).

Donald, D.B. 1997. Relationship between year-class strength for Goldeyes and selected environmental variables during the first year of life. Transactions of the American Fisheries Society 126: 361-368.

Duan, Q.S., S. Sorooshian, and V.K. Gupta. 1992. Effective and efficient global optimization for conceptual rainfall runoff models. Water Resources Research 28: 1015-1031.

Dunham, J.B. and G.L. Vinyard. 1997. Relationships between body mass, population density, and the self-thinning rule in stream-living salmonids. Canadian Journal of Fisheries and Aquatic Sciences 54: 1025-1030.

East, P. and P. Magnan. 1991. Some factors regulating piscivory of brook trout, *Salvelinus fontinalis*, in lakes of the Laurentian Shield. Canadian Journal of Fisheries and Aquatic Sciences 48: 1735-1743.

Edwards, E.A. 1983a. Habitat suitability index models: Bigmouth buffalo. U.S. Department of the Interior, Fish and Wildlife Service, Washington, DC. FWS/OBS-82/10.34.

Edwards, E.A. 1983b. Habitat suitability index models: Longnose sucker. U.S. Department of the Interior, Fish and Wildlife Service, Washington, DC. FWS/OBS-82/10.35.

Edwards, E.A. and K.A. Twomey. 1982a. Habitat suitability index models: Common carp. U.S. Department of the Interior, Fish and Wildlife Service, Washington, DC. FWS/OBS-82/10.12.

Edwards, E.A. and K.A. Twomey. 1982b. Habitat suitability index models: Smallmouth buffalo. U.S. Department of the Interior, Fish and Wildlife Service, Washington, DC. FWS/OBS-82/10.13.

Edwards, E.A., M. Bacteller, and O.E. Maughan. 1982a. Habitat suitability index models: Slough darter. U.S. Department of the Interior, Fish and Wildlife Service, Washington, DC. FWS/OBS-82/10.9.

Edwards, E.A., G. Gebhart, and O.E. Maughan. 1983a. Habitat suitability index models: Smallmouth bass. U.S. Department of the Interior, Fish and Wildlife Service, Washington, DC. FWS/OBS-82/10.36.

Edwards, E.A., H. Li, and C.B. Schreck. 1983b. Habitat suitability index models: Longnose dace. U.S. Department

of the Interior, Fish and Wildlife Service, Washington, DC. FWS/OBS-82/10.33.

Edwards, E.A., D.A. Krieger, M. Bacteller, and O.E. Maughan. 1982b. Habitat suitability index models: Black crappie. U.S. Department of the Interior, Fish and Wildlife Service, Washington, DC. FWS/OBS-82/10.6.

Edwards, E.A., D.A. Krieger, G. Gebhart, and O.E. Maughan. 1982c. Habitat suitability index models: White crappie. U.S. Department of the Interior, Fish and Wildlife Service, Washington, DC. FWS/OBS-82/10.7.

Elrod, J.H. and R. O'Gorman. 1991. Diet of juvenile lake trout in southern Lake Ontario in relation to abundance and size of prey fishes, 1979-1987. Transactions of the American Fisheries Society 120: 290-302.

Elston, D.A. 1992. Sensitivity analysis in the presence of correlated parameter estimates. Ecological Modelling 64: 11-22.

Enge, K.M. and R. Mulholland. 1985. Habitat suitability index models: Southern and gulf flounders. U.S. Department of the Interior, Fish and Wildlife Service, Washington, DC. Biological Report 82(10.92).

Erickson, R.J. and J.M. McKim. 1990. A model for exchange of organic chemicals at fish gills: flow and diffusion limitations. Aquatic Toxicology 18: 175-198.

Everson, D.A. and D.H. Boucher. 1998. Tree species-richness and topographic complexity along the riparian edge of the Potomac River. Forest Ecology and Management 109: 305-314.

Facey, D.E. and G.D. Grossman. 1992. The relationship between water velocity, energetic costs, and microhabitat use in four North American stream fishes. Hydrobiologia 239: 1-6.

Fenneman, N.M. 1938. Physiography of the Eastern United States. McGraw-Hill, New York.

Galperin, B., L.H. Kantha, S. Hassid, and A. Rosati. 1988. A quasi-equilibrium turbulent energy model for geophysical flows. Journal of the Atmospheric Sciences 45: 55-62.

Garman, G.C. and L.A. Nielsen. 1982. Piscivory by stocked brown trout (*Salmo trutta*) and its impact on the nongame fish community of Bottom Creek, Virginia. Canadian Journal of Fisheries and Aquatic Sciences 39: 862-869.

Gatz, A.J. and S.M. Adams. 1994. Patterns of movement of centrarchids in two warmwater streams in eastern Tennessee. Ecology of Freshwater Fish 3: 35-48.

Giersch, C. 1991. Sensitivity analysis of ecosystems: an analytical treatment. Ecological Modelling 53: 131-146.

Giese, G.L., J.L. Eimers, and R.W. Coble. 1997. Simulation of ground-water flow in the coastal plain aquifer system of North Carolina, in Regional Aquifer-System Analysis—Northern Atlantic Coastal Plain. U.S. Geological Survey.

Professional Paper 1404–M.

Gillen, A.L., R.A. Stein, and R.F. Carline. 1981. Predation by pellet-reared muskellunge on minnows and bluegills in experimental systems. *Transactions of the American Fisheries Society* 110: 197-209.

Gobas, F.A.P.C. and D. Mackay. 1987. Dynamics of hydrophobic organic chemical bioconcentration in fish. *Environmental Toxicology and Chemistry* 6: 495-504.

Gobas, F.A.P.C., A. Opperhuizen, and O. Hutzinger. 1986. Bioconcentration of hydrophobic chemicals in fish: relationship with membrane permeation. *Environmental Toxicology and Chemistry* 5: 637-646.

Goldstein, R.M., J.C. Stauffer, P.R. Larson, and D.L. Lorenz. 1996. Relation of physical and chemical characteristics to streams fish communities in the Red River of the North basin, Minnesota and North Dakota, 1993-5. U.S. Geological Survey, Mounds View, MN. Water Resources Investigations Report 96-4227.

Gordoa, A. and C.M. Duarte. 1992. Size-dependent density of the demersal fish off Namibia: patterns within and among species. *Canadian Journal of Fisheries and Aquatic Sciences* 49: 1990-1993.

Graham, P.H., L.S. Costello, and H.J. Mallon. 1974. Estimation of imperviousness and specific curb length for forecasting stormwater quality and quantity. *Journal Water Pollution Control Federation* 46: 717-725.

Grant, J.W.A. and D.L. Kramer. 1990. Territory size as a predictor of the upper limit to population density of juvenile salmonids in streams. *Canadian Journal of Fisheries and Aquatic Sciences* 47: 1724-1737.

Gregory, S.V., F.J. Swanson, W.A. McKee, and K.W. Cummins. 1991. An ecosystem perspective of riparian zones - focus on links between land and water. *BioScience* 41: 540-551.

Grossman, G.D. and R.E. Ratajczak, Jr. In review. A multi-factorial study of population regulation in a benthic stream fish (*Cottus bairdi*). *Ecological Monographs*.

Grossman, G.D., P.B. Moyle, and J.O. Whittaker, Jr. 1982. Stochasticity in structural and functional characteristics of an Indiana stream fish assemblage: a test of community theory. *American Naturalist* 120: 423-454.

Grossman, G.D., R.E. Ratajczak, Jr., M. Crawford, and M.C. Freeman. 1998. Assemblage organization in stream fishes: effect of environmental variation and interspecific interactions. *Ecological Monographs* 68: 395-420.

Håkanson, L. 1995. Optimal size of predictive models. *Ecological Modelling* 78: 195-204.

Hale, R.S. 1996. Threadfin shad use as supplemental prey in reservoir white crappie fisheries in Kentucky. *North American Journal of Fisheries Management* 16: 619-632.

Hale, S.S., T.E. McMahon, and P.C. Nelson. 1985. Habitat suitability index models and instream flow suitability

curves: Chum salmon. U.S. Department of the Interior, Fish and Wildlife Service, Washington, DC. Biological Report 82(10.108).

Hambright, K.D. 1991. Experimental analysis of prey selection by largemouth bass: role of predator mouth width and prey body depth. *Transactions of the American Fisheries Society* 120: 500-508.

Hamilton, K. and P.C. Nelson. 1984. Habitat suitability index models and instream flow suitability curves: White bass. U.S. Department of the Interior, Fish and Wildlife Service, Washington, DC. Biological Report 82(10.89).

Hamrick, J.M. 1992. A three-dimensional environmental fluid dynamics computer code: theoretical and computational aspects. The College of William and Mary, School of Marine Science, Virginia Institute of Marine Science, Gloucester Point, VA. Special Report 317 in Applied Marine Science and Ocean Engineering.

Hamrick, J.M. 1994. Linking hydrodynamic and biogeochemical transport models for estuarine and coastal waters. *In Estuarine and Coastal Modeling, Proceedings of the 3rd International Conference. Edited by M.L. Spaulding.* American Society of Civil Engineers, New York, NY. pp. 591-608

Hamrick, J.M. 1996. User's Manual For The Environmental Fluid Dynamics Computer Code. The College of William and Mary, School of Marine Science, Virginia Institute of Marine Science, Gloucester Point, VA. Special Report No. 331 in Applied Marine Science and Ocean Engineering.

Hamrick, J.M. and M.Z. Moustafa. 1995. Development of the Everglades wetlands hydrodynamic model: 1. Model formulation and physical processes representation. *Water Resources Research* (submitted).

Hamrick, J.M. and T.S. Wu. 1997. Computational design and optimization of the EFDC/HEM3D surface water hydrodynamic and eutrophication models. *In Next Generation Environmental Models and Computational Methods. Edited by G. Delich and M.F. Wheeler.* Society of Industrial and Applied Mathematics, Philadelphia, PA. pp. 143-156

Hanson, P.C., T.B. Johnson, D.E. Schindler, and J.F. Kitchell. 1997. Fish bioenergetics 3.0 for Windows. University of Wisconsin, Sea Grant Institute, Madison, WI. U.S. Department of Commerce, National Technical Information Service PB2000100305.

Harned, D.A., G. McMahon, T.B. Spruill, and M.D. Woodside. 1995. Water quality assessment of the Albemarle-Pamlico drainage basin, North Carolina and Virginia – Characterization of suspended sediment, nutrients, and pesticides. U.S. Geological Survey. Open File Report 95 – 191.

Hawkes, C.L., D.L. Miller, and W.G. Layher. 1986. Fish ecoregions of Kansas: stream fish assemblage patterns and associated environmental correlates. *Environmental Biology of Fishes* 17: 267-279.

Hayes, D.B., C.P. Ferreri, and W.W. Taylor. 1996. Linking fish habitat to their population dynamics. *Canadian Journal of Fisheries and Aquatic Sciences* 53(Supp.): 383-390.

- Hickman, T. and R.F. Raleigh. 1982. Habitat suitability index models: Cutthroat trout. U.S. Department of the Interior, Fish and Wildlife Service, Washington, DC. FWS/OBS-82/10.5.
- Hicks, R.W.B. and S.D. Woods. 2000. Pollutant load, population growth and land use. Water Environment Research Foundation, Progress Newsletter 11: 10.
- Hill, J. and G.D. Grossman. 1987. Home range estimates for three North American stream fishes. *Copeia* 1987: 376-380.
- Hocutt, C.H., R.E. Jenkins, and J.R. Stauffer, Jr. 1986. Zoogeography of the fishes of the central Appalachians and central Atlantic Coastal Plain. *In* The zoogeography of North American freshwater fishes. *Edited by* C.H. Hocutt and E.O. Wiley. John Wiley & Sons, New York. pp. 161 - 211
- Hubert, W.A., S.H. Anderson, P.D. Southall, and J.H. Crance. 1984. Habitat suitability index models and instream flow suitability curves: Paddlefish. U.S. Department of the Interior, Fish and Wildlife Service, Washington, DC. FWS/OBS-82/10.80.
- Hubert, W.A., R.S. Helzner, L.A. Lee, and P.C. Nelson. 1985. Habitat suitability index models and instream flow suitability curves: Artic grayling riverine populations. U.S. Department of the Interior, Fish and Wildlife Service, Washington, DC. Biological Report 82(10.110).
- Hughes, R.M., P.R. Kaufmann, A.T. Herlihy, T.M. Kincaid, L. Reynolds, and D.P. Larsen. 1998. A process for developing and evaluating indices of fish assemblage integrity. *Canadian Journal of Fisheries and Aquatic Sciences* 55: 1618-1631.
- Hurst, T.P. and D.O. Conover. 1998. Winter mortality of young-of-the-year Hudson River striped bass (*Morone saxatilis*): size-dependent patterns and effects on recruitment. *Canadian Journal of Fisheries and Aquatic Sciences* 55: 1122-1130.
- Inskip, P.D. 1982. Habitat suitability index models: Northern pike. U.S. Department of the Interior, Fish and Wildlife Service, Washington, DC. FWS/OBS-82/10.17.
- Jackson, D.A., K.M. Somers, and H.A. Harvey. 1992. Null models and fish communities: evidence of nonrandom patterns. *American Naturalist* 139: 930-951.
- Jager, H.I., H.E. Cardwell, M.J. Sale, M.S. Bevelhimer, C.C. Coutant, and W. van Winkle. 1997. Modelling the linkages between flow management and salmon recruitment in rivers. *Ecological Modelling* 103: 171-191.
- Jakeman, A.J. and G.M. Hornberger. 1993. How much complexity is warranted in a rainfall-runoff model? *Water Resources Research* 29: 2637-2649.
- Jaworska, J.S., K.A. Rose, and L.W. Barnthouse. 1997. General response patterns of fish populations to stress: an

- evaluation using an individual-based model. *Journal of Aquatic Ecosystem Stress and Recovery* 6: 15-31.
- Jenkins, R.E. and N.M. Burkhead. 1993. *Freshwater fishes of Virginia*. American Fisheries Society, Bethesda, MD.
- Jensen, A.L., S.A. Spigarelli, and M.M. Thommes. 1982. PCB uptake by five species of fish in Lake Michigan, Green Bay of Lake Michigan, and Cayuga Lake, New York. *Canadian Journal of Fisheries and Aquatic Sciences* 39: 700-709.
- Johnson, B.H., K.W. Kim, R.E. Heath, B.B. Hsieh, and H.L. Butler. 1993. Validation of three-dimensional hydrodynamic model of Chesapeake Bay. *Journal of Hydrologic Engineering* 119: 2-20.
- Johnson, B.L., D.L. Smith, and R.F. Carline. 1988. Habitat preferences, survival, growth, foods, and harvests of walleye and walleye × sauger hybrids. *North American Journal of Fisheries Management* 8: 292-304.
- Johnson, J.H., D.S. Dropkin, and P.G. Schaffer. 1992. Habitat use by a headwater stream fish community in north-central Pennsylvania. *Rivers* 3: 69-79.
- Johnston, J.M. 2001. A scientific and technological framework for evaluating risk in Ecological Risk Assessments. *In Modeling of Environmental Chemical Exposure and Risk. Edited by J.B.H.J. Linders*. Kluwer Academic Publishers, Dordrecht, Netherlands. pp. 133-150
- Johnston, T.A., M.N. Gaboury, R.A. Janusz, and L.R. Janusz. 1995. Larval fish drift in the Valley River, Manitoba: influences of abiotic and biotic factors, and relationships with future year-class strengths. *Canadian Journal of Fisheries and Aquatic Sciences* 52: 2423-2431.
- Jones, K.B., K.H. Ritters, J.D. Wickham, R.D. Tankersley, Jr., R.V. O'Neill, D.J. Chaloud, E.R. Smith, and A.C. Neale. 1997. *An ecological assessment of the United States mid-Atlantic region*. U.S. Environmental Protection Agency. EPA/600/R-97/130.
- Juanes, F. 1986. Population density and body size in birds. *American Naturalist* 128: 921-929.
- Juanes, F., R.E. Marks, K.A. McKown, and D.O. Conover. 1993. Predation by age-0 bluefish on age-0 anadromous fishes in the Hudson River estuary. *Transactions of the American Fisheries Society* 122: 348-356.
- Jude, D.J., F.J. Tesar, S.F. Deboe, and T.J. Miller. 1987. Diet and selection of major prey species by Lake Michigan salmonines, 1973-1982. *Transactions of the American Fisheries Society* 116: 677-691.
- Karr, J.R. 1981. Assessment of biotic integrity using fish communities. *Fisheries* 6: 21-27.
- Karr, J.R. and I.J. Schlosser. 1978. Water resources and the land-water interface. *Science* 201: 229-234.
- Karr, J.R., K.D. Fausch, P.L. Angermeier, P.R. Yant, and I.J. Schlosser. 1986. *Assessing biological integrity in*

running waters: a method and its rationale. Illinois Natural History Survey. Special Publication No. 5.

Keeley, E.R. and J.W.A. Grant. 1995. Allometric and environmental correlates of territory size in juvenile Atlantic salmon (*Salmo salar*). Canadian Journal of Fisheries and Aquatic Sciences 52: 186-196.

Knight, R.L., F.J. Margraf, and R.F. Carline. 1984. Piscivory by walleyes and yellow perch in western Lake Erie. Transactions of the American Fisheries Society 113: 677-693.

Knight, W. 1968. Asymptotic growth: An example of nonsense disguised as mathematics. Journal of the Fisheries Research Board of Canada 25: 1303-1307.

Kostecki, P.T. 1984. Habitat suitability index models: Spotted seatrout. U.S. Department of the Interior, Fish and Wildlife Service, Washington, DC. FWS/OBS-82/10.75.

Krieger, D.A., J.W. Terrell, and P.C. Nelson. 1983. Habitat suitability information: Yellow perch. U.S. Department of the Interior, Fish and Wildlife Service, Washington, DC. FWS/OBS-82/10.55.

Kuczera, G. 1983. Improved parameter inference in catchment models. 1. Evaluating parameter uncertainty. Water Resources Research 19: 1151-1172.

Lee, L.A. and J.W. Terrell. 1987. Habitat suitability index models: Flathead catfish. U.S. Department of the Interior, Fish and Wildlife Service, Washington, DC. Biological Report 82(10.152).

Leidy, G.R. and R.M. Jenkins. 1977. The development of fishery compartments and population rate coefficients for use in reservoir ecosystem modeling. U.S. Department of Interior, Fish and Wildlife Service, Fayetteville, AR. Report Y-77-1.

Leonard, P.M. and D.J. Orth. 1988. Use of habitat guilds to determine instream flow requirements. North American Journal of Fisheries Management 8: 399-409.

Lewis, W.M., R. Heidinger., W. Kirk, W. Chapman, and D. Johnson. 1974. Food intake of the largemouth bass. Transactions of the American Fisheries Society 103: 277-280.

Lloyd, O.B., C.R. Barnes, and M.D. Woodside. 1991. National water-quality assessment program - the Albemarle-Pamlico drainage. U.S. Geological Survey. Open-file Report 91-156.

Lobb, M.D., III and D.J. Orth. 1991. Habitat use by an assemblage of fish in a large warmwater stream. Transactions of the American Fisheries Society 120: 65-78.

Loehle, C. 1997. A hypothesis testing framework for evaluating ecosystem model performance. Ecological Modelling 97: 153-165.

- Lorenzen, K. 1996. The relationship between body weight and natural mortality in juvenile and adult fish: a comparison of natural ecosystems and aquaculture. *Journal of Fish Biology* 49: 627-647.
- Loveland, T.R. and D.M. Shaw. 1996. Multi-resolution land characterization: Building collaborative partnerships., pp. 79-85. In J.M. Scott, T.H. Tear and F.W. Davis [eds.], *Gap Analysis: A landscape approach to biodiversity planning*. American Society for Photogrammetry and Remote Sensing (ASPRS) Symposium, Charlotte, NC.
- Lowrance, R., R. Todd, J. Fail, Jr., O. Hendrickson, Jr., R. Leonard, and L. L. Asmussen. 1984. Riparian forests as nutrient filters in agricultural watersheds. *BioScience* 34: 374-377.
- Lumb, A.M., R.B. McCammon, and J.L. Kittle, Jr. 1994. A Manual for an Expert System (HSPEXP) for Calibration of the Hydrologic Simulation Program - Fortran. U.S. Geological Survey. Water-Resources Investigations Report 94-4168.
- Lyons, J. 1996. Patterns in the species composition of fish assemblages among Wisconsin streams. *Environmental Biology of Fishes* 45: 329-341.
- Mackay, D. 1982. Correlation of bioconcentration factors. *Environmental Science and Technology* 16: 274-278.
- Madenjian, C.P., T.J. DeSorcie, and R.M. Stedman. 1998. Ontogenic and spatial patterns in diet and growth of lake trout in Lake Michigan. *Transactions of the American Fisheries Society* 127: 236-252.
- Madenjian, C.P., S.R. Carpenter, G.E. Eck, and M.A. Miller. 1993. Accumulation of PCBs by lake trout (*Salvelinus namaycush*): an individual-based model approach. *Canadian Journal of Fisheries and Aquatic Sciences* 50: 97-109.
- Marcus, M.D., W.A. Hubert, and S.H. Anderson. 1984. Habitat suitability index models: Lake trout (exclusive of the Great Lakes). U.S. Department of the Interior, Fish and Wildlife Service, Washington, DC. FWS/OBS-82/10.84.
- Margenau, T.L., P.W. Rasmussen, and J.M. Kampa. 1998. Factors affecting growth of northern pike in small Wisconsin lakes. *North American Journal of Fisheries Management* 18: 625-639.
- Matthews, W.J. 1982. Small fish community structure in Ozark streams: structured assembly patterns or random abundance of species? *American Midland Naturalist* 107: 42-54.
- Matthews, W.J. 1998. *Patterns in freshwater fish ecology*. Chapman & Hall, New York, NY.
- Mattingly, H.T. and M.J. Butler, IV. 1994. Laboratory predation on the Trinidadian guppy: implications for size-selective predation hypothesis and guppy life history evolution. *Oikos* 69: 54-64.
- May, R.M. 1973. *Stability and Complexity in Model Ecosystems*. Princeton University Press, Princeton, NJ.
- McGurk, M.D. 1993. Allometry of herring mortality. *Transactions of the American Fisheries Society* 122: 1035-

1042.

McGurk, M.D. 1999. Size dependence of natural mortality rate of sockeye salmon and kokanee in freshwater. *North American Journal of Fisheries Management* 19: 376-396.

McMahon, G. and O.B. Lloyd, Jr. 1995. Water-quality assessment of the Albemarle-Pamlico Drainage Basin, North Carolina and Virginia - Environmental setting and water-quality issues. U.S. Geological Survey. Open-File Report 95-136.

McMahon, T.E. 1982. Habitat suitability index models: Creek chub. U.S. Department of the Interior, Fish and Wildlife Service, Washington, DC. FWS/OBS-82/10.4.

McMahon, T.E. 1983. Habitat suitability index models: Coho salmon. U.S. Department of the Interior, Fish and Wildlife Service, Washington, DC. FWS/OBS-82/10.49.

McMahon, T.E. and J.W. Terrell. 1982. Habitat suitability index models: Channel catfish. U.S. Department of the Interior, Fish and Wildlife Service, Washington, DC. FWS/OBS-82/10.2.

McMahon, T.E., J.W. Terrell, and P.C. Nelson. 1984a. Habitat suitability information: Walleye. U.S. Department of the Interior, Fish and Wildlife Service, Washington, DC. FWS/OBS-82/10.56.

McMahon, T.E., G. Gebhart, O.E. Maughan, and P.C. Nelson. 1984b. Habitat suitability index models and instream flow suitability curves: Spotted bass. U.S. Department of the Interior, Fish and Wildlife Service, Washington, DC. FWS/OBS-82/10.72.

McMahon, T.E., G. Gebhart, O.E. Maughan, and P.C. Nelson. 1984c. Habitat suitability index models and instream flow suitability curves: Warmouth. U.S. Department of the Interior, Fish and Wildlife Service, Washington, DC. FWS/OBS-82/10.67.

Mellor, G.L. and T. Yamada. 1982. Development of a turbulence closure model for geophysical fluid problems. *Reviews of Geophysics and Space Physics* 20: 851-875.

Menhinick, E.F. 1991. The freshwater fishes of North Carolina. North Carolina Wildlife Resources Commission, Raleigh, NC.

Miall, A.D. 1985. Architectural-element analysis: A new method of facies analysis applied to fluvial deposits. *Earth-Science Reviews* 22: 261-308.

Miller, D.L., P.M. Leonard, R.M. Hughes, J.R. Karr, P.B. Moyle, L.H. Schrader, B.A. Thompson, R.A. Daniels, K.D. Fausch, G.A. Fitzhugh, J.R. Gammon, D.B. Halliwell, P.L. Angermeier, and D.J. Orth. 1988. Regional applications of an index of biotic integrity for use in water resource management. *Fisheries* 13: 12-20.

- Miller, T.J., L.B. Crowder, J.A. Rice, and F.P. Binkowski. 1992. Body size and the ontogeny of the functional response in fishes. *Canadian Journal of Fisheries and Aquatic Sciences* 49: 805-812.
- Minns, C.K. 1995. Allometry of home range size in lake and river fishes. *Canadian Journal of Fisheries and Aquatic Sciences* 52: 1499-1508.
- Minor, J.D. and E.J. Crossman. 1978. Home range and seasonal movements of muskellunge as determined by radiotelemetry. *American Fisheries Society Special Publication* 11: 146-153.
- Mittelbach, G.G. and L. Persson. 1998. The ontogeny of piscivory and its ecological consequences. *Canadian Journal of Fisheries and Aquatic Sciences* 55: 1454-1465.
- Moore, C.M., R.J. Neves, J.J. Ney, and D.K. Whitehurst. 1985. Utilization of alewives and gizzard shad by striped bass in Smith Mountain Lake, Virginia. *Proceeding of the Annual Conference of the Southeastern Association of Fish and* 39: 108-115.
- Moser, G.A. and M.S. McLachlan. 2001a. The influence of dietary concentration on the absorption and excretion of persistent lipophilic organic pollutants in the human intestinal tract. *Chemosphere* 45: 201-211.
- Moser, G.A. and M.S. McLachlan. 2001b. Partitioning of polychlorinated biphenyls and hexachlorobenzene into human faeces. *Chemosphere* 46: 449-457.
- National Research Council. 2001. *Assessing the TMDL Approach to Water Quality Management*. National Academy Press, Washington, DC.
- NCARP. 2002. Trophy fish guidelines. North Carolina Angler Recognition Program. http://www.ncwildlife.org/pg03_Fishing/pg3c1.htm
- NCDENR. 1996. Roanoke River Basinwide Water Quality Plan. North Carolina Department of Environment and Natural Resources, Division of Water Quality, Raleigh, NC.
- NCDENR. 1997a. Chowan River Basinwide Water Quality Plan. North Carolina Department of Environment and Natural Resources, Division of Water Quality, Raleigh, NC.
- NCDENR. 1997b. Annual Report of Fish Kill Events. North Carolina Department of Environment and Natural Resources, Division of Water Quality. <http://www.esb.enr.state.nc.us/Fishkill/1997KillRept.pdf>
- NCDENR. 1998. Annual Report of Fish Kill Events. North Carolina Department of Environment and Natural Resources, Division of Water Quality. <http://www.esb.enr.state.nc.us/Fishkill/98killrept.pdf>
- NCDENR. 1999a. Tar-Pamlico River Basinwide Water Quality Plan. North Carolina Department of Environment and Natural Resources, Division of Water Quality, Raleigh, NC.

- NCDENR. 1999b. Annual Report of Fish Kill Events. North Carolina Department of Environment and Natural Resources, Division of Water Quality. <http://www.esb.enr.state.nc.us/Fishkill/99killrept.pdf>
- NCDENR. 2000. Annual Report of Fish Kill Events. North Carolina Department of Environment and Natural Resources, Division of Water Quality. <http://www.esb.enr.state.nc.us/Fishkill/2000killrep.pdf>
- NCDENR. 2001. Annual Report of Fish Kill Events. North Carolina Department of Environment and Natural Resources, Division of Water Quality. <http://www.esb.enr.state.nc.us/Fishkill/01killrep.pdf>
- NCDENR. 2002a. Chowan River Basin: Albamarle-Pamlico National Estuary Program. North Carolina Department of Environment and Natural Resources. http://h2o.enr.state.nc.us/nep/chowan_river_basin.htm
- NCDENR. 2002b. Neuse River Basin: Albamarle-Pamlico National Estuary Program. North Carolina Department of Environment and Natural Resources. http://h2o.enr.state.nc.us/nep/neuse_river_basin.htm
- NCDENR. 2002c. Roanoke River Basin: Albamarle-Pamlico National Estuary Program. North Carolina Department of Environment and Natural Resources. http://h2o.enr.state.nc.us/nep/roanoke_river_basin.htm
- NCDENR. 2002d. Tar-Pamlico River Basin: Albamarle-Pamlico National Estuary Program. North Carolina Department of Environment and Natural Resources. http://h2o.enr.state.nc.us/nep/tarpamlico_river_basin.htm
- NCDENR. 2002e. Basinwide Planning Program, NC River Basin Statistics. North Carolina Department of Environment and Natural Resources, Division of Water Quality. http://h2o.enr.state.nc.us/basinwide/basinwide_stats.htm
- NCDHHS. 2001. Roanoke River Fish Consumption Advisory for Dioxin. North Carolina Department of Health and Human Services. <http://www.dhhs.state.nc.us/pressrel/10-10-01a.htm>
- NCDHHS. 2002. Fish Consumption Advisories. North Carolina Department of Health and Human Services. <http://www.schs.state.nc.us/epi/fish/current.html>
- NCNEWP. 202. North Carolina Atlas of Freshwater Mussels & Endangered Fish. North Carolina Nongame and Endangered Wildlife Program. http://www.ncwildlife.org/pg07_WildlifeSpeciesCon/pg7b1.htm
- NCWRC. 2002. North Carolina Inland Fishing, Hunting and Trapping Regulations Digest 2002-2003. North Carolina Wildlife Resources Commission, Raleigh, NC. http://216.27.49.98/pg02_Regs/Regs_Digest.pdf
- Newcombe, C.P. and D.D. MacDonald. 1991. Effects of suspended sediments on aquatic ecosystems. North American Journal of Fisheries Management 11: 72-82.
- Nilsson, C., A. Ekblad, and M. Dynesius. 1994. A comparison of species richness and traits of riparian plants between a major river channel and its tributaries. Journal of Ecology 82: 281-295.

- Norstrom, R.J., A.E. McKinnon, and A.S.W. deFreitas. 1976. A bioenergetics-based model for pollutant accumulation by fish. Simulation of PCB and methylmercury residue levels in Ottawa River yellow perch (*Perca flavescens*). Journal of the Fisheries Research Board of Canada 33: 248-267.
- Norton, J.P. 1996. Roles of deterministic bounding in environmental modelling. Ecological Modelling 86: 157-161.
- Page, L.M. and B.M. Burr. 1991. A Field Guide to Freshwater Fishes. Houghton Mifflin, Boston, MA.
- Paller, M.H. 1994. Relationships between fish assemblage structure and stream order in South Carolina Coastal Plain streams. Transactions of the American Fisheries Society 123: 150-161.
- Paller, M.H., M.J.M. Reichert, and J.M. Dean. 1996. Use of fish communities to assess environmental impacts in South Carolina coastal plain streams. Transactions of the American Fisheries Society 125: 633-644.
- Paloheimo, J.E. and L.M. Dickie. 1965. Food and growth of fishes. I. A growth curve derived from experimental data. Journal of the Fisheries Research Board of Canada 22: 521-542.
- Pardue, G.B. 1983. Habitat suitability index models: Alewife and blueback herring. U.S. Department of the Interior, Fish and Wildlife Service, Washington, DC. FWS/OBS-82/10.58.
- Park, R.A. 2000a. AQUATOX for Windows, version 1.69 Volume 2: Technical documentation. U.S. Environmental Protection Agency, Office of Water, Washington, DC. EPA/823/R-00/007.
- Park, R.A. 2000b. AQUATOX for Windows, version 1.69 Volume 3: Model Validation Reports. U.S. Environmental Protection Agency, Office of Water, Washington, DC. EPA/823/R-00/008.
- Parker, R.R. and P.A. Larkin. 1959. A concept of growth in fishes. Journal of the Fisheries Research Board of Canada 16: 721-745.
- Parsons, J.W. 1971. Selective food preferences of walleyes of the 1959 year class in Lake Erie. Transactions of the American Fisheries Society 100: 474-485.
- Pearsons, T.N., H.W. Li, and G.A. Lamberti. 1992. Influence of habitat complexity on resistance to flooding and resilience of stream fish assemblages. Transactions of the American Fisheries Society 121: 427-436.
- Peterjohn, W.T. and D.L. Correll. 1984. Nutrient dynamics in an agricultural watershed: observations on the role of a riparian forest. Ecology 65: 1466-1475.
- Peters, R.H. and J.V. Raelson. 1984. Relations between individual size and mammalian population density. American Naturalist 124: 498-517.
- Peterson, I. and J.S. Wroblewski. 1984. Mortality rates of fishes in the pelagic ecosystem. Canadian Journal of

Fisheries and Aquatic Sciences 41: 1117-1120.

Planty Tabacchi, A., E. Tabacchi, R.J. Naiman, C. Deferrari, and H. Decamps. 1996. Invasability of species-rich communities in riparian zones. *Conservation Biology* 10: 598-607.

Poff, N.L. and J.D. Allan. 1995. Functional organization of stream fish assemblages in relation to hydrologic variability. *Ecology* 76: 606-627.

Popper, K. 1959. *The Logic of Scientific Discovery*. Harper, New York, NY.

Prince, A. 2002. The Upper Tar River Basin: Swift Creek and Fishing Creek Subbasins. North Carolina Natural Heritage Program. http://www.ncwildlife.org/pg07_WildlifeSpeciesCon/images/img_7b1c_forestmemo2.pdf

Rahel, F.J., J.D. Lyons, and P.A. Cochran. 1984. Stochastic or deterministic regulation of assemblage structure? It may depend on how the assemblage is defined. *American Naturalist* 124: 583-589.

Raleigh, R.F. 1982. Habitat suitability index models: Brook trout. U.S. Department of the Interior, Fish and Wildlife Service, Washington, DC. FWS/OBS-82/10.24.

Raleigh, R.F. and P.C. Nelson. 1985. Habitat suitability index models and instream flow suitability curves: Pink salmon. U.S. Department of the Interior, Fish and Wildlife Service, Washington, DC. Biological Report 82(10.109).

Raleigh, R.F., W.J. Miller, and P.C. Nelson. 1986a. Habitat suitability index models and instream flow suitability curves: Chinook salmon. U.S. Department of the Interior, Fish and Wildlife Service, Washington, DC. Biological Report 82(10.122).

Raleigh, R.F., L.D. Zuckerman, and P.C. Nelson. 1986b. Habitat suitability index models and instream flow suitability curves: Brown trout. U.S. Department of the Interior, Fish and Wildlife Service, Washington, DC. Biological Report 82(10.124) [First printed as: FWS/OBS-82/10.71, September 1984].

Raleigh, R.F., T. Hickman, R.C. Solomon, and P.C. Nelson. 1984. Habitat suitability information: Rainbow trout. U.S. Department of the Interior, Fish and Wildlife Service, Washington, DC. FWS/OBS-82/10.60.

Randall, R.G., J.R.M. Kelso, and C.K. Minns. 1995. Fish production in freshwaters: Are rivers more productive than lakes? *Canadian Journal of Fisheries and Aquatic Sciences* 52: 631-643.

Reeves, G.H., L.E. Benda, K.M. Burnett, P.A. Bisson, and J.R. Sedell. 1995. A disturbance-based ecosystem approach to maintaining and restoring freshwater habitats of evolutionary significant units of anadromous salmonids in the Pacific Northwest. *American Fisheries Society Symposium* 17: 334-349.

Reice, S.R. 1994. Nonequilibrium determinants of biological community structure. *American Scientist* 82: 424-435.

- Richards, R.J. 1959. A flexible growth function for empirical use. *Journal of Experimental Botany* 10: 290-300.
- Richter, B.D., D.P. Braun, M.A. Mendelson, and L.L. Master. 1997. Threats to imperiled freshwater fauna. *Conservation Biology* 11: 1081-1093.
- Ricker, W.E. 1979. Growth rates and models. *In Fish Physiology, Vol. VIII. Edited by W.S. Hoar, D.J. Randall and J.R. Brett. Academic Press, Inc., Orlando, FL. pp. 677-743*
- Robinson, J.G. and K.H. Redford. 1986. Body size, diet and population density of neotropical forest mammals. *American Naturalist* 128: 665-680.
- Roell, M.J. and D.J. Orth. 1998. Indirect effects of fishery exploitation and pest control in a riverine food web. *North American Journal of Fisheries Management* 18: 337-346.
- Rosati, A.K. and K. Miyakoda. 1988. A general circulation model for upper ocean simulation. *Journal of Physical Oceanography* 18: 1601-1626.
- Rose, D.R. and A.A. Echelle. 1981. Factor analysis of associations of fishes in Little River, central Texas, with an interdrainage comparison. *American Midland Naturalist* 106: 379-391.
- Schlösser, I.J. 1987. A conceptual framework for fish communities in small warmwater streams. *In Community and evolutionary ecology of North American stream fishes. Edited by W.J. Matthews and D.C. Heins. University of Oklahoma Press, Norman, OK. pp. 17-24*
- Schlösser, I.J. 1995. Critical landscape attributes that influence fish population dynamics in headwater streams. *Hydrobiologia* 303: 71-81.
- Schnute, J. 1981. A versatile growth model with statistically stable parameters. *Canadian Journal of Fisheries and Aquatic Sciences* 38: 1128-1140.
- Schueler, T. 1994. The importance of imperviousness. *Watershed Protection Techniques* 1: 100 -111.
- Scott, M.C. and L.W. Hall, Jr. 1997. Fish assemblages as indicators of environmental degradation in Maryland Coastal Plain streams. *Transactions of the American Fisheries Society* 126: 349-360.
- Sharitz, R.R., L.R. Boring, D.H. Van Lear, and J.E. Pinder, III. 1992. Integrating ecological concepts with natural resource management of southern forests. *Ecological Applications* 2: 226-237.
- Sheldon, A.L. and G.K. Meffe. 1995. Path analysis of collective properties and habitat relationships of fish assemblages in coastal plain streams. *Canadian Journal of Fisheries and Aquatic Sciences* 52: 23-33.
- Shuter, B.J. 1990. Population-level indicators of stress. *American Fisheries Society Symposium* 8: 145-166.

- Sikora, W.B. and J.P. Sikora. 1982. Habitat suitability index models: Southern kingfish. U.S. Department of the Interior, Fish and Wildlife Service, Washington, DC. FWS/OBS-82/10.31.
- Sleavin, W.J., S. Prisloe, L. Giannotti, and D.L. Civco. 2000. Measuring impervious surfaces for non-point source pollution modeling, 2000 American Society for Photogrammetry and Remote Sensing (ASPRS) Annual Convention, Washington, DC.
- Smith, E.R. 2000. An overview of EPA's Regional Vulnerability Assessment (ReVA) Program. *Environmental Monitoring and Assessment* 64: 9-15.
- Smock, L.A. and E. E. Gilinsky. 1992. Coastal plain blackwater streams. *In Biodiversity of Southeastern United States: Aquatic Communities. Edited by C.T. Hacknet, S.M. Adams and W.H. Martin.* John Wiley & Sons, New York, NY. pp. 271-313
- Smock, L.A., G.M. Metzler, and J.E. Gladden. 1989. Role of debris dams in the structure and function of low-gradient headwater streams. *Ecology* 70: 764-775.
- Smoger, R.A. and P.L. Angermeier. 1998. Relations between fish metrics and measures of anthropogenic disturbance in three IBI regions in Virginia. *In Assessing the sustainability and biological integrity of water resources using fish communities. Edited by T.P. Simon.* CRC Press, Boca Raton, FL. pp. 585-610
- Smolarkiewicz, P.K. 1984. A fully multidimensional positive definite advection transport algorithm with small implicit diffusion. *Journal of Computational Physics* 54: 325-362.
- Smolarkiewicz, P.K. and T.L. Clark. 1986. The multidimensional positive definite advection transport algorithm: further development and applications. *Journal of Computational Physics* 67: 396-438.
- Smolarkiewicz, P.K. and W.W. Grabowski. 1990. The multidimensional positive definite advection transport algorithm: nonoscillatory option. *Journal of Computational Physics* 86: 355-375.
- Smolarkiewicz, P.K. and L.G. Margolin. 1993. On forward-in-time differencing for fluids: extension to a curvilinear framework. *Monthly Weather Review* 121: 1847-1859.
- Sorooshian, S., Q. Duan, and V.K. Gupta. 1993. Calibration of rainfall-runoff models: application of global optimization to the Sacramento Soil Moisture Accounting Model. *Water Resources Research* 29: 1185-1194.
- Spruill, T.B., D.A. Harned, P.M. Ruhl, J.L. Eimers, G. McMahon, K.E. Smith, D.R. Galeone, and M.D. Woodside. 1998. Water-quality in the Albemarle-Pamlico drainage basin, North Carolina and Virginia, 1992-95. U.S. Geological Survey. Circular 1157.
- Stankowski, S.J. 1972. Population Density as an Indirect Indicator of Urban and Suburban Land-Surface Modifications. U.S. Department of the Interior, Geological Survey. Professional Paper 800-B.

- Steingrímsson, S.O. and J.W.A. Grant. 1999. Allometry of territory size and metabolic rate as predictors of self thinning in young-of-year Atlantic salmon. *Journal of Animal Ecology* 68: 17-86.
- Stickney, R.R. and M.L. Cuenco. 1982. Habitat suitability index models: Juvenile spot. U.S. Department of the Interior, Fish and Wildlife Service, Washington, DC. FWS/OBS-82/10.20.
- Stiefvater, R.J. and S.P. Malvestuto. 1985. Seasonal analysis of predator-prey size relationships in West Point Lake, Alabama-Georgia. *Proceedings of the Annual Conference of the Southeastern Association of Fish and Wildlife* 39: 19-27.
- Stier, D.J. and J.H. Crance. 1985. Habitat suitability index models and instream flow suitability curves: American shad. U.S. Department of the Interior, Fish and Wildlife Service, Washington, DC. Biological Report 82(10.88).
- Storck, T.W. 1986. Importance of gizzard shad in the diet of largemouth bass in Lake Shelbyville, Illinois. *Transactions of the American Fisheries Society* 115: 21-27.
- Strange, E.M., P.B. Moyle, and T.C. Foin. 1992. Interactions between stochastic and deterministic processes in stream fish community assembly. *Environmental Biology of Fishes* 36: 1-15.
- Stuber, R.J. 1982. Habitat suitability index models: Black bullhead. U.S. Department of the Interior, Fish and Wildlife Service, Washington, DC. FWS/OBS-82/10.14.
- Stuber, R.J., G. Gebhart, and O.E. Maughan. 1982a. Habitat suitability index models: Bluegill. U.S. Department of the Interior, Fish and Wildlife Service, Washington, DC. FWS/OBS-82/10.8.
- Stuber, R.J., G. Gebhart, and O.E. Maughan. 1982b. Habitat suitability index models: Green sunfish. U.S. Department of the Interior, Fish and Wildlife Service, Washington, DC. FWS/OBS-82/10.15.
- Stuber, R.J., G. Gebhart, and O.E. Maughan. 1982c. Habitat suitability index models: Largemouth bass. U.S. Department of the Interior, Fish and Wildlife Service, Washington, DC. FWS/OBS-82/10.16.
- Summers, J.K., H.T. Wilson, and J. Kou. 1993. A method for quantifying the prediction uncertainties associated with water quality models. *Ecological Modelling* 65: 161-176.
- Taylor, C.M. 1996. Abundance and distribution within a guild of benthic stream fishes: local processes and regional patterns. *Freshwater Biology* 36: 385-396.
- Thomann, R.V. 1989. Bioaccumulation model of organic chemical distribution in aquatic food chains. *Environmental Science and Technology* 23: 699-707.
- Thomann, R.V. and J.P. Connolly. 1984. Model of PCB in the Lake Michigan lake trout food chain. *Environmental Science and Technology* 18: 65-71.

- Thyer, M., G. Kuczera, and B.C. Bates. 1999. Probabilistic optimization for conceptual rainfall-runoff models: a comparison of the shuffled complex evolution and simulated annealing algorithms. *Water Resources Research* 35: 767-773.
- Timmons, T.J., W.L. Shelton, and W.D. Davies. 1980. Differential growth of largemouth bass in West Point Reservoir, Alabama-Georgia. *Transactions of the American Fisheries Society* 109: 176-186.
- Tonn, W.M., C.A. Paszkowski, and T.C. Moermond. 1986. Competition in *Umbra-Perca* fish assemblages: experimental and field evidence. *Oecologia* 69: 126-133.
- Toole, C.L., R.A. Barnhart, and C.P. Onuf. 1987. Habitat suitability index models: Juvenile English sole. U.S. Department of the Interior, Fish and Wildlife Service, Washington, DC. Biological Report 82(10.133).
- Townsend, C.R. 1989. The patch dynamics concept of stream community ecology. *Journal of the North American Benthological Society* 8: 36-50.
- Trial, J.G., C.S. Wade, J.G. Stanley, and P.C. Nelson. 1983a. Habitat suitability information: Common shiner. U.S. Department of the Interior, Fish and Wildlife Service, Washington, DC. FWS/OBS-82/10.40.
- Trial, J.G., C.S. Wade, J.G. Stanley, and P.C. Nelson. 1983b. Habitat suitability information: Fallfish. U.S. Department of the Interior, Fish and Wildlife Service, Washington, DC. FWS/OBS-82/10.48.
- Trial, J.G., J.G. Stanley, M. Bacteller, G. Gebhart, O.E. Maughan, and P.C. Nelson. 1983c. Habitat suitability information: Blacknose dace. U.S. Department of the Interior, Fish and Wildlife Service, Washington, DC. FWS/OBS-82/10.41.
- Turchin, P. 1995. Population regulation: old arguments and a new synthesis. *In* *Populations dynamics: new approaches and synthesis*. Edited by N. Cappuccino and P.W. Price. Academic Press, San Diego, CA. pp. 19-40
- Twomey, K.A., K.L. Williamson, and P.C. Nelson. 1984a. Habitat suitability index models and instream flow suitability curves: White sucker. U.S. Department of the Interior, Fish and Wildlife Service, Washington, DC. FWS/OBS-82/10.64.
- Twomey, K.A., G. Gebhart, O.E. Maughan, and P.C. Nelson. 1984b. Habitat suitability index models and instream flow suitability curves: Redear sunfish. U.S. Department of the Interior, Fish and Wildlife Service, Washington, DC. FWS/OBS-82/10.79.
- USEPA. 1994. The Quality of Our Nation's Water: 1992. U.S. Environmental Protection Agency, Office of Water, Washington, DC. EPA/841/F-94/002.
- USEPA. 1998. U.S. EPA Reach File 1 (RF1) for the Conterminous United States in BASINS. U.S. Environmental Protection Agency, Office of Science and Technology, Office of Science and Technology, Washington, DC.

<http://www.epa.gov/waterscience/basins/metadata/rfl.htm>.

USEPA. 1999. HSPFParm: An Interactive Database of HSPF Model Parameters, Version 1.0. U.S. Environmental Protection Agency, Office of Water, Washington, DC. EPA/823/R-99/004.

USEPA. 2000a. BASINS Technical Note 6: Estimating Hydrology and Hydraulic Parameters for HSPF. U.S. Environmental Protection Agency, Office of Water, Washington, DC. EPA/823/R-00/012.

USEPA. 2000b. Better Assessment Sciences Integrating Point and Nonpoint Sources (BASINS). U.S. Environmental Protection Agency, Office of Water, Office of Science and Technology, Washington, DC.

USGS. 1998. Water Quality in the Albemarle-Pamlico Drainage Basin, North Carolina and Virginia, 1992-95:. U.S. Geological Survey Circular 1157. <http://water.usgs.gov/pubs/circ/circ1157/nawqa91.6.html#21462>

Vannote, R.L., G.W. Minshall, K.W. Cummins, J.R. Sedell, and C.E. Cushing. 1980. The river continuum concept. *Canadian Journal of Fisheries and Aquatic Sciences* 37: 130-137.

Vecchia, A.V. and R.L. Cooley. 1987. Simultaneous confidence and prediction intervals for nonlinear regression models with application to a groundwater flow model. *Water Resources Research* 23: 1237-1250.

Verry, E.S. and D.R. Timmons. 1982. Waterborne nutrient flow through an upland-peatland watershed in Minnesota. *Ecology* 63: 1456-1467.

Vogelmann, J.E., T. Sohl, and S.M. Howard. 1998. Regional characterization of land cover using multiple sources of data. *Photogrammetric Engineering and Remote Sensing* 64: 45-57.

Vogelmann, J.E., S.M. Howard, L. Yang, C.R. Larson, B.K. Wylie, and J.N. Van Driel. 2001. Completion of the 1990's National Land Cover Data Set for the conterminous United States. *Photogrammetric Engineering and Remote Sensing* 67: 650-662.

Waide, J.B. and J.R. Webster. 1976. Engineering Systems Analysis: Applicability to Ecosystems. *In Systems Analysis and Simulation in Ecology: Volume IV. Edited by B.C. Patten. Academic Press, New York, NY. pp. 330-371*

Wallach, D. and M. Genard. 1998. Effect of uncertainty in input and parameter values on model prediction error. *Ecological Modelling* 105: 337-345.

Wang, Q.J. 1991. The genetic algorithm and its application to calibrating conceptual rainfall-runoff models. *Water Resources Research* 27: 2467-2471.

Wanzenböck, J. and F. Schiemer. 1989. Prey detection in cyprinids during early development. *Canadian Journal of Fisheries and Aquatic Sciences* 46: 995-1001.

- Wardle, D.A., O. Zackrisson, G. Hornberg, and C. Gallet. 1997. The influence of island area on ecosystem properties. *Science* 277: 1296-1299.
- Weinstein, M.P. 1986. Habitat suitability index models: Inland silverside. U.S. Department of the Interior, Fish and Wildlife Service, Washington, DC. Biological Report 82(10.120).
- Werner, E.E. 1974. The fish size, prey size, handling time relation in several sunfishes and some implications. *Journal of the Fisheries Research Board of Canada* 31: 1531-1536.
- Whittier, T.R., R.M. Hughes, and D.P. Larsen. 1988. Correspondence between ecoregions and spatial patterns in stream ecosystems in Oregon. *Canadian Journal of Fisheries and Aquatic Sciences* 45: 1264-1278.
- Wilcove, D.S., D. Rothstein, J. Dubow, A. Phillips, and E. Losos. 1998. Quantifying threats to imperiled species in the United States. *BioScience* 48: 607-615.
- Williams, J.E., J.E. Johnson, D.A. Hendrickson, S. Contreras-Balderas, J.D. Williams, M. Navarro-Mendoza, D.E. McAllister, and J.E. Deacon. 1989. Fishes of North America: endangered, threatened, or of species concern. *Fisheries* 14: 2-20.
- Williamson, K.L. and P.C. Nelson. 1985. Habitat suitability index models and instream flow suitability curves: Gizzard shad. U.S. Department of the Interior, Fish and Wildlife Service, Washington, DC. Biological Report 82(10.112).
- Winston, M.R., C.M. Taylor, and J. Pigg. 1991. Upstream extirpation of four minnow species due to damming of a prairie stream. *Transactions of the American Fisheries Society* 120: 98-105.
- Yalkowsky, S.H., O.S. Carpenter, G.L. Flynn, and T.G. Slunick. 1973. Drug absorption kinetics in goldfish. *Journal of Pharmaceutical Sciences* 62: 1949-1954.
- Yang, M.S. and P.A. Livingston. 1988. Food habits and daily ration of Greenland halibut, *Reinhardtius hippoglossoides*, in the eastern Bering Sea. *Fishery Bulletin* 86: 675-690.
- Yant, P.R., J.R. Karr, and P.L. Angermeier. 1984. Stochasticity in stream fish communities: an alternative interpretation. *American Naturalist* 124: 573-582.
- Yapo, P.O., H.V. Gupta, and S. Sorooshian. 1998. Multi-objective global optimization for hydrologic models. *Journal of Hydrology* 204: 83-97.
- Yokoo, Y., S. Kazama, M. Sawamoto, and H. Nishimura. 2001. Regionalization of lumped water balance model parameters based on multiple regression. *Journal of Hydrology* 246: 209-222.
- Zandbergen, P., J. Houston, and H. Schreier. 1999. Comparative Analysis of Methodologies for Measuring Imperviousness of Watersheds in the Georgia Basin. University of British Columbia, Institute for Resources and Environment. Prepared for Fisheries & Oceans Canada, Habitat & Enhancement Branch, Vancouver, BC.

